SATHYABAMA
INSTITUTE OF SCIENCE AND TECHNOLOGY
(DEEMED TO BE UNIVERSITY)
Accredited "A" Grade by NAAC | 12B Status by UGC | Approved by AICTE
www.sathyabama.ac.in

SCHOOL OF MECHANICAL ENGINEERING
DEPARTMENT OF MECHATRONICS ENGINEERING

UNIT I – INTRODUCTION

Micro Electro Mechanical Systems (MEMS)

SMR1301

1. Why MEMS?

1.1. What is MEMS and comparison with microelectronics?

Micro Electro Mechanical Systems or MEMS is a term coined around 1989 by Prof. R. Howe [1] and others to describe an emerging research field, where mechanical elements, like cantilevers or membranes, had been manufactured at a scale more akin to microelectronic circuit than to lathe machining. But MEMS is not the only term used to describe this field and from its multicultural origin it is also known as Micro machines, a term often used in Japan, or as Microsystem Technology (MST), in Europe. However, if the etymology of the word is more or less well known, the dictionaries are still mum about an exact definition.

It appears that these devices share the presence of features below 100 µm that are not machined using standard machining but using other techniques globally called microfabrication technology. Of course, this simple definition would also include microelectronics, but there is a characteristic that electronic circuits do not share with MEMS. While electronic circuits are inherently solid and compact structures, MEMS have holes, cavity, channels, cantilevers, membranes, etc, and, in some way, resemble „mechanical" parts. This has a direct impact on their manufacturing process. Actually, even when MEMS are based on silicon, microelectronics process needs to be adapted to cater for thicker layer deposition, deeper etching and to introduce special steps to free the mechanical structures. Then, many more MEMS are not based on silicon and can be manufactured in polymer, in glass, in quartz or even in metal. Thus, if similarities between MEMS and microelectronics exist, they now clearly are two distinct fields. Actually, MEMS needs a completely different set of mind, where next to electronics, mechanical and material knowledge plays a fundamental role.

1.2. Why MEMS technology

1.2.1. Advantages offered

The development of a MEMS component has a cost that should not be misevaluated but the technology has the possibility to bring unique benefits. The reasons that prompt the use of MEMS technology can be classified broadly in three classes: - miniaturization of existing devices, like for example the production of silicon based gyroscope which reduced existing devices weighting several kg and with a volume of 1000cm^3 to a chip of a few grams contained in a 0.5cm^3 package. - Development of new devices based on principles that do not work at larger scale. A typical example is given by the biochips where electrical field are used to pump the reactant around the chip. This so called electro-osmotic effect based on the existence of a drag force in the fluid works only in channels with dimension of a fraction of one mm, that is, at micro-scale. - Development of new tools to interact with the micro-world. In 1986 H. Rohrer and G. Binnig at IBM were awarded the Nobel prize in physics for their work on scanning tunnelling microscope. This work heralded the development of a new class of microscopes (atomic force microscope, scanning near-field optical microscope…) that shares the presence of micro machined sharp micro-tips with radius below 50nm. This micro-tool was used to position atoms in complex arrangement, writing Chinese character or helping verify some prediction of quantum mechanics. Another example of this class of MEMS devices at a slightly larger scale would be the development of micro-grippers to handle cells for analysis. By far miniaturization is often the most important driver behind MEMS development. The common perception is that miniaturization reduces cost, by decreasing material consumption and allowing batch fabrication, but an important collateral benefit is also in the increase of applicability. Actually, reduced mass and size allow placing the MEMS in places where a traditional system won"t have been able to fit. Finally, these two effects concur to increase the total market of the miniaturized device compared to its costlier and bulkier ancestor. A typical example is brought by the accelerometer developed as a replacement for traditional airbag triggering sensor and that is now used in many appliances, as in digital cameras to help stabilize the image or even in the contact-less game controller integrated with the latest hand phones.However often miniaturization alone cannot justify the development of new MEMS. After all if the bulky component is small enough, reliable enough, and particularly cheap then there is probably no reason to miniaturize it. Micro-fabrication process cost cannot usually compete with metal sheet punching or other conventional mass production methods. But MEMS technology allows something different, at the same time you make the component smaller you can make it better. The airbag crash sensor gives us a good example of the added value that can be brought by developing a MEMS device. Some non-MEMS crash sensors are based on a metal ball retained by a rolling spring or a magnetic field. The ball moves in response to a rapid car deceleration and shorts two contacts inside the sensor. A simple and cheap method, but the ball can be blocked or contact may have been contaminated and when your start your engine, there is no easy way to tell if the sensor will work or not. MEMS devices can have a built-in self-test feature, where a micro-actuator will simulate the effect of deceleration and allow checking the integrity of the system every time you start up the engine. Another advantage that MEMS can bring relates with the system integration. Instead of having a series of external components (sensor, inductor…) connected by wire or soldered to a printed circuit board, the MEMS on silicon can be integrated directly with the electronics. Whether it is on the same chip or in the same package it results in increased reliability and decreased assembly cost, opening new application opportunities. As we see, MEMS technology not only makes the things smaller but often makes them better.

1.2.2. Diverse products and markets

The previous difficulty we had to define MEMS stems from the vast number of products that fall under the MEMS umbrella. The MEMS component currently on the market can be broadly divided in six categories (Table 1.1), where next to the well-known pressure and inertia sensors produced by different manufacturer like Motorola, analogy Devices, Sensor or Delphi we have many other products. The micro-fluidic application is best known for the inkjet printer head popularized by Hewlett Packard, but they also include the burgeoning bio MEMS market with micro analysis system like the capillary electrophoresis system from Agilent or the DNA chips. Optical MEMS includes the component for the fibre optic telecommunication like the switch based on a moving mirror produced by Sercalo. They also include the optical switch matrix that is now waiting for the recovery of the telecommunication industry. This component consists of 100s of micro-mirror that can redirect the light from one input fibre to one output fibre, when the fibres are arranged either along a line (proposed by the now defunct Optical Micro Machines) or in a 2D configuration (Lambda router from Lucent). Moreover MOEMS deals with the now rather successful optical projection system that is competing with the LCD projector. The MEMS products are based either on an array of torsional micro-mirror in the Texas Instrument Digital Light Processor (DLP) system or on an array of controllable grating as in the Grating Light Valve (GLV) from Silicon Light Machines. RF MEMS is also emerging as viable MEMS market. Next to passive components like high-Q inductors produced on the IC surface to replace the hybridized component as proposed by MEMSCAP we find RF switches and soon micromechanical filters. But the list does not end here and we can find micro machined relays (MMR) produced for example by Omron, HDD read/write head and actuator or even toys, like the autonomous micro-robot EMRoS produced by EPSON.

Product category	Example
Pressure sensor	Manifold pressure (MAP), tire pressure, blood pressure…
Inertia sensor	Accelerometer, gyroscope, crash sensor…
Microfluidics / bioMEMS	Inkjet printer nozzle, micro-bio-analysis systems, DNA chips…
Optical MEMS / MOEMS	Micro-mirror array for projection (DLP), micro-grating array for projection (GLV), optical fiber switch, adaptive optics…
RF MEMS	High Q-inductor, switches, antenna, filter…
Others	Relays, microphone, data storage, toys…

Table 1.1: MEMS products example

In 2002 these products represented a market of about 3.2B$, with roughly one third in inkjet printer nozzle, one third in pressure sensor and the rest split between inertia sensors, RF MEMS, optical MEMS, projection display chip and bio MEMS . Of course the MEMS market overall value is still small compared to the 180B$ IC industry – but there are two aspects that still make it very interesting: - it is expected to grow at an annual rate of 18% for the foreseeable future, much higher than any projection for IC industry; - MEMS chips have a large leveraging effect, and in the average a MEMS based systems will have 8 times more value than the MEMS chip price (e.g., a DLP projector is about 10 times the price of a MEMS DLP chip). This last point has created very large difference between market studies, whether they reported market for components alone or for systems. The number cited above is in the average of other studies and represent the market for the MEMS components alone.

1.2.3. Economy of MEMS manufacturing and applications

However large the number of opportunities is, it should not make companies believe that they can invest in any of these fields randomly. For example, although the RF MEMS market seems to be growing fuelled for the appetite for smaller wireless communication devices, it seems to grow mostly through internal growth. Actually the IC foundries are developing their own technology for producing, for example, high-Q inductors, and it seems that an external provider will have a very limited chance to penetrate the market. Thus, market opportunities should be analysed in detail to eliminate the false perception of a large market, taking into consideration the targeted customer inertia to change and the possibility that the targeted customer himself develop MEMS based solution. In that aspect, sensors seems an easy target being simple enough to allow full development within small business unit and having a large base of customers – however, an optical switch matrix is riskier because its value is null without the system that is built by a limited number of customers, which most probably have the capabilities to develop in house the MEMS component anyway. Some MEMS products already achieve high volume and benefit greatly from the batch fabrication technique. For example more than 100 millions MEMS accelerometers are sold every year in the world – and with newer use coming, this number is still growing fast. But large numbers in an open market invariably means also fierce competition and ultimately reduced prices. Long are gone the days where a MEMS accelerometer could be sold 10$ a piece - it is now less than 2$ and still dropping. Currently, the next target is a 3-axis accelerometer in a single package for about 4$, so that it can really enter the toys industry. Note that there may be a few exceptions to this rule. Actually, if the number of unit sold is also very large, the situation with the inkjet printer nozzle is very different. Canon and Hewlett Packard developed a completely new product, the inkjet printer, which was better than earlier dot matrix printer, creating a captive market for its MEMS based system. This has allowed HP to repeatedly top the list of MEMS manufacturer with sales in excess of 600M$. This enviable success is unfortunately most probably difficult to emulate. But these cases should not hide the fact that MEMS markets are essentially niche markets. Few product will reach the million unit/year mark and currently among the more than 300 companies producing MEMS only a dozen have sales above 100m$/year. Thus great care should be taken in balancing the research and development effort, because the difficulty of developing new MEMS from scratch can be daunting and the return low. For example, although Texas Instrument is now reaping the fruit of its Digital Light Processor selling between 1996 and 2004 more than 4 million chips for a value now approaching 200m$/year, the development of the technology by L. Hornbeck took more than 10 years . Few start-up companies will ever have this opportunity. Actually it is not clear for a company what the best approach for entering the MEMS business is, and we observe a large variety of business model with no clear winner. For many years in microelectronics industry the abundance of independent foundries and Packaging companies has made fabless approach a viable business model. However it is an approach only favoured by a handful of MEMS companies, and it seems for good reasons. A good insight in the polymorphism of MEMS business can be gained by studying the company MEMS Tech, now a holding listed on the Kuala Lumpur Mesdaq (Malaysia) and having office in Detroit, Kuala Lumpur and Singapore. Singapore is actually where everything started in the mid-90"s for MEMS Tech with the desire from an international company (EG&G) to enter the MEMS sensor market. They found a suitable partner in Singapore at the Institute of Microelectronics (IME), a research institute with vast experience in IC technology. This type of cooperation has been a frequent business model for MNC willing to enter MEMS market, by starting with ex-house R&D contract development of a component. EG&G and IME designed an accelerometer, patenting along the way new fabrication process and developing a cheap plastic packaging process. Finally the R&D went well enough and the complete clean room used for the development was spun-off and used for the production of the accelerometer. Here, we have another typical start up model, where IP developed in research institute and university ends up building a company. This approach is very typical of MEMS development, with a majority of the existing MEMS companies having been spun-off from a public research institute or a university.

A few years down the road the fab continuously produced accelerometer and changed hands to another MNC before being bought back in 2001 by its management. During that period MEMS Tech was nothing else but a component manufacturer providing off-the-shelf accelerometer, just like what Motorola, Texas Instrument and others are doing. But after the buyout, MEMS Tech needed to diversify its business and started proposing fabrication services. It then split in two entities: the fab, now called Sensfab, and the packaging and testing unit, Senzpak. Three years later, the company had increased its „off-the-shelf" product offering, proposing accelerometer, pressure sensor, microphones and one IR camera developed in cooperation with local and overseas university. This is again a typical behaviour of small MEMS companies where growth is fuelled by cooperation with external research institutions. Still at the same time MEMS Tech proposes wafer fabrication, packaging and testing services to external companies. This model where products and services are mixed is another typical MEMS business model, also followed by Silicon Microstructures in the USA, Colybris in Switzerland, MEMSCAP in France and some other. Finally, in June 2004 MEMS Tech went public on the Mesdaq market in Kuala Lumpur. The main reason why the company could survives its entire series of avatar, is most probably because it had never overgrown its market and had the wisdom to remain a small company, with staff around 100 persons. Now, with a good product portfolio and a solid base of investor it is probably time for expansion.

1.3. Major drivers for MEMS technology

From the heyday of MEMS research at the end of the 1960s, started by the discovery of silicon large Piezo resistive effect by C. Smith [4] and the demonstration of anisotropic etching of silicon by J. Price [5] that paved the way to the first pressure sensor, one main driver for MEMS development has been the automotive industry. It is really amazing to see how many MEMS sensor a modern car can use! From the first oil pressure sensors, car manufacturer quickly added manifold and tire pressure sensors, then crash sensors, one, then two and now up to five accelerometers. Recently the gyroscopes made their apparition for anti-skidding system and also for navigation unit – the list seems without end. Miniaturized pressure sensors were also quick to find their ways in medical equipment for blood pressure test. Since then biomedical application have drained a lot of attention from MEMS eveloper, and DNA chip or micro-analysis system are the latest successes in the list. Because you usually sell medical equipment to doctors and not to patients, the biomedical market has many features making it perfect for MEMS: a niche market with large added value. Actually cheap and small MEMS sensors have many applications. Digital cameras have been starting using accelerometer to stabilize image, or to automatically find image orientation. Accelerometers are also being used in new contactless game controller or mouse. These two later products are just a small part of the MEMS–based system that the computer industry is using to interface the arid beauty of digits with our human senses. The inkjet printer, DLP based projector, head-up display with MEMS scanner are all MEMS based computer output interfaces. Additionally, computer mass storage uses a copious amount of MEMS, for example, the hard-disk drive nowadays based on micro machined GMR head and dual stage MEMS micro-actuator. Of course in that last field more innovations are in the labs, and most of them use MEMS as the central reading/writing element. The telecommunication industry has fuelled the biggest MEMS R&D effort so far, when at the turn of the millennium, 10s of companies started developing optical MEMS switch and similar components. We all know too well that the astounding 2D-switch matrix developed by Optical Micro Machines (OMM) and the 3D-matrix developed in just over 18 months at Lucent are now bed tale stories. However within a few years they placed optical MEMS as a serious contender for the future extension of the optical network, waiting for the next market rebound. Wireless telecommunications are also using more and more MEMS components. MEMS are slowly sipping into hand phone replacing discrete elements one by one, RF switch, microphone, filters – until the dream of a $1mm^3$ hand phone becomes true (with vocal recognition for numbering of course!). The latest craze seems to be in using accelerometers (again) inside hand phone to convert them into game controller, the ubiquitous hand phone becoming even more versatile. Large displays are another consumer product that may prove to become a large market for MEMS. Actually, if plasma and LCD TV seems to become more and more accepted, their price is still very high and recently vendors start offering large display based on MEMS projector at about half the price of their flat panel cousin. Projector based system can be very small and yet provide large size image. Actually, for the crown of the largest size the DLP projecting system from TI is a clear winner as evidenced by the digital cinema theatres that are burgeoning all over the globe. For home theatre the jury is still debating – but MEMS will probably get a good share at it and DLP projector and similar technologies won"t be limited to PowerPoint presentation. Finally, it is in the space that MEMS are finding an ultimate challenge and already some MEMS sensors have been used in satellite. The development of micro (less than 100kg) and nano (about 10kg) satellites is bringing the mass and volume advantage of MEMS to good use and some project are considering swarms of nano satellite each replete with micro machined systems.

1.4. Mutual benefits between MEMS and microelectronics

The synergies between MEMS development and microelectronics are many. Actually MEMS clearly has its roots in microelectronics, as H. Nathanson at Westinghouse reported in 1967 the "resonant gate transistor" [6], which is now considered to be the first MEMS. This device used the resonant properties of a cantilevered beam acting as the gate of a field-effect transistor to provide electronic filtering with high-Q. But even long after this pioneering work, the emphasis on MEMS based on silicon was clearly a result of the vast knowledge on silicon material and on silicon based micro fabrication gained by decades of research in microelectronics. Even quite recently the SOI technology developed for ICs has found a new life with MEMS. But the benefit is not unilateral and the MEMS technology has indirectly paid back this help by nurturing new electronic product. MEMS brought muscle and sight to the electronic brain, enabling a brand new class of embedded system that could sense, think and act while remaining small enough to be placed everywhere. As a more direct benefit, MEMS can also help keep older microelectronics fab running. Actually MEMS devices most of the times have minimum features size of a several µm, allowing the use of older generation IC fabrication equipment that otherwise will have just been dumped. It is even possible to convert a complete plant and analogy. Devices have redeveloped an older BiCMOS fabrication unit to successfully produce their renowned smart MEMS accelerometer. Moreover, as we have seen, MEMS component often have small market and although batch fabrication is a must, a large part of the MEMS production is still done using 4” (100 mm) and 6” (150 mm) wafers – and could use 5-6 years old IC production equipment. But this does not mean that equipment manufacturer cannot benefit from MEMS. Actually MEMS fabrication has specific needs (deeper etch, double side alignment, wafer bonding, thicker layer…) with a market large enough to support new product line. For example, firms like STS and Alcatel-Adixen producing MEMS deep RIE or EVGroup and Suss for their wafer bonder and double side mask aligner have clearly understood how to adapt their know-how to the MEMS fabrication market.

2.0 Scaling Laws in Miniaturization

2.1 Introduction to Scaling

Scaling theory is a value guide to what may work and what may not work when we start to design the world of micro.Three general scale sizes: (a) Astronomical

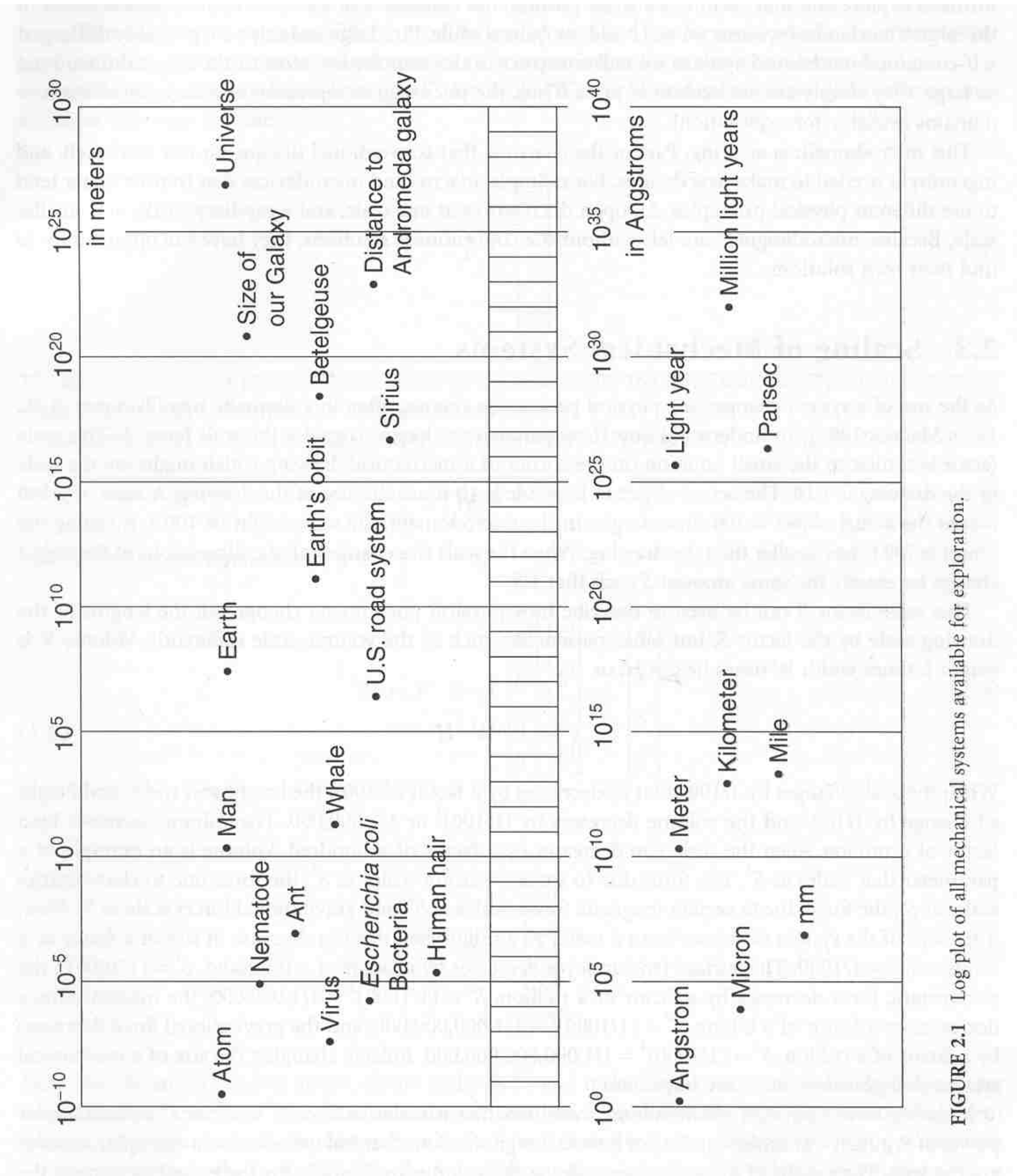

FIGURE 2.1 Log plot of all mechanical systems available for exploration.

objects; (b) Macro-objects;

(c) micro-objects.

- Things effective at one of these scale sizes often are insignificant at another scale size.
- Examples:
  - ➢ Gravitational forces dominate on an astronomical scale (e.g., the earth

moves around the sun), but not on smaller scales.

- ➢ Macro-sized motors use magnetic forces for actuation, but micro-sized ones usually use electrostatic fields instead of magnetic.

(Reference: MEMS Handbook, edited by Mohamed Gad-el-Hak, CRC Press)

Two types of scaling laws:

1. The first type: depends on the size of physical objects.
2. The second type: involves both the size and material properties of the system.

2.2 Scaling in Geometry

Surface and volume are two physical quantities that are frequently involved in micro-device design.

- Volume: related to the mass and weight of a device, which are related to both mechanical and thermal inertial.

  (thermal inertial: related to the heat capacity of a solid, which is a measure of how fast we can heat or cool a solid. → important in designing a thermal actuator)

- Surface: related to pressure and the buoyant forces in fluid mechanics, as well as heat absorption or dissipation by a solid in convective heat transfer.

Surface to volume ration (*S/V* ratio)

- $S \propto l^2$; $V \propto l^3$
- $S/V \propto l^{-1}$
- As the size *l* decreases, its *S/V* ratio increases.
- Examples
  - ➢ *S/V* ratio of an elephant (10^{-4}) vs. of a dragonfly (10^{-1})

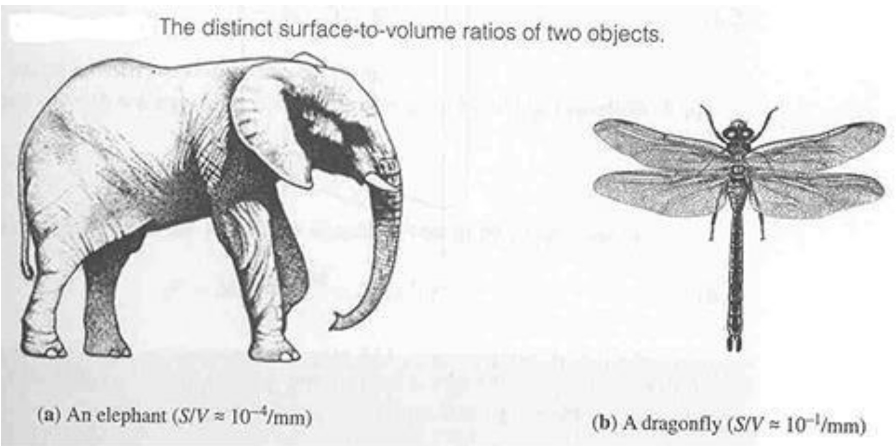

Fig 2.2 Distinct surface to volume ratios of two objects

➤ An elephant and a flea (Fig 2.2) have cells of about the same size. Too large a cell will not have enough surfaces for substance exchanges with its surroundings to support the active metabolism within, unless it is highly elongated like a vertebrate nerve cell, increasing the *S/V* ratio. (Biochemistry by Mathews *et al.*) (fig 2.3).

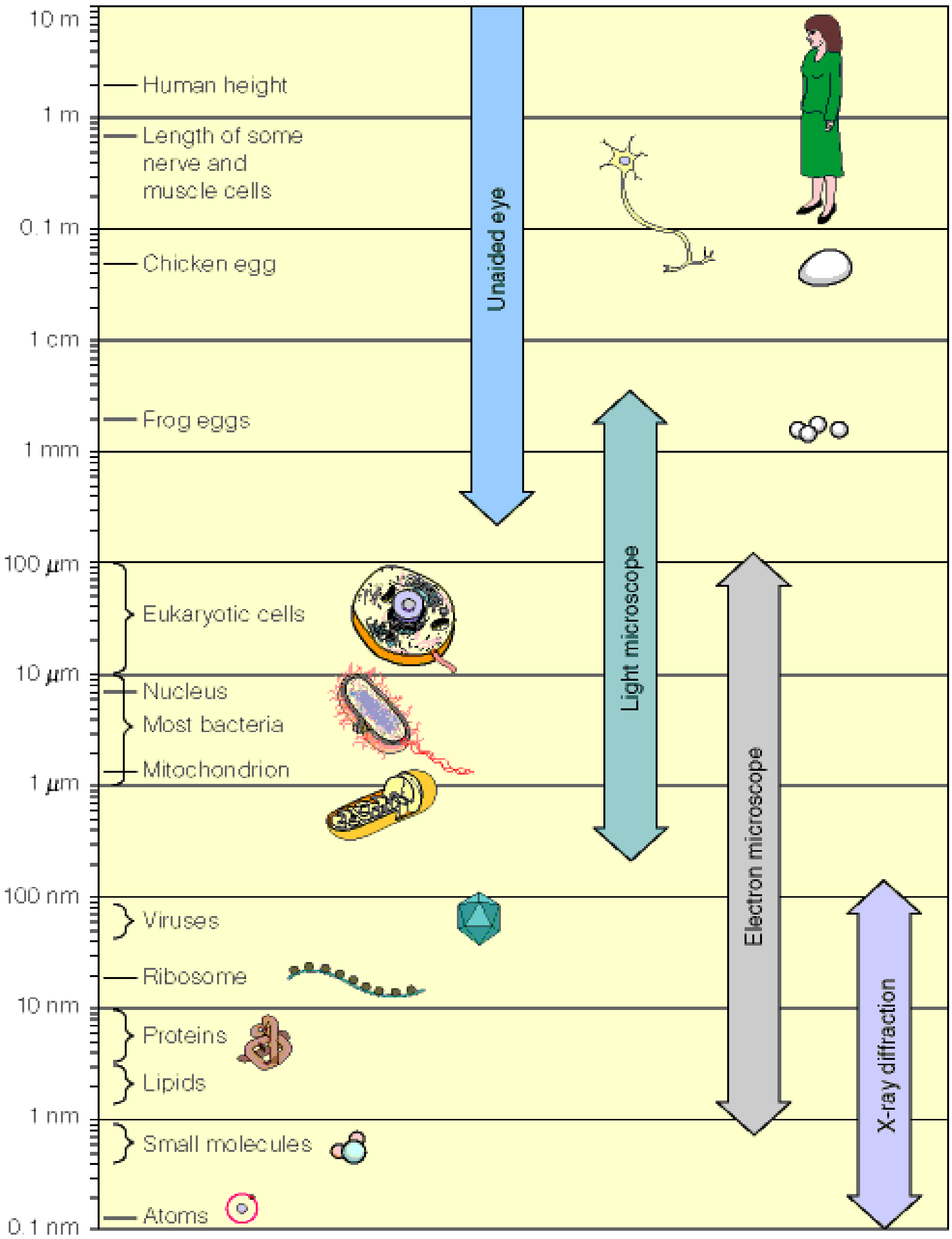

Figure 2.3 shows Range of sizes of objects studied by biochemists and biologists. (Biochemistry by Mathews et al.)

Eukaryotes - Organisms whose cells are compartmentalized by internal cellular membranes to produce a nucleus and organelles.

2.3 Scaling in Rigid-Body Dynamics

2.3.1 Scaling in Dynamic Forces

$$s = v_0 t + \frac{1}{2} a t^2$$

By letting $v_0 = 0$,

$$a = \frac{2s}{t^2}$$

$$F = Ma = \frac{2sM}{t^2}$$

2.3.2 The Trimmer Force Scaling Vector

Trimmer (1989) proposed a unique matrix to represent force scaling with relative parameters of acceleration a, time t, and power density P/V_0 (table 2.1)

Force scaling factor:

$$F = [l^F] = \begin{bmatrix} l^1 \\ l^2 \\ l^3 \\ l^4 \end{bmatrix}$$

Acceleration a:

$$a = [l^F][l^3]^{-1} = \begin{bmatrix} l^1 \\ l^2 \\ l^3 \\ l^4 \end{bmatrix} [l^{-3}] = \begin{bmatrix} l^{-2} \\ l^{-1} \\ l^0 \\ l^1 \end{bmatrix}$$

Time t:

$$t = \sqrt{\frac{2sM}{F}} \propto ([l^1][l^3][l^{-F}])^{0.5} = \begin{bmatrix} l^{1.5} \\ l^1 \\ l^{0.5} \\ l^0 \end{bmatrix}$$

Power Density P/V_0:

Since $P = \frac{W}{t} = \frac{F \cdot s}{t}$, thus

$$\frac{P}{V_0} = \frac{Fs}{tV_0}$$

$$\Rightarrow \frac{P}{V_0} = \frac{[l^F][l^1]}{([l^1][l^3][l^{-F}])^{0.5}[l^3]} = \begin{bmatrix} l^{-2.5} \\ l^{-1} \\ l^{0.5} \\ l^2 \end{bmatrix}$$

Table 2.1 | Scaling laws for rigid-body dynamics

Order	Force scale F	Acceleration a	Time t	Power density P/V_0
1	l^1	l^{-2}	$l^{1.5}$	$l^{-2.5}$
2	l^2	l^{-1}	l^1	l^{-1}
3	l^3	l^0	$l^{0.5}$	$l^{0.5}$
4	l^4	l^1	l^0	l^2

2.4 Scaling in Electrostatic Forces

In Fig. 2.4, the electric potential energy induced in the parallel plates is:

$$U = -\frac{1}{2}CV^2 = -\frac{\varepsilon_r \varepsilon_0 WL}{2d}V^2$$

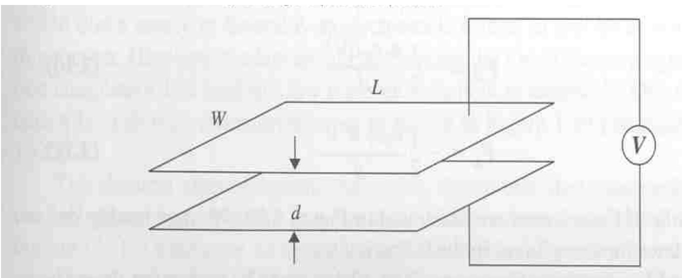

Fig 2.4 Electrically charged parallel plates

Breakdown voltage

- The voltage required to initiate discharge.
- For $d > 10\mu m$, $V \propto l^1$ (see Fig. 2.5)

$$\Rightarrow U \propto \frac{(l^0)(l^0)(l^1)(l^1)(l^1)^2}{l^1} = l^3 \tag{6.11}$$

- A factor of 10 decrease in linear dimension will decrease the potential energy by a factor of 1000.

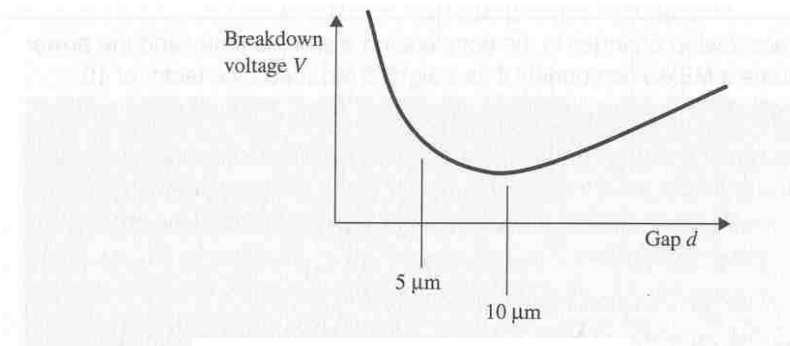

Fig 2.5 Paschen's effect

In Fig. 2.6, the electrostatic forces are,

$$F_d = -\frac{\partial U}{\partial d} = -\frac{1}{2}\frac{\varepsilon_r \varepsilon_0 WLV^2}{d^2}$$

$$F_W = -\frac{\partial U}{\partial W} = \frac{1}{2}\frac{\varepsilon_r \varepsilon_0 LV^2}{d}$$

$$F_L = -\frac{\partial U}{\partial L} = \frac{1}{2}\frac{\varepsilon_r \varepsilon_0 WV^2}{d}$$

- F_d, F_W, and $F_L \propto (l^2)$
  - A 10 times reduction in the plate sizes means a 100 times decrease in the induced electrostatic forces.

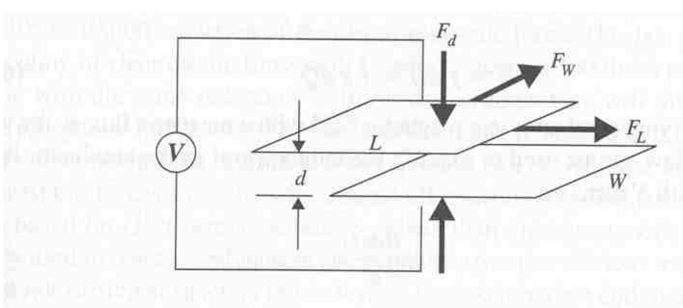

Fig2.6 Electrostatic forces in charged parallel plates

2.5 Scaling in Electromagnetic Forces

In this section, it is shown that electromagnetic actuation is not scaled down nearly as favorably as electrostatic forces.

- The electromagnetic forces can be induced in a conductor or a conducting loop in a magnetic field **B** by passing current *i* in the conductor.
- The electromotive force (emf) is the force that drives the electrons through the conductor.

If 10 times reduction in size (l)

$\Rightarrow$ Electromagnetic force: 10,000 times reduction

Comparison: Electrostatic force: only 100 times reduction

Conclusion: Electromagnetic force is less favorable in scale-down than Electromagnetic force.

2.6 Scaling in Electricity

Examples: Microsystem actuation by electrostatic, piezoelectric, and thermal resistance heating.

Electric Resistance: $R = \frac{\rho L}{A} \propto l^{-1}$

where ρ, L, and A are the resistivity, length, and cross-sectional area, respectively.

where V is the applied voltage $\propto l^0$

Electric field energy density: $u = \frac{1}{2}\varepsilon E^2 \propto l^{-2}$

where the dielectric permittivity $\varepsilon \propto l^0$, and the electric field E$\propto l^{-1}$.

Example: For a system that carries its own power, the available power $E_{av} \propto l^3$.

$$\Rightarrow \frac{P}{E_{av}} \propto l^{-2}.$$

- That is, a 10 times reduction of *l* leads to 100 times greater power loss due to the resistance increase.
- Disadvantage of scaling down of power supply systems.

2.7 Scaling in Fluid Mechanics

In Fig. 2.7, moving the top plate to the right induces the motion of the fluid.

- Newtonian flow: $\tau \propto \frac{d\theta}{dt}$, or $\tau = \mu\frac{d\theta}{dt} = \mu\frac{dV}{dy}$

  where τ: shear stress; μ: coefficient of viscosity;

  dθ/dt: strain rate; V: fluid velocity.

- Thus, $\mu = \frac{\tau}{R_S}$

  where $R_s = V_{max}/h$

- Rate of volumetric fluid flow: $Q = A_s V_{ave}$
- where A_s: cross-sectional area for the flow; V_{ave}: average velocity of the fluid.

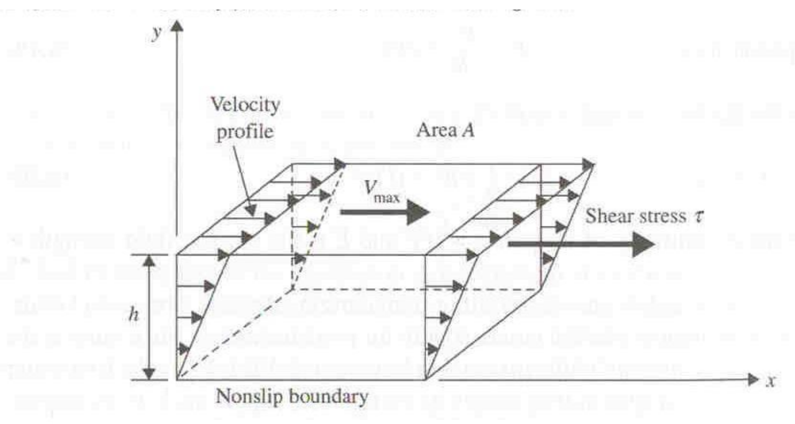

Fig .2.7 Velocity profile of a volume of moving fluid

Renolds number: $\mathrm{Re} = \dfrac{\rho V L}{\mu}$

where ρ: fluid density; V & L: characteristic velocity and length scales of the flow.

- Re $\propto$ (inertial forces)/(viscousforce)
- Macro flows: high inertial forces → high Re → turbulence flow
- Micro flows: high viscosity → low Re → laminar flow

p.s.: (1) turbulence flow: fluctuating and agitated;

(2) laminar flow: smooth and steady;

(3) transition from laminar to turbulent: 10^3~10^5

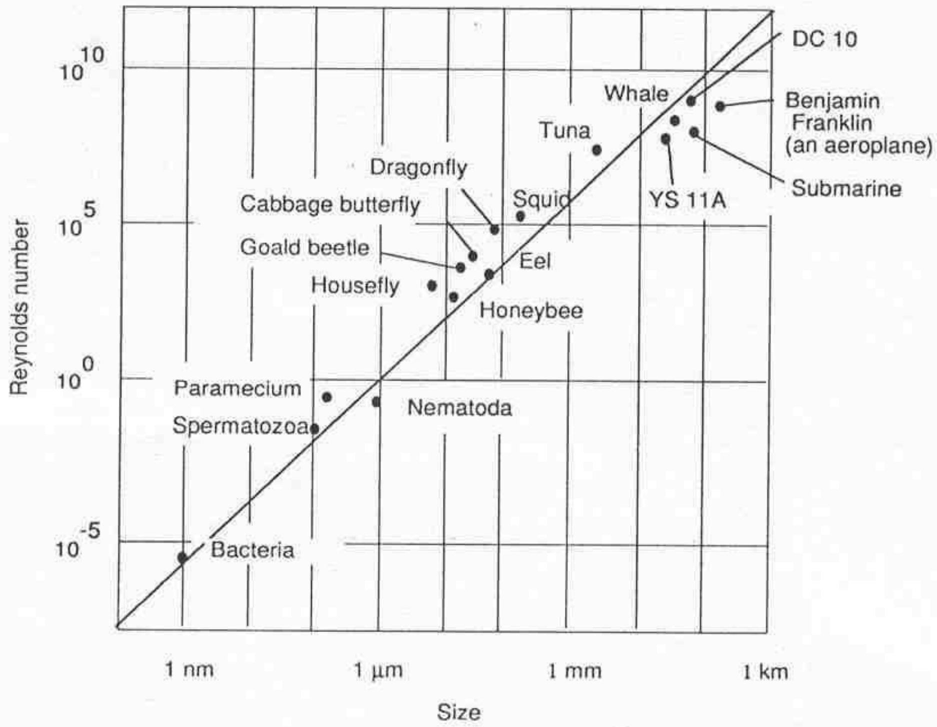

Relation between size (length) of mobile machines and Reynolds numbers of their fluid environments (adopted from Hayashi (1988)). The Reynolds number becomes around 1 when mobile machines are around 1 mm. The Reynolds number expresses the ratio between inertial force and viscous resistance. Therefore, if the machine is less than 1 mm viscous resistance dominates the dynamics. (YS 11A is a twin-engined plane.)

(from “Micromachines: A New Era in Mechanical Engineering,” by Iwao Fujimasa, Oxford University Press, 1996)

- In Fig. 2.8, with the pressure drop ΔP over the length L, the rate of volumetric flow of the fluid is (Hagen-Poiseuille law),

$$\Theta = \pi a^4 \Delta P / 8\mu L \qquad (6.24)$$

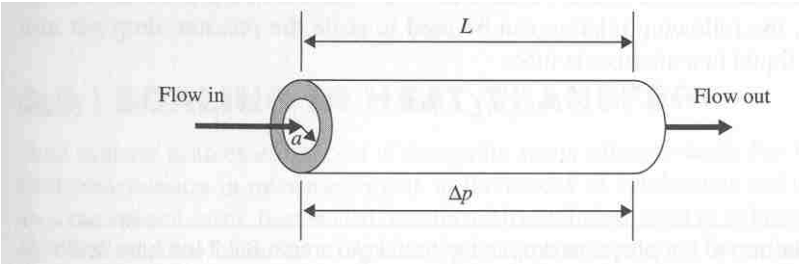

Fig 2.8 Fluid flow in a small circular conduit

- With $V_{ave} = \dfrac{Q}{\pi a^2}$, $\Delta P = \dfrac{8\mu V_{ave} L}{a^2}$
- Thus, $Q \propto a^4$; $\dfrac{\Delta P}{L} \propto a^{-2}$

2.8 Scaling in Heat Transfer

6.8.1 Scaling in Heat Conduction

Scaling of Heat Flux

Heat conduction in solid is governed by the Fourier law,

➢ $q_x = -k \dfrac{\partial T\,(x, y, z, t)}{\partial x}$

where q_x: heat flux along the x axis; k: thermal conductivity of the solid; $T(x,y,z,t)$: temperature field.

Rate of heat conduction: $Q = qA = -kA \dfrac{\Delta T}{\Delta x}$

For solids in meso- and microscales,

$$Q \propto (l^2)(l^{-1}) = l^1$$

That is, reduction in size leads to the decrease of total heat flow.

Scaling in Submicrometer Regime

In the submicrometer regime, the thermal conductivity is,

$$k = \frac{1}{3} cV\lambda \propto l^1$$

where c, V, and λ are specific heat, molecular velocity, and average mean free path, respectively.

- Thus, $Q \propto (l^1)(l^1) = l^2$
- A reduction in size of 10 would lead to a reduction of total heat flow by 100.

Scaling in Effect of Heat Conduction in Solids of Meso- and Micro-scales

A dimensionless number, called the Fourier number, F_0 is used to determine the time increments in a transient heat conduction analysis.

- $$F_0 = \frac{\alpha t}{L^2}$$

where α: thermal diffusivity of the material, and *t*: time for heat to flow across the characteristic length *L*.

Scaling in Heat Convection Heat transfer in fluid is in the mode of convection (Newton's cooling law),

$$Q = qA = hA\Delta T$$

where *Q*: total heat flow between two plates; *q*: heat flux; *A*: cross-sectional area for the heat flow; *h*: heat transfer coefficient; ΔT : temperature difference between these two points.

- *h*: depends primarily on the fluid velocity, which does not play a significant role in the scaling of the heat flow.
- Thus, in meso- and micro-regimes, $Q \propto A \propto l^2$

For the cases in which gases pass in narrow channels at submicro-meter scale,

- ➢ The classical heat transfer theories based on continuum fluids break down.
- ➢ The seemingly convective heat transfer has in fact become conduction of heat among the gas molecules as the effect of the boundary layer becomes a dominant factor.
- ➢ In Fig. 6.9, $H < 7\lambda$ where λ =65nm for gases, and 1.3 μm for liquids.

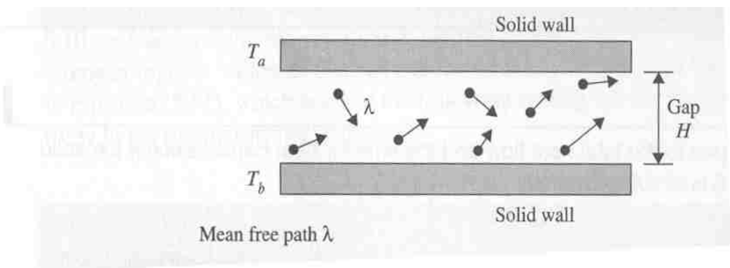

Fig 3.9 Gas flow in a micro channel

- $\lambda \propto \frac{1}{\rho}$
- $k = \frac{1}{3} cV\lambda$
- $V = \sqrt{\frac{8kT}{\pi m}}$
  where *T*: mean temperature of the gas; and *m*: molecular weight of the gas.
- Effective heat flux:

$$q_{eff} = \frac{k\Delta T}{H + 2\varepsilon}$$

where ΔT : temperature difference between two plates; ε: depends on the gases entrapped between two plates, $2.4\lambda<\varepsilon<2.9\lambda$ for air, O_2, N_2, CO_2, methane, and He, and $\varepsilon=11.7\lambda$ with $H>7\lambda$ for H_2.

3. Materials for MEMS and Microsystems

3.1 Introduction

Many Microsystems use microelectronics materials such as silicon, and gallium arsenide for the sensing and actuating elements.

- Reasons: (1) dimensionally stable;
  (2) Well-established fabricating and packaging techniques.

However, there are other materials used for MEMS and Microsystems products:

- Such as quartz and Pyrex, polymers and plastics, and ceramics. (not common in microelectronics)

3.2 Substrates and Wafers

Substrate:

- In microelectronics, substrate is a flat macroscopic object on which micro fabrication processes take place [Ruska, 1987].
- In microsystems, a substrate serves an additional purpose:
  - Act as signal transducer besides supporting other transducers that convert mechanical actions to electrical outputs or vice versa.

Wafer:

- In semiconductors, the substrate is a single crystal cut in slices from a larger piece call a wafer (which can be of silicon or other single crystalline materials such as quartz or gallium arsenide).
- In microsystems, there are two types of substrate materials:

3.2.1 Active substrate material.

3.2.2 Passive substrate material.

Material classifications:

- Insulators: electric resistivity $\rho > 10^8$ Ω-cm
- Semiconductors: $10^{-3} < \rho < 10^8$ Ω-cm
- Conductors: $\rho < 10^{-3}$ Ω-cm

Table 3.1 Typical electrical resistivity of insulators, semiconductors and conductors

Materials	Approximate electrical resistivity ρ, Ω-cm	Classification
Silver (Ag)	10^{-6}	Conductors
Copper (Cu)	$10^{-5.8}$	
Aluminum (Al)	$10^{-5.5}$	
Platinum (Pt)	10^{-5}	
Germanium (GE)	10^{-3}–$10^{1.5}$	Semiconductors
Silicon (Si)	10^{-3}–$10^{4.5}$	
Gallium arsenide (GaAs)	10^{-3}–10^{8}	
Gallium phosphide (GaP)	10^{-2}–$10^{6.5}$	
Oxide	10^{9}	Insulators
Glass	$10^{10.5}$	
Nickel (pure)	10^{13}	
Diamond	10^{14}	
Quartz (fused)	10^{18}	

In MEMS, common substrate materials (silicon Si, germanium Ge , gallium arsenide GaAs fig 3.5) all fall in the category of semiconductors. Why?

- They are at the borderline between conductors and insulators, so they can be made either a conductor or an insulator as needed.

  → Can be converted to a conducting material by doping (p- or n-type).
- The fabrication processes (e.g., etching) and the required equipment have already been developed for these materials.

3.3 Active Substrate Materials

Active substrate materials are primarily used for sensors and actuators in Microsystems.

- Typical materials: Si, GaAs, Ge, and quartz.

  (All except quartz are classified as semiconductors in Table 3.1)
- Have a cubic crystal lattice with tetrahedral atomic bond.
- Reason for active substrate materials: dimensional stability

  → Insensitive to environmental conditions.

  → A critical requirement for sensors and actuators with high precision.
- Each atom carries 4 electrons in the outer orbit, and shares these 4 electrons with its 4 neighbors.

3.4 Silicon as A substrate Material

3.4.1 The Ideal Substrate for MEMS

- Single-crystal silicon is the most widely used substrate material for MEMS and microsystem. The reasons are:
  - 3.4.1.1 (a) Mechanically stable; (b) can be integrated with electronics for signal transduction on the same substrate.
  - 3.4.1.2 An ideal structural material because of high Young's modulus (which can better maintain a linear relationship between applied load and the induced deformation) and light weight.
    - 3.4.1.2.1 About the same as steel (about 2×10^5 MPa)
    - 3.4.1.2.2 As light as aluminum with a mass density of about 2.3 g/cm^3.
  - 3.4.1.3 High melting point at 1400℃
    - 3.4.1.3.1 About twice as high as that of aluminum.
    - 3.4.1.3.2 Dimensionally stable.
  - 3.4.1.4 Low thermal expansion coefficient
    - 3.4.1.4.1 About 8 times smaller than that of steel.
    - 3.4.1.4.2 More than 10 times smaller than that of aluminum.
  - 3.4.1.5 (a) Show virtually no mechanical hysteresis

    → An ideal candidate material for sensors and actuators.

    (b) Extremely flat and accept coatings and additional thin-film layers for building microstructures and conducting electricity.
  - 3.4.1.6 Treatment and fabrication processes for silicon substrate are well established and documented.

3.4.2 Single Crystal Silicon and Wafer

- The Czochralski (CZ) method: is the most popular one to produce pure silicon crystal. (Fig. 3.1)
  - The raw silicon in the form of quartzite are melted in a quartz crucible with carbon (coal, coke, wood chips, etc.), which is placed in a furnace.

    $$SiC+SiO_2 \rightarrow Si+CO+SiO$$
  - A "seed" crystal is brought into contact with the molten silicon to form a larger crystal (a large bologna-shaped boule).
  - The silicon boule is then ground to a perfect circle, then sliced to form thin disks, which are then chemically-lap polished for finishing.

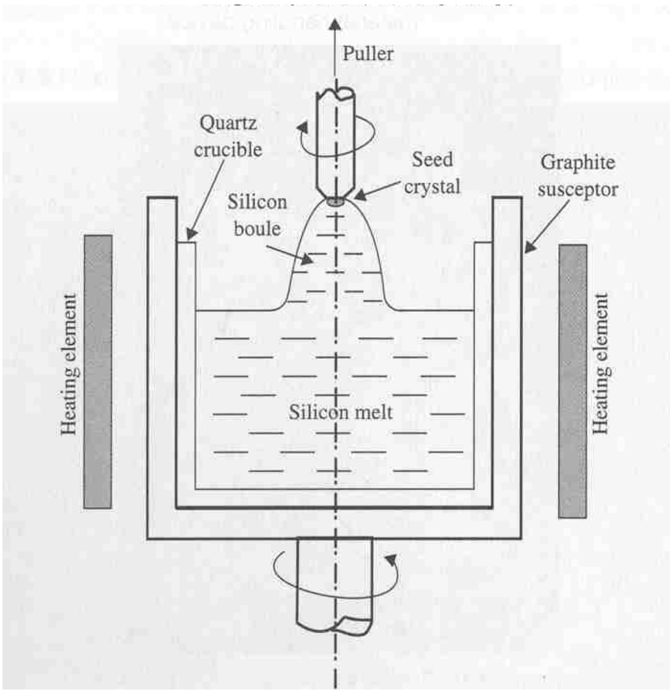

Fig 3.1 The Czochralski method for growing single crystals (Ruska [1987])

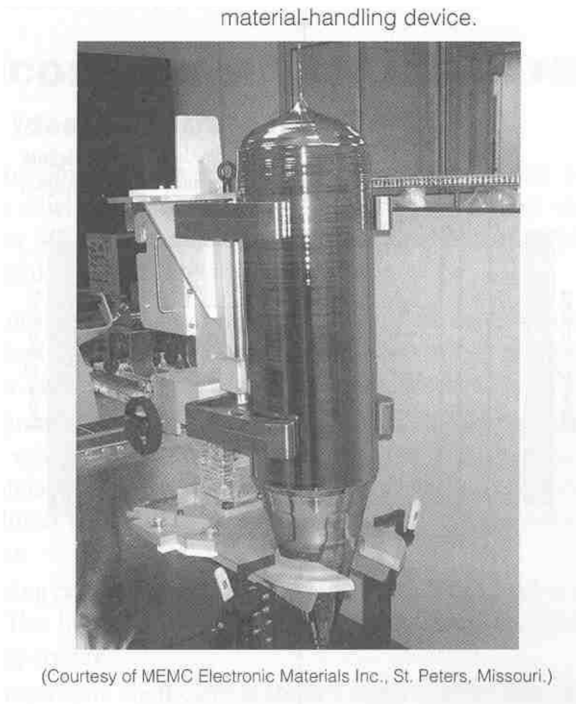

- Wafer sizes:
  - 100 mm (4 in) diameter × 500μm thick
  - 150 mm (6 in) diameter × 750μm thick
  - 200 mm (8 in) diameter × 1mmthick
  - 300 mm (12 in) diameter × 750μm thick(tentative)

- Silicon substrates often are expected to carry electric charges.
  - Require p or n doping of the wafers either by ion implantation or by diffusion
  - n-type dopants: phosphorus [P], arsenic [As], and antimony[Sb]
  - p-type dopants: boron [B]

3.4.3 Crystal Structural

- Silicon: has basically a face-centered cubic (FCC) unit cell, called a *lattice* (as shown in Fig. 3.4).
  - Lattice constant b=0.543 nm.
  - Crystal structure of silicon: more complex

    → Two penetrating face-centered cubic crystals, as shown in Fig. 3.4.

    → 4 additional atoms in the interior of the FCC.

    → 18 atoms in a unit cell.

    → Spacing between adjacent atoms in the diamond sub cell: 0.235 nm.
  - Asymmetrical and non-uniform lattice distance: exhibits anisotropic) thermo physical and mechanical characteristics.

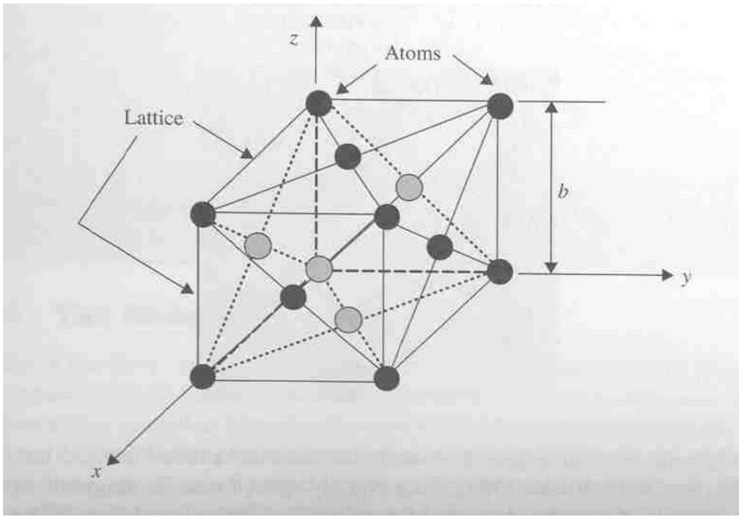

Fig 3.4 A typical face center cubic unit cell

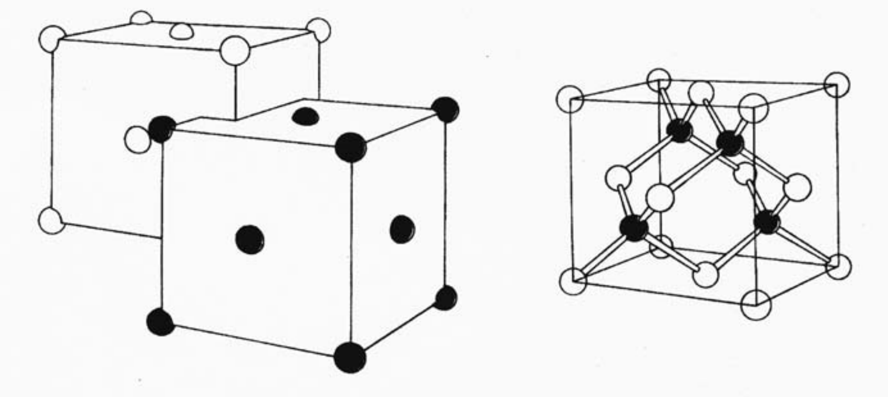

Fig 3.5 The diamond-type lattice can be constructed from two interpenetrating face-centered cubic unit cells. Si forms four covalent bonds, making tetrahedrons.

- Crystal structure of GaAs:

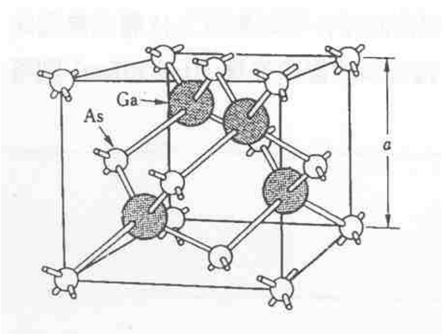

Fig 3.6 Crystal structure of GaAs

3.4.4 The Miller Indices

- Because of the skew distribution of atoms in a silicon crystal, it is important to designate the principal orientations as well as planes in the crystal (fig 3.7 and 3.8).

- Miller Indices:
  - ➢ A plane that intercepts x, y, and z axes at a, b, and c, can be expressed as:

$$\frac{x}{a}+\frac{y}{b}+\frac{z}{c}=1$$

  - ➢ Above Equation can be rewritten as:

$$hx+ky+mz=1$$

where h=1/a, k=1/b, and m=1/c.

  - ➢ (hkm): designate the plane, and <hkm>: designate the direction normal to the plane.
  - ➢ Examples:

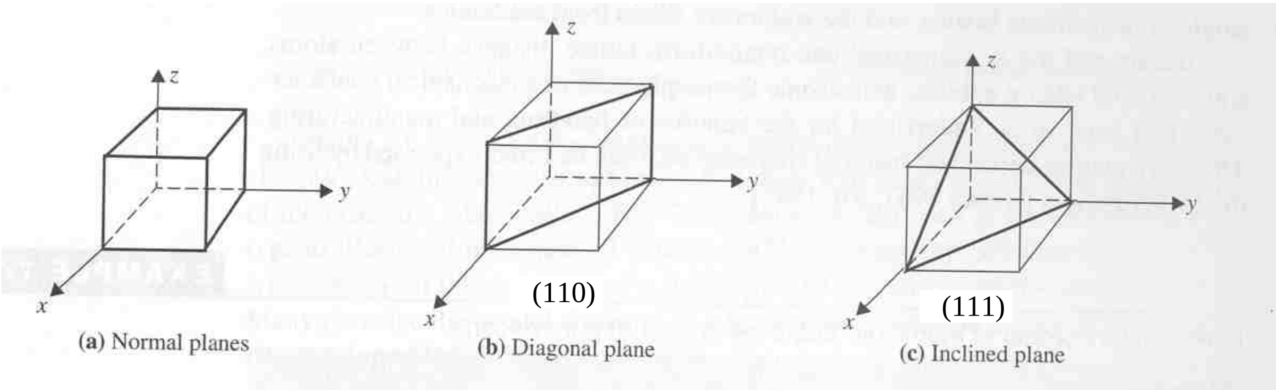

Fig 3.7 Designation of the planes of a cubic crystal

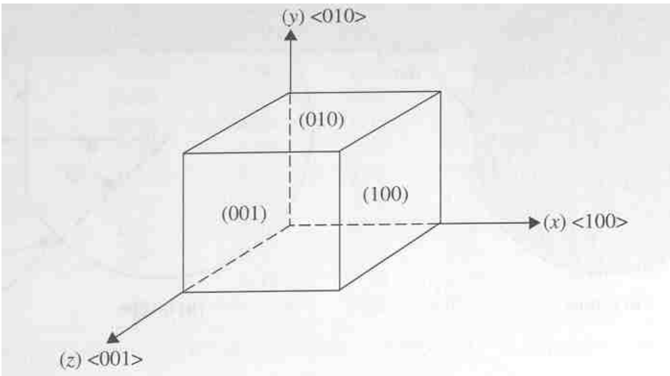

Fig 3.8 Silicon Crystal Structure and planes and Orientation

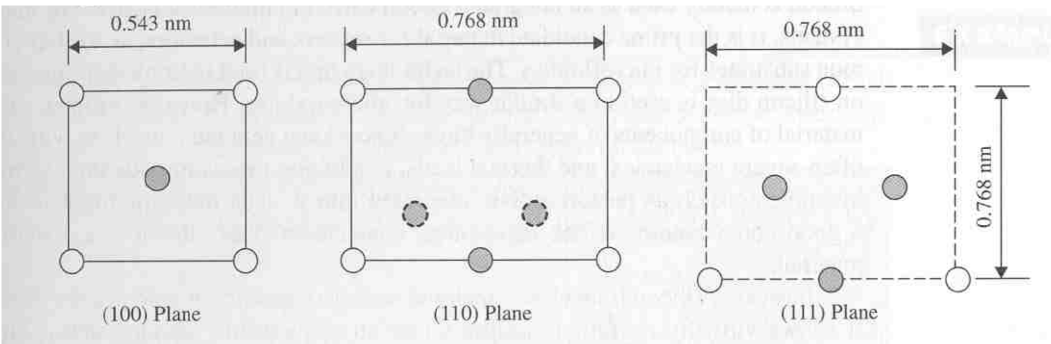

Fig 3.9 Silicon atoms on three designated planes

In Fig. 3.9,

- The lattice distances between adjacent atoms are shortest on (111) plane.
- These shortest lattice distance makes the attractive forces between atoms stronger on (111) than those on the (100) and (110) planes.
- On the (111) plane, the growth of crystal is the slowest, and the fabrication processes will proceed slowest.

- Primary flats and secondary flats are used to indicate the crystal orientation and dopant type of the wafers.

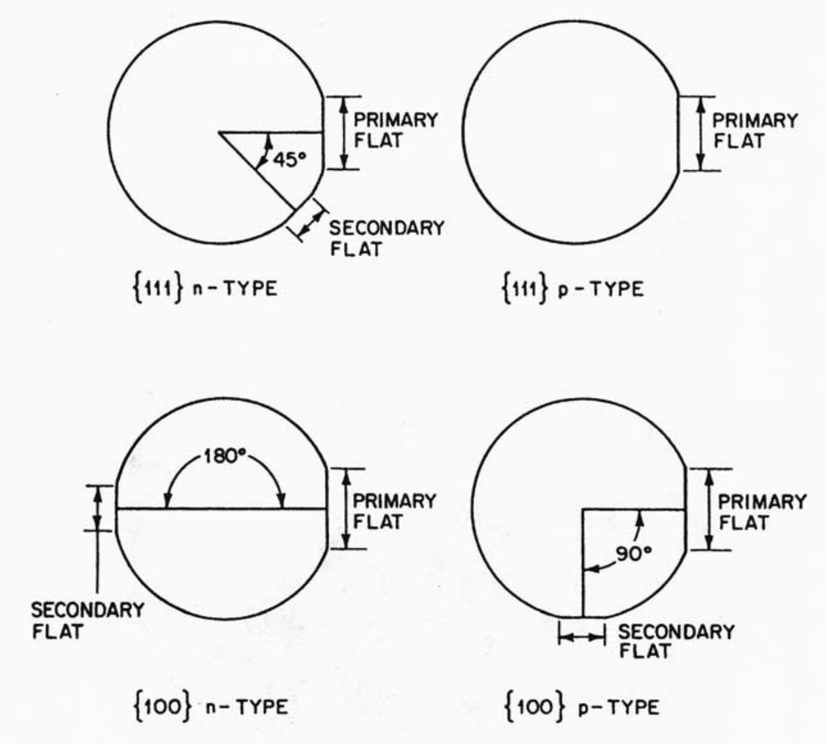

Fig.3.10 Primary and secondary flats on silicon wafers.

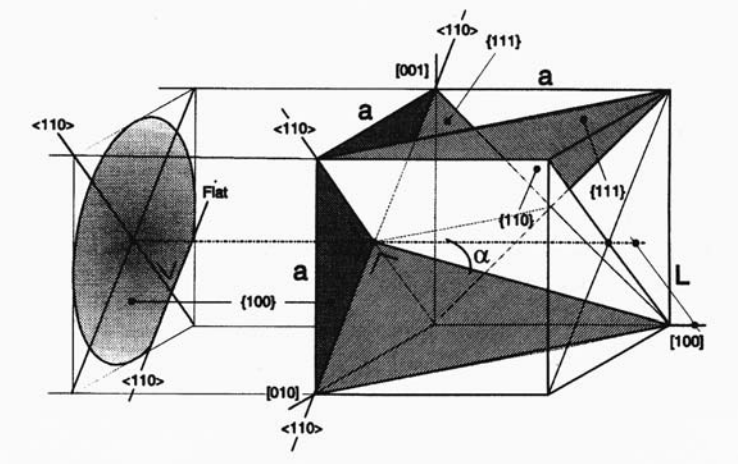

Fig. 3.11 (100) silicon wafer with reference to the unity cube and its relevant planes. (From E. Peeters, "Process Development for 3D Silicon Microstructures, with Application to Mechanical Sensor Design," KUL, Belgium, 1994.[42] Reprinted with permission.)

3.4.5 Mechanical Properties of Silicon

- Silicon, as the material of 3-D structures, needs to withstand often-severe mechanical and thermal loads, in addition to accommodating electrical instruments.

- Silicon is an ideal sensing and actuating material because
  3.4.5.1 It is an elastic material with no plasticity or creep below 800℃.
  3.4.5.2 Show virtually no fatigue failure.

- Disadvantages:
  1. brittle
  2. weak resistance to impact loads
  3. Anisotropic which makes stress analysis of the structures tedious.

- Young's moduli and shear moduli in three directions:

Table 3.2 The diverse Young's moduli of elasticity of silicon crystals

Miller index for orientation	Young's modulus E, GPa	Shear modulus G, GPa
<100>	129.5	79.0
<110>	168.0	61.7
<111>	186.5	57.5

Material	σ_y, 10^9 N/m²	E, 10^{11} N/m²	ρ, g/cm³	c, J/g-°C	k, W/cm-°C	α, 10^{-6}/°C	T_M, °C
Si	7.00	1.90	2.30	0.70	1.57	2.33	1400
SiC	21.00	7.00	3.20	0.67	3.50	3.30	2300
Si_3N_4	14.00	3.85	3.10	0.69	0.19	0.80	1930
SiO_2	8.40	0.73	2.27	1.00	0.014	0.50	1700
Aluminum	0.17	0.70	2.70	0.942	2.36	25	660
Stainless steel	2.10	2.00	7.90	0.47	0.329	17.30	1500
Copper	0.07	0.11	8.9	0.386	3.93	16.56	1080
GaAs	2.70	0.75	5.30	0.35	0.50	6.86	1238
Ge		1.03	5.32	0.31	0.60	5.80	937
Quartz	0.5-0.7	0.76-0.97	2.66	0.82-1.20	0.067.0.12	7.10	1710

*Principal source for semiconductor material properties: *Fundamentals of Microfabrication*, Marc Madou, CRC Press, 1997

Legend: σ_y = yield strength, E = Young's modulus, ρ = mass density, c = specific heat, k = thermal conductivity, α = coefficient of thermal expansion, T_M = melting point.

Table 3.3 Mechanical and thermo physical properties of MEMS materials

- Bulk material properties of silicon, silicon compounds, and other active substrate materials:

3.5 Silicon Compounds

- 3 often-used silicon compounds:

  3.5.1 Silicon dioxide (SiO_2)

  3.5.2 Silicon Carbide (SiC)

  3.5.3 Silicon Nitride (Si_3N_4)

3.5.1 Silicon Dioxide (SiO_2)

- Three principal uses of SiO_2:
  1. as a thermal and electric insulator (see Table 3.5);
  2. as a mask in the etching of silicon substrates;

     (∵ SiO_2 has much stronger resistance to most etchants than silicon)
  3. as a sacrificial layer in the surface micromachining.

- Properties:

Table 3.5 Properties of silicon di oxide

Properties	Values
Density, g/cm^3	2.27
Resistivity, Ω-cm	$\geq 10^{16}$
Relative permittivity	3.9
Melting point, °C	~1700
Specific heat, J/g-°C	1.0
Thermal conductivity, W/cm-°C	0.014
Coefficient of thermal expansion, ppm/°C	0.5

Source: Ruska [1987].

- Oxidation: by heating silicon in an oxidant (e.g., O_2) with or without steam.

  (a) Dry oxidation:

  $$Si + O_2 \rightarrow SiO_2$$

  (b) Wet oxidation in steam:

  $$Si + 2H_2O \rightarrow SiO_2 + 2H_2$$

- Oxidation is effectively a diffusion process Diffusivity of SiO_2 at 900°C in dry oxidation:

  (a) 4×10^{-19} cm^2/s for arsenic(As)-doped silicon (n-type);

  (b) 3×10^{-19} cm^2/s for boron(B)-doped silicon (p-

type); Note: Steam would accelerate the oxidation process.

3.5.2 Silicon Carbide (SC)

- Properties and usages:
  4. dimensional and chemical stability at high temperature
     (a) strong resistance to oxidation at very high temperature
     (b) deposited over MEMS components to protect them from extreme temperature
  5. The thin SiC film can be patterned by dry etching with aluminum masks, and can be further used as passivation layer (protective layer) in micromachining for the underlying silicon layer.

     (∵ SiC can resist common etchants such as KOH and HF.)

- SiC: a by-product in producing single crystal silicon boule
  - ➢ Intense heating of the carbon raw materials (coal, coke, wood chips, etc.) would results in SiC sinking to the bottom of the crucible).

- The SiC film: produced by various deposition techniques.

3.5.3 Silicon Nitride (Si_3N_4)

- Superior properties attractive for MEMS:
  - ➢ An excellent barrier to diffusion of water and ions (e.g., sodium)
  - ➢ Ultra strong resistance to oxidation and many etchants
    → Suitable for masks for deep etching.

- Applications:
  - Optical waveguides
  - Encapsulants to prevent diffusion of water and other toxic fluid into the substrate.
  - High-strength electric insulators and ion implantation masks.

- Production Processes:
  - ➢ Produced from silicon containing gases and NH_3:

    $$3SiCl_2H_2 + 4NH_3 \rightarrow Si_3N_4 + 6HCl + 6H_2$$

  - ➢ Can be produced by both LPCVD (low pressure chemical vapor deposition) and PECVD (plasma-enhanced chemical vapor deposition) processes. Note: plasma
  - ➢ Properties: listed in Tables 3.6

Table 3.6 Selected properties of silicon nitride

Properties	LPCVD	PECVD
Deposition temperature, °C	700–800	250–350
Density, g/cm³	2.9–3.2	2.4–2.8
Film quality	Excellent	Poor
Relative permittivity	6–7	6–9
Resistivity, Ω-cm	10^{16}	10^{6}–10^{15}
Refractive index	2.01	1.8–2.5
Atom % H	4–8	20–25
Etch rate in concentrated HF	200 Å/min	
Etch rate in boiling HF	5–10 Å/min	
Poisson's ratio	0.27	
Young's modulus, GPa	385	
Coefficient of thermal expansion, ppm/°C	1.6	

Source: Madou [1997].

3.5.2 Polycrystalline Silicon

- Polysilicon is a principal material in surface micromachining (fig 3.12).

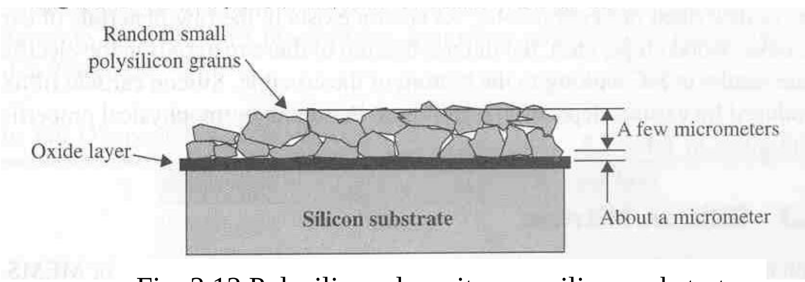

Fig. 3.12 Polysilicon deposits on a silicon substrate

- Production process:
  - LPCVD is frequently used for depositing polycrystalline silicon onto silicon. → Temperature: 600 to 650°C

- Applications and properties:
  - In IC industry: resistors, gates for transistors, thin-film transistors, etc.
  - Highly doped polysilicon can reduce the resistivity of polysilicon to produce conductors and control switches.

    → Ideal material for micro resistors as well as easy ohmic contacts.
  - Poly silicon can be treated as isotropic material in structural and thermal analyses (due to its crystals in random sizes and orientations).
  - Table 3.7: list some key properties of poly silicon and other materials.

Table 3.7 Comparison of Mechanical properties of polysilicon and other materials

Materials	Young's modulus, GPa	Poisson's ratio	Coefficient of thermal expansion, ppm/°C
As substrates:			
Silicon	190	0.23	2.6
Alumina	415		8.7
Silica	73	0.17	0.4
As thin films:			
Polysilicon	160	0.23	2.8
Thermal SiO_2	70	0.2	0.35
LPCVD SiO_2	270	0.27	1.6
PECVD SiO_2			2.3
Aluminum	70	0.35	25
Tungsten	410	0.28	4.3
Polymide	3.2	0.42	20–70

Source: Madou [1997].

3.6 Silicon Piezoresistors

- Definition of piezoresistance :
  - A change in electric resistance of solids when subjected to stress fields.

- Both p- ad n-type silicon exhibit excellent piezoresistive effect.

- Due to anisotropic in p- and n-type silicon, the relationship between the resistance change and the stress field is more complex:

$$\{\Delta R\} = [\pi]\{\sigma\}$$

where $\{\Delta R\} = \{\Delta R_{xx} \quad \Delta R_{yy} \quad \Delta R_{zz} \quad \Delta R_{xy}$ infinitesimally small cubic piezoresistiv components $\{\sigma\} = \{\sigma_{xx} \quad \sigma_{yy} \quad \sigma_{zz} \quad \sigma_{xy}$ coefficient matrix, which has the form:

$$[\pi] = \begin{bmatrix} \pi_{11} & \pi_{12} & \pi_{12} & 0 & 0 & 0 \\ \pi_{12} & \pi_{11} & \pi_{12} & 0 & 0 & 0 \\ \pi_{12} & \pi_{12} & \pi_{11} & 0 & 0 & 0 \\ 0 & 0 & 0 & \pi_{44} & 0 & 0 \\ 0 & 0 & 0 & 0 & \pi_{44} & 0 \\ 0 & 0 & 0 & 0 & 0 & \pi_{44} \end{bmatrix}$$

➢ That is,

$$\begin{aligned} \Delta R_{xx} &= \pi_{11}\sigma_{xx} + \pi_{12}(\sigma_{yy} + \sigma_{zz}) \\ \Delta R_{yy} &= \pi_{11}\sigma_{yy} + \pi_{12}(\sigma_{xx} + \sigma_{zz}) \\ \Delta R_{zz} &= \pi_{11}\sigma_{zz} + \pi_{12}(\sigma_{xx} + \sigma_{yy}) \\ \Delta R_{xy} &= \pi_{44}\sigma_{xy} \\ \Delta R_{xz} &= \pi_{44}\sigma_{xz} \\ \Delta R_{yz} &= \pi_{44}\sigma_{yz} \end{aligned}$$

➢ π_{11} and π_{12} are associated with the normal stress components, whereas π_{44} is related to the shearing stress components.

➢ In Fig 3.14, The change of electric resistance can be expressed as

$$\frac{\Delta R}{R} = \pi_L \sigma_L + \pi_T \sigma_T$$

where π_L and π_T denote the piezoresistive coefficients along the Longitudinal and tangential directions, respectively.

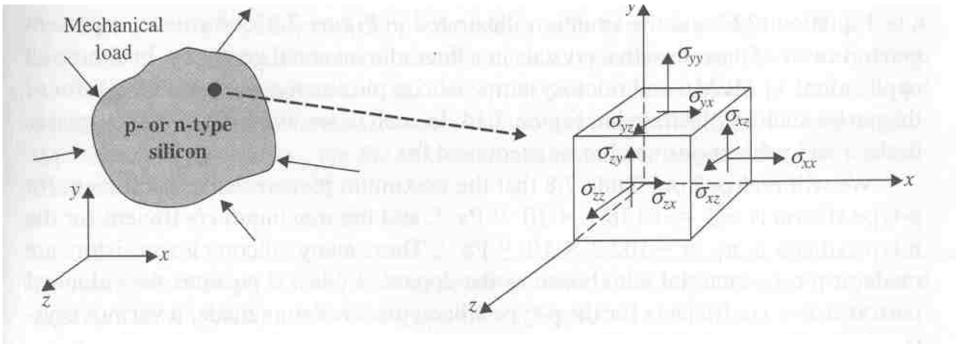

Fig 3.13 A Silicon Piezo resistance subjected to a stress field

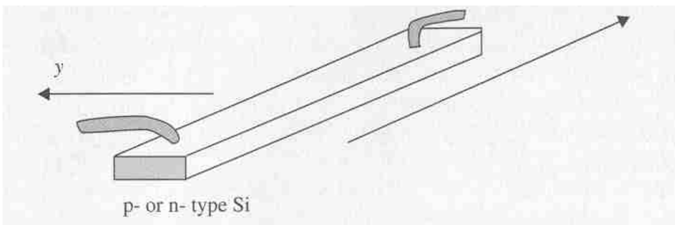

Fig 3.14 Silicon Strain Gauge

Table 3.8 Resistivity and Piezo resistive coefficients of silicon at room temperature in <100> orientation

Materials	Resistivity, Ω-cm	π_{11}*	π_{12}*	π_{44}*
p silicon	7.8	+6.6	−1.1	+138.1
n silicon	11.7	−102.2	+53.4	−13.6

*in 10^{-12} cm^2/dyne or in 10^{-11} m^2/N (or Pa^{-1})

Source: French and Evans [1988].

3.7 Gallium Arsenide (GaAs)

- GaAs
  - A compound semiconductor
  - Advantages
    - ➢ A prime candidate material for photonic device due to its highmobility of electrons (7 times higher than silicon, see Table 3.9)

      → easier for electric current to flow in the material
    - ➢ Superior thermal insulator with excellent dimensional stability at high temperature

Table 3.9 Electron mobility of selected materials at 300K

Materials	Electron mobility, $m^2/V\text{-}s$
Aluminum	0.00435
Copper	0.00136
Silicon	0.145
Gallium arsenide	0.850
Silicon oxide	~0
Silicon nitride	~0

Source: Kwok [1997].

  - Disadvantages
    - ➢ More difficult to process than silicon
    - ➢ Low yield strength (one-third of that of silicon)
    - ➢ More expensive than silicon due to its low use
  - Comparison of GaAs and silicon (Table 3.10)

Table 3.10 Comparision of GaAs and Silicon in micromachining

Properties	GaAs	Silicon
Optoelectronics	Very good	Not good
Piezoelectric effect	Yes	No
Piezoelectric coefficient, pN/°C	2.6	Nil
Thermal conductivity	Relatively low	Relatively high
Cost	High	Low
Bonding to other substrates	Difficult	Relatively easy
Fracture	Brittle, fragile	Brittle, strong
Operating temperature	High	Low
Optimum operating temp., °C	460	300
Physical stability	Fair	Very good
Hardness, GPa	7	10
Fracture strength, GPa	2.7	6

Source: Madou [1997].

3.8 Quartz

- Quartz
  - A compound of SiO_2
  - Unit cell in the shape of tetrahedron
  - Orientation: (Senturia, 2001)
    - ➢ Not based on miller indices
    - ➢ Some basic orientations, such as *X*-cut and *Z*-cut quartz, refer to the crystalline axes normal to the plane of the wafer.
    - ➢ However, some others, such as *AT*-cut quartz, refer to off-axis orientations that are selected for specific temperature insensitivities of their piezoelectric or mechanical properties.
  - An ideal material for sensor because of its near absolute thermal dimensional Stability
  - A desirable material in microfluidics applications in biomedical analyses
    - ➢ Inexpensive
    - ➢ Work well in electrophoretic fluid transportation due to its excellent electric insulation properties
    - ➢ Transparent to ultraviolet light which is good for the purpose of species detection
  - Hard to machine
    - ➢ Could use “diamond cutting” or “ultrasonic cutting”
    - ➢ Can be etched chemically by HF/NH_4F into the desired shape
  - More dimensionally stable than silicon
  - More flexibility in geometry than silicon

Table 3.11 some properties of quartz

Properties	Value $\parallel Z$	Value $\perp Z$	Temperature dependency
Thermal conductivity, cal/cm-s°/C	29×10^{-3}	16×10^{-3}	↓ with T
Relative permittivity	4.6	4.5	↓ with T
Density, kg/m^3	2.66×10^3	2.66×10^3	
Coefficient of thermal expansion, ppm/°C	7.1	13.2	↑ with T
Electrical resistivity, Ω/cm	0.1×10^{15}	20×10^{15}	↓ with T
Fracture strength, GPa	1.7	1.7	↓ with T
Hardness, GPa	12	12	

Source: Madou [1997].

3.9 Piezoelectric Crystals

- Piezoelectric crystals
  - Piezoelectric effect:
    - Produce a voltage when subjected to an applied force
    - The application of voltage to the crystal can change its shape.

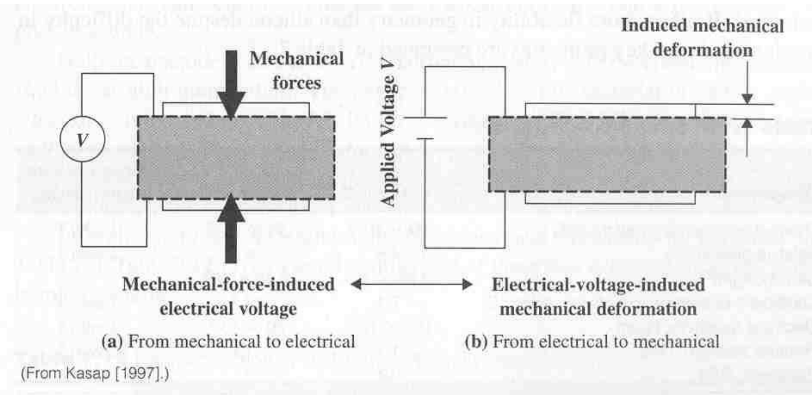

Fig 3.15 Conversion of Mechanical and electrical energies by piezoelectric crystals

- Natural crystals: quartz, tourmaline, and sodium potassium tartrate
- Synthesized crystals: Rochelle salt, barium titanate, and lead zirconate titanate (PZT)
- Its structure should have no center of symmetry
  - ➢ The applied stress will alter the separation between the positive and negative charge sites in an elementary cell, leading to a net polarization at the crystal surface.

    → result in an electric field with voltage potential
- Applications
  - ➢ High voltage generation via the application of high compressive stress

    → Can be used as an impact detonation device.

    → can be used to send signals for depth detection in a sonar System
  - ➢ In MEMS: used as actuators and dynamic signal transducers for pressure sensors and accelerometers.
  - ➢ Used in pumping mechanisms for microfluidic flows as well as for inkjet printer heads.

- Effectiveness of the conversion of mechanical to electrical energy and vice versa can be assessed by the electromechanical conversion factor K:

$$K^2 = \frac{\text{output of mechanical energy}}{\text{input of electrical energy}}$$

or

$$K^2 = \frac{\text{output of electrical energy}}{\text{input of mechanical energy}}$$

- The electric field produced by stress

$$V = f\sigma$$

  where V: generated electric field in V/m; f: constant coefficient; σ: applied stress in pascals (Pa)

- The mechanical strain produced by the electric field

$$\varepsilon = dV$$

  where : induced strain; V: applied electric field in V/m; d: piezoelectric coefficient (see Table 7.14)

- Relation between f and d:

$$\frac{1}{fd} = E$$

where E: the Young's modulus

Fig 3.12 Piezo electric coefficients of selected materials

Piezoelectric crystals	Coefficient d, 10^{-12} m/V	Electromechanical conversion factor K
Quartz (crystal SiO_2)	2.3	0.1
Barium titanate ($BaTiO_3$)	100–190	0.49
Lead zirconate titanate, PZT ($PbTi_{1-x}Zr_xO_3$)	480	0.72
$PbZrTiO_6$	250	
$PbNb_2O_6$	80	
Rochelle salt ($NaKC_4H_4O_6$-$4H_2O$)	350	0.78
Polyvinylidene fluoride, PVDF	18	

Source: Kasap [1997], Askeland [1994].

3.10 Polymers

- Polymers
  - Include diverse materials such as plastics, adhesives, Plexiglas, and Lucite
  - Become increasingly popular materials for MEMS and Microsystems
  - Examples in MEMS and microsystems:
    - Plastic cards approximately 150 mm wide containing 1000 micro channels for microfluidic electrophoretic systems by the biomedical industry (Lipman, 1999)
    - Epoxy resins and adhesives such as silicone rubber used in packing Made up of long chains of organic, mainly hydrocarbon)

    molecules
  - Characteristics:
    - Low mechanical strength
    - Low melting point
    - Poor electric conductivity
  - Thermoplastics and thermosets: 2 groups of common polymers
    - Thermoplastics: easily formed to the desired shape
    - Thermosets: have better mechanical strength and temperature resistance up to 350°C

3.10.1 Polymer as Industrial Materials

- Applications:
  - Used as insulators, sheathing, capacitor films in electric

devices, and die pads in integrated circuits.

- Advantages
  - Light weight
  - Ease in processing
  - Low cost of raw materials and processes for producing polymers
  - High corrosion resistance
  - High electrical resistance
  - High flexibility in structures
  - High dimensional stability
  - Great variety

3.10.2 Polymers for MEMS and Microsystems

- Applications:

1. Photoresist polymers: used as masks for creating desired patterns on substrates by photolithography
2. Photoresist polymers: used to produce the prime mold in the LIGA process.
3. Conductive polymers: used as organic substrates.
4. Ferroelectric polymers (which behave like piezoelectric crystals): used as a source of actuation in micro devices such as those for micro pumping
5. Thin Langmuir-Blodgett (LB) film: used for multilayer microstructures
6. Used as a coating substances for capillary tubes to facilitate electro-osmotic flow in microfluidics
7. Thin polymer films: used as electric insulators in micro devices and as a dielectric substances in micro capacitors.
8. Used for electromagnetic interference (EMI) and radio-frequency interference (RFI,) shielding in Microsystems.
9. Used for the encapsulation of micro sensors and packaging of other Microsystems.

3.10.3 Conductive Polymers

- For some application, polymers have to be made electrically conductive.
  - By nature, polymers: poor electric conductors (Table 3.13).
  - Polymers can be made electrically conductive by the following 3 methods:

1. Pyrolysis:
   - A pyro polymer based on phthalonitrile resin: by adding an amine heated above 600℃

Table 3.13 Electric conductivity of selected materials

Materials	Electric conductivity, S/m*
Conductors:	
Copper	10^6–10^8
Carbon	10^4
Semiconductors:	
Germanium	10^0
Silicon	10^{-4}–10^{-2}
Insulators:	
Glass	10^{-10}–10^{-8}
Nylon	10^{-14}–10^{-12}
SiO_2	10^{-16}–10^{-14}
Polyethylene	10^{-16}–10^{-14}

*S/m = siemens per meter. Siemens = Ω^{-1} = A^2-s^3/kg-m^2

2. Doping

Examples:

- For polyacetylenes (PA): Dopants such as Br_2, I_2, AsF_5, $HClO_4$, and H_2SO_4 to produce p-type polymers, and sodium naphthalide in tetrahydrofuran (THF, [1071] for the n-type polymer.
- For PPP and PPS: see page 265

A. Insertion of Conductive Fibers Incorporate conductive fillers (e.g., carbon, aluminum flakes, stainless steel, gold, and silver fibers) into both thermosetting and thermoplastic polymer structures.

B. Other inserts include semiconducting fibers (nanometers in length), e.g., silicon and germanium.

3.10.4 The Langmuir-Blodgett (LB) Film

- LB film
  - made by a special process (LB process) to produce thin polymer films
  - involves spreading volatile solvent over surface-active materials
  - The LB process can produce more than a single monolayer structure (i.e., create a multi-layer structure).

  → regarded as an alternative micro manufacturing technique.

- Applications:

1. Ferroelectric polymer thin films
   - Such as polyvinylidene fluoride (PVDF)
   - Applications: (a) sound transducers in air and water, (b) tactile

Sensors, (c) biomedical applications (such as I. Tissue-compatible implants, II. Cardiopulmonary sensors, and III. Implantable transducers and sensors for prosthetics and rehabilitation devices)

- See Table 7.14 for the piezoelectric coefficient of PVDF.

2. Coating materials with controllable optical properties

- widely used in broadband optical fibers

3. Micro sensors

Principle of Fig. 7.20:

- The electric conductivity of the polymer sensing element will change when it is exposed to a specific gas.

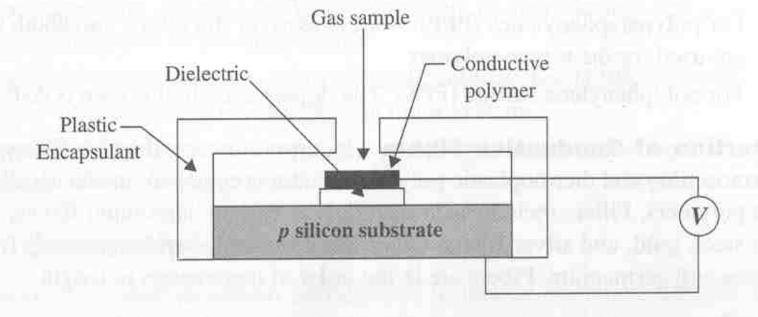

Fig 3.16 Micro sensor using polymer

3.11 Packaging Mate

- Distinction between the IC packaging and the microsystems packaging:
  - For IC: to protect from the hostile operating environment.
  - For microsystems: in addition to protection, it is required to be in contact with the media that are sources of action.

- Materials for microsystem packaging:
  - Include those for IC packaging:

    (a) wires made of noble metals at silicon die level,

    (b) metal layers for lead wires,

    (c) Solders or die/constraint base attachments, etc.
  - Also include metal and plastics.

- Consider the microsystem packaging in Fig. 3.17:

  (a) Use aluminum or gold metal films as ohmic contacts to the Piezo resistors that are diffused in the silicon diaphragm.

(b) Similar materials: used for the lead wires to the inter connects outside the casing.

(c) Casing: made of plastic or stainless steel

(d) Constrain base: made of glass (e.g., Pyrex) or ceramics (e.g., alumina)

(e) Adhesives that attach the silicon die to the constraint base: can be

   i) tin-lead solder alloys (thin metal layers needs to be sputtered at the joints to facilitate the soldering P;

   ii) epoxy resins

   iii) or Room-temperature vulcanizing (RTV) silicone rubber.

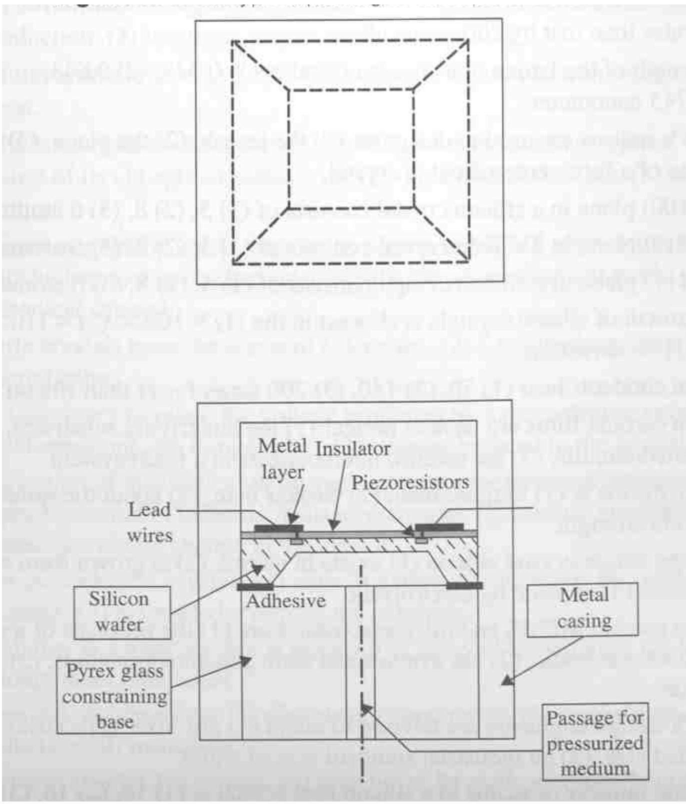

Fig 3.17 A typical packaged micro pressure sensor

SATHYABAMA
INSTITUTE OF SCIENCE AND TECHNOLOGY
(DEEMED TO BE UNIVERSITY)
Accredited "A" Grade by NAAC | 12B Status by UGC | Approved by AICTE
www.sathyabama.ac.in

SCHOOL OF MECHANICAL ENGINEERING
DEPARTMENT OF MECHATRONICS ENGINEERING

UNIT II

FABRICATION OF MEMS –SMR 1301

Silicon wafer manufacturing

1 Introduction

The first step in integrated circuit (IC) fabrication is preparing the high purity single crystal Si wafer. This is the starting input to the fab. Typically, *Si wafer* refers to a single crystal of Si with a *specific orientation*, *dopant type, and resistivity* (determined by dopant concentration). Typically, Si (100) or Si (111) wafers are used. The numbers (100) and (111) refers to the orientation of the plane parallel to the surface. The wafer should have structural defects, like dislocations, below a certain permissible level and impurity (undesired) concentration of the order of *ppb* (parts per billion). Consider the *specs* (specifications) of a 300 mm wafer shown in table 1 below. The thickness of the wafer is less than 1 *mm*, while its diameter is 300 *mm*. Also, the wafers must have the 100 plane parallel to the surface, to within◦2 deviation, and typical impurity levels should be of the order of *ppm* or less with metallic impurities of the order of *ppb*. For doped wafers, there shouldbe specific amounts of the desired dopants (*p* or *n* type) to get the required resistivity.

Table 1: Specs of a typical 300 mm wafer used in fabrication. The specifications include the dimensions, orientation, resistivity, and oxygen and carbon impurity content.

Specs	**Value**
Diameter	300 ± 0.02 mm
Thickness	$775 \pm 25\ \mu m$
Orientation	$100 \pm 2^{\circ}$
Resistivity	$> 1\ \Omega - m$
Oxygen concentration	20-30 *ppm*
Carbon concentration	< 0.2 *ppm*

Table 2: Impurities in MGS, after the submerged arc electrode process.

Element	**Concentration (*ppm*)**
Al	1000-4350
B	40-60
Ca	245-500
Fe	1550-6500
P	20-50
Cu	15-45

2 Poly Si manufacture

The starting material for Si wafer manufacture is called *Electronic grade Si* (EGS). This is an ingot of Si that can be shaped and cut into the final wafers. EGS should have impurity levels of the order of *ppb*, with the desired doping levels, so that it matches the chemical composition of the final Si wafers. The doping levels are usually back calculated from resistivity measurements. To get EGS, the starting material is called *Metallurgical grade Si* (MGS). The first step is the synthesis of MGS from the ore.
The starting material for Si manufacture is *quartzite* (SiO_2) or *sand*. The ore is reduced to Si by mixing with coke and heating in a submerged elec- trode arc furnace. The SiO_2 reacts with excess C to first form SiC. At high temperature, the SiC reduces SiO_2 to form Si. The overall reaction is given by

$$SiC\,(s) + SiO_2\,(s) \rightarrow Si\,(l) + SiO\,(g) + CO\,(g) \tag{1}$$

The *Si*(*l*) formed is removed from the bottom of the furnace. This is the MGS and is around 98% pure. The schematic of the reducing process is shown in figure 1. Typical impurities and their concentrations in MGS is tabulated in 2. MGS is used for making alloys. From table 2 it can be seen that the main

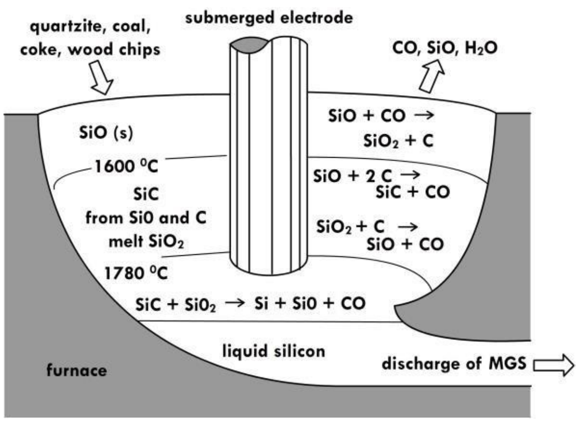

Figure 1: Schematic of the submerged arc electrode process. SiO_2 is mixed with coke and heated. It first forms SiC, which further reacts with the remaining SiO_2 forming silicon. The temperature is maintained above the melting point of silicon so that the molten semiconductor is removed from the bottom. Adapted from Synthesis and purification of bulk semiconductors - Barron and Smith metallic impurities are Al and Fe. Further purification is needed to make EGS since the impurity concentration must be reduced to *ppb* levels. One of the techniques for converting MGS to EGS is called the **Seimens process**. In this the Si is reacted with HCl gas to form tricholorosilane, which is in gaseous form.

$$Si\,(s) \; + \; 3HCl\,(g) \; \rightarrow \; SiHCl_3\,(g) \; + H_2\,(g) \qquad (2)$$

This process is carried out in a *fluidized bed reactor* at 300°C, where the trichlorosilane gas is removed and then reduced using H_2 gas.

$$2SiHCl_3\,(g) \; + \; 2H_2\,(g) \; \rightarrow \; 2Si\,(s) \; + \; 6HCl\,(g) \qquad (3)$$

The process flow is shown in figure 2. A Si rod is used to nucleate the reduced Si obtained from the silane gas, as shown in figure 3. During the conversion of silicon to trichlorosilane impurities are removed and process can be cycled to increase purity of the formed Si. The final material obtained is the EGS. This is a polycrystalline form of Si, like MGS, but has much smaller impurity levels, closer to what is desired in the final single crystal wafer. The impurities in EGS are tabulated in 3. EGS is still polycrystalline and needs to be converted into a single crystal Si ingot for producing the wafers.

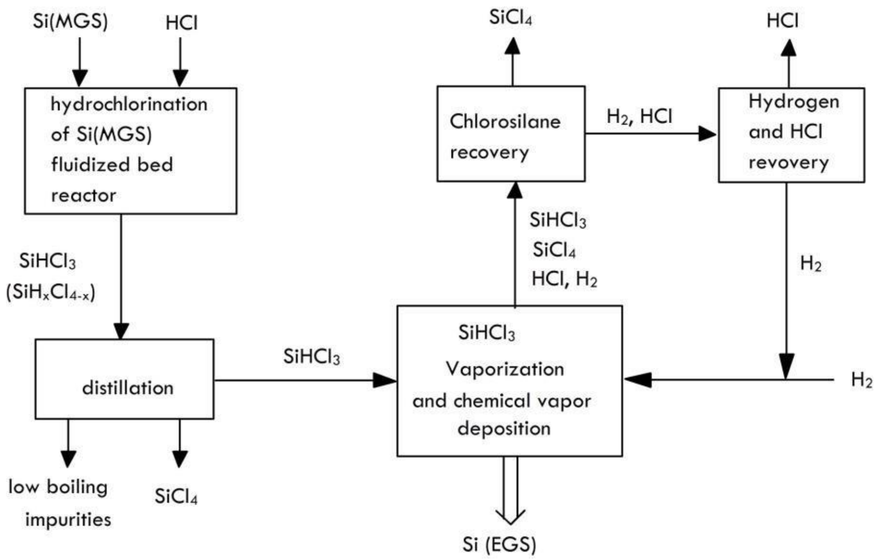

Figure 2: Schematic of the process to purify MGS to obtain EGS. The process involves conversion of silicon to trichlorosilane gas, which is purified, and then reduced to obtain silicon. Adapted from Synthesis and purification of bulk semiconductors - Barron and Smith

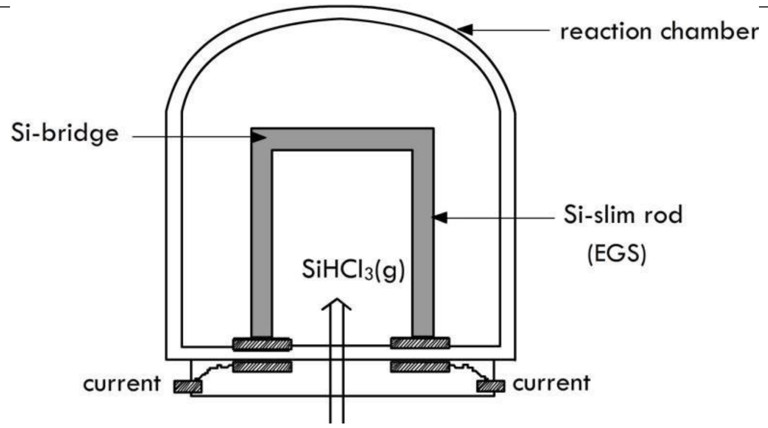

Figure 3: The Seimens deposition reactor where the purified Si is condensed. This is the electronic grade Si, same purity level as Si wafers, but polycrystalline. Adapted from Synthesis and purification of bulk semiconductors - Barron and Smith

Table 3: Impurities in EGS, after purification from MGS. Compared to table 2, the concentration levels of the metals have dropped to *ppb* levels.

Element	**Concentration (*ppb*)**
As	<0.001
Sb	<0.001
B	<0.1
C	100-1000
Cu	0.1
Fe	0.1-1
O	100-400
P	<0.3

3 Single crystal Si manufacture

There are two main techniques for converting polycrystalline EGS into a single crystal ingot, which are used to obtain the final wafers.

1. **Czochralski technique (CZ)** - this is the dominant technique for manufacturing single crystals. It is especially suited for the large wafers that are currently used in IC fabrication.

2. **Float zone technique** - this is mainly used for small sized wafers. The float zone technique is used for producing specialty wafers that have low oxygen impurity concentration.

3.1 Czochralski crystal growth technique

A schematic of this growth process is shown in figure 4. The various components of the process are

1. Furnace
2. Crystal pulling mechanism
3. Ambient control - atmosphere
4. Control system

The starting material for the CZ process is electronic grade silicon, which is melted in the furnace. To minimize contamination, the crucible is made of SiO_2 or SiN_x. The drawback is that at the high temperature the inner liner of the crucible also starts melting and has to replaced periodically. The

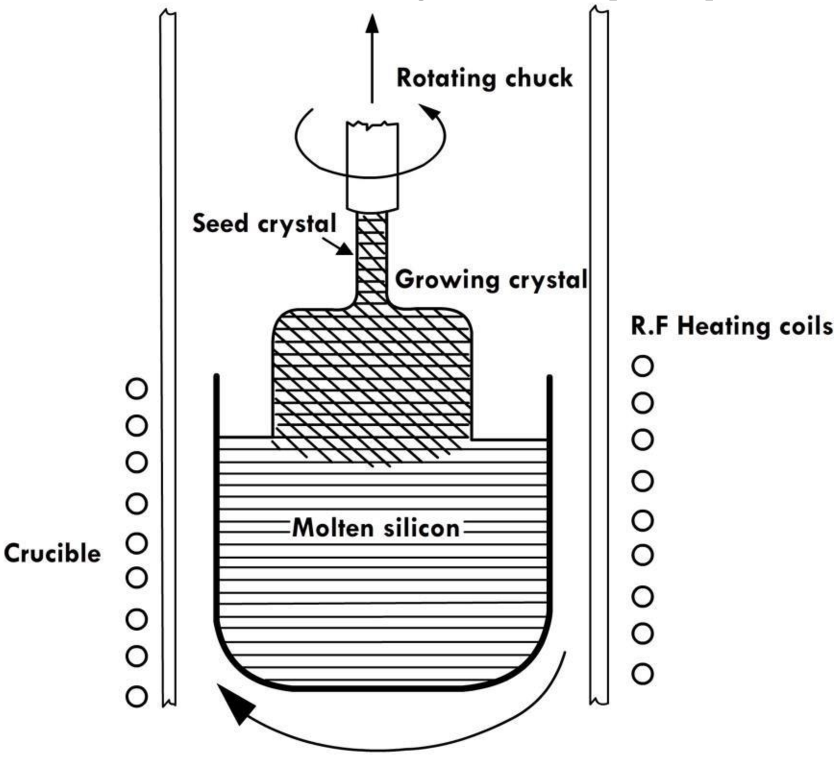

Figure 4: Schematic of the Czochralski growth technique. The polycrystalline silicon is melted and a single crystal seed is then used to nucleate a single crystal ingot. The seed crystal controls the orientation of the single crystal. Adapted from *Microchip fabrication - Peter van Zant.*

Figure 5: Single crystal Si ingot. This is further processed to get the wafers that are used for fabrication. Source *http://www.chipsetc.com/silicon-wafers.html*

furnace is heated above 1500 $^{\circ}$C, since Si melting point is 1412 $^{\circ}$C. A small seed crystal, with the *desired orientation of the final wafer*, is dipped in the molten Si and slowly withdrawn by the crystal pulling mechanism. The seed crystal is also rotated while it is being pulled, to ensure uniformity across the surface. The furnace is rotated in the direction opposite to the crystal puller. The molten Si sticks to the seed crystal and starts to solidify with the same orientation as the seed crystal is withdrawn. Thus, a single crystal ingot is obtained. To create doped crystals, the dopant material is added to the Si melt so that it can be incorporated in the growing crystal. The process control, i.e. speed of withdrawal and the speed of rotation of the crystal puller, is crucial to obtain a good quality single crystal. There is a feedback system that control this process. Similarly there is another ambient gas control system. The final solidified Si obtained is the single crystal ingot. A 450 *mm* wafer ingot can be as heavy as 800 *kg*. A picture of a such an ingot is show in figure 5.

3.2 Float zone technique

The float zone technique is suited for small wafer production, with low oxygen impurity. The schematic of the process is shown in figure 6. A polycrystalline EGS rod is fused with the single crystal seed of desired orientation. This is taken in an inert gas furnace and then melted along the length of the rod by a traveling radio frequency (RF) coil. The RF coil starts from the fused region, containing the seed, and travels up, as shown in figure 6. When the molten region solidifies, it has the same orientation as the seed. The furnace is filled with an inert gas like argon to reduce gaseous impurities.

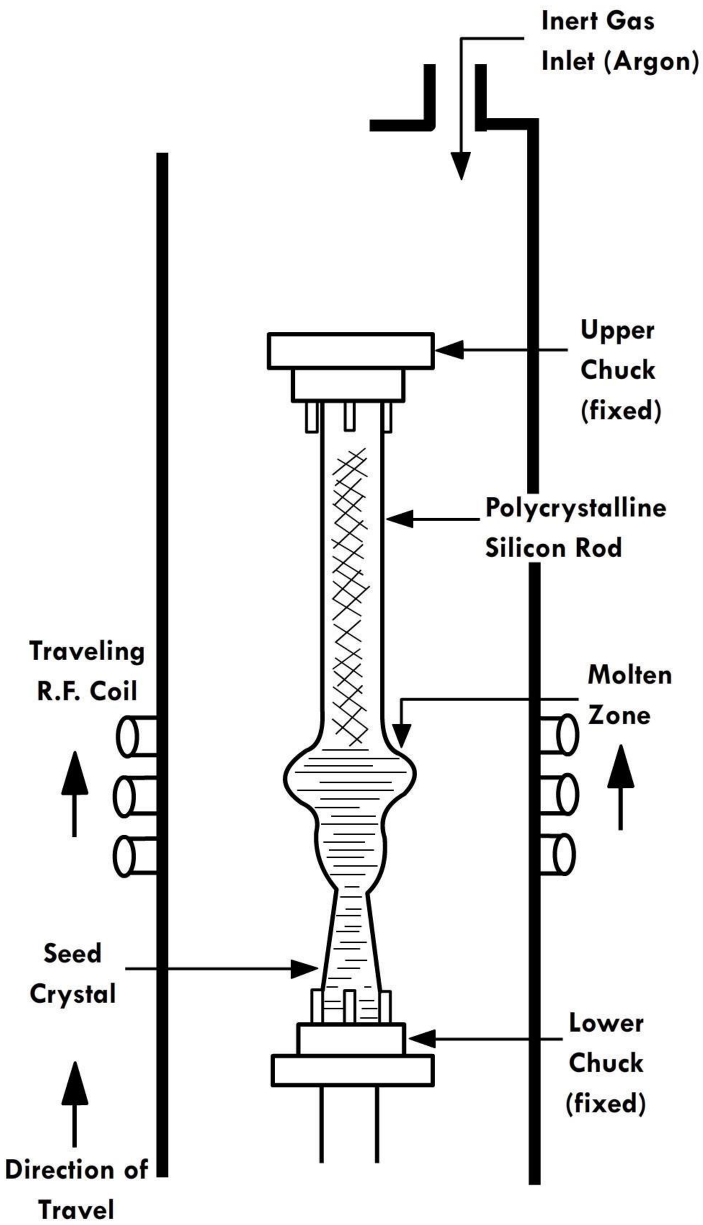

Figure 6: Schematic of the float zone technique. The polycrystalline ingot is fused with a seed crystal and locally melted by a traveling radio frequency coil. As the ingot melts and resolidifes it has the same orientation as the seed. Adapted from Microchip fabrication - Peter van Zant.

Also, since no crucible is needed it can be used to produce oxygen ’free’ Si wafers. The difficulty is to extend this technique for large wafers, since the process produces large number of dislocations. It is used for small specialty applications requiring low oxygen content wafers.

4 Wafer manufacturing

After the single crystal is obtained, this needs to be further processed to produce the wafers. For this, the wafers need to be shaped and cut. Usually, industrial grade diamond tipped saws are used for this process. The shaping operations consist of two steps

1. The seed and tang ends of the ingot are removed.
2. The surface of the ingot is ground to get an uniform diameter across the length of the ingot.

Before further processing, the ingots are checked for resistivity and orientation. Resistivity is checked by a four point probe technique and can be used to confirm the dopant concentration. This is usually done along the length of the ingot to ensure uniformity. Orientation is measured by x-ray diffraction at the ends (after grinding).
After the orientation and resistivity checks, one or more *flats* are ground along the length of the ingot. There are two types of flats.

1. **Primary flat** - this is ground relative to a specific crystal direction. This acts as a visual reference to the orientation of the wafer.
2. **Secondary flat** - this used for identification of the wafer, dopant type and orientation.

The different flat locations are shown in figure 7. *p*-type (111) Si has only one flat (primary flat) while all other wafer types have two flats (with different orientations of the secondary flats). The primary flat is typically longer than the secondary flat. Consider some typical specs of 150 *mm* wafers, shown in table 4. Bow refers to the flatness of the wafer while Δt refers to the thickness variation across the wafer.
After making the flats, the individual wafers are sliced per the required thickness. Inner diameter (ID) slicing is the most commonly used technique. The cutting edge is located on the inside of the blade, as seen in figure 8. Larger wafers are usually thicker, for mechanical integrity.
After cutting, the wafers are chemically etched to remove any damaged and

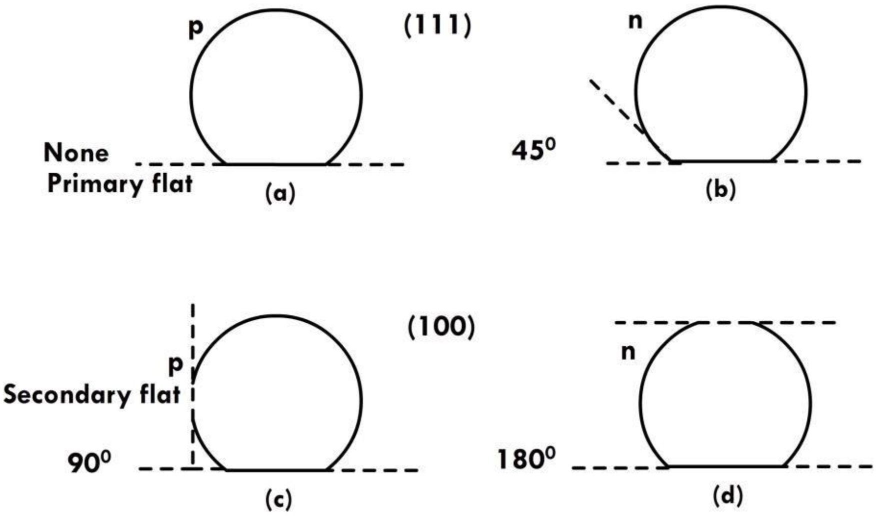

Figure 7: Flats for the different wafer types and orientations. All orientations and doping types have a primary flat, while there are different secondary flats for different types (a) p(111) (b) n(111) (c) p(100) and (d) n(100). Adapted from Microchip fabrication - Peter van Zant.

Table 4: Specs of a typical 150 mm wafer

Specs	**Value**
Diameter	150 ± 0.5 mm
Thickness	675 ± 25 μm
Orientation	100 ± 1°
Bow	60 μm
Δt	50 μm
Primary flat	55-60 mm
Secondary flat	35-40 mm

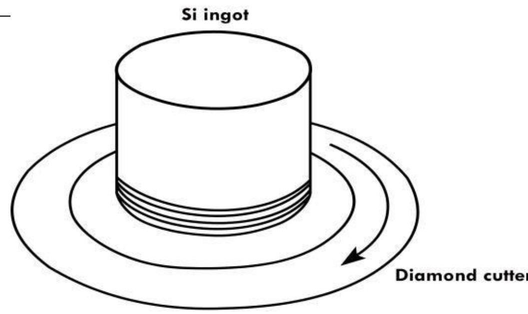

Figure 8: Inner diameter wafer slicing, used for cutting the ingots into indi- vidual wafers. The thickness is slightly higher than the final required thick- ness to account for material loss due to polishing. Adapted from Microchip fabrication - Peter van Zant.

contaminated regions. This is usually done in an acid bath with a mixture of hydrofluoric acid, nitric acid, and acetic acid. After etching, the surfaces are polished, first a rough abrasive polish, followed by a chemical mechanical pol- ishing (CMP) procedure. In CMP, a slurry of fine SiO_2 particles suspended in aqueous NaOH solution is used. The pad is usually a polyester material. Polishing happens both due to mechanical abrasion and also reaction of the silicon with the NaOH solution.

Wafers are typically single side or double side polished. Large wafers are usually double side polished so that the backside of the wafers can be used for patterning. But wafer handling for double side polished wafers shouldbe carefully controlled to avoid scratches on the backside. Typical 300 *mm* wafers used for IC manufacture are handled by robot arms and these are made of ceramics to minimize scratches. Smaller wafers (3” and 4” wafers) used in labs are usually single side polished. After polishing, the wafers are subjected to a final inspection before they are packed and shipped to the faThe fabrication of microelectromechanical systems (MEMS) uses some of the same processes and tools used to fabricate integrated circuits (IC) (e.g., deposition, photolithography, etch). However, MEMS technology has altered or enhanced some of these processes, as well as added new processes, in order to build mechanical devices such as microfluidic channels, gears, cantilevers, micro motors, comb drives and gyroscopes. Because of the techniques used in some of these new processes and methods, MEMS fabrication is also called micromachining. This unit provides an overview of three widely used MEMS micromachining methods:

- Surface Micromachining
- Bulk Micromachining
- LIGA (Lithography, Galvanoformung (electroforming), and Abformung (molding)

Each of these processes requires a clean environment to reduce particle contamination during fabrication.

5. Introduction to MEMS fabrication

Many of MEMS fabrication processes use batch fabrication techniques where more than one wafer is processed at a time, as well as tools and infrastructure similar to that used in the manufacturing of integrated circuits or computer chips. By incorporating this existing technology, MEMS fabrication (also called micromachining) has allowed for the manufacturing of micro and nano-sized devices at lower cost and increased reliability when compared to macro-sized equivalent components. This is especially true for sensors and actuators. These microdevices also tend to be quite rugged. They respond quickly while consuming little power and they occupy very small volumes.

MEMS micromachining techniques allow for the construction of three-dimensional (3D) micro-sized structures, components, and various elements on or within a substrate (usually silicon). In some cases, micromachining is the utilization of modified IC manufacturing processes in conjunction with other processes such as deep bulk etching, laser assisted chemical vapor deposition, electroplating, and molding techniques.

Three widely used MEMS fabrication methods are

- surface micromachining,
- bulk micromachining, and
- LIGA (Lithography, Galvanoformung (electroforming), and Abformung (molding).

Below are scanning electron microscope (SEM) images of products from each type of micromachining process. The far left SEM shows microchambers and channels fabricated using bulk micromachining. The middle SEM shows layers of gears made possible through surface micromachining. The left SEM is a waveguide produced by Sandia National Laboratories using LIGA.

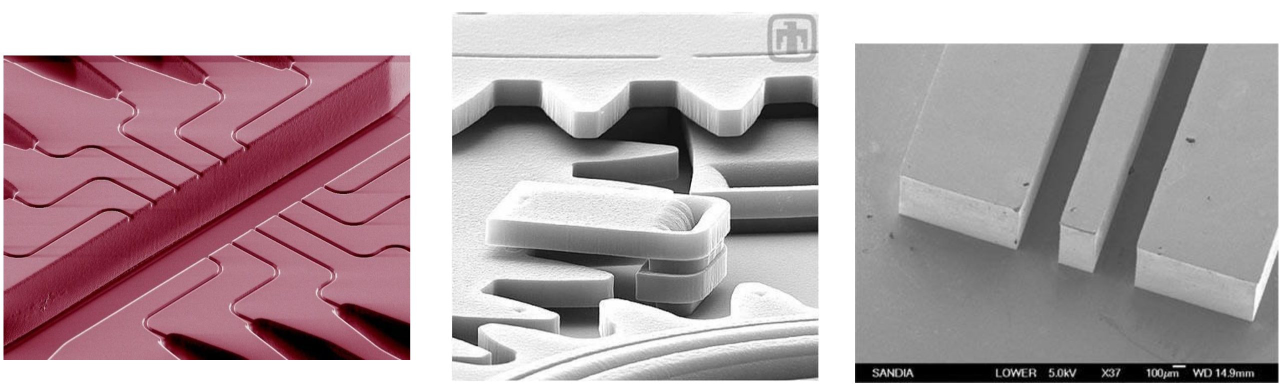

Fig. 9 [The SEMs of the gears and waveguide are courtesy of Sandia National Laboratories. The microfluidic channels are courtesy of BioPOETS Lab, Berkeley]

Surface micromachining constructs thin mechanical components and systems on the surface of a substrate by alternately depositing, patterning and etching thin films. Bulk micromachining etches into a substrate to form 3D mechanical elements such as channels, chambers and valves. When combined with wafer bonding, surface and bulk micromachining allow for the fabrication of complex mechanical devices. LIGA processes combine collimated x-ray lithography with electroplating and molding techniques to create high aspect ratio (tall and thin) structures or deep cavities needed for certain types of MEMS devices. This unit takes a closer look at each of three widely used micromachining processes: bulk, surface and LIGA.

5.1 Objectives

- Identify the distinguishing elements of bulk micromachining, surface micromachining and LIGA.
- Identify microsystems and microsystem components that are constructed using each of the three micromachining processes.

***5.2* Terminology** *Definitions for these key terms are found in the glossary at the end of this unit.*

Anisotropic etch
Aspect Ratio
Bulk etch
Bulk Micromachining
Chemical Mechanical Polishing (CMP)
Deposition
Electroforming
Electroplating
Isotropic etch
LIGA
Oxidation
Photolithography
Release etch
Sacrificial Layer
Structural Layer
Surface micromachining

5.3 Surface Micromachining

Surface micromachining is a process that uses thin film layers deposited on the surface of a substrate to construct structural components for MEMS. Unlike bulk micromachining that builds components within a substrate, surface micromachining builds on top of the substrate. The scanning electron microscope (SEM) image shows microgears that were fabricated using surface micromachining.

Fig. 10 These gears are very thin, 2 to 3 microns in thickness (or height), but can be hundreds of microns wide. Each gear tooth is smaller than the diameter of a red blood cell (8 to 10 microns). These gears rotate above the surface of the substrate. [SEM courtesy of Sandia National Laboratories]

Surface micromachining uses many of the same techniques, processes, and tools as those used to build integrated circuits (ICs) or more specifically CMOS (Complementary Metal Oxide Semiconductor) components. This process is used to fabricate micro-size components and structures by depositing, patterning, and etching a series of thin film layers on a silicon substrate. This creates an ideal situation for integrating microelectronics with micromechanics. Electronic logic circuits can be fabricated at the same time and on the same chip as the mechanical devices. The 3-axes MEMS accelerometer below shows three surface micromachined accelerometers (mechanical components) on the same chip as their electronic control circuits.

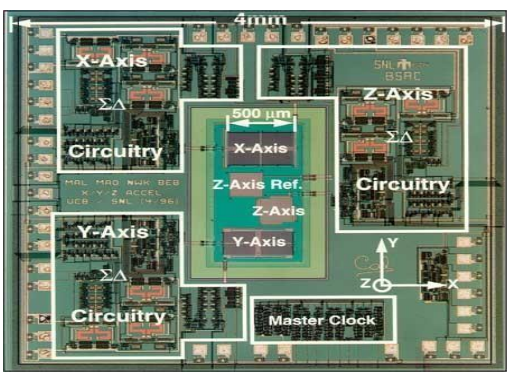

Fig. 10 Integrated 3-axes silicon micro accelerometer [Image courtesy of Sandia National Laboratories]

The main difference between CMOS fabrication and surface micromachining is that the circuits constructed for CMOS allow for the movement or flow of electrons while the structures constructed with surface micromachining (e.g., cantilevers, gears, mirrors, switches) move matter. In order to

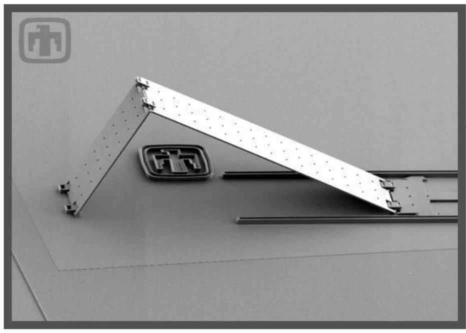

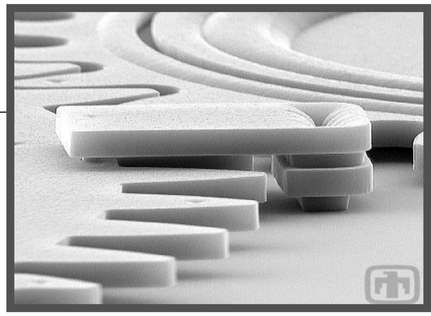

Fig.11. Pop-up Mirror (left) and geartrain with alignment pin (right) [SEM images courtesy of Sandia National Laboratories]

move matter and to create moveable structures, spaces must be incorporated between moveable components during the fabrication process. For example, optical flip mirrors *(fig.11)* cannot move nor can a gear *(fig 11)* rotate on an axis unless there is space to allow for movement.

The spaces between components are fabricated using sacrificial layers. A sacrificial layer is deposited between two structural layers to provide the needed gap. Once the device is complete and all of the structural layers are formed, the sacrificial layers are removed, *releasing* the component(s) so that it is free to move. The graphic below shows the construction of a microcantilever. A sacrificial layer is deposited on top of the substrate. A structural layer is then deposited on top of the sacrificial layer. Once the structure is defined and etched, the sacrificial layer is removed; the cantilever is *released* and is free to flex.

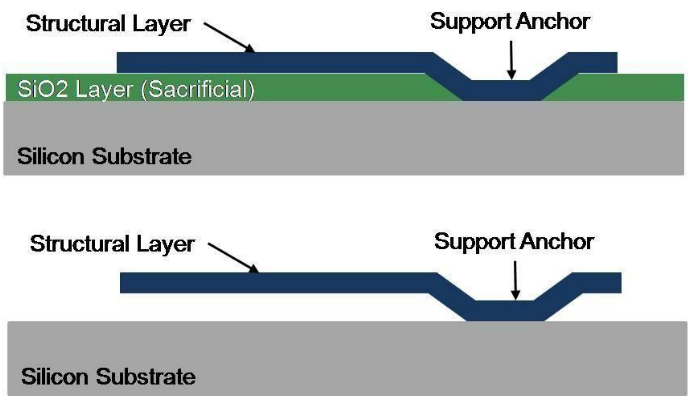

Some of the moving parts in the structural layers are so thin (2 to 3 microns) and have such a low aspect ratio (ratio of height to width) that they are sometimes referred to as “2.5 D” rather than 3 D.

Surface micromachining is based on the deposition and etching of alternating structural and sacrificial layers on top of a substrate. The most commonly used substrate is silicon; however, less expensive substrates such as glass and plastic are also used. Glass substrates are used for MEMS applications such as DNA microarrays, implantable sensors, components for flat screen displays, and solar cells. Plastic substrates are used for various microfluidics applications and bioMEMS applications as well as for the fabrication of surface micromachined beams, diaphragms and cantilevers.

What is a Sacrificial Layer?

Complicated components such as movable gear transmissions and chain drives can be constructed using surface micromachining because of its use of the sacrificial layer. Let’s take a look at how sacrificial devices are used to construct macro-size structures.The image below shows a cross-sectional view of a keystone bridge. This structure is made by first constructing a wooden scaffold. Cut stones are placed on top of the scaffold, following its outline. The final stone at the apex is called the keystone, thus the name – Keystone bridge. Once this stone is in place, the scaffolding is removed and the bridge remains in place. The scaffold is only used to provide support and shape during the construction process, and then it is sacrificed (removed). Thus the term sacrificial layer.

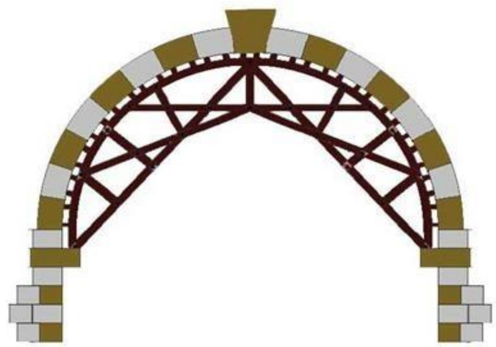

When constructing MEMS there are many possible combinations of sacrificial and structural layers. The combination used is dependent upon the device(s) being constructed. Below are two surface micromachined MEMS that require different process flows. Notice the layering required for the gears and the gear with its alignment clip *(left)* vs. the pop-up mirror (right). Obviously, the gears would require more structural/sacrificial layers than the pop-up mirror.

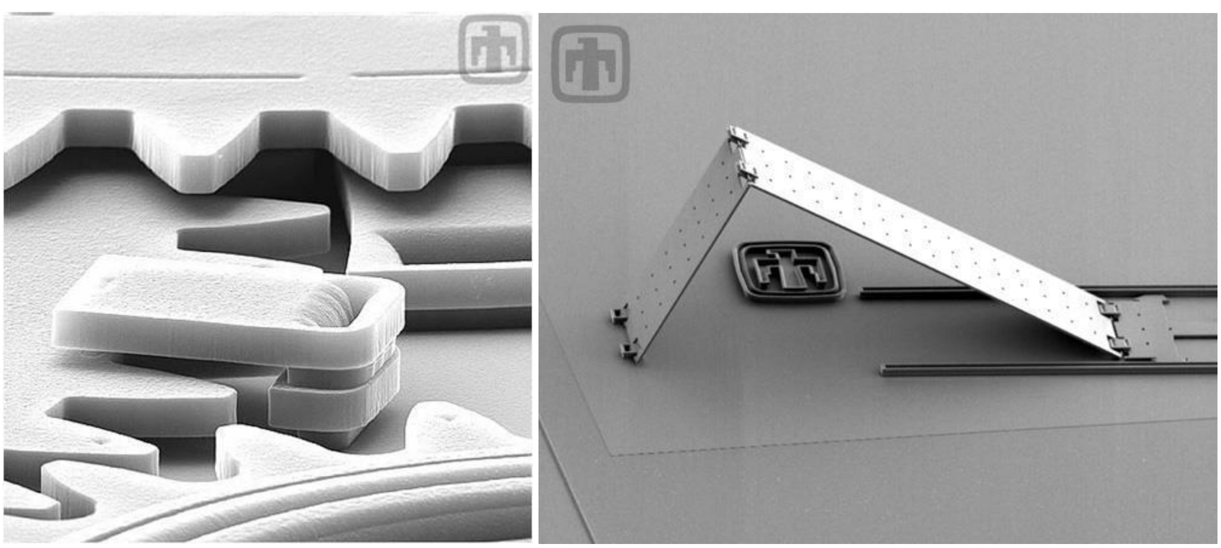

Fig.12 [SEM images courtesy of Sandia National Laboratories]

5.4 Surface Micromachining Materials

Materials used in surface micromachining are generally the same as those used in CMOS processing techniques but they serve a different function in the mechanical components.

- Silicon dioxide (SiO_2 or oxide) is the film most commonly used as a sacrificial layer and hard mask.
- Polysilicon crystalline (poly) is the most commonly used film as a structural layer.
- Silicon nitride is a thin film used for membranes (in devices such pressure sensors), as insulating material, and as a hard mask.
- Self-assembled monolayer (SAM) coatings are deposited at different steps to make the surfaces hydrophobic, and to reduce friction and wear of rubbing parts.

Surface Micromachining Layers and Processes

Silicon Dioxide (SiO_2 or oxide)

The first step of surface micromachining is to grow a thin film of silicon dioxide into the surface of the silicon wafer (substrate). This first SiO_2 layer acts as an insulator and a scaffold (space). It is thermally grown in a thermal oxidation furnace. The picture on the left is of a six (6) process chamber horizontal oxidation furnace (fig 13). The graphic on the right illustrates the components of each chamber. This is a batch process; therefore, several cassettes (boats) of wafers are processed at one time.

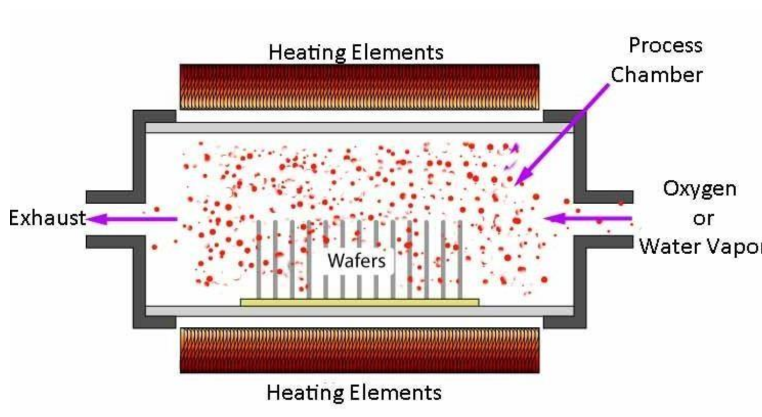

Fig.13 Diagram of an oxidation furnace's process chamber Horizontal Thermal Oxidation Furnace [Photo courtesy of University of New Mexico, Manufacturing Training and Technology Center (UNM/MTTC)]

Two oxidation methods are used in thermal oxidation: dry and wet oxidation. Dry oxidation uses oxygen gas (O_2) to form SiO_2.

Si (solid) + O_2 (gas) → SiO_2 (solid)

Wet oxidation uses steam or water vapor to form SiO_2.

Si (solid) + $2H_2O$ (vapor) → SiO_2 (solid) + $2H_2$ (gas)

In both processes, dry and wet, the process temperature affects the rate of oxidation (the rate at which the SiO_2 layer grows). The higher the temperature, the greater the oxidation rate (amount of oxide growth / time). Also, wet oxidation has a higher oxidation rate than dry oxidation at any given temperature. This effect can be seen in the oxidation of iron and the formation of rust (iron oxide). Rust grows much faster in humid climates than in dry climates (Florida vs. New Mexico); thus, the oxidation rate is higher in Florida than in New Mexico.

A variety of Chemical Vapor Deposition (CVD) fig. 14 processes are used to deposit subsequent structural and sacrificial layers. CVD is the most widely used deposition method. The films deposited during CVD are a result of the chemical reaction between the reactive gas(es) and between the reactive gases and the atoms of the substrate surface. CVD processes used in surface micromachining include the following:

- Atmospheric pressure chemical vapor deposition (APCVD) system - uses atmospheric pressure or 1 atm in the reaction chamber.
- Low pressure CVD (LPCVD) system - uses a vacuum pump to reduce the pressure inside the reaction chamber to a pressure less than 1 atm.
- Plasma-enhanced CVD (PECVD) - uses a low pressure chamber and a plasma to provide higher deposition rates at lower temperatures than a LPCVD system. *(see graphic below of a PECVD)*
- High Density, Plasma Enhanced, CVD (HDPECVD) uses a magnetic field to increase the density of the plasma within the chamber resulting in much higher deposition rates.

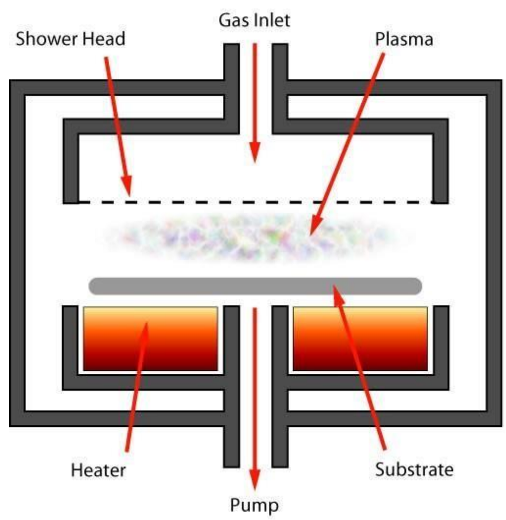

Fig .14. Plasma-enhanced CVD System

Metal layers which are used as conductive layers are deposited using Physical Vapor Deposition (PVD) processes such as sputtering and evaporation. Once a layer has been deposited, it needs to be patterned. This is done through photolithography, a process used to transfer the pattern on a reticle or mask to a thin coating on the wafer's surface.

Photolithography uses a coating of light sensitive material called photoresist which is developed after exposure to patterned light. When a positive photoresist is used, the exposed resist is removed during develop. The resist which is not exposed, remains on the wafer surface and protects the underlying surface from the subsequent etch. *(See graphic below)*

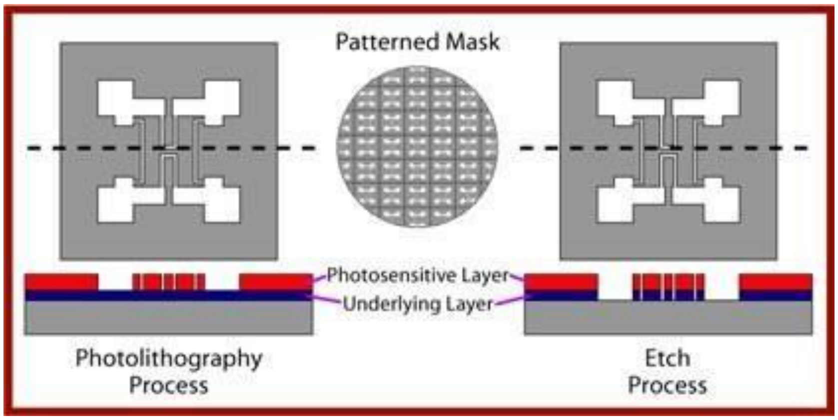

After the develop process, the exposed areas of the underlying layer are etched (removed) using either a wet or dry etch process. Once the resist pattern has been transferred to the underlying material layer, the remaining resist is removed (resist strip) leaving the patterned material layer.

5.5 Chemical Mechanical Polishing (CMP)

As you add layers, the topography at the surface gets bumpy or uneven. This unevenness can affect subsequent processes such as deposition and photolithography, but it can also affect the movement of components upon release. The more layers a MEMS device requires, the more uneven the surface becomes after each new layer. Remember that each layer usually requires a deposition, photolithography, and etch step. Therefore, some processes require that an oxide deposition be followed by chemical mechanical polish (CMP) fig15. The CMP removes the "bumpiness" of the oxide surface prior to the deposition of the next layer. The graphics below show the bumpiness of an oxide layer after being deposited on top of an etched structural layer and its "flatness" after a CMP.

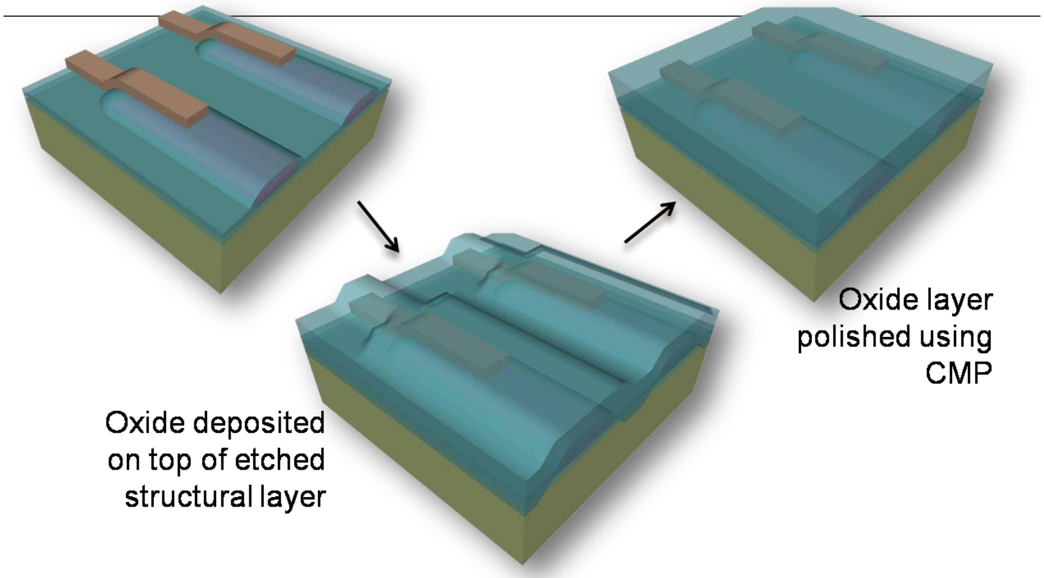

Fig.15 [Graphic images courtesy of Khalil Najafi, University of Michigan]

CMP is used to flatten the topography. Sandia National Laboratories developed a CMP process for MEMS which is similar to that used in CMOS manufacturing. A thick layer of sacrificial oxide is deposited followed with a polish (CMP). The polish removes the topography making the top of the sacrificial layer very smooth. The next structural layer is then deposited. This structural layer is flat on the bottom allowing the structure to move freely once the sacrificial layer is removed.

The image in the left (fig. 16) shows the severe topography resulting if no CMP is done. Compare this to the image on the right (fig. 16). In this case a polish is performed between the sacrificial and structural layer depositions. The conformal nature of oxide deposition is negated by polishing the surface prior to the structural layer deposition.

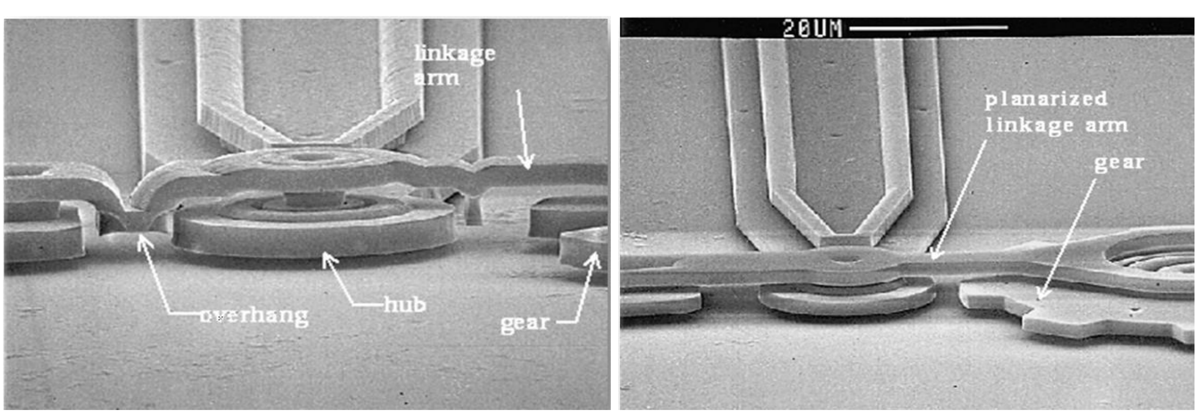

Fig 16. Without CMP (left image), With CMP (right image)
[Scanning Electron Microscope (SEM) images courtesy of Sandia National Laboratories]

5.6 Building a MEMS using Surface Micromachining

The linkage system in the graphic is an example of a surface micromachining process that requires several structural and sacrificial layers. During fabrication, the sacrificial oxide layers define the components' topographical shapes (structural layers) and the vertical spaces between them. Let's take a look at how such a device is fabricated fig.17.

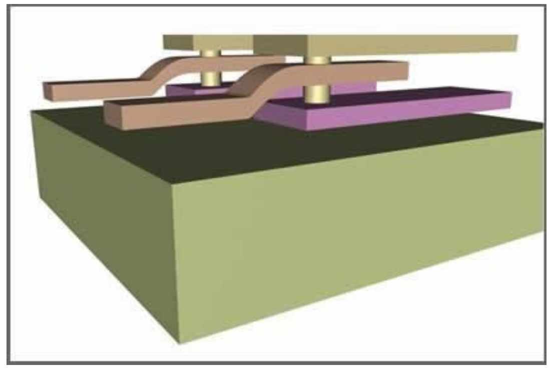

Fig 17. [Graphic image courtesy of Khalil Najafi, University of Michigan]

- A sacrificial (oxide) layer is first deposited on the substrate.
- The first polysilicon layer is deposited on top of the oxide layer.
- This polysilicon layer is patterned and etched and forms the first set of cantilevers.
- A second oxide layer is deposited on top of the etched polysilicon layer.
- The second structural layer or polysilicon layer is deposited, patterned and etched. This forms the second set of cantilevers.
- The third oxide layer (sacrificial layer) is deposited.
- At this point, the surface has become extremely bumpy; therefore, this oxide deposition is followed by a CMP.
- Two holes are etched through the top oxide layer providing an opening to the polysilicon layer below it. These holes are needed to begin forming the posts which support the cantilevers and allow rotation.
- To continue fabricating the posts, holes are etched into the second polysilicon layer.
- Another layer of oxide is deposited on the surface and into the two holes. This is the last sacrificial layer.
- The third polysilicon layer is now deposited, patterned and etched. This layer forms the top set of cantilevers.
- The oxide films below each structural layer provide the necessary space for the middle cantilever to move after all of the oxide layers have been removed and the cantilevers released.
- The last step of this process is to remove the oxide layers from between the structural layers using a wet etch process of a hydrofluoric acid (HF) solution.
- Once the sacrificial layers are removed, the middle cantilever is free to rotate.

These steps - 1) oxide deposition, 2) structural layer deposition, pattern, etch, 3) sacrificial etch – can be repeated several times when fabricating a complex moving structure such as the linkage system, a gear transmission, an accelerometer, and other MEMS devices.

To view a step-by-step presentation of this process, stop here and watch the narrated presentation "Linkage Assembly Fabrication".

An important advantage of using surface micromachining over bulk micromachining is that it is very compatible with CMOS processing. This compatibility allows mechanical devices to be built at the same time as the electronic logic circuits. Also, the cost of fabrication is generally lower since this technology uses the same equipment as the semiconductor industry. Many MEMS startup companies purchase used equipment from the semiconductor industry allowing for lower startup costs. MEMS component parts are generally 1 micron or larger in scale which is compatible with 1990's semiconductor equipment capabilities. *(Note: Simultaneous fabrication of electronic logic circuits and mechanical components require the logic circuits to be encapsulated before the mechanical release step of the process; otherwise, the silicon dioxide insulation for the logic circuits would be etched along with the sacrificial layers for the mechanical components.)*

The downside of surface micromachining is that the mechanical components are very close together (a few microns) and they are flat. This can cause stiction. Stiction occurs when two, very flat surfaces come into contact and stick together; often, the two parts cannot be separated.

A limitation of surface micromachining is that its processes can generally create only low aspect ratio devices, which is ideal for comb drives and gear drives. However, MEMS devices such as micro-channels and reservoirs require high aspect ratios; therefore, other micromachining processes are required.

5.7 Surface Micromachining Components

In spite of its limitations, surface micromachining is used to fabricate many MEMS components:

- Comb Drives
- RF Switch
- Gears and chains
- Surface acoustical wave (SAW) sensors
- Inertial sensors
- Cantilevers
- Torsional Ratching Actuators (TRA)

5.8 Bulk Micromachining

Bulk micromachining is a process that defines structures by electively removing or etching into a substrate. This is not a new concept. In fact, bulk etch has existed in nature for eons. Have you ever seen a natural bridge or arch like the natural arch shown in the picture 18 to the right? This arch was formed by water and wind eroding (or etching) into and eventually, through the sandstone.

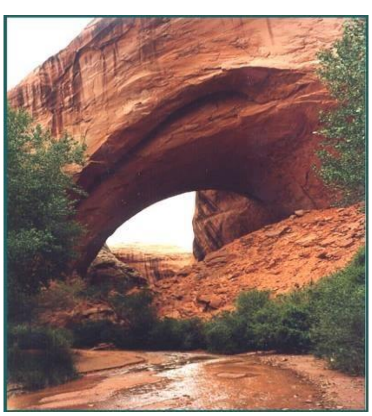

Fig.18 Natural Arch, Coyote anyon, Utah [Photo courtesy of Bob Willis]

The men that carved the faces into Mt. Rushmore fig. 19 *(below left)* and the native Americans that constructed cliff dwellings *(below right)* into the side of mountains used an bulk etch process. Imagine what it took to start with a flat surface like the side of a mountain and end up with such definitive structures as the ones seen in the pictures below. When you look carefully at these pictures you can see that bulk etching is a subtractive process as well as a highly selective process. These are not random carvings.

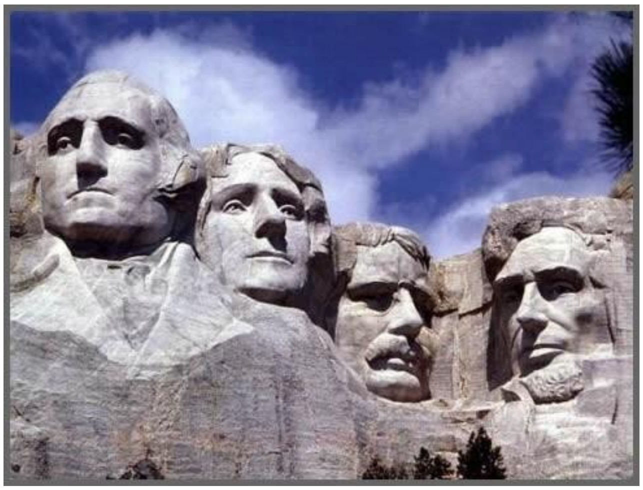

Fig.19 Mt. Rushmore, South Dakota
[Photo courtesy of the National Park Service]

Mesa Verde National Park, Colorado
[Photo courtesy of the Barbara Lopez]

In MEMS fabrication bulk micromachining uses the entire thickness of the silicon wafer (or substrate) to form microsystem structures that can result in high aspect ratios. In bulk micromachining monocrystalline silicon wafers are selectively etched to form 3-D MEMS devices. Bulk micromachining is used to

- remove relatively large amounts of a silicon substrate,
- construct high aspect ratio structures such as fluidic channels and chambers ***(see fig 20),*** alignment grooves, and
- construct sensors including micro pressure sensors, cantilever arrays, and accelerometers. Some of these latter components are fabricated using both bulk and surface micromachined components.

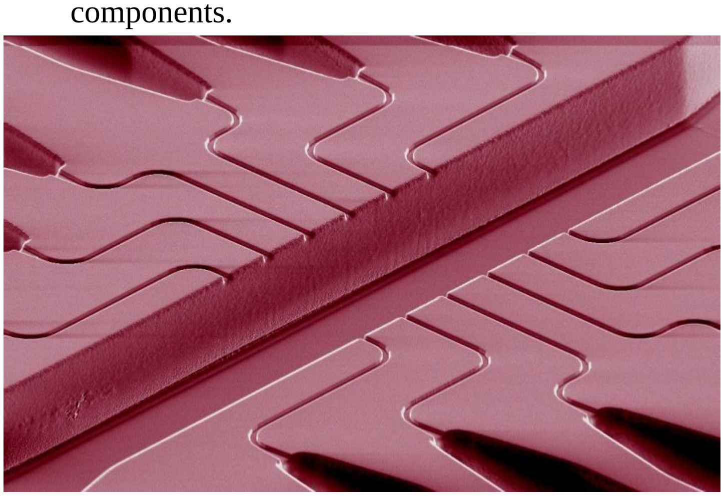

Fig.20 Microfluidic channels with high aspect ratio fluidic chambers [SEM Image courtesy of Berkeley. Ref: C. Ionescu- Zanetti, R. M. Shaw, J. Seo, Y. Jan, L. Y. Jan, and L. P. Lee (PNAS, 2005)]

5.9 The Bulk Micromachining Process

Bulk etch is a subtractive process in which the silicon substrate is selectively removed. Specific etchants are chosen that remove substrate material either isotropically (the same in all directions) or anisotropically (not the same in all direction). The anisotropic wet etching of silicon takes advantage of the crystalline structure of the silicon wafer to remove select material following the planes of the silicon crystal. This selectivity is possible due to the knowledge that certain plane orientations etch much faster than other planes (e.g., the (100) plane etches approximately 400 times faster than the (111) plane).

An example of bulk etching in MEMS fabrication is in the construction of a MEMS pressure sensor. A MEMS pressure sensor *(fig 21)* consists of a silicon nitride thin film deposited onto the surface of a silicon substrate. This layer of silicon nitride acts as the diaphragm or membrane of the pressure sensor. A thin film of gold is deposited on top of the silicon nitride, then patterned and etched to form a Wheatstone bridge sensing circuit. In order for the membrane to move up and down with changes in pressure, it must be "released". To release the membrane, the silicon substrate beneath the membrane is removed by etching the backside of the wafer.

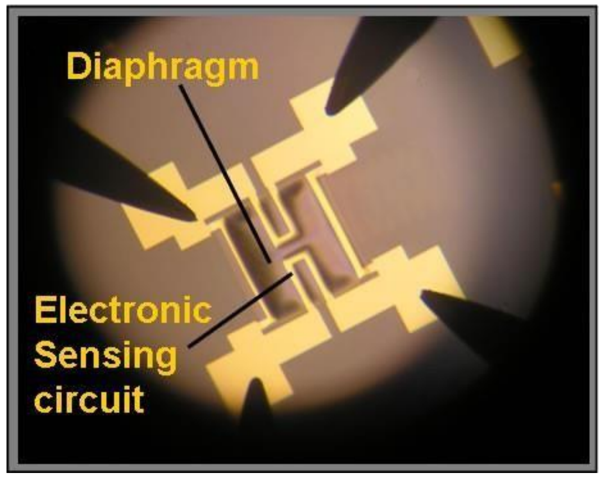

Fig. 21. [Pressure Sensor image courtesy of MTTC/UNM]

The picture to the right shows the backside of a MEMS pressure sensor and the result of a bulk etch using a solution of potassium hydroxide (KOH) and water. The KOH etchant solution selectively etches the crystalline silicon along a specific plane. In the picture you can see that the etchant preferentially etched the (100) plane of the silicon (the wafer surface in this case) while simultaneously etching the (111) plane. The (111) plane etches about 400 times slower than the (100) plane. This allows for a controlled etch in which an inverted pyramid shaped opening of a specific size is created. The etch of the (100) plane stops when it hits the silicon nitride which is impervious to the KOH. For the purpose of this etch, the silicon nitride layer is the etch stop layer. For the purpose of the pressure sensor, the silicon nitride serves as the membrane or diaphragm on which the sensing circuit is constructed.

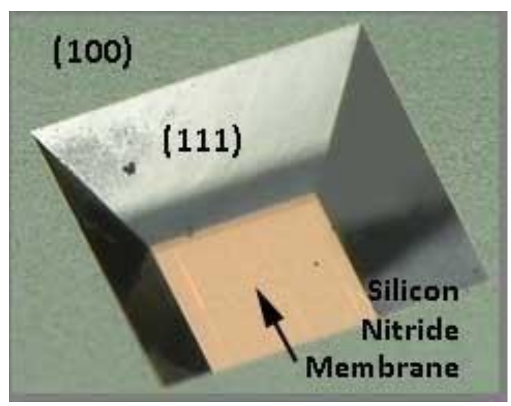

5.10 Bulk Combined with Surface Micromachining

The previous example of the pressure sensor is actually a MEMS fabrication process that uses both bulk micromachining and surface micromachining. Bulk etch is used to remove a select section the thickness of the substrate from beneath a patterned thin film (silicon nitride). Surface micromachining is used to pattern the backside as well as to create a metal electronic sensing circuit on the frontside of the wafer. Below is the process used to fabricate this MEMS pressure sensor.

- A thin film of silicon nitride is deposited onto both sides (frontside / backside) of the wafer.
- The backside nitride is patterned and plasma etched creating the openings for the chamber (the inverted pyramid shown in a previous image). In this application the silicon nitride is used as a hard mask.
- Prior to creating the chambers within the substrate, the metal electronic sensing circuit is fabricated on the frontside silicon nitride. The surface micromachining processes - deposition, pattern and etch – are used to create the electronic sensing circuit by depositing chrome, then gold thin films on top of the silicon nitride, patterning the chrome/gold layers, then etching the chrome/gold to form the electronic circuit.
- The last step is to anisotropically etch the backside chambers using a potassium hydroxide (KOH) solution. For this bulk etch process, the backside silicon nitride acts as a patterned mask, while the frontside silicon nitride is the etch stop (i.e., the anisotropic etch stops when all of the silicon is removed within the holes of the mask and the frontside silicon nitride is reached).
- The frontside silicon nitride directly over the backside chamber operates as the pressure sensor's diaphragm because it can now deflect up or down with changes in pressure.

The images below show the frontside and backside, respectively, of a finished pressure sensor (far right circuit in both images).

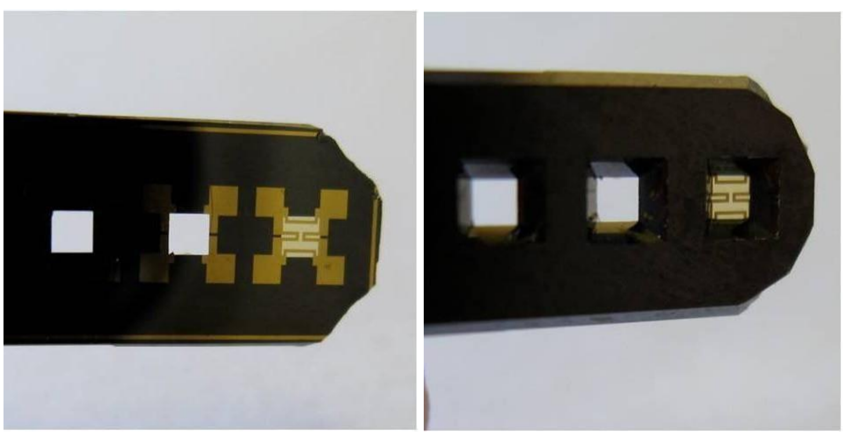

Fig .22. MEMS pressure sensor frontside (left) showing electronic sensing circuit etch in a gold film layer and backside (right) showing the chamber (look closely and you can see the beveled edges). [Images courtesy of UNM/MTTC]

5.11 Wet and Dry Etch in Bulk Micromachining

Wet and dry etch techniques have been developed to provide the various shapes needed for MEMS devices. *(See graphic below)* Grooves and slots are used in assembly, such as putting multiple wafers together with different devices on each wafer. V-shaped grooves are also used to finely align fiber optics to micro optical components. Nozzles are used for devices such as inkjet printheads, cavities for open volumes or chambers in pumps or voids under membranes, and channels to pass fluids through. These shapes are formed by using different processes that create either an isotropic or anisotropic profile.

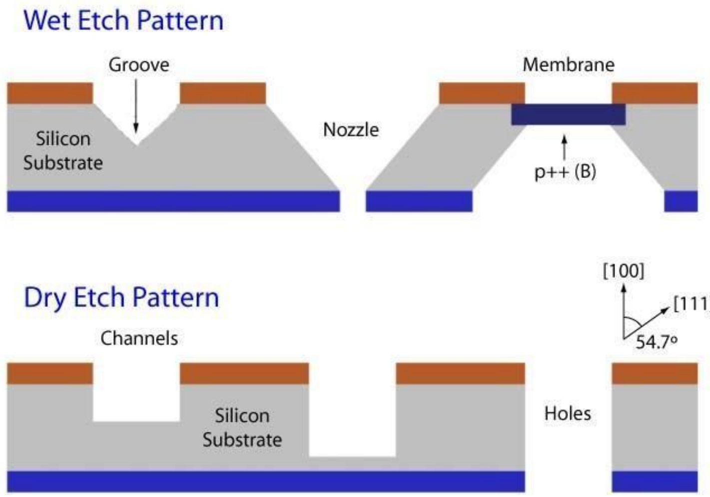

Anisotropic vs. Isotropic Profiles

Bulk micromachining uses etch processes that result in both isotropic and anisotropic etch profiles. The result (isotropic or anisotropic) depends on the etchant used and the selectivity of that etchant to the material being etched.

Anisotropic etches prefer one direction over another and may be dependent upon the crystalline structure (crystal orientation) of the substrate. As you saw previously with the backside etch of the pressure sensor, the etch process etches certain planes more rapidly than others (i.e., the (100) plane faster than the (111) plane). This etch rate selectivity where the selectivity varies with crystal plane orientation, provides the ability to use anisotropic etching techniques to produce specific shapes such as pyramidal cavities and v-shaped trenches.

Isotropic etch does not prefer a given direction over another. This is an etch equal in all directions as illustrated in the graphic. The typical cross sectional profile is that of a champagne glass or concave shape. It is not dependent upon crystal orientation, but rather upon the ability of the etchant to react with the material to be etched creating a volatile by-product that detaches from the wafer. Isotropic etching is characterized by its distinct profile and its undercutting of the thin film used as the etch mask. Isotropic profiles can be achieved using both wet and dry etch processes. A wet isotropic etch is used to remove the sacrificial layer from underneath a structural layer. A dry isotropic etch is used to create some of the structures and shapes needed for MEMS. The graphic below illustrates the isotropic profile versus the anisotropic profile. Anisotropic profiles can also be the result of a dry plasma reactive ion etches. The side-walls can be vertical or at an angle to the wafer plane.

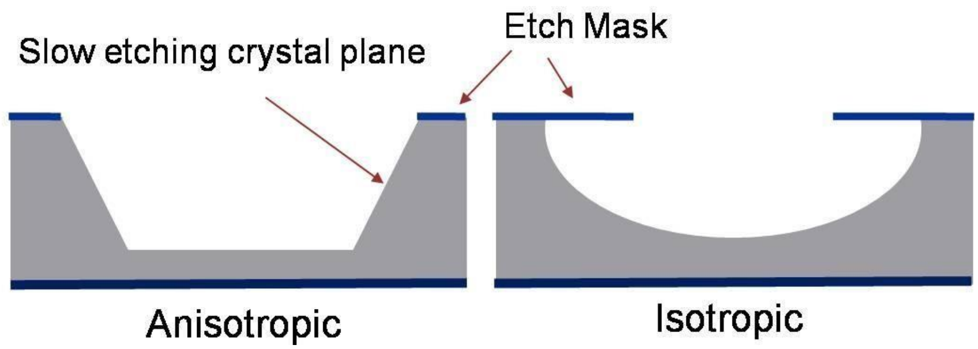

Wet Etch Anisotropic Etchants

In bulk micromachining wet etching can result in either isotropic or anisotropic structures depending upon the etchant and the material being etched. The following etchants yield anisotropic profiles when etching crystalline material such as silicon:

- Potassium Hydroxide (KOH)
- Ethylene Diamine Pyrocathechol (EDP)
- Tetramethyl Ammonum Hydroxide (TMAH)
- Sodium Hydroxide (NaOH)
- N_2H_4-H_2O (Hydrazine)

Costs, etch rates (i.e., how fast something etches), resulting surface roughness, selectivity between the mask material and material to be etched, relative etch ratios between the different crystal planes, safety issues, and process compatibility are some of the variables used when selecting one etchant over another.

Dry Etch

Dry etch bulk processes use reactive vapor etchants usually in a plasma environment, or through bombarding the exposed substrate by sputtering with high energy particles. Dry etch is generally well controlled and capable of higher resolutions than wet etch. Dry etch can produce both isotropic and anisotropic profiles with critical dimensions much less than 1 µm.Compared to wet etch tools, tools used for dry etching are more expensive and usually have a larger footprint, taking up more space in the manufacturing area. Dry etch does not leave large quantities of hazardous liquids needing to be properly disposed of; however, some of the etchants and the etched by-product (exhaust gasses) can be quite hazardous, requiring filters and neutralization systems..

Four dry etch processes used in bulk micromachining include the following:

- Deep Reactive ion etch (DRIE)
- Isotropic Plasma Etching
- Sputter Etching (ion milling)
- Vapor Phase Etching

5.12 Bulk Micromachining Components

The following components are MEMS structures that are possible only through the use of bulk micromachining processes.

- Cantilever Arrays
- Nozzles
- Microfluidic channels
- Needle Arrays
- AFM Probes
- Membranes
- Chambers
- Through wafer connections

5.13 LIGA

(Lithographie (Lithography)**, G**alvanoformung (electroforming), and **A**bformung (molding).

LIGA was developed in the early 1980's at the Karlsruhe Nuclear Research Center in Germany to produce nozzles for uranium enrichment processes. The image to the right is a SEM of one of these nozzles.

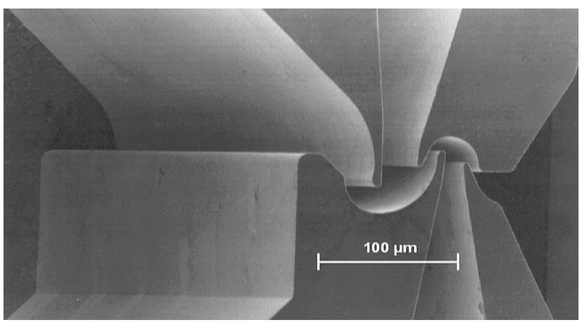

Fig.23. LIGA micro machined nozzles [Image courtesy of Wenn du Benutzer Captain Bligh,Source: Wikipedia]

LIGA is an additive, lithographic process which allows for the fabrication of complex, three dimensional structures with very high aspect ratios exceeding 100:1.[6] These structures can have sub-micron size features with heights of several millimeters and widths of only a few microns (e.g., probes, pin, electrodes, gears, waveguides, and molds). LIGA is also a type of HARMST process – High Aspect Ratio Micro-Structure Technology. LIGA molds allow for mass-production of micro-sized HARMST components. These components as well as other LIGA components can be fabricated using polymers, metals and moldable materials.The graphic below illustrates high aspect ratio posts that can be fabricate using the LIGA process and made from a variety of different materials.

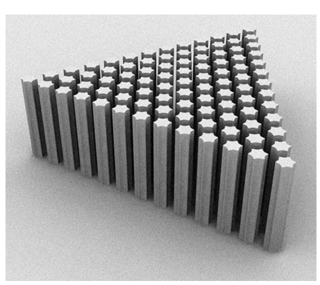

LIGA uses the collimated x-rays produced by synchrotron radiation to illuminate thick x-ray sensitive materials such as PMMA (polymethylmethacrylate), also known as acrylic glass or Plexiglas. As with a basic photolithography process, the PMMA layer is patterned under a lithographic mask using an x-ray exposure. Instead of a mask consisting of a chrome pattern on quartz as in UV photolithography, LIGA utilizes gold on beryllium as the mask materials. Gold blocks x-rays while the beryllium is transparent to x-rays. The PMMA is exposed by the x-rays and the pattern is developed (like photoresist). Since the x-rays are well collimated, they travel in a straight line and have a large depth of focus. This results in patterning sharp, tall, thin or deep structures or cavities within the PMMA after the develop process. Nickel and other metals are electroplated into these cavities. After electroplating, the PMMA is removed leaving the metal structures. These structures can be used individually, or as stamps, or molds to create thousands of like structures in plastic. Hot plastic embossing and injection molding are used with the LIGA fabricated molds.

Fig. 24. This LIGA micromachined gear is used for a mini electromagnetic motor
[Image courtesy of Sandia National Laboratories]

5.14 LIGA Process

The LIGA process consists of the following basic steps:

- Expose
- Develop
- Electroform (Electroplate)
- Strip
- Replicate or Release

Let’s take a look at each of these steps.

Expose

Once the PMMA is applied to the substrate or base, synchrotron radiation patterns the PMMA through a gold on beryllium mask. Like photoresist, the radiation modifies the PMMA so that the exposed material can be removed with a suitable or selective developer solution.

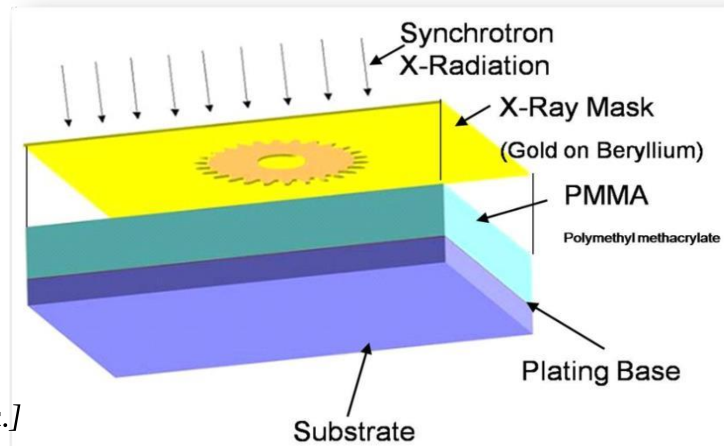

Fig. 25. The graphic shows the radiation, the mask and the PMMA layer. The mask has the pattern of a micro-gear.
[Graphic courtesy of HT MicroAnalytical, Inc.]

<u>Develop</u>

With the use of a developer solution, the exposed PMMA is removed leaving a mold with high aspect ratio cavities, holes, or trenches. Fig.26

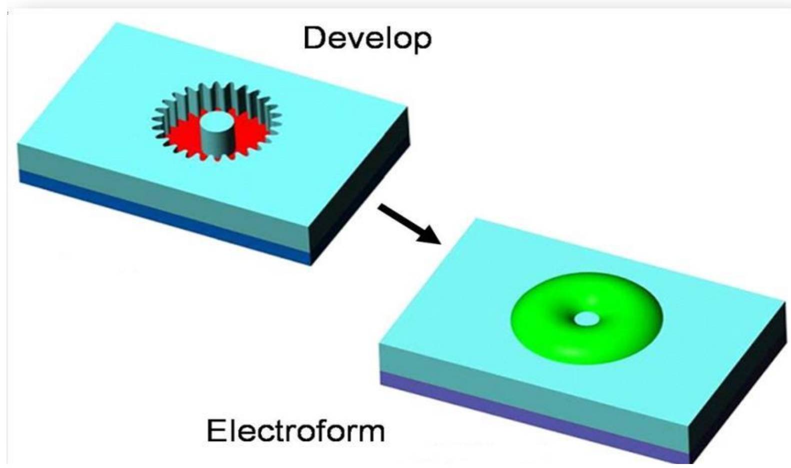

<u>Electroform</u>
The cavities created in the develop step are filled with a metal (e.g., nickel, copper, gold, or various alloys) through electroforming processes.

Fig.26 [Graphics courtesy of HT MicroAnalytical, Inc.]

Electroforming is “the fabrication of simple and complicated components by means of electroplating.” Electroplating *(graphic right)* is a process in which a positive and a negative electrode are submerged in an electrolyte solution. The negative electrode (i.e., cathode) is the object or holds the object or substrate to be coated. In LIGA fabrication the cathode (also referred to as the mandrel) is the 3-D PMMA structure that is formed by the expose and develop processes.

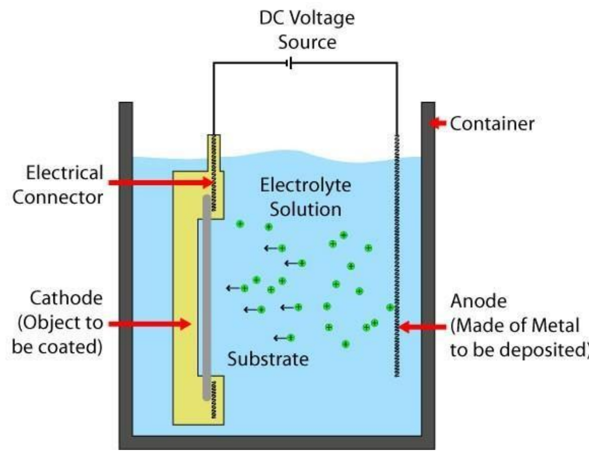

During electroplating metallic positive ions (cations) released from the anode are attracted to the negatively charged cathode. When the cations reach the substrate they are neutralized by the electrons of the cathode, reducing them to metallic form. This process continues until the substrate is coated with the desired thickness.

Electroforming differs from electroplating in that it yields a much thicker layer of metal on the substrate or mandrel than the electroplating processes. In electroforming a metal object is produced (or reproduced) by coating the mandrel with the desired thickness of metal. At the end of the process, the mandrel may be removed, resulting in a self-supporting object. In electroplating the su bstrate is coated with a thin layer of metal which adheres to the substrate becoming a permanent

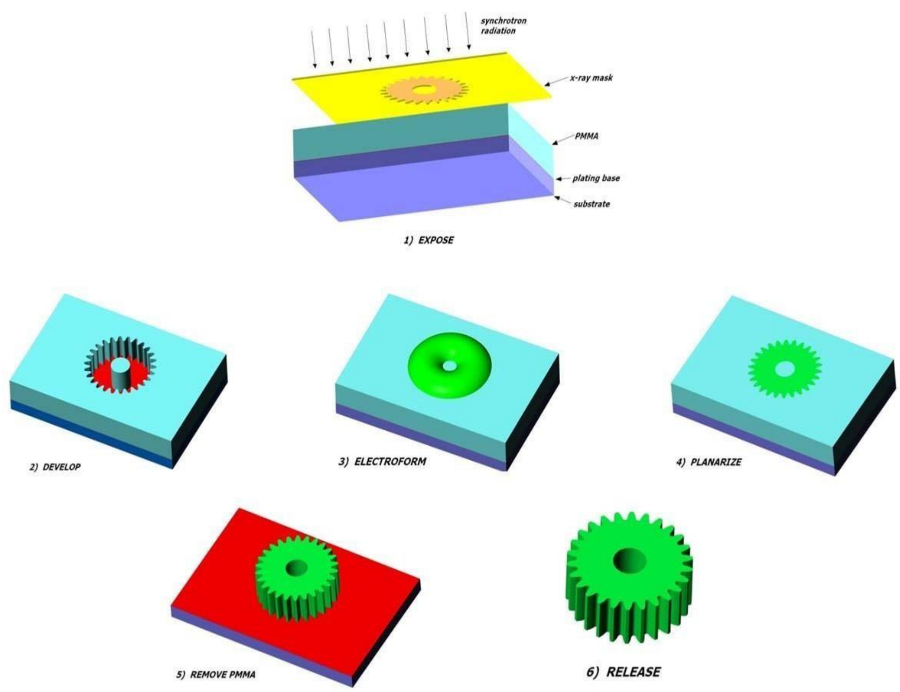

Fig. 27. [Graphic courtesy of HT MicroAnalytical, Inc.]

part of the object (e.g., chrome faucet, jewelry, hardware).The following graphic illustrates how the mandrel takes shape after the develop step (2) of LIGA fabrication. In the electroforming process, metal is deposited within the cavity using the process of electroplating. However, the electroplating process continues (in this case) until the cavity is completely filled. Once the surface has been planarized, the PMMA removed and the metal form released, a self-supporting object remains, in this case – a metal micro gear.

Strip

After electroforming a CMP may be performed to flatten the surface. Once the surface has been polished (planarized), the PMMA is removed or stripped. Depending on the component, the remaining structure could be used to make molds or the end product. The graphic shows these three steps (CMP, strip, release) for a microgear.

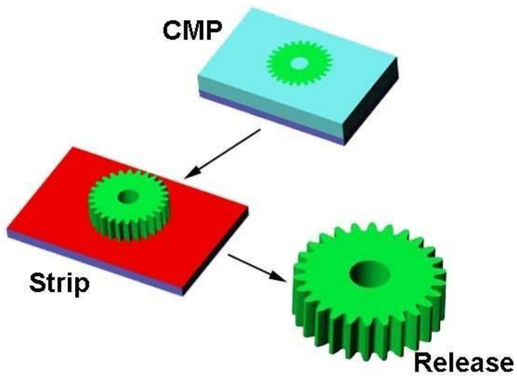

Fig. 28.[Graphics courtesy of HT MicroAnalytical, In

The LIGA process enables the creation of micro-sized high aspect ratio components that are

- free-standing,
- attached to the substrate, or
- metal inserts for injection molding.

LIGA's ability to incorporate "multi-layer wafer-scale processing extends the additive approach to accommodate interfaces and packaging." LIGA components require extensive, unique metrology to ensure quality products.[8]

What type of MEMS components would fall into these three categories and would probably be fabricated using LIGA processing?

Here are some graphics of parts and structures that can be build using LIGA micromachining processes. Note the very high aspect ratios. What are some of the applications which would require such tall structures?

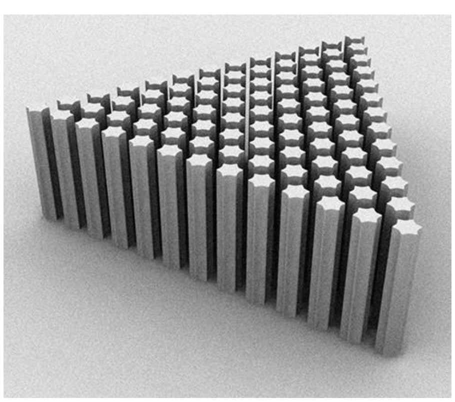
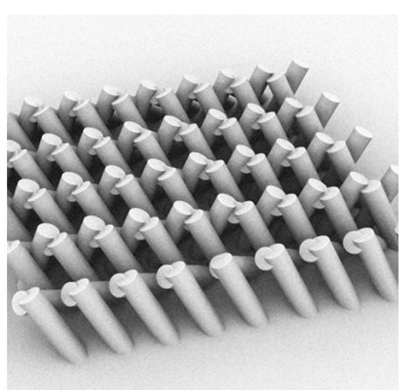
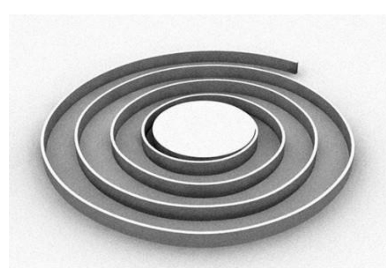

The left image represents high aspect ratio posts. Such posts can be fabricated from a LIGA mold or build into the PMMA and released. The middle image represents angled structures that can be fabricated using a LIGA process. Again, notice the high aspect ratio of the components. The right image is of a coiled spring. This would be a very difficult component to fabricate using surface or bulk micromachining. However, such components are possible with a LIGA process.

Glossary

Anisotropic etch – this etch is highly directional. The etch rate varies with direction resulting in straight or sloped sidewalls. An example of a wet anisotropic etch is the application of KOH solution to silicon crystal; the etch rate of the (110) plane is approximately 400 times faster than the etch rate along the (111) plane.

Aspect ratio - The height of an etched feature divided by its width in the case of a tall structure, or the width divided by the depth in the case of a channel.

Bulk etch - A subtractive process in which the silicon substrate is selectively removed in relatively large amounts.

Bulk Micromachining - A process that defines structures by selectively removing or etching inside a substrate. This results in deep channels, or large, free-standing structures.

Chemical Mechanical Polishing (CMP) – A process used to flatten the topography of the wafer's surface as new layers are deposited.

Deposition - A process that deposits a material onto an object. Typically, thin films are deposited in Microsystems fabrication using chemical vapor deposition, physical vapor deposition (evaporation) or even oxide growth.

Electroforming – A process used to coat an object with a metal or metal alloy. This process uses a positive and negative electrode submerged in an electrolyte solution. This is similar to electroplating but provides for thicker coatings. The resulting structures are often used as a stamp or mold used in hot-plastic embossing or injection molding, respectively.

Electroplating - The process of using electrical current to coat an electrically conductive object with a layer of metal. The film is typically much thinner than what is done in electroforming.

Isotropic Etch – Etching is done at the same rate in all directions. Resulting structures have concave cross-sections, bowl-shaped.

LIGA (**Li**thography**, G**alvanoformung, and **A**bformung) - An additive, lithographic process which allows for the fabrication of complex, three dimensional structures with very high aspect ratios exceeding 100:1.

Oxidation - The process used to grow a uniform, high quality layer of silicon dioxide (SiO_2) on the surface of a silicon substrate.

Photolithography - The transfer of a pattern or image from one medium to another, as from a mask to a thin film deposited on a silicon wafer.

Release etch – An etch process designed to remove material (sacrificial layer or bulk material) from underneath the structural layer without affecting the structural layer itself. The removed sacrificial layers provide space so the mechanical parts can move.

Sacrificial Layer - A layer deposited between structural layers for mechanical separation and isolation. This layer is removed during a "release etch" to free the structural layers and to allow mechanical devices to move. (Silicon dioxide, photoresist, polycrystalline silicon)

Structural Layer - A layer having the mechanical and electrical properties needed for the component being constructed. (doped polycrystalline silicon, silicon nitride, some metals such as chrome, gold and aluminum-copper)

Surface micromachining - A micromachining process that uses layers of thin films deposited on the surface of a substrate to construct structural components for MEMS.

Synchrotron – A type of cyclic particle accelerator that synchronizes a magnetic field and electric field with a traveling particle beam.

Synchrotron radiation – The electromagnetic radiation emitted by charged particles moving close to the speed of light within a synchrotron.

x-ray – A form of electromagnetic radiation having a wavelength in the range 0.01 nanometer (nm) to 10 nm.

SATHYABAMA
INSTITUTE OF SCIENCE AND TECHNOLOGY
(DEEMED TO BE UNIVERSITY)
Accredited "A" Grade by NAAC | 12B Status by UGC | Approved by AICTE
www.sathyabama.ac.in

SCHOOL OF MECHANICAL ENGINEERING
DEPARTMENT OF MECHATRONICS ENGINEERING

Unit – III: DESIGN CONSIDERATIONS BASED ON MICROMECHANICS

Micro Electro Mechanical Systems (MEMS): SMR1301

Lectures on
MEMS and MICROSYSTEMS DESIGN and MANUFACTURE

Chapter 4
Engineering Mechanics for Microsystems Design

Structural integrity is a primary requirement for any device or engineering system regardless of its size.

The theories and principles of engineering mechanics are used to assess:

(1) Induced stresses in the microstructure by the intended loading, and
(2) Associated strains (or deformations) for the dimensional stability, and the deformation affecting the desired *performance* by this microstructural component.

Accurate assessment of stresses and strains are critical in microsystems design not only for the above two specific purposes, but also is required in the design for signal transduction, as many signals generated by sensors are related to the stresses and strains Induced by the input signals.

HSU 2008

Chapter Outline

Static bending of thin plates

Mechanical vibration analysis

Thermomechanical analysis

Fracture mechanics analysis

Thin film mechanics

Overview of finite element analysis

Mechanical Design of Microstructures

Theoretical Bases:

- Linear theory of elasticity for stress analysis
- Newton's law for dynamic and vibration analysis
- Fourier law for heat conduction analysis
- Fick's law for diffusion analysis
- Navier-Stokes equations for fluid dynamics analysis

Mathematical models derived from these physical laws are valid for micro-components > 1 μm.

Mechanical Design of Microsystems

Common Geometry of MEMS Components

Beams:

Microrelays, gripping arms in a micro tong, beam spring in micro accelerometers

Plates:

- Diaphragms in pressure sensors, plate-spring in microaccelerometers, etc
- Bending induced deformation generates signals for sensors and relays using beams and plates

Tubes:

Capillary tubes in microfluidic network systems with electro-kinetic pumping (e.g. electro-osmosis and electrophoresis)

Channels:

Channels of square, rectangular, trapezoidal cross-sections in microfluidic network.

- **Component geometry unique to MEMS and microsystems:**

  Multi-layers with thin films of dissimilar materials

Recommended Units (SI) and Common Conversion Between SI and Imperial Units in Computation

Units of physical quantities:

Length:	m
Area:	m^2
Volume:	m^3
Force:	N
Weight:	N
Velocity:	m/s
Mass:	g
Mass density:	g/cm^3
Pressure:	Pa

Common conversion formulas:

1 kg = 9.81 m/s^2
1kgf = 9.81 N
1 μm = 10^{-6} m
1 Pa = 1 N/m^2
1 MPa = 10^6 Pa = 106 N/m^2

1 m = 39.37 in = 3.28 ft
1 N = 0.2252 lb_f (force)
1 kg_f = 2.2 lb_f (weight)
1 MPa = 145.05 psi

Static Bending of Thin Plates

We will deal with a situation with thin plates with fixed edges subjected to laterally applied pressure:

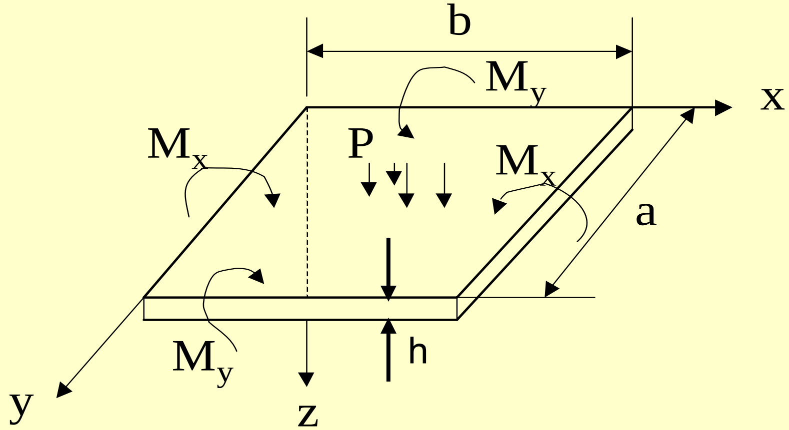

in which, P = applied pressure (MPa)

M_x, M_y = bending moments about respective y and x-axis (N-m/m)

h = thickness of the plate (m)

The governing differential equation for the induced deflection, w(x,y) of the plate is:

$$\left(\frac{\partial^2}{\partial x^2}+\frac{\partial^2}{\partial y^2}\right)\left(\frac{\partial^2 w}{\partial x^2}+\frac{\partial^2 w}{\partial y^2}\right)=\frac{p}{D} \qquad (4.1)$$

with D = flexural rigidity, $D=\dfrac{E\,h^3}{12(1-\nu^2)}$ (4.2)

in which E = Young's modulus (MPa), and ν = Poisson's ratio

Static Bending of Thin Plates-Cont'd

Once the induced deflection of the plate w(x,y) is obtained from the solution of the governing differential equation (4.1) with appropriate boundary conditions, the bending moments and the maximum associated stresses can be computed by the following expressions:

Bending moments (4.3a,b,c):

$$M_x = -D\left(\frac{\partial^2 w}{\partial x^2} + \nu \frac{\partial^2 w}{\partial y^2}\right)$$

$$M_y = -D\left(\frac{\partial^2 w}{\partial y^2} + \nu \frac{\partial^2 w}{\partial x^2}\right)$$

$$M_{xy} = D(1-\nu)\frac{\partial^2 w}{\partial x \partial y}$$

Bending stresses (4.4a,b,c):

$$(\sigma_{xx})_{\max} = \frac{6(M_x)_{\max}}{h^2}$$

$$(\sigma_{yy})_{\max} = \frac{6(M_y)_{\max}}{h^2}$$

$$(\sigma_{xy})_{\max} = \frac{6(M_{xy})_{\max}}{h^2}$$

Special cases of bending of thin plates

Bending of circular plates

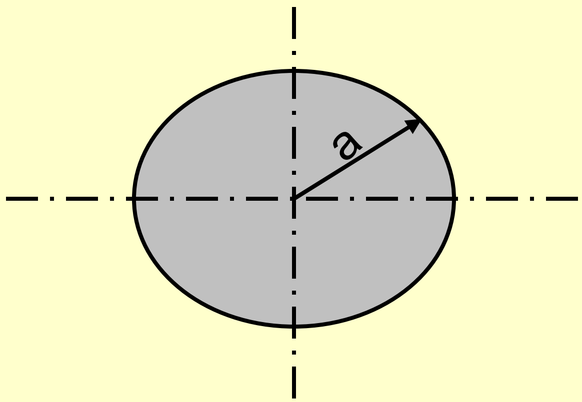

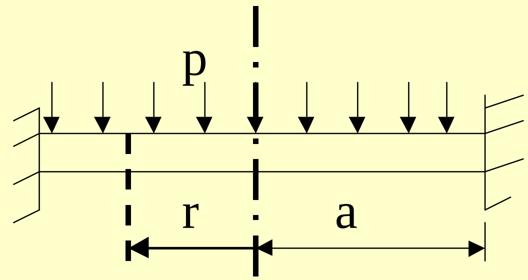

Let W = total force acting on the plate, W = (πa)p and m=1/ν

The maximum stresses in the r and θ-directions are:

$$(\sigma_{rr})_{\max} = \frac{3W}{4\pi h^2} \quad \text{and} \quad (\sigma_{\theta\theta})_{\max} = \frac{3\nu W}{4\pi h^2} \qquad (4.5a,b)$$

Both these stresses at the center of the plate is: $\sigma_{rr} = \sigma_{\theta\theta} = \dfrac{3\nu W}{8\pi h^2}$ (4.6)

The maximum deflection of the plate occurs at the center of the plate:

$$w_{\max} = -\frac{3W(m^2-1)a^2}{16\pi E m^2 h^3} \qquad (4.7)$$

Example 4.1 (p.113)

Determine the minimum thickness of the circular diaphragm of a micro pressure sensor made of Silicon as shown in the figure with conditions:

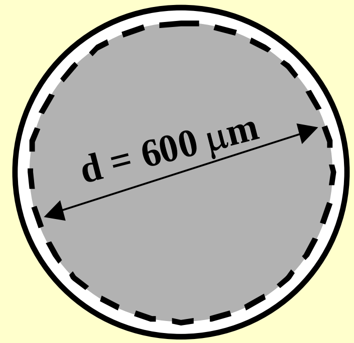

Diameter d = 600 μm; Applied pressure p = 20 MPa
Yield strength of silicon σ_y = 7000 MPa
E = 190,000 MPa and ν = 0.25.

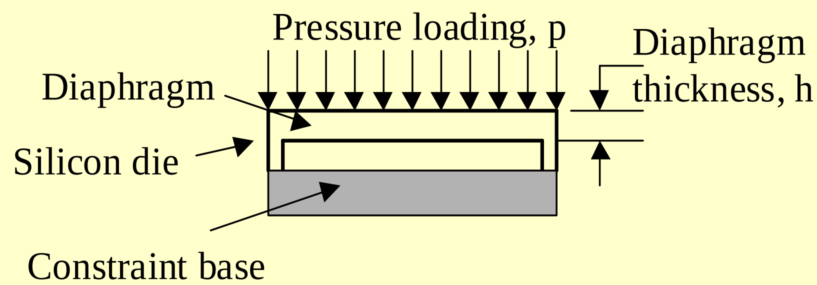

Solution:

$$(\sigma_{rr})_{max} = \frac{3W}{4\pi h^2} \longrightarrow h = \sqrt{\frac{3W}{4\pi(\sigma_{rr})_{max}}}$$

$$(\sigma_{\theta\theta})_{max} = \frac{3\nu W}{4\pi h^2} \longrightarrow h = \sqrt{\frac{3\nu W}{4\pi(\sigma_{\theta\theta})_{max}}}$$

Use the condition that $\sigma_{rr} < \sigma_y$ = 7000 MPa and $\sigma_{\theta\theta} < \sigma_y$ = 7000 MPa, and

$W = (\pi a^2)p = 3.14 \times (300 \times 10^{-6})^2 \times (20 \times 10^6) = 5.652$ N, we get the minimum thickness of the "plate" to be:

$$h = \sqrt{\frac{3x5.652}{4x3.14x(7000x10^6)}} = 13.887x10^{-6}\ m$$ or **13.887 μm**

Special cases of bending of thin plates-Cont'd

Bending of rectangular plates

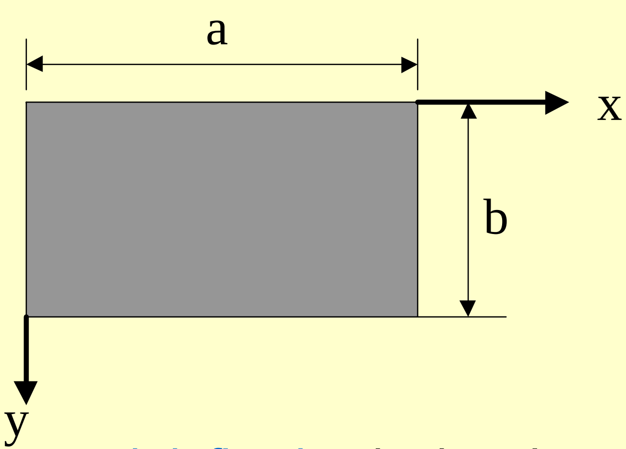

The maximum stress and deflection in the plate are:

$$(\sigma_{yy})_{\max} = \beta \frac{p\,b^2}{h^2} \quad \text{and} \quad w_{\max} = \alpha \frac{p\,b^4}{E\,h^3} \qquad \text{(4.8 and 4.9)}$$

in which coefficients **α** and **β** can be obtained from Table 4.1:

a/b	1	1.2	1.4	1.6	1.8	2.0	∞
α	0.0138	0.0188	0.0226	0.0251	0.0267	0.0277	0.0284
β	0.3078	0.3834	0.4356	0.4680	0.4872	0.4974	0.5000

Example 4.2 (p.115)

A rectangular diaphragm, 13.887 μm thick has the plane dimensions as shown in the figure. The diaphragm is made of silicon. Determine the maximum stress and deflection when it is subjected to a normal pressure, P = 20 MPa. All 4 edges of the diaphragm are fixed.

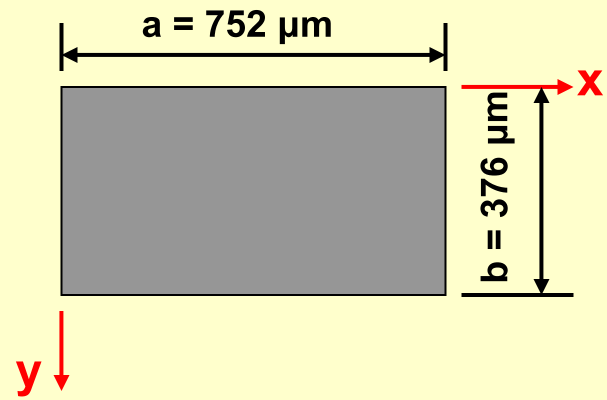

Solution:

We will first determine α = 0.0277 and β = 0.4974 with a/b = 752/376 = 2.0 from the Given Table. Thus, from available formulas, we get the maximum stress:

$$(\sigma_{yy})_{\max} = \beta \frac{p\,b^2}{h^2} = 0.4974 \frac{(20x10^6)(376x10^{-6})^2}{(13.887x10^{-6})^2} = 7292.8x10^6\,Pa$$

and the maximum deflection:

$$w_{\max} = -\alpha \frac{p\,b^4}{E\,h^3} = -\alpha \frac{pb}{E}\left(\frac{b}{h}\right)^3 = -\frac{0.0277x(20x10^6)x376x10^{-6}}{190000x10^6}\left(\frac{376x10^{-6}}{13.887x10^{-6}}\right)^3 = -21.76x10^{-6}\,m$$

at the center (centroid) of the plate

Special cases of bending of thin plates-Cont'd

Bending of square plates:

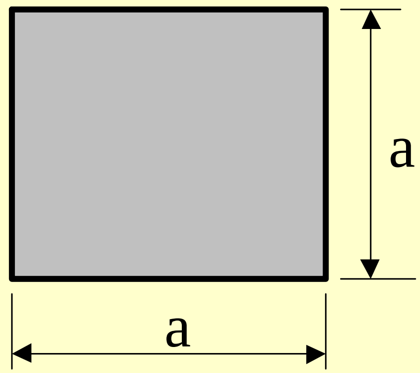

The maximum stress occurs at the middle of each edge: $\sigma_{max} = \frac{0.308\,p\,a^2}{h^2}$ (4.10)

The maximum deflection occurs at the center of the plate: $w_{max} = -\frac{0.0138\,p\,a^4}{E\,h^3}$ (4.11)

The stress and strain at the center of the plate are:

$\sigma = \frac{6p(m+1)a^2}{47m\,h^2}$ and $\varepsilon = \frac{1-\nu}{E}\sigma$ (4.12 and 4.13)

Square diaphragm (idealized as a square plate) is the sensing element in many micro pressure sensors

Example 4.3 (p.116)

Determine the maximum stress and deflection in a square plate made of silicon when is subjected to a pressure loading, p = 20 MPa. The plate has edge length, a = 532 μm and a thickness, h = 13.887 μm.

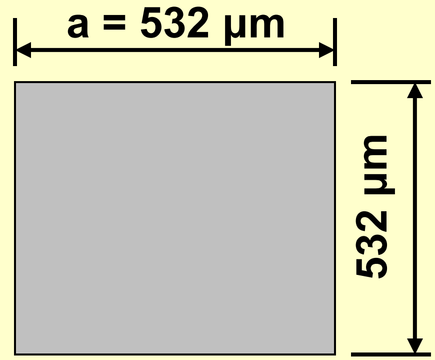

Solution:

From the given formulas, we have the maximum stress to be:

$$\sigma_{\max} = \frac{0.308\,pa^2}{h^2} = \frac{0.308x(20x10^6)(532x10^{-6})^2}{(13.887x10^{-6})^2} = 9040x10^6 \;\; Pa$$

and the maximum deflection:

$$w_{\max} = -\frac{0.0138\,p\,a^4}{Eh^3} = -\frac{0.0138\,pa}{E}\left(\frac{a}{h}\right)^3 =$$

$$-\frac{0.0138(20x10^6)x532x10^{-6}}{190000x10^6}\left(\frac{532x10^{-6}}{13.887x10^{-6}}\right)^3 = -43x10^{-6}\; m$$ or w_{max} = 43 μm

Geometric effect on plate bending

Comparison of results obtained from Example 4.1, 4.2 and 4.3 for plates made of silicon having same surface area and thickness, subjecting to the same applied pressure indicate saignificant difference in the induced maximum stresses and deflections:

Geometry	Maximum Stress (MPa)	Maximum Deflection (μm)
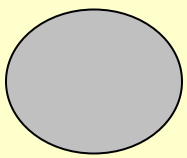	7000	55.97
	7293	21.76
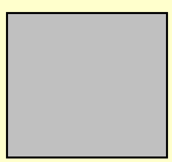	**9040** highest stress output	43.00

The circular diaphragm is most favored from design engineering point of view.
The square diaphragm has the highest induced stress of all three cases. It is favored geometry for pressure sensors because the high stresses generated by applied pressure loading – result in high sensitivity..

Example 4.4

(p. 118)

Determine the maximum stress and deflection in a square diaphragm used in a micro pressure sensor as shown in the figure. The maximum applied pressure is p = 70 MPa.

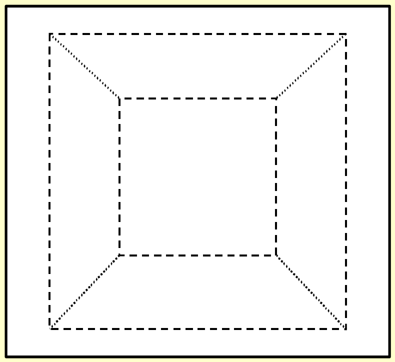

View on Section "A-A"

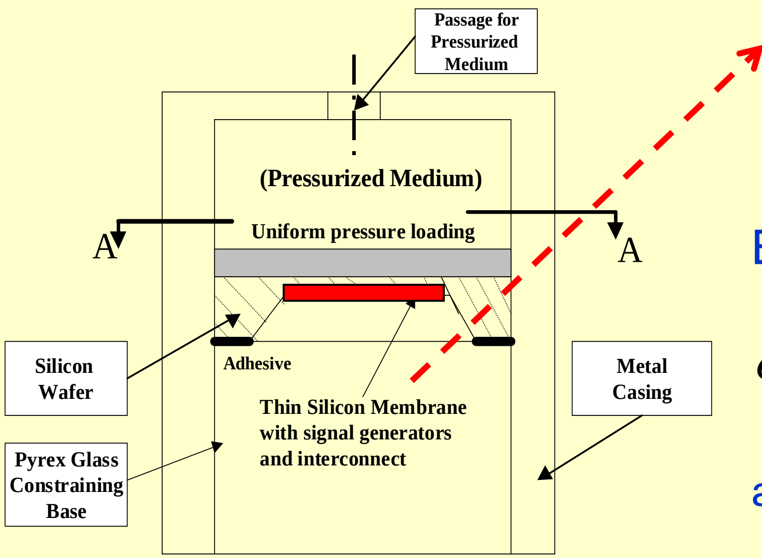

Detail of the Silicon die and diaphragm:

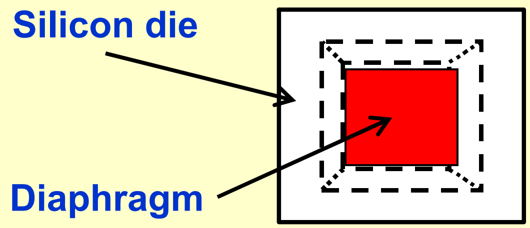

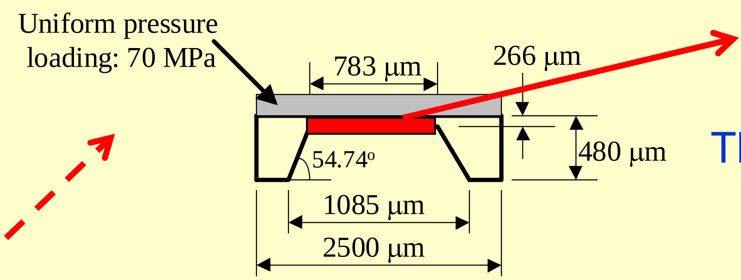

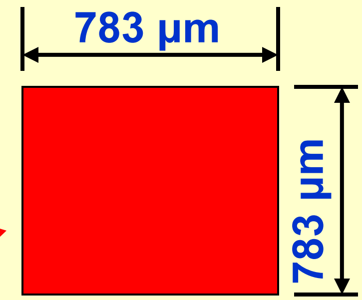

Thickness h = 266 μm

By using the formulas for square plates, we get:

$$\sigma_{\max} = \frac{0.308x70x10^6 x(783x10^{-6})^2}{(266x10^{-6})^2} = 186.81MPa$$

and the maximum deflection:

$$w_{\max} = -\frac{0.0138x70(783x10^{-6})^4}{190000(266x10^{-6})^3} = -10153x10^{-11} m$$

or 0.1015 μm (downward)

Mechanical Vibration Analysis

Mechanical vibration principle is used in the design of micro-accelerometer, which is a common MEMS device for measuring forces induced by moving devices.

Microaccelerometers are used as the sensors in automobile air bag deployment systems.

We will outline some key equations involved in mechanical vibration analysis and show how they can be used in microaccelerometer design.

Overview of Simple Mechanical Vibration Systems

(a) Free vibration: (b) Damped vibration: (c) Forced vibration:

Circular frequency:

$$\omega = \sqrt{\frac{k}{m}}$$

Natural frequency:

$$f = \frac{\varpi}{2\pi}$$

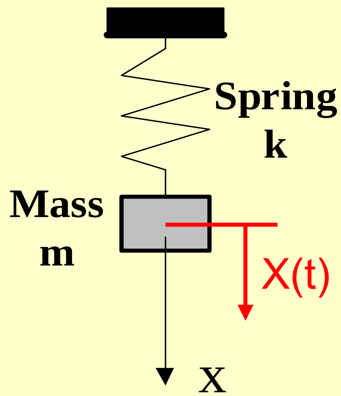

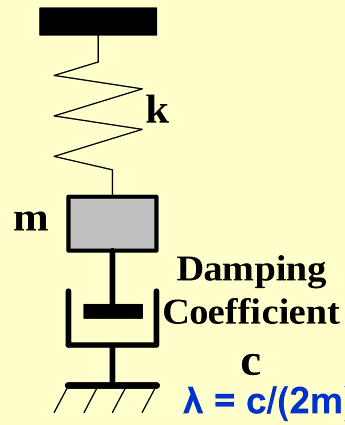

λ = c/(2m)

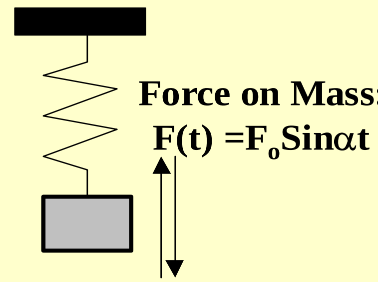

X(t) = instantaneous position of the mass, or the displacement of the mass at time t.
X(t) is the solution of the following differential equation with C_1 and C_2 being constants:

$$m\frac{d^2X(t)}{dt^2} + kX(t) = 0$$ Eq. (4.14) for **Case (a)** → $X(t) = C_1 \cos(\omega t) + C_2 \sin(\omega t)$

$$m\frac{d^2X(t)}{dt^2} + c\frac{dX(t)}{dt} + kX(t) = 0$$ Eq. (4.19) for **Case (b)** →

$$X(t) = e^{-\lambda t}\left(C_1 e^{t\sqrt{\lambda^2-\omega^2}} + C_2 e^{-t\sqrt{\lambda^2-\omega^2}}\right)$$ for $\lambda^2 - \omega^2 > 0$

$$X(t) = e^{-\lambda t}(C_1 + C_2 t)$$ for $\lambda^2 - \omega^2 = 0$

$$X(t) = e^{-\lambda t}\left(C_1 \cos\sqrt{\omega^2-\lambda^2}\,t + C_2 \sin\sqrt{\omega^2-\lambda^2}\,t\right)$$ for $\lambda^2 - \omega^2 < 0$

$$m\frac{d^2X(t)}{dt^2} + kX(t) = F_o Sin(\alpha t)$$ Eq (4.21) for **Case (c)** → $$X(t) = \frac{F_o}{\omega(\omega^2-\alpha^2)}\left(-\alpha Sin\omega t + \omega Sin\alpha t\right)$$

In a special case of which **α = ω** → **Resonant vibration:** $$X(t) = \frac{F_o}{2\omega^2} Sin\omega t - \frac{F_o}{2\omega} t Cos\omega t$$

Example 4.6 (p.121)

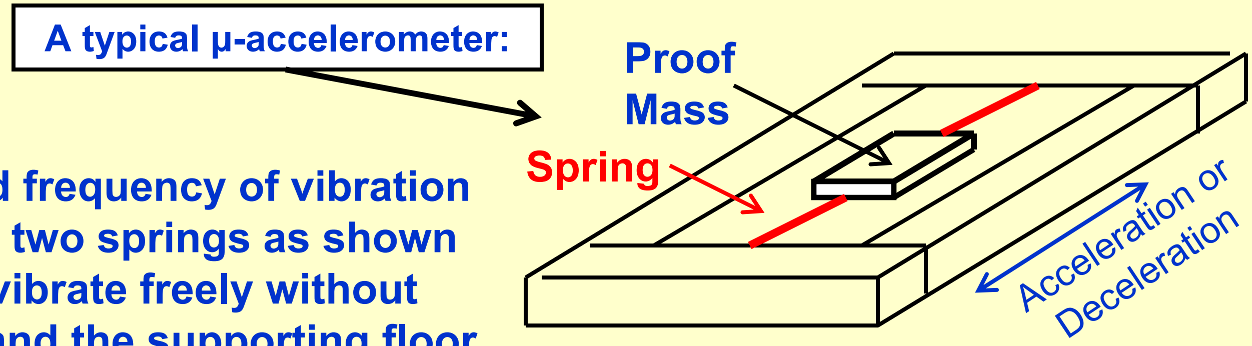

Determine the amplitude and frequency of vibration of a 10-mg mass attached to two springs as shown in the figure. The mass can vibrate freely without friction between the rollers and the supporting floor. Assume that the springs have same spring constant $k_1 = k_2 = k = 6 \times 10^{-5}$ N/m in both tension and compression. The vibration begins with the mass being pulled to the right with an amount of δ_{st} = 5 μm.
(as induced by acceleration or deceleration)

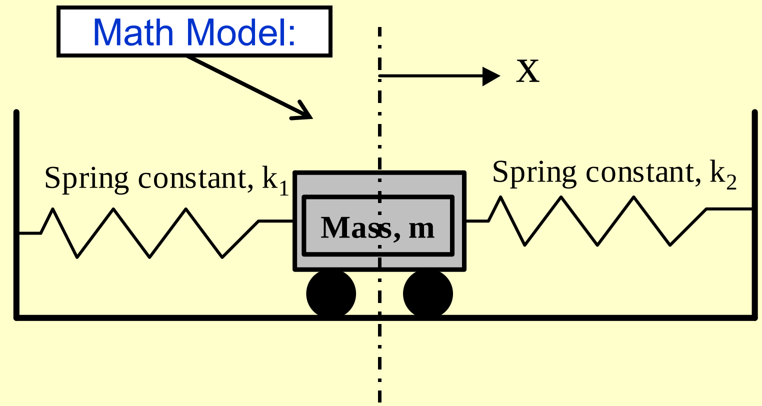

<u>Solution:</u>

We envisage that the mass in motion is subjected to two spring forces:

One force by stretching the spring ($F_1 = k_1x$) + the other by compressing ($F_2 = k_2x$).

Also If the spring constants of the two springs are equal, ($k_1 = k_2$).

And also each spring has equal magnitudes of its spring constants in tension and Compression. We will have a situation:

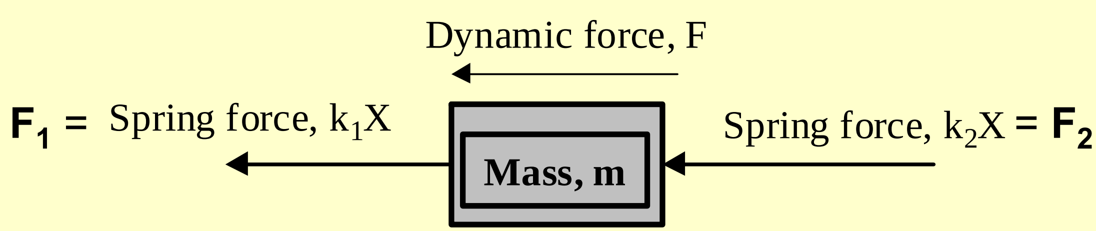

In which $F_1 = F_2$ **, This is the situation that is called "Vibration with balanced force"**

Example 4.6-Cont'd

Since the term kX(t) in the differential equation in Eq. (4.14) represent the "spring force" acting on the vibrating mass, and the spring force in this case is twice the value.

We may replace the term kX(t) in that equation with (k+k)X(t) or 2kX(t) as:

$$m\frac{d^2X(t)}{dt^2} + 2k\,X(t) = 0$$

with the conditions: $X(0) = \delta_{st}$ = 5 μm, and $\left.\frac{dX(t)}{dt}\right|_{t=0} = 0$ (zero initial velocity)

The general solution of the differential equation is: $X(t) = C_1 \cos(\omega t) + C_2 \sin(\omega t)$, in which $C_1 = \delta_{st} = 5 \times 10^{-6}$ m and $C_2 = 0$ as determined by the two conditions.

Thus, the instantaneous position of the mass is: $X(t) = 5x10^{-6} \cos(\omega t)$ meter

The corresponding maximum displacement is $X_{max} = 5x10^{-6}$ m

The circular frequency, ω in this case is:

$$\omega = \sqrt{\frac{2k}{m}} = \sqrt{\frac{(6+6)x10^{-5}}{10^{-5}}} = 3.464\ rad/s$$

Microaccelerometers

Micro accelerometers are used to measure the acceleration (or deceleration) of a moving solid (e.g. a device or a vehicle), and thereby relate the acceleration to the associated dynamic force using Newton's 2nd law: F(t) = M a(t), in which M = mass of the moving solid and a(t) = the acceleration at time t.

An accelerator requires: a proof mass (m), a spring (k), and damping medium (c), in which k = spring constant and c = damping coefficient.

Early design of microaccelerators have the following configurations:

Conventional accelerometers →

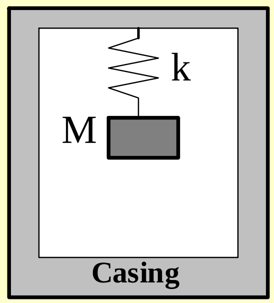

(a) Spring-mass

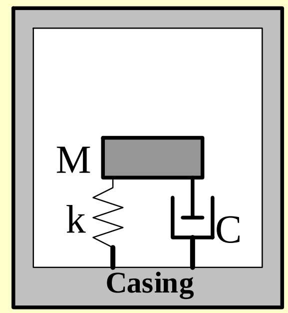

(b) Spring-mass-dashpot

Microaccelerometers →

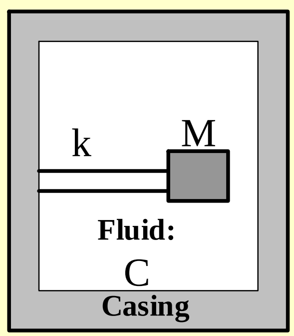

(c)Beam-Mass

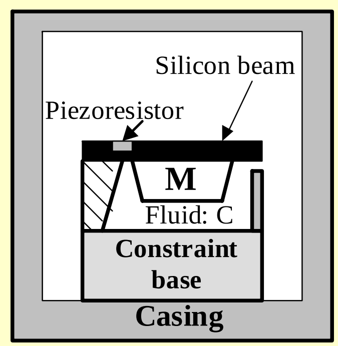

(d) Beam-attached mass

Design Theory of Accelerometers

In a real-world application, the accelerometer is attached to a moving solid. We realize that the amplitude of the vibrating proof mass in the accelerometer may not necessarily be in phase with the amplitude of vibration of the moving solid (the base).

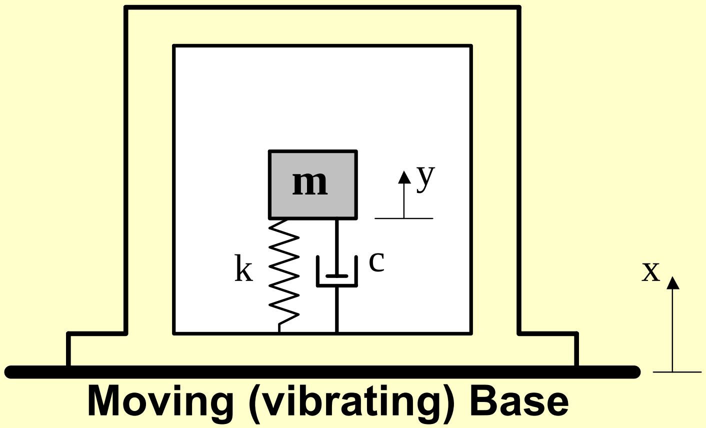

x(t) = the amplitude of vibration of the base

Assume x(t) = X sin(ωt) – a harmonic motion

y(t) = the amplitude of vibration of proof mass in the accelerometer from its initial static equilibrium position.

z(t) = the relative (or net) motion of the proof mass, m

Hence **z(t) = y(t) – x(t)** (4.26)

The governing differential equation for z(t) is:

$$m\ddot{z}(t) + c\dot{z}(t) + kz(t) = mX\,\omega^2\,Sin\omega t \qquad (4.29)$$

Once z(t) is obtained from solving the above equation with appropriate initial conditions, we may obtain the acceleration of the proof mass in a relative movement as:

$$\ddot{z}(t) = \frac{d^2 z(t)}{dt^2}$$

Design Theory of Accelerometers-Cont'd

The solution of z(t) with initial conditions: z(0) = 0 and $\left.\frac{dz(t)}{dt}\right|_{t=0} = 0$ is:

$$\mathbf{z(t) = Z\sin(\omega t - \Phi)} \qquad (4.30)$$

in which the maximum magnitude, Z of z(t) is:

$$Z = \frac{\omega^2 X}{\sqrt{\left(\frac{k}{m} - \omega^2\right)^2 - \left(\frac{\omega c}{m}\right)^2}} \qquad (4.31a)$$

where X = maximum amplitude of vibration of the base. The phase angle difference, Φ between the input motion of x(t) and the relative motion, z(t) is:

$$\phi = \tan^{-1} \frac{\frac{\omega c}{m}}{\frac{k}{m} - \omega^2} \qquad (4.31b)$$

Design Theory of Accelerometers-Cont'd

An alternative form for the maximum amplitude of the relative vibration of the proof mass in the accelerometer, Z is:

$$Z = \frac{\omega^2 X}{\omega_n^{\;2} \sqrt{\left[1 - \left(\frac{\omega}{\omega_n}\right)^2\right]^2 + \left[2h \frac{\omega}{\omega_n}\right]^2}} \qquad (4.32a)$$

where ω = frequency of the vibrating base; ω_n is the circular natural frequency of the accelerometer with:

$$\omega_n = \sqrt{\frac{k}{m}}$$

The parameter, $h = c/c_c$ = the ratio of the damping coefficients of the damping medium in the micro accelerometer to its critical damping with $c_c = 2m\omega_n$

For the case of which the frequency of the vibrating base, ω is much smaller than the natural frequency of the accelerometer, ω_n, i.e. **$\omega \ll \omega_n$**:

$$Z \doteq -\frac{a_{base,\max}}{\omega_n^2} \qquad (4.33)$$

Design of Accelerometers

The engineer may follow the following procedure in the design of appropriate microaccelerometer for a specific application:

(1) Set the target maximum amplitude of vibration, X of the base (e.g., a vehicle or a machine) and the anticipated frequency of vibration, i.e. ω.

(2) Select the parameters: m, k, c and calculate ω_n and h.

(3) Compute the maximum relative amplitude of vibration of the proof mass, Z using the available formulas.

(4) Check if the computed Z is within the range of measurement of the intended transducer, e.g. piezoresistors, piezoelectric, etc.

(5) Adjust the parameters in Step (2) if the computed Z is too small to be measured by the intended transducer.

Design of Accelerometers-Cont'd

Spring constant of simple beams

Simple beams are commonly used to substitute the coil springs in microaccelerometers. It is thus necessary to calculate the “equivalent spring constant” of these beam springs.

Since the spring constant of an elastic solid, whether it is a coil spring or other geometry, is define as **k = Force/Deflection** (at which the force is applied), we may derive the spring constant for the three simple beam configurations to be:

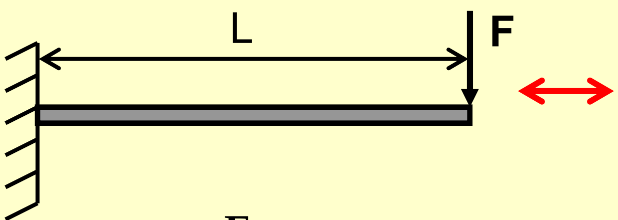

$$k = \frac{Applied force, F}{Induced deflection, \delta} = \frac{3EI}{L^3}$$

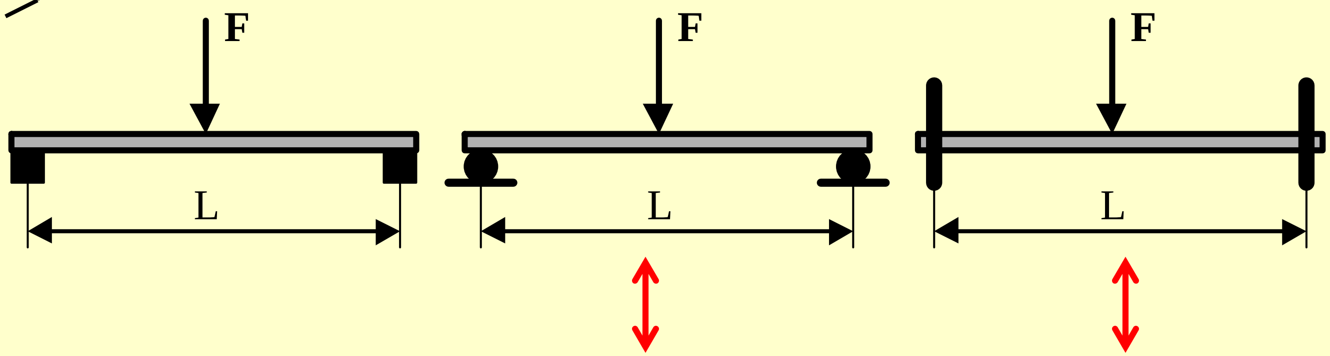

$$k = \frac{48EI}{L^3}$$

$$k = \frac{192EI}{L^3}$$

in which E = Young's modulus; I = section moment of inertia of beam cross-section.

Design of Accelerometers-Cont'd

Damping coefficients

In microaccelerometers, the friction between the immersed fluid and the contacting surfaces of the moving proof mass provides damping effect.

There are two types of "damping" induced by this affect:

(a) Squeeze film damping:

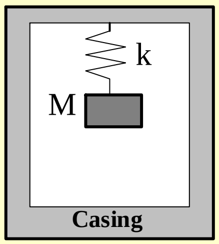

(a) Spring-mass

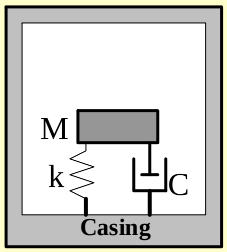

(b) Spring-mass-dashpot

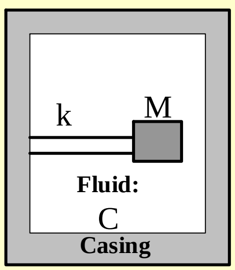

(c)Beam-Mass

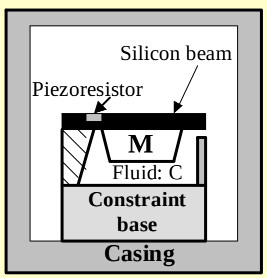

(d) Beam-attached mass

(b) Micro damping in shear:

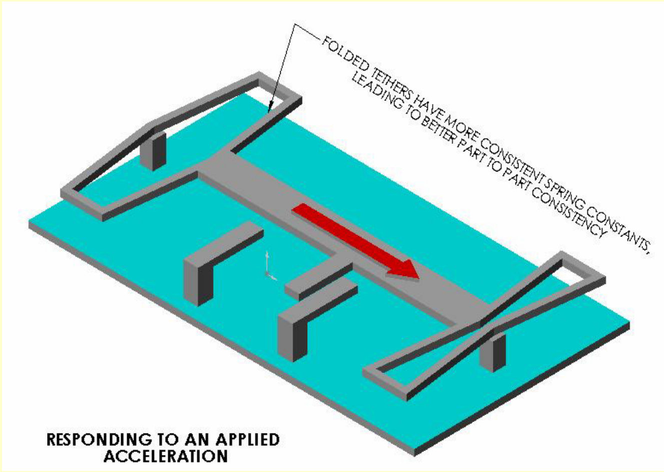

Numerical values of damping coefficients depend on the geometry of the vibrating solid components and the fluid that surround them.

Example 4.10 (p.133)

Determine the displacement of the proof mass from its neutral equilibrium
Position of a balanced-force microaccelerometer illustrated below:

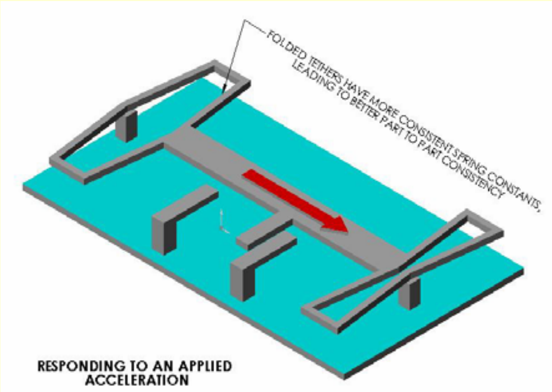

The structure of this accelerometer
can be graphically represented below:

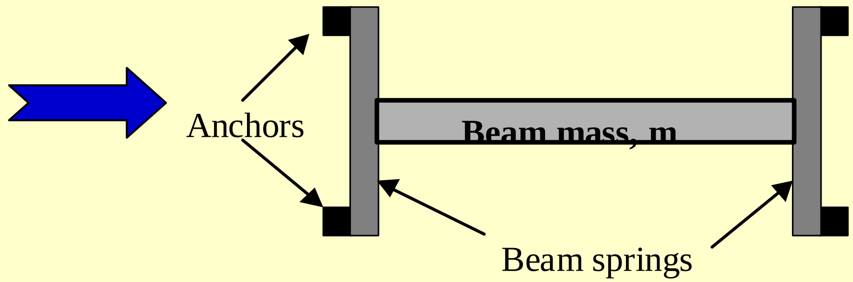

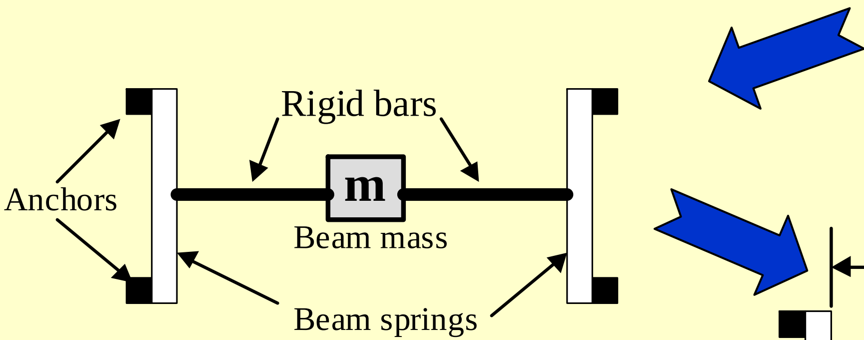

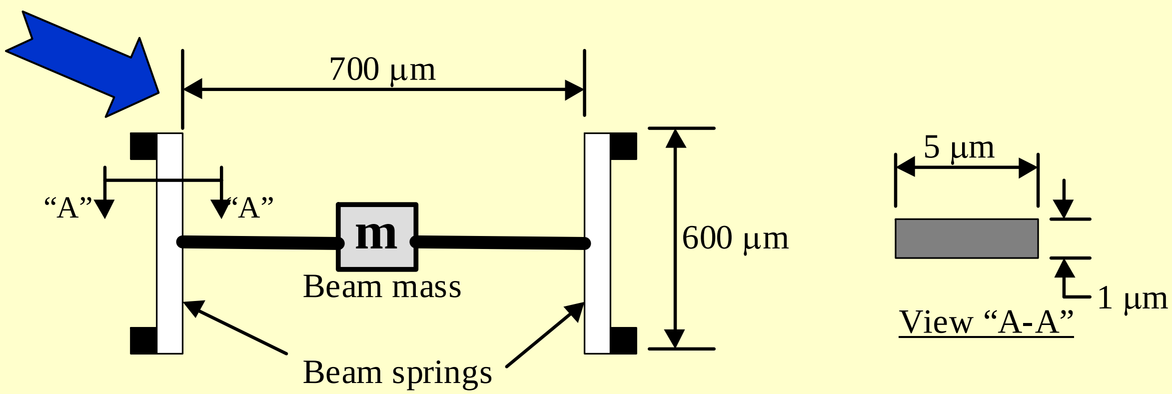

With: b = 10^{-6} m, B = 100×10^{-6} m, L = 600×10^{-6} m and L_b = 700×10^{-6} m, we have from Example 4.9 the moment of inertia of beam spring cross-section to be:
I = 10.42×10^{-24} m^4

For simply-support beam spring: k = 0.44 N/m, ω_n = 23,380 rad/s
For rigidly fixed beam spring: k = 1.76 N/m and ω_n = 147,860 rad/s

Assume the "rigidly held beam spring case is adopted, the equation of motion of the proof mass is:

$$\frac{d^2X(t)}{dt^2} + \omega^2 X(t) = 0$$

with initial conditions: $X(t)\big|_{t=0} = 0$ initial position

, and $\left.\frac{dX(t)}{dt}\right|_{t=0} = 50\ km/h = 13.8888\ m/s$ initial velocity

The solution of the equation of motion with the given initial conditions is:

$$X(t) = 9.3932x10^{-5}\ Sin(147.86t)$$

leading to X(1 ms) = -2.597×10^{-5} m or 26 μm opposite to the direction of deceleration.

(a) Damping coefficient in a squeeze film:

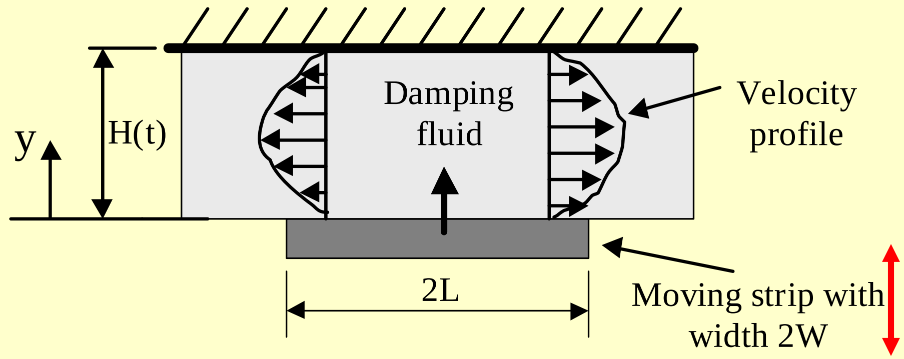

The **damping coefficient** can be found to be: $c = 16\, f\left(\frac{W}{L}\right) W^3 L\, H_o^3$
where H_o = nominal thickness of the thin film.

The function, $f\left(\frac{W}{L}\right)$ can be obtained by the following Table 4.2:

$\frac{W}{L}$	$f\left(\frac{W}{L}\right)$	$\frac{W}{L}$	$f\left(\frac{W}{L}\right)$
0	1.00	0.6	0.60
0.1	0.92	0.7	0.55
0.2	0.85	0.8	0.50
0.3	0.78	0.9	0.45
0.4	0.72	1.0	0.41
0.5	0.60		

Example 4.11 (p.136)

Estimate the damping coefficient of a micro accelerometer using a cantilever beam spring as illustrated.

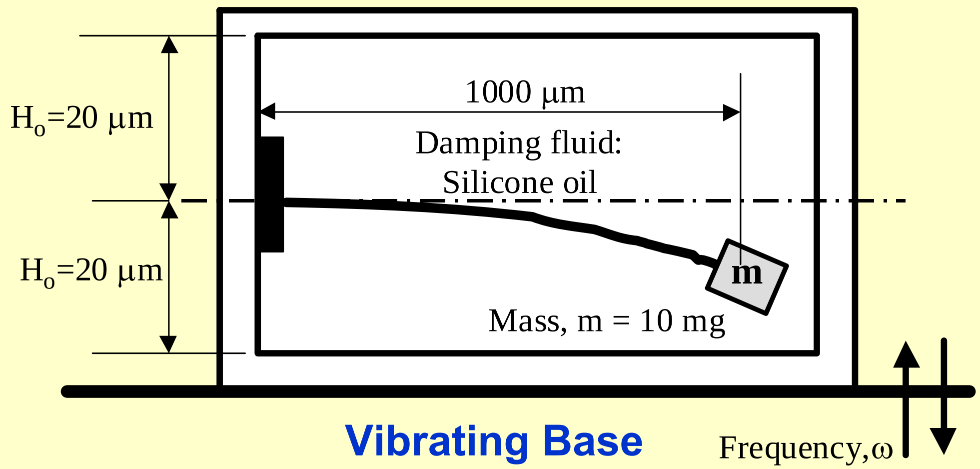

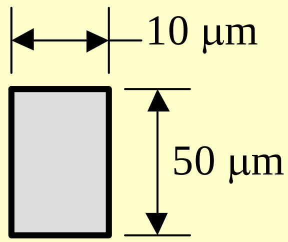

Beam cross-section

We have the beam dimensions as: 2L = 1000x10^{-6} m and 2W = 10x10^{-6} m →

W/L = 0.01 → F(W/L) = 0.992 from Table 4.2.

The nominal film thickness, H_o = 20x10^{-6} m. From Eq. (4.38) we get: c = 8x10^{-33} N-s/m.

(b) Micro damping in shear:

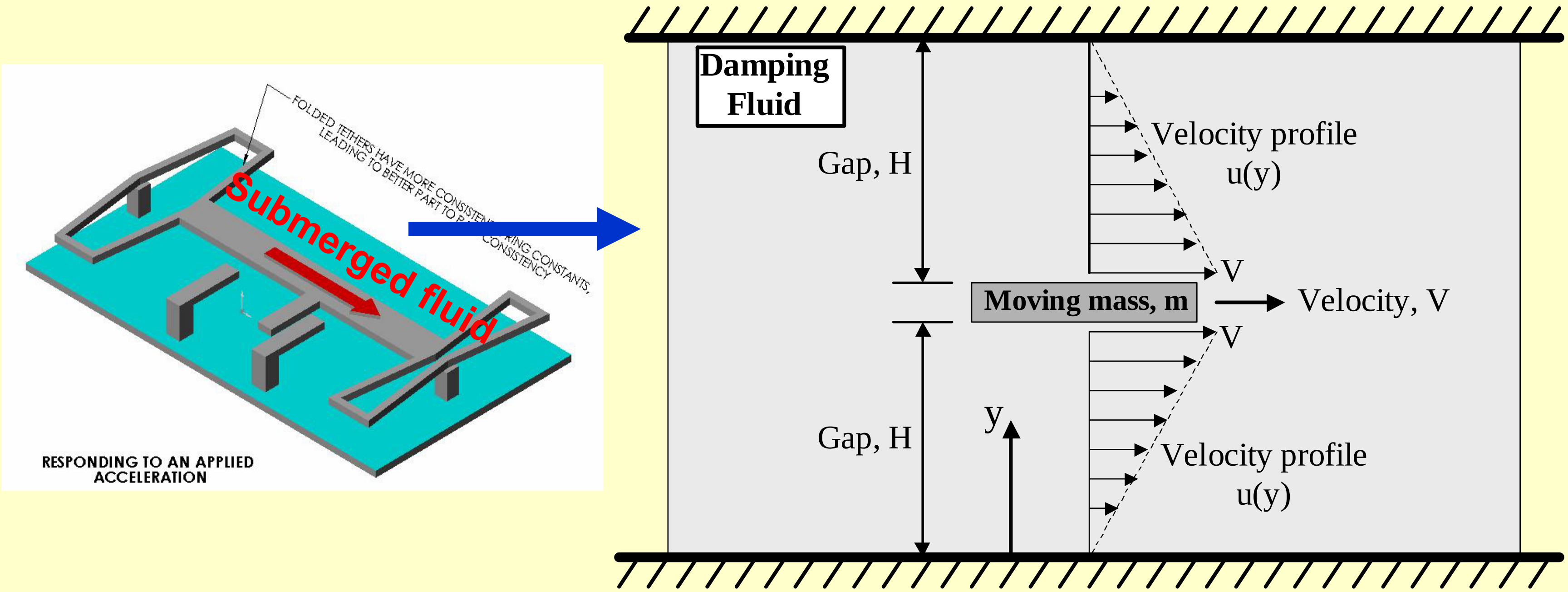

The damping coefficient, c may be computed from the following expression:

$$c = \frac{F_D}{V} = \frac{2\mu L b}{H} \qquad \text{N-s/m} \qquad (4.43)$$

where L = length of the beam (m); b = the width of the beam (m); H = gaps (m)
μ = dynamic viscosity of the damping fluid (N-s/m^2), see Table below.

Dynamic Viscosity for Selected Fluids (in 10^{-6} N-s/m^2)

A.Compressible fluids:

	0°C	20°C	60°C	100°C	200°C
Air	17.08	18.75	20.00	22.00	25.45
Helium	18.60	19.41	21.18	22.81	26.72
Nitrogen	16.60	17.48	19.22	20.85	24.64

B. Non-compressible fluids:

	0°C	20°C	40°C	60°C	80°C
Alcohol	1772.52	1199.87	834.07	591.80	432.26
Kerosene	2959.00	1824.23	1283.18	971.96	780.44
Fresh water	1752.89	1001.65	651.65	463.10	351.00
Silicone oil*		740			

Example 4.12 (p.139)

Estimate the damping coefficient in a balanced-force microaccelerometer as illustrated, with (a) air, and (b) silicone oil as damping media. The sensor operates at 20°C.

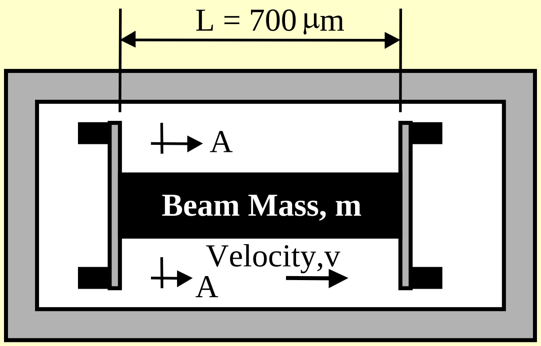

Top View

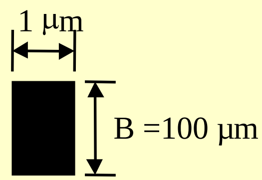

View "A-A"

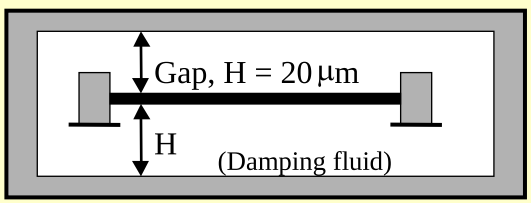

Elevation

Eq. (4.43) is used for the solutions.

We have L = 700x10^{-6} m and b = 5x10^{-6} m and the gap, H = 10x10^{-6} m.

The dynamic viscosities for air and silicone oil at 20°C may be found from Table 4.3 to be:

μ_{air} = 18.75x10^{-6} N-s/m^2, and

μ_{si} = 740x10^{-6} N-s/m^2

Thus, the damping coefficient with air is:

$$c = \frac{2\mu_{air} Lb}{H} = \frac{2(18.75x10^{-6})(700x10^{-6})(100x10^{-6})}{20x10^{-6}} = 2.625x10^{-12} \text{ N-s/m}$$

and the damping coefficient with silicone oil is:

$$c = \frac{2\mu_{si} Lb}{H} = \frac{2(740x10^{-6})(700x10^{-6})(100x10^{-6})}{20x10^{-6}} = 1.036x10^{-10} \text{ N-s/m}$$

Example 4.14 Design of an inertia sensor for airbag deployment system in automobiles (p.142)

Two vehicles with respective masses, m_1 and m_2 traveling in opposite directions at velocities V_1 and V_2 as illustrated. Each vehicle is equipped with an inertia sensor (or micro accelerometer) built with cantilever beam as configured in Example 4.8.

Estimate the *deflection* of the proof mass in the sensor in vehicle 1 with mass m_1, and also the *strain* in the two piezoresistors embedded underneath the top and bottom surfaces of the beam near the support after the two vehicles collide.

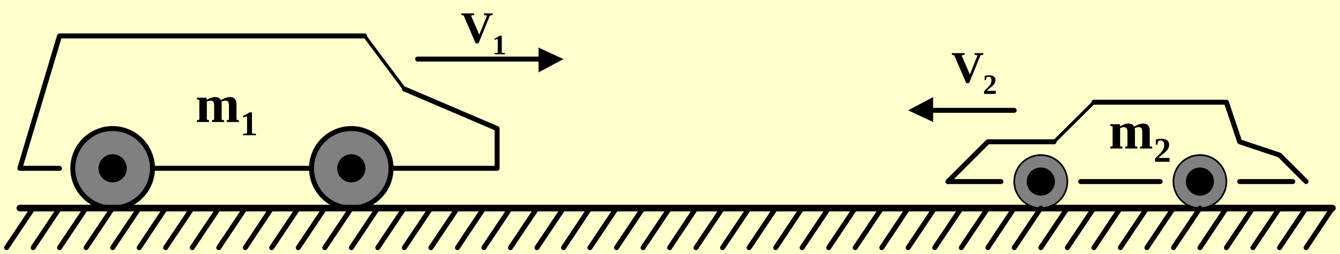

m_1 = 12,000 Kg, m_2 = 8000 Kg; V_1 = V_2 = 50 Km/h

Solution:

Let us first look into the property of the "beam spring" used in Example 4.8, and have:

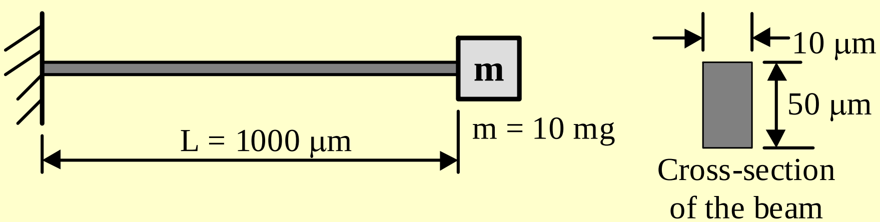

$$I = \frac{(10x10^{-6})(50x10^{-6})^3}{12} = 0.1042x10^{-18} \quad \text{m}^4$$

$$k = \frac{3(190000x10^{6})(0.1042x10^{-18})}{(1000x10^{-6})^3} = 59.39 \quad \text{N/m}$$

$$\omega_n = \sqrt{\frac{k}{m}} = \sqrt{\frac{59.39}{10^{-5}}} = 2437 \quad \text{Rad/s}$$

Postulation: The two vehicles will tangle together after the collision, and the entangled vehicles move at a velocity V as illustrated:

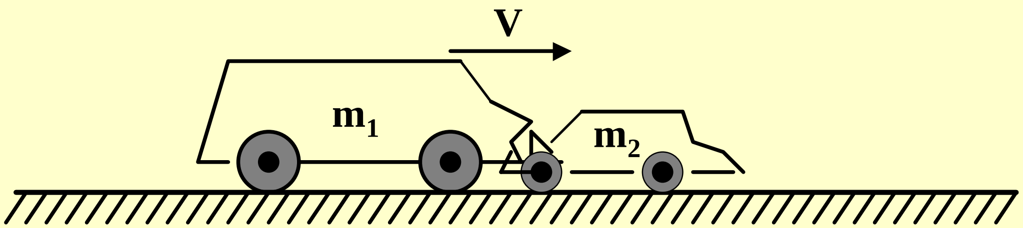

Thus, by law of conservation of momentum, we should have the velocity of the entangled vehicles to be:

$$V = \frac{m_1 V_1 - m_2 V_2}{m_1 + m_2} = \frac{12000x50 - 8000x50}{12000 + 8000} = 10 \quad \text{Km/h}$$

The decelerations of the two vehicles are:

$\ddot{X} = \dfrac{V - V_1}{\Delta t}$ for vehicle with m_1, and $\ddot{X} = \dfrac{V - V_2}{\Delta t}$ for vehicle with m_2

in which Δt = time required for deceleration.

Let us assume that it takes 0.5 second for vehicle 1 to decelerate from 50 Km/hr to 10 Km/hr after the collision. Thus the time for deceleration of the vehicle m_1 is Δt = 0.5 second, in the above expressions.

We may thus compute the deceleration of vehicle m1 to be:

$$\ddot{X} = a_{base} = \frac{(10-50)x10^3/3600}{0.5} = -22.22 \quad \text{m/s}^2$$

Let ω = frequency of vibration of the vehicles.

Assume that $\omega << \omega_n$, (ω_n =the natural frequency of the accelerometer = 2437 rad/s^2).

Consequently, we may approximate the amplitude of vibration of the proof mass in the accelerometer using Eq. (4.33) as:

$$Z \doteq -\frac{a_{base}}{\omega_n^2} = -\frac{-22.22}{(2437)^2} = 3.74x10^{-6} \quad \text{m, or } 3.74\ \mu\text{m}$$

We thus have the maximum deflection of the cantilever beam of 3.74 μm at the free end in the accelerometer. The equivalent force acting at the free-end is:

$$F = \frac{3EIZ}{L^3} = \frac{3(1.9x10^{11})(0.1042x10^{-18})(3.74x10^{-6})}{(1000x10^{-6})^3} = 2.2213x10^{-4} \quad \text{N}$$

From which, we may compute the maximum bending moment at the support to be:

$M_{max} = FL$ in which L is the length of the beam. The numerical value of M_{max} is:

$$M_{max} = 2.2213x10^{-4}\, x10^{-3} = 2.2213x10^{-7}$$ N-m

The corresponding maximum stress,σ_{max} is:

$$\sigma_{max} = \frac{M_{max} C}{I} = \frac{(2.2213x10^{-7})(25x10^{-6})}{0.1042x10^{-18}} = 532.95x10^{5}$$ N/m² or Pa

and the corresponding max. strain is obtained by using the Hooke's law to be:

$$\varepsilon_{max} = \frac{\sigma_{max}}{E} = \frac{53.30x10^{5}}{190x10^{9}} = 02.81x10^{-4} = 0.0281\%$$

Depending on the transducer used in the microaccelerometer, the maximum stress, $\boldsymbol{\sigma_{max}}$ can produce a resistance change in the case of "piezoresistors". Alternatively, the maximum strain, $\boldsymbol{\varepsilon_{max}}$ will produce a change of voltage if "piezoelectric crystal" is used as the transducer. (Detail descriptions available in Chapter 7)

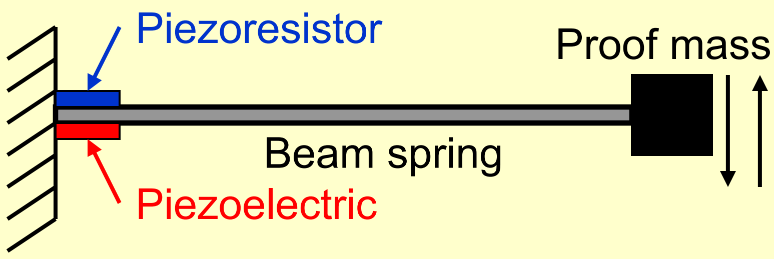

THERMOMECHANICS

Thermomechanics relates mechanical effects (stresses, strains and deformation) induced by thermal forces (temperature difference or heat flow) – common phenomena in microsystems.

Other thermal-induced effects on solid physical behavior:

1. Material property changes:

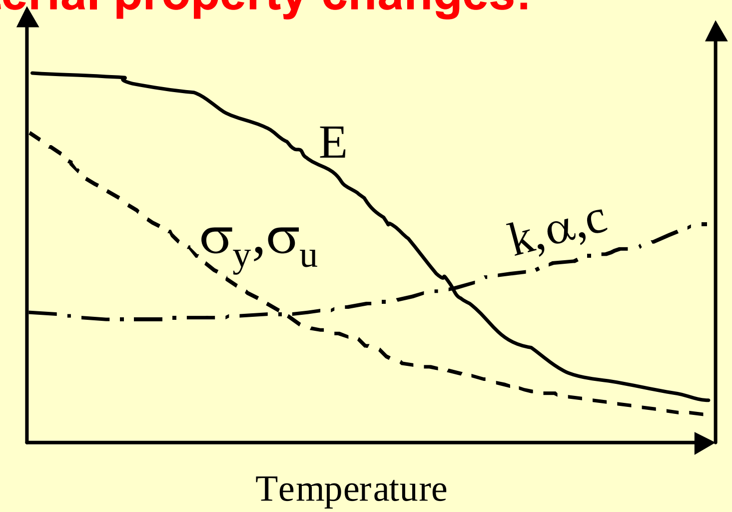

LEGEND:
E = Young's modulus
σ_y= Plastic yield strength
σ_u= Ultimate tensile strength
k = Thermal conductivity
c = Specific heat
α = Coefficient of thermal expansion

Table 4-4 Temperature-Dependent Thermophysical Properties of Silicon

Temperature, K	Specific Heat, J/g-K	Coefficient of Thermal Expansion, 10^{-6}/K
200	0.557	1.406
220	0.597	1.715
240	0.632	1.986
260	0.665	2.223
280	0.691	2.432
300	0.713	2.616
400	0.785	3.253
500	0.832	3.614
600	0.849	3.842

Other thermal-induced effects on solid physical behavior (cont'd):

2. Creep deformation:

Structure changes its shape with time without increase of mechanical load:

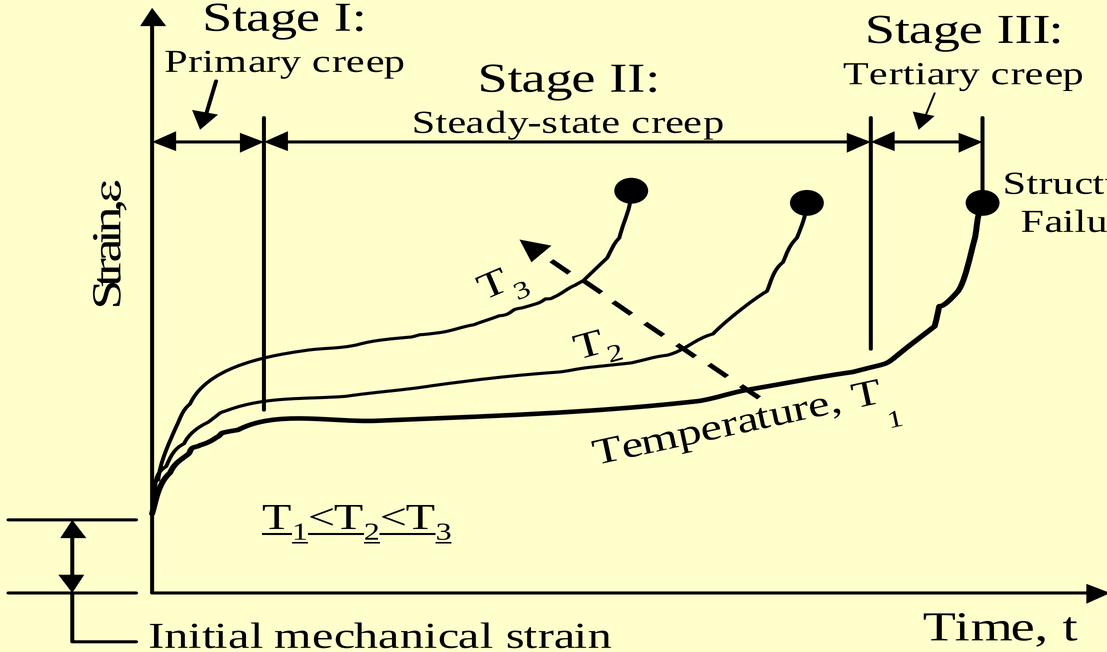

Silicon and silicon compounds have strong creep resistance. Creep is not a problem.

It is the polymer materials and many solder alloys that have this problem.

Thermal Stress and Strain Analysis

A simple physical phenomenon:

Solids expand when they are heated up and contract when they are cooled down.

Constraints to such shape change will cause "stresses" in the solids.

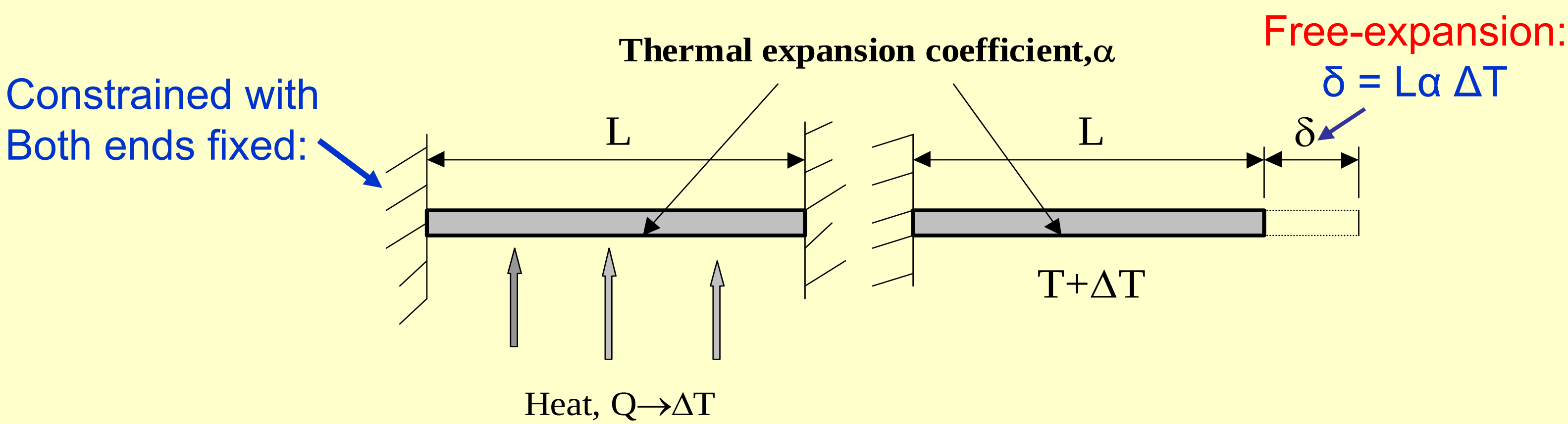

Induced thermal stress with both ends fixed: $\sigma_T = -E\,\varepsilon_T = -\alpha\, E\, \Delta T$

where E = Young's modulus; ε_T = thermal strain; ΔT = temperature rise from reference temperature (room temperature)

Application of Thermal Expansion of Bi-strip Materials in MEMS:

(S. Timoshenko "Analysis of Bi-metal thermostats," J. of Optical society of America, 11, 1925, 00. 233-255)

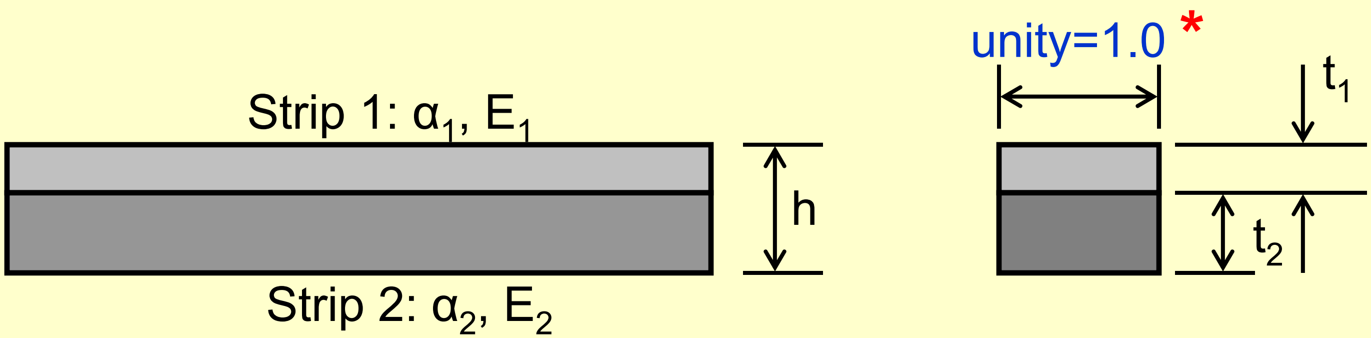

The bi-metallic strip will bend when it is subjected to a temperature rise of $\Delta T = T - T_o$.
The strip will bend into the following shape if $t_2 > t_1$ and $\alpha_2 > \alpha_1$:

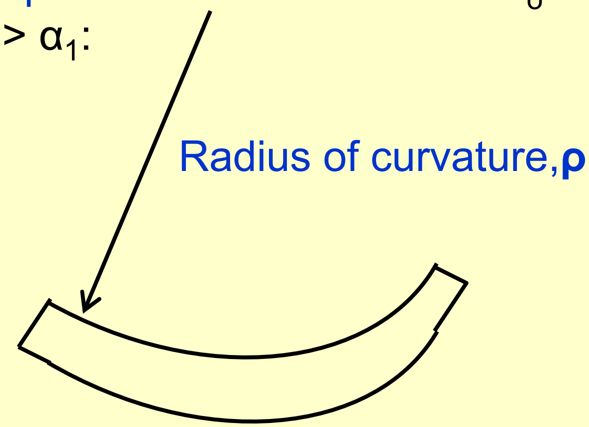

In which ρ = radius of curvature of the bent strip.

If we let: **m** = t_1/t_2 and **n** = E_1/E_2.

Since the strips are of rectangular shape with a unity width, the moment of inertia for strip 1 and strip 2 are:

$$I_1 = \frac{t_1^3}{12} \quad and \quad I_2 = \frac{t_2^3}{12}$$

The radius of curvature, ρ can be obtained by the following expression:

$$\frac{1}{\rho} = \frac{6(1+m)^2(\alpha_1 - \alpha_2)\Delta T}{h\left[3(1+m)^2 + (1+mn)\left(m^2 + \frac{1}{mn}\right)\right]} \qquad \text{Eq. (4.49)}$$

✓

***The unity width is used to simplify the derivation. The width of the strip does not affect the curvature of the bent beam.**

For a special case when $t_1 = t_2 = h/2$ $\longrightarrow$ m = 1, we have:

$$\frac{1}{\rho} = \frac{24(\alpha_2 - \alpha_1)\Delta T}{h\left(14 + n + \frac{1}{n}\right)}$$

Further, if $E_1 \approx E_2$ $\rightarrow$ $n \approx 1$, we may further simplify the expression to give:

$$\frac{1}{\rho} = \frac{3}{2}\frac{(\alpha_2 - \alpha_1)\Delta T}{h}$$

or in another way:

$$\checkmark \quad \rho = \frac{2h}{3(\alpha_2 - \alpha_1)\Delta T}$$

which is identical to Eq. (4.51) in the textbook.

Example 4.17 (p.154)

A micro actuator made up by a bi-layered strip using oxidized silicon beam is illustrated below. A resistant heating film is deposited on the top of the oxide layer. Estimate the interfacial force and the movement of the free-end of the strip with a temperature rise, $\Delta T = 10^oC$. Use the following material properties:

Young's modulus: $E_{SiO2} = E_1 = 385000$ MPa; $E_{Si} = E_2 = 190000$ MPa

Coefficients of thermal expansion: $\alpha_{SiO2} = \alpha_1 = 0.5x10^{-6}/^oC$; $\alpha_{Si} = \alpha_2 = 2.33x10^{-6}/^oC$

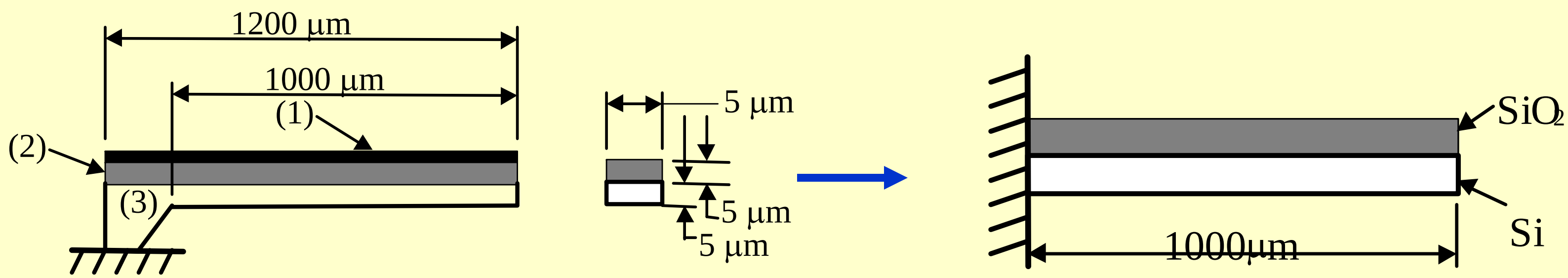

(1) Electric resistant heater
(2) Silicon dioxide coating
(3) Silicon

Solution:

Use Eq. (4.49) to compute the interface force: $F = \dfrac{(\alpha_2 - \alpha_1)T}{8} \dfrac{hb}{\left(\dfrac{1}{E_1} + \dfrac{1}{E_2}\right)}$

$$F = \frac{(2.33x10^{-6} - 0.5x10^{-6})10}{8} \frac{(10x10^{-6})(5x10^{-6})}{\dfrac{1}{385000x10^6} + \dfrac{1}{190000x10^6}} = 14.55x10^{-6} \text{ N}$$

The radius of curvature of the bent beam can be computed from Eq. (4.50):

$$\rho = \frac{2(10x10^{-6})}{3(2.33x10^{-6} - 0.5x10^{-6})10} = 0.3643 \text{ m}$$

In reality, however, we will design the actuator for the end movement to the desired amount.

Thus, we have to translate the radius of curvature of the actuated beam to that amount by taking the following approach:

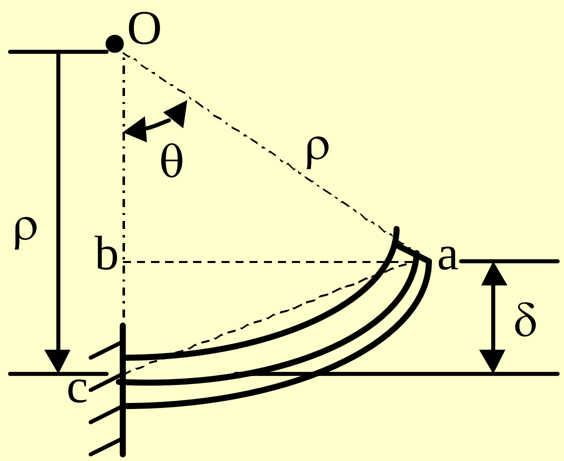

The angle, θ can be evaluated by the following approximation:

$$\frac{\theta}{arc(ac)} \approx \frac{\theta}{line(ac)} = \frac{\theta}{1000x10^{-6}} = \frac{360}{2.2878}$$

from which we may compute the end movement, δ to be:

$$\delta \approx \rho - \rho Cos\theta = 0.3643 - 0.3643 Cos(0.1574^o) = 1.373x10^{-6} \text{ m, or } 1.37\ \mu\text{m}$$

Example 4.18 (p.156)

If the same bi-layer beam described in Example 4.17 is used, but with the thickness of the SiO_2 film being reduced to 2 μm and the total thickness, h remains to be 10 μm, meaning the thickness of the Si beam being increased to 8 μm. Estimate what will be the change in the actuated strip.

Solution:

We have in this case, $t_1 = t_{SiO2} = 2\times10^{-6}$ m and $t_2 = t_{Si} = 8\times10^{-6}$ m, which leads to:

$m = t_1/t_2 = 2/8 = 0.25$, and $n = E_1/E_2 = 385000/190000 = 2.026$.

By using the previously derived equation to compute the radius of curvature:

$$\frac{1}{\rho} = \frac{6\left(1+m\right)^2\left(\alpha_1-\alpha_2\right)\Delta T}{h\left[3\left(1+m\right)^2+\left(1+mn\right)\left(m^2+\frac{1}{mn}\right)\right]}$$

Thus, by substituting the appropriate values into the above expression, we get:

$$\frac{1}{\rho} = \frac{6\left(1+0.25\right)^2\left(0.5\times10^{-6}-2.33\times10^{-6}\right)\times10}{10\times10^{-6}\left[3\left(1+0.25\right)^2+\left(1+0.25\times2.026\right)\left(0.25^2+\frac{1}{0.25\times2.026}\right)\right]} = -2.187$$

or **ρ = - 0.4572 m**, which leads to the end deflection, **δ = 1.73 μm** (downward with –ve ρ)

Design of thermal-actuated relay using bi-layer beams:

We realize the fact that the actuation of this type of relays is due to the fact that dissimilar materials with different coefficient of thermal expansion are the reason for its bending when it is subjected to a temperature rise.

In the above formulation in Eq. (4.49), we realize that the “Stiffness” ratio, i.e. $n = E_1/E_2$ is a part of the equation used to calculate the radius of curvature of the bent beam.

The curve at the right depicts the effect of the stiffness relating to the thickness ratio: $m = t_1/t_2$ that could affect the strip movement, despite the fact that

$$\alpha_{si}\ (= \alpha_2)\ /\ \alpha_{SiO2}\ (= \alpha_1) = 5$$

But $E_{si}\ (=E_2)/E_{SiO2}\ (=E_1) = 0.4935$

Higher $n = t_1/t_2$ means thicker SiO_2 portion and thus stiffer the bi-layer strip.

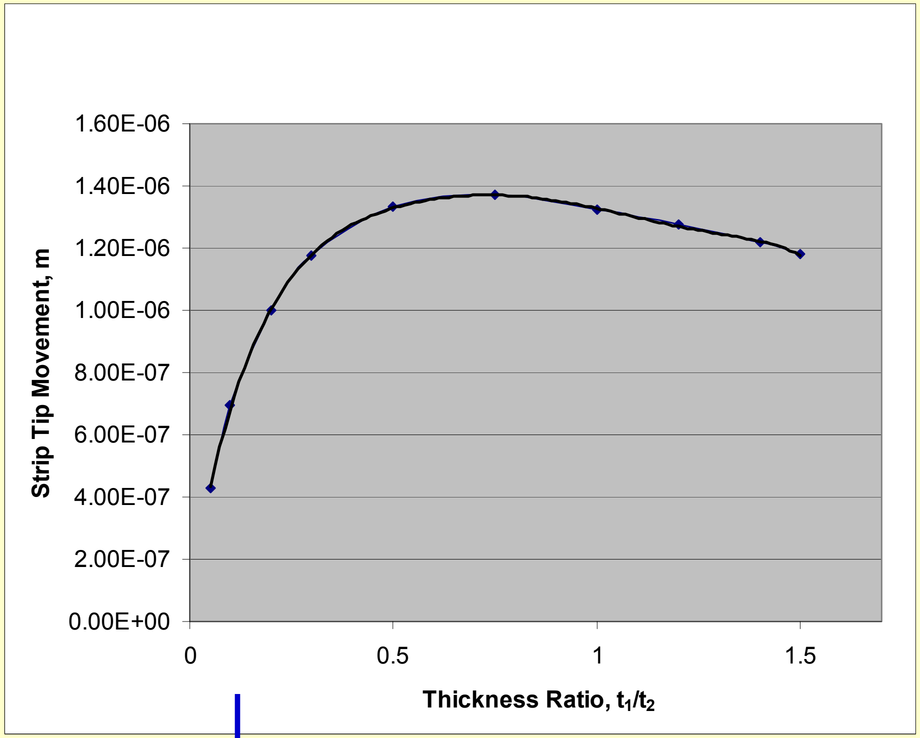

Thicker SiO_2 layer

Thermal Stresses (and Strains)

Thermal stresses and strains in a solid structure can be induced in three conditions:

(1) Uniform temperature rise (or fall) in structure with constrained boundaries;

(2) Non-uniform temperature in structure with partial boundaries constrained;

(3) Non-uniform temperature in structure with no constrained boundaries.

Designation of stresses (strains) in a solid in a 3-dimensional space:

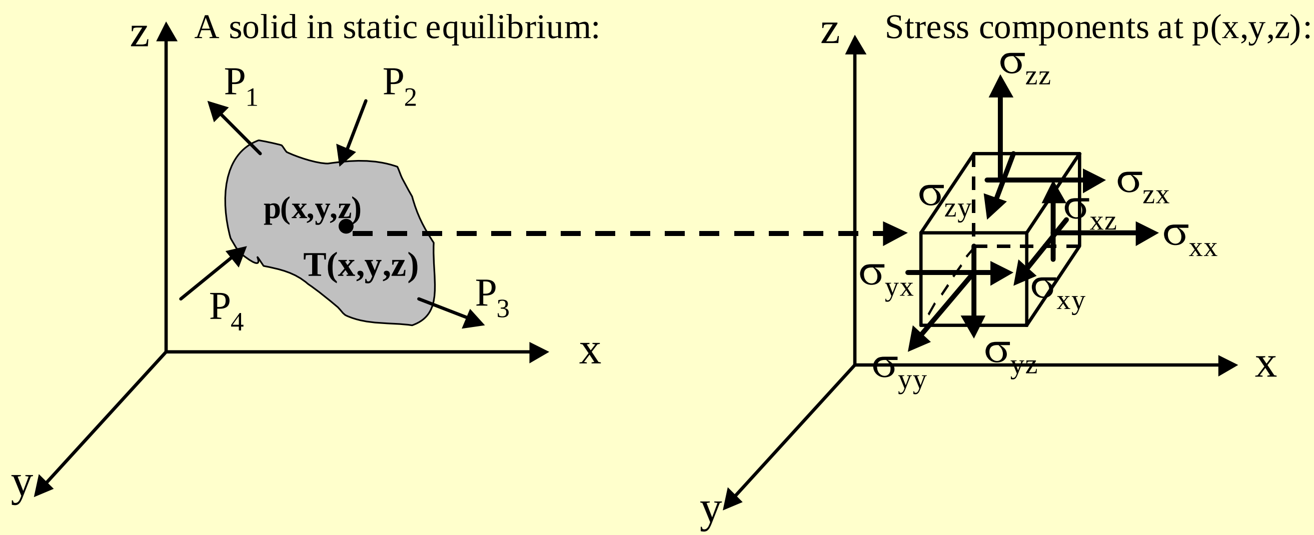

The stress component: σ_{xy} in which the subscript **x** = the axis that is perpendicular to the plane of action. The subscript **y** = the direction of the stress component.

Thermal Stresses in Thin Plates with Temperature Variation Through the Thickness

(p.158)

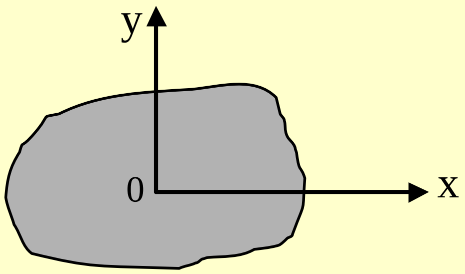

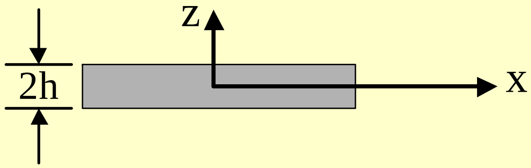

Being a **thin** plate, the stress components along the z-axis are negligible. We thus have the situation:

σ_{xx} (x,y,z) = f_1(z) and **σ_{yy} (x,y,z) = f_2(z)**

$\sigma_{zz} = \sigma_{xz} = \sigma_{yx} = \sigma_{yz} = 0$ with temperature variation,

with T = T(z) is specified.

Thermal stresses

$$\sigma_{xx} = \sigma_{yy} = \frac{1}{1-\nu}\left[-\alpha E T(z) + \frac{1}{2h} N_T + \frac{3z}{2h^3} M_T\right] \qquad (4.52)$$

Thermal strains

$$\varepsilon_{xx} = \varepsilon_{yy} = \frac{1}{E}\left[\frac{1}{2h} N_T + \frac{3z}{2h^3} M_T\right] \qquad (4.53a)$$

$$\varepsilon_{zz} = -\frac{2\nu}{(1-\nu)E}\left(\frac{N_T}{2h} + \frac{3z}{2h^3} M_T\right) + \frac{1+\nu}{1-\nu}\alpha T(z) \qquad (4.53b)$$

$\varepsilon_{xy} = \varepsilon_{yz} = \varepsilon_{zx} = 0$

where **N_T = thermal force** = $N_T = \alpha E \int_{-h}^{h} T(z)dz$ (4.55a)

and **M_T = thermal moment** = $M_T = \alpha E \int_{-h}^{h} T(z) z dz$ (4.55b)

Displacement components

In x-direction: $$u = \frac{x}{E}\left(\frac{N_T}{2h} + \frac{3z}{2h^3}M_T\right)$$ (4.54a)

In y-direction: $$v = \frac{y}{E}\left(\frac{N_T}{2h} + \frac{3z}{2h^3}M_T\right)$$ (4.54b)

In z-direction: $$w = -\frac{3M_T}{4h^3E}\left(x^2 + y^2\right) + \frac{1}{(1-\nu)E}\left[(1+\nu)\alpha E\int_o^z T(z)dz - \frac{\nu z}{h}N_T - \frac{3\nu z^2}{2h^3}M_T\right]$$ (4.54c)

with thermal force, N_T and thermal moment, M_T to be:

$$N_T = \alpha E\int_{-h}^{h} T(z)dz$$ (4.55a)

and $$M_T = \alpha E\int_{-h}^{h} T(z)zdz$$ (4.55b)

Thermal Stresses in Beams with -Temperature Variation in the Depth

Let us consider the situation as illustrated below, with z = depth direction:

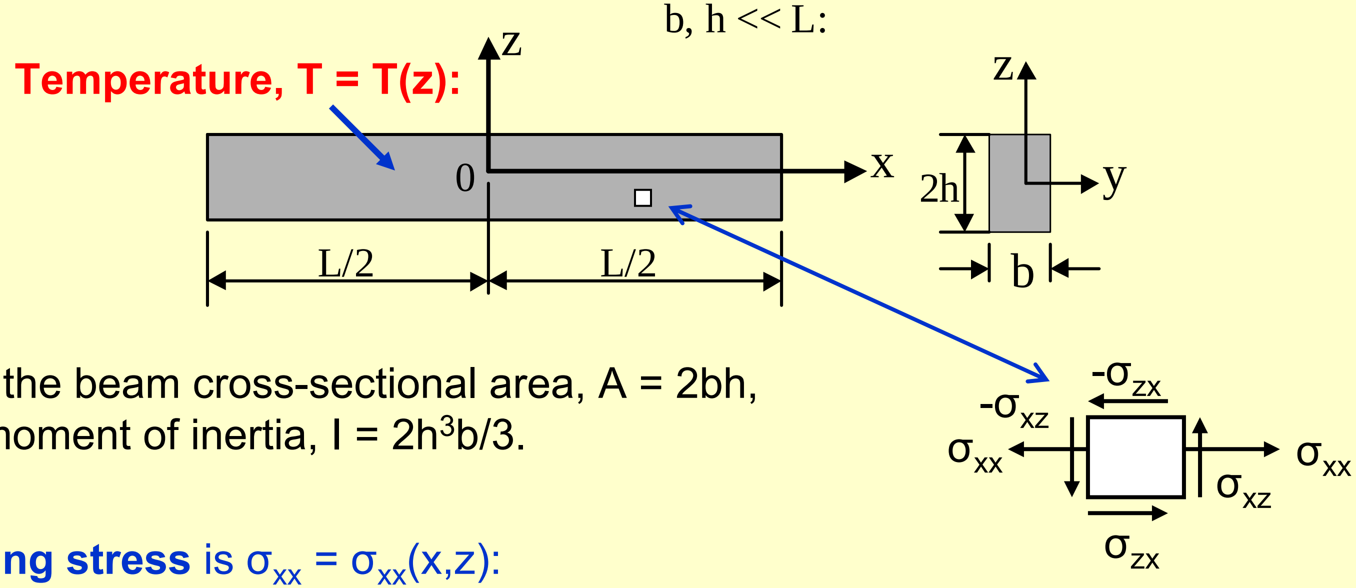

We have the beam cross-sectional area, A = 2bh, and the moment of inertia, $I = 2h^3b/3$.

The **bending stress** is $\sigma_{xx} = \sigma_{xx}(x,z)$:

$$\sigma_{xx}(x,z) = -\alpha E T(z) + \frac{b N_T}{A} + \frac{z(b M_T)}{I} \tag{4.56}$$

The shearing stresses: $\sigma_{xz} = \sigma_{zx} = 0$

The two associate strain components are:

$$\varepsilon_{xx}(x,z) = \frac{1}{E}\left[\frac{b N_T}{A} + \frac{z}{I}(b M_T)\right] \tag{4.57a}$$

$$\varepsilon_{zz}(x,z) = -\frac{\nu}{E}\left[\frac{b N_T}{A} + \frac{z}{I}(b M_T)\right] + \left(\frac{1+\nu}{E}\right)\alpha T(z) \tag{4.57b}$$

Thermal Stress in Beams – Cont'd

The deflections

In the x-direction:

$$u(x,z) = \frac{x}{E}\left[\frac{b\,N_T}{A} + \frac{z}{I}(b\,M_T)\right] \tag{4.58a}$$

In the z-direction:

$$w(x,z) = -\frac{b\,M_T}{2EI}x^2 - \frac{\nu}{E}\left[\frac{b\,N_T}{A}z + \frac{z^2}{2I}(b\,M_T)\right] + \alpha\left(\frac{1+\nu}{E}\right)\int_0^z T(z)dz \tag{4.58b}$$

with thermal force, N_T and thermal moment, M_T to be:

$$N_T = \alpha E \int_{-h}^{h} T(z)dz \tag{4.55a}$$

and

$$M_T = \alpha E \int_{-h}^{h} T(z)z\,dz \tag{4.55b}$$

The **curvature** of the bent beam is: $$\frac{1}{\rho} \approx -\frac{b\,M_T}{EI} \tag{4.59}$$

Type text here

Example 4.19 (p.160)

Determine the thermal stresses and strains as well as the deformation of a thin beam at 1 μsec after the top surface of the beam is subjected to a sudden heating by the resistance heating of the attached thin copper film. The temperature at the top surface resulting from the heating is 40°C. The geometry and dimensions of the beam is illustrated below. The beam is made of silicon and has the following material properties (refer to Table 7.3, p. 257):

Mass density, ρ = 2.3 g/cm^3; specific heats, c = 0.7 J/g-°C;
Thermal conductivity, k = 1.57 w/cm-°C (or J/cm-°C-sec);
Coefficient of thermal expansion, α = 2.33 x 10^{-6}/°C;
Young's modulus, E = 190000 x 10^{6} N/m^2; and Poisson's ratio, ν = 0.25.

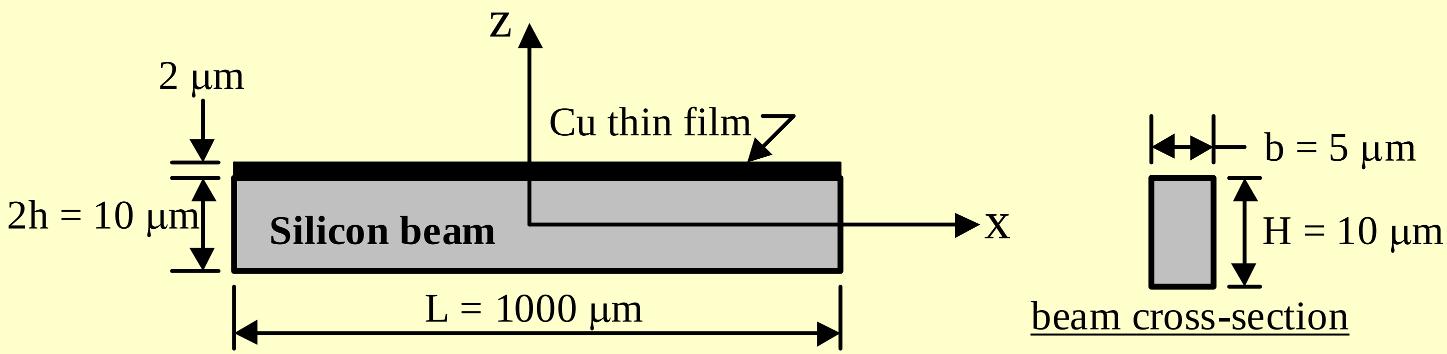

NOTE: This is not a bi-material strip. It is a beam made of a single material – silicon. Thermal stresses and deformations occur because of the uneven temperature distribution in beam (from top to bottom) in early stage of heating.

The Cu heating film is so thin that it does not affect the mechanical deformation or stresses in the structure.

Solution:

Solution procedure includes:

(1) Use the "heat conduction equation (Eq.(4.60)) to solve for temperature distribution in beam, i.e. T(z,t) with the boundary conditions of T(5 μm,t) = 40°C, and T(-5 μm,t) = 20°C as the case in the problem:

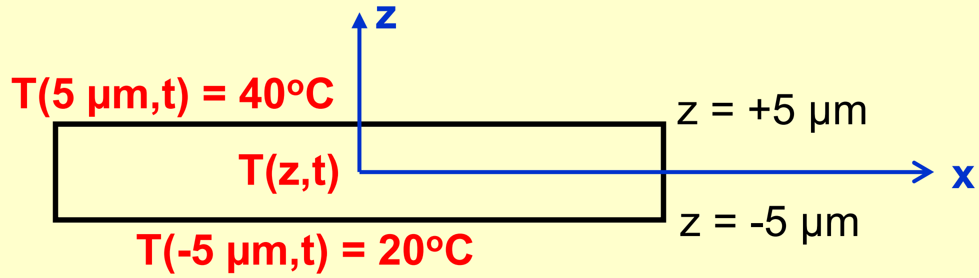

(2) Exact solution of T(z,t) for this problem is beyond the scope of this chapter.

(3) Instead, we use an approximate solution for the temperature distribution along the depth of the beam at **t = 1 μs** to be: **$T(z) = 2.1x10^6 z + 28.8$** °C

(4) We may thus use Eqs. (4.55a) and (4.55b) to calculate the thermal force and thermal moment.

$$N_T = \alpha E \int_{-h}^{h} T(z)dz = (2.33x10^{-6})(190000x10^6)\int_{-5x10^{-6}}^{5x10^{-6}} (2.1x10^6 z + 28.8)dz = 127.5$$

$$M_T = \alpha E \int_{-h}^{h} T(z)zdz = (2.33x10^{-6})(190000x10^6)\int_{-5x10^{-6}}^{5x10^{-6}} (2.1x10^6 z + 28.8)zdz = 77.4725x10^{-6} \text{ N-m}$$

(5) Once N_T and M_T are computed, we may calculate the maximum bending stress using Eq. (4.56):

$$\sigma_{xx}(z,1\mu s) = -(2.33x10^{-6})(190000x10^{6})(2.1x10^{6}z + 28.8)$$

$$+\frac{(5x10^{-6})127.5}{5x10^{-11}} + \frac{z(5x10^{-6})(77.4725x10^{-6})}{4.167x10^{-22}}$$

$$= -4.427x10^{5}(2.1x10^{6}z + 28.8) + 127.5x10^{5} + 92.95x10^{10}z \quad \text{Pa}$$

(6) From which, the maximum bending stress to be σ_{max} = -500 Pa at z = 5 μm

(7) The associated thermal strain components may be computed using Eqs. (4.57a) and (4.57b):

$$\varepsilon_{xx}(z) = \frac{1}{190000x10^{6}}\left[\frac{(5x10^{-6})127.5}{5x10^{-11}} + \frac{z(5x10^{-6}x77.4725x10^{-6})}{4.167x10^{-22}}\right]$$

$$= 67.11x10^{-6}(1 + 0.73x10^{5}z)$$

The thermal strain in z-direction is:

$$\varepsilon_{zz}(z) = 0.25(-67.11x10^{-6})(1+0.73x10^{5}z)$$

$$+\frac{1+0.25}{190000x10^{6}}(2.33x10^{-6})(2.1x10^{6}z+28.8)$$

$$= (-16.78x10^{-6} - 1.23z) + (3.22x10^{-11}z + 44.15x10^{-17})$$

(8) From which, we have the maximum strains to be:

$\varepsilon_{xx,max} = \varepsilon_{xx}(5x10^{-6}) = 91.61x10^{-6} = 0.0092\%$ and

$\varepsilon_{zz,max} = \varepsilon_{zz}(5x10^{-6}) = -22.93x10^{-6} = -0.0023\%$

(9) The displacements, or **deflection of the beam**, at the top free corners with x = ± 500 μm and z = +5 μm can be computed using Eqs. (4.58a) and (4.58b):

Deflection in the x-direction:

$$u=\frac{500x10^{-6}}{190000x10^{6}}\left[\frac{(5x10^{-6})127.5}{5x10^{-11}}+\frac{(5x10^{-6})(5x10^{-6})(77.47x10^{-6})}{4.167x10^{-22}}\right]=0.046 \quad \mu m$$

The deflection in normal (z)-direction to the beam:

$$w=-\frac{(5x10^{-6})(77.47x10^{-6})(500x10^{-6})^{2}}{2(190000x10^{6})(4.167x10^{-22})}$$
$$-\frac{0.25}{190000x10^{6}}\left[\frac{(5x10^{-6})127.5}{5x10^{-11}}(5x10^{-6})+\frac{(5x10^{-6})^{2}(5x10^{-6})(77.47x10^{-6})}{2(4.167x10^{-22})}\right]$$
$$+\frac{1+0.25}{190000x10^{6}}(2.33x10^{-6})\int_{0}^{5x10^{-6}}(2.1x10^{6}z+28.8)zdz=-0.612\mu m$$

(10) The curvature of the bent beam as estimated from Eq. (4.58) is:

$$\frac{1}{\rho}=-\frac{(5x10^{-6})(77.47x10^{-6})}{(190000x10^{6})(4.167x10^{-22})}=-4.892 \quad m^{-1}$$

Application of Fracture Mechanics in MEMS and Microsystems Design

Many MEMS and microsystems components are made of layers of thin films using physical or chemical vapor deposition methods (Chapter 8)**.**

These structures are vulnerable to failure in "de-lamination", or fracture at the interfaces.

Linear elastic fracture mechanics (LEFM) theories are used to assess the integrity of these structures.

Fracture mechanics was first introduced by Griffith in 1921 in the study of crack propagation in glasses using energy balance concept. It was not a practical engineering tool due to the difficulty in accurately measure the "surface energy" required in the calculation.

The LEFM was developed in 1963 by US naval research institute in studies unexpected fracture of many "liberty" class ships built in WWII.

The essence of the LEFM is to formulate the stress/strain fields near tips of cracks in elastic solids.

Stress Intensity Factors

A “crack” existing inside an elastic solid subjected to a mechanical and/or thermal loading. A stress field is induced in the solid due to the loading. The stress components in a point located near the crack tip can be shown as:

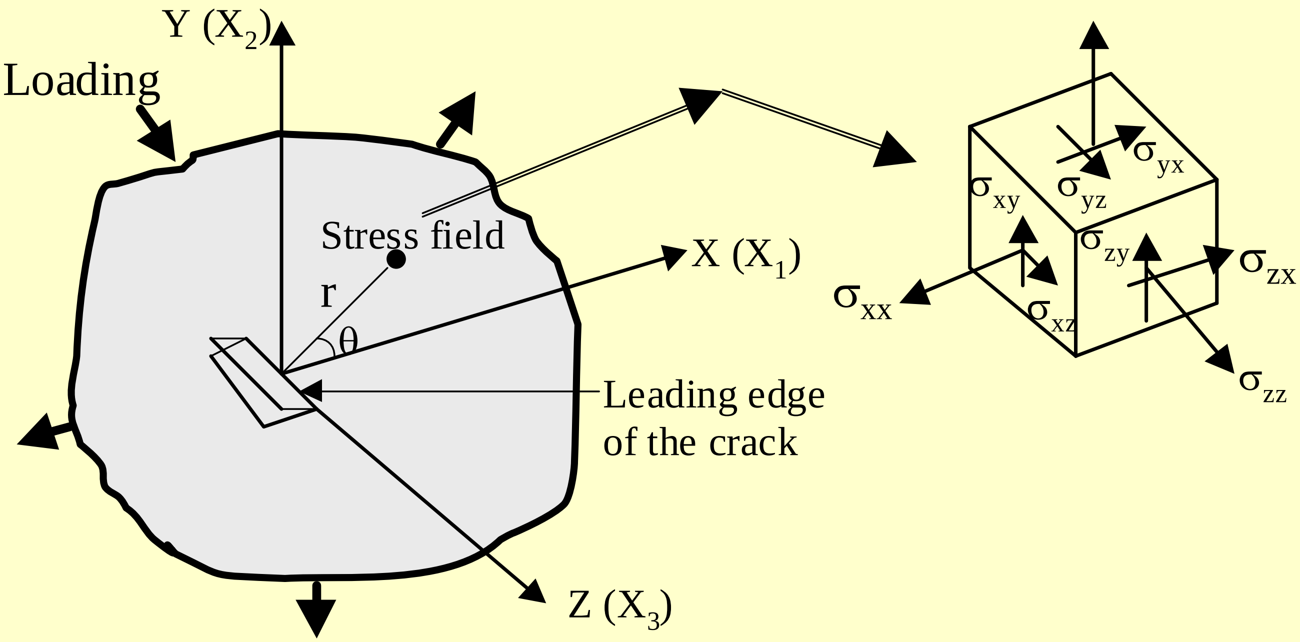

Stress Intensity Factors-cont'd

The "Three modes" of fracture of solids:

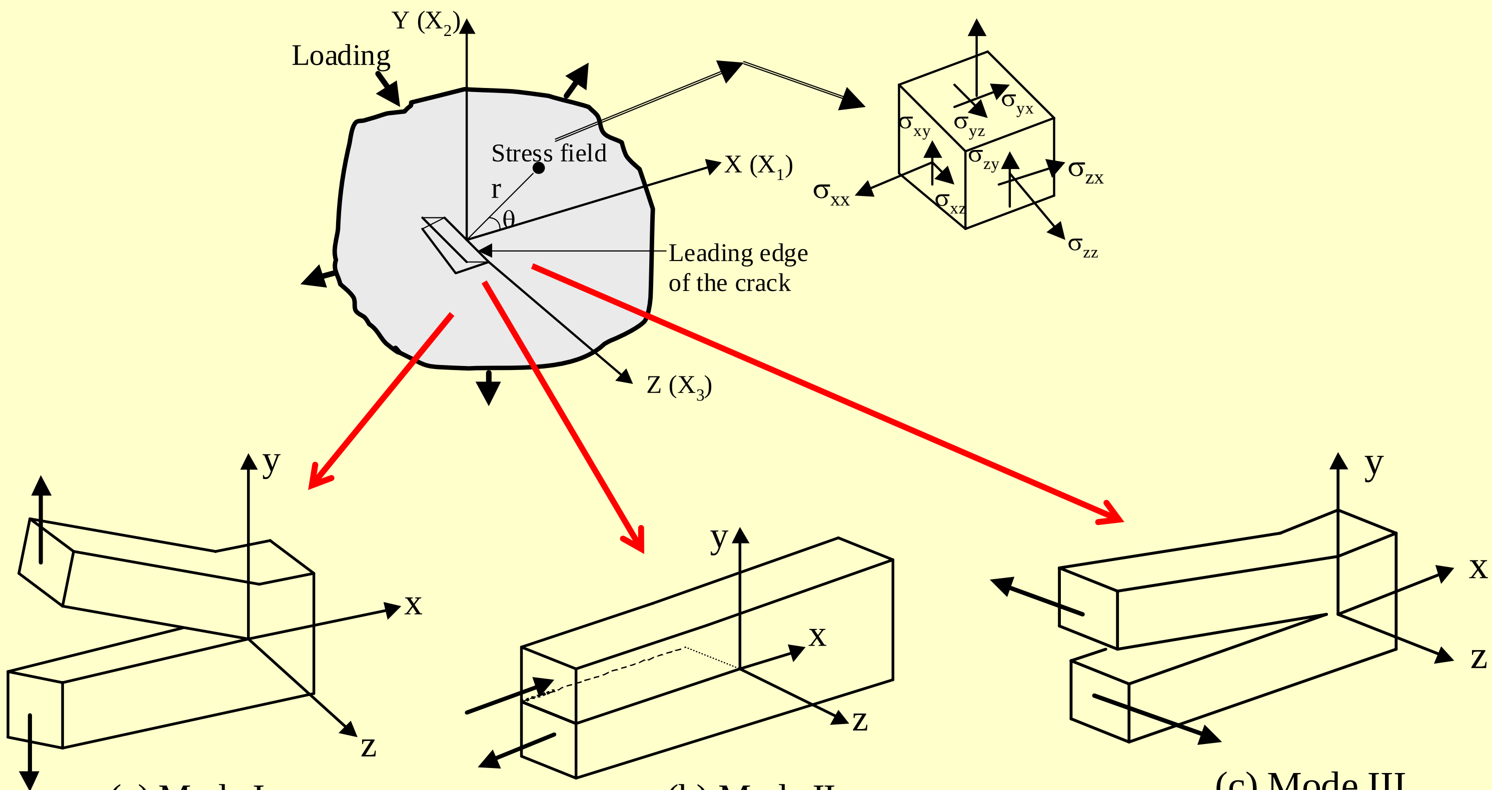

(a) Mode I
The Opening mode

(b) Mode II
The Shearing mode

(c) Mode III
The Tearing mode

Stress Intensity Factors-cont'd

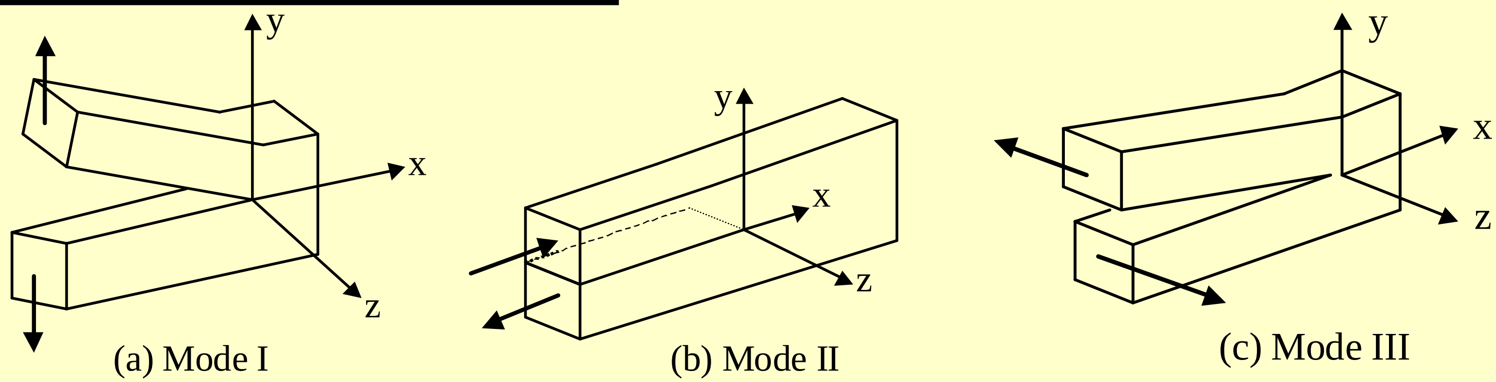

(The Opening mode) **(The Shearing mode)** **(The Tearing mode)**

Near-tip stress components in three modes:

$$\sigma_{ij} = \frac{K_I \text{ or } K_{II} \text{ or } K_{III}}{\sqrt{r}} f_{ij}(\theta)$$

Note:

$$\sigma_{ij} \to \infty \quad when \quad r \to 0$$

Near-tip displacement components:

$$u_i = K_I \text{ or } K_{II} \text{ or } K_{III} \sqrt{r}\, g_i(\theta)$$

Stress intensity factors:

K_I = stress intensity factor for Mode I fracture
K_{II} = stress intensity factor for Mode II fracture
K_{III} = stress intensity factor for Mode III fracture

Fracture Toughness, Kc

Fracture toughness, Kc is a material property that sets the limits for the three modes of fracture, e.g. K_{IC}, K_{IIC} and K_{IIIC} to be the limiting values of K_I, K_{II} and K_{III} respectively.

So, in practice, Kc is used to assess the "stability" of an existing crack in the following ways:

$K_I > K_{IC}$	unstable crack in Mode I fracture
$K_{II} > K_{IIC}$	unstable crack in Mode II fracture
$K_{III} > K_{IIIC}$	unstable crack in Mode III fracture.

Numerical values of Kc are measured by laboratory testing as described in Section 4.5.2 of the textbook for K_{IC}

Interfacial Fracture Mechanics

MEMS and microsystems components made of multi-layers of thin films are vulnerable to interfacial fracture – delamination of layers.

Interface of two dissimilar materials subject to mixed Mode I and Mode II fracture at the interface:

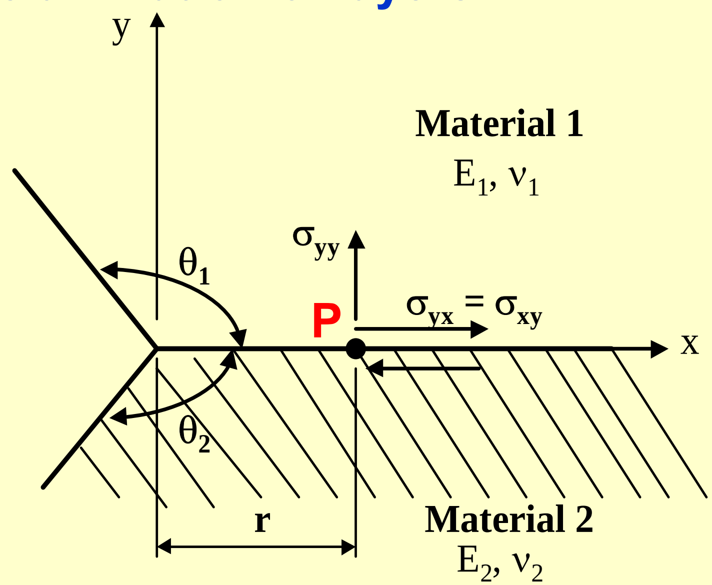

Stress components at Point P are:

$$\sigma_{ij} = \frac{K_I \text{ or } K_{II}}{r^{\lambda}} + L_{ij}\,\ell n(r) + terms$$

where λ = singularity parameter

If P is very close to the tip of the interface, i.e. $r \longrightarrow 0$, the contribution of the term L_{ij} is small, thus leads to:

$$\sigma_{ij} = \frac{K_I \text{ or } K_{II}}{r^{\lambda}}$$

$$\sigma_{yy} = \frac{K_I}{r^{\lambda_I}}$$ **for the opening mode**

$$\sigma_{xy} = \frac{K_{II}}{r^{\lambda_{II}}}$$ **for the shearing mode**

Interfacial Fracture Mechanics-Cont'd

Determination of: K_I, K_{II} and λ_I, λ_{II}:

$$\sigma_{yy} = \frac{K_I}{r^{\lambda_I}} \qquad\qquad \sigma_{xy} = \frac{K_{II}}{r^{\lambda_{II}}}$$

After taking logarithms on the above expressions:

$$\ell n(\sigma_{yy}) = -\lambda_I \,\ell n(r) + \ell n(K_I) \quad \textbf{and} \quad \ell n(\sigma_{xy}) = -\lambda_{II}\,\ell n(r) + \ell n(K_{II})$$

Plot the above expressions in logarithm scale for the desired values:

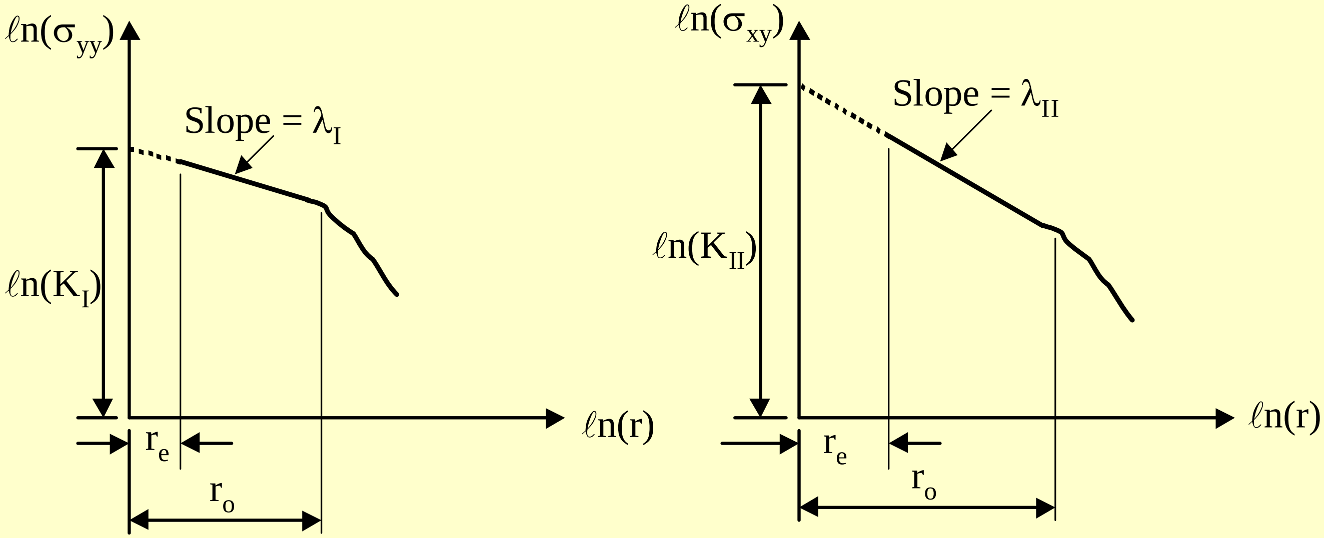

(a) Mode I fracture (b) Mode II fracture

Interfacial Fracture Mechanics-Cont'd

Failure (Fracture) Criteria

$$\left(\frac{K_I}{K_{IC}}\right)^2 + \left(\frac{K_{II}}{K_{IIC}}\right)^2 = 1 \qquad (4.69)$$

in which KIC and KIIC are experimentally determined fracture toughness from "mixed Mode I and II" situations.

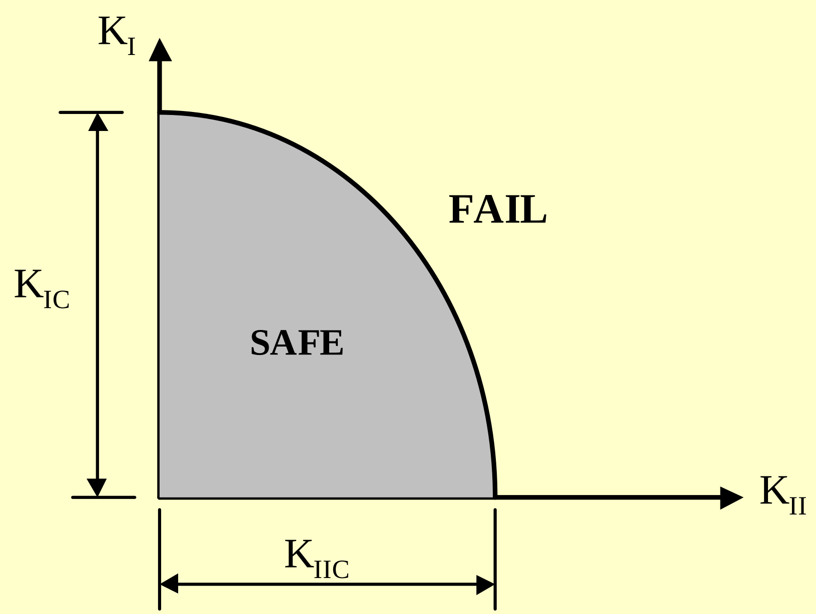

Thin Film Mechanics (p.172)

A common practice in MEMS and microsystems fabrication is to deposit thin films of a variety of materials onto the surface of silicon substrates.

These films usually are in the order of sub-micrometer or a few micrometers thick.

Due to the fact that the overall microcomponent structures are minute in size, thin films made of different materials can effect the overall stiffness, and thus the strength of the structures.

Quantitative assessment of induced stresses in thin films after they are produced on the top of the base materials is not available for the following two reasons:

(1) These films are so thin that the unusual forces such as molecular forces (or van der Waals) forces become dominant forces. There is no reliable way to assess such forces quantitatively at the present time.

(2) Another major source that induces stresses in thin films is "residual stresses" resulting from fabrication processes.

Total stress in thin films is expressed as: $\sigma = \sigma_{th} + \sigma_m + \sigma_{int}$ (4.70)

where σ_{th} = thermal stress; σ_m = due to mechanical loads; σ_{int} = intrinsic stresses.

The intrinsic stresses are normally determined by empirical means.

Overview of Finite Element Stress Analysis (p.173)

Finite element method (FEM) is a powerful tool in stress analysis of MEMS and microsystems of complex geometry, loading and boundary conditions.

Commercial FEM codes include: ANSYS, ABAQUS, IntelliSuites, MEMCad, etc.

The essence of FEM is to discretize (divide) a structure made of continuum into a finite number of "elements" interconnected at "nodes." Elements are of specific geometry.

One may envisage that smaller and more elements used in the discretized model produces better results because the model is closer to the original continuum.

Continuum mechanics theories and principles are applied on the individual elements, and the results from individual elements are "assembled" to give results of the overall Structure.

I/O in FEM for Stress Analysis

- **Input information to FE analysis:**

(1) General information:

- **Profile of the structure geometry.**
- **Establish the coordinates:**

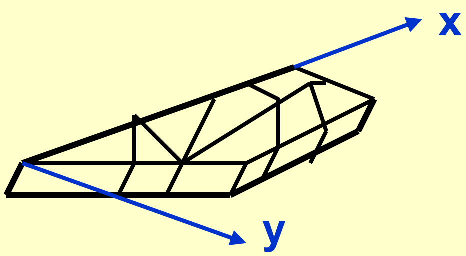

x-y for plane

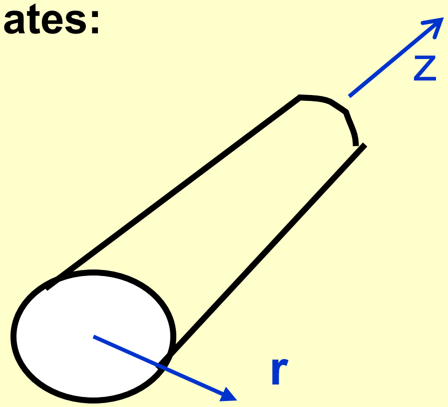

r-z for axi-symmetrical

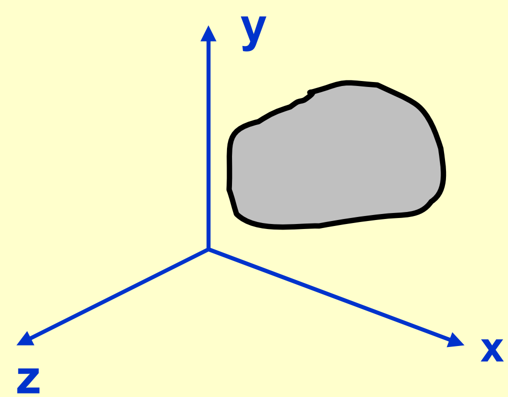

x-y-z for 3-dimensional geometry

(2) Develop FE mesh (i.e. discretizing the structure):

Use automatic mesh generation by commercial codes.

User usually specifies desirable density of nodes and elements in specific regions.
(Place denser and smaller elements in the parts of the structure with abrupt change of geometry where high stress/strain concentrations exist)

(3) Material property input:

<u>In stress analysis</u>: **Young's modulus, E; Poisson ratio, ν; Shear modulus of elasticity, G; Yield strength, σ_y; Ultimate strength, σ_u.**

<u>In heat conduction analysis</u>: **Mass density, ρ; Thermal conductivity, k; Specific heat, c; Coefficient of linear thermal expansion coefficient, α.**

(4) Boundary and loading conditions:

<u>In stress analysis</u>: **Nodes with constrained displacements (e.g. in x-, y- or z-direction); Concentrated forces at specified nodes, or pressure at specified element edge surfaces.**

<u>In heat conduction analysis</u>: **Given temperature at specified nodes, or heat flux at specified element edge surfaces, or convective or radiative conditions at specified element surfaces.**

● Output from FE analysis

(1) Nodal and element information

Displacements at nodes.

Stresses and strains in each element:

- **Normal stress components in x, y and z directions;**
- **Shear stress components on the xy, xz and yz planes;**
- **Normal and shear strain components**
- **Max. and min. principal stress components.**
- **The von Mises stress defined as:**

$$\bar{\sigma} = \frac{1}{\sqrt{2}}\sqrt{\left(\sigma_{xx}-\sigma_{yy}\right)^2+\left(\sigma_{xx}-\sigma_{zz}\right)^2+\left(\sigma_{yy}-\sigma_{zz}\right)^2+6\left(\sigma_{xy}^2+\sigma_{yz}^2+\sigma_{xz}^2\right)} \quad (4.71)$$

The von Mises stress is used to be the "representative" stress in a multi-axial stress situation.

It is used to compare with the yield strength, σ_y for plastic yielding, and to σ_u for the prediction of the rupture of the structure, often with an input safety factor.

Application of FEM in stress analysis of silicon die in a pressure sensor:

by V. Schultz, MS thesis at the MAE Dept., SJSU, June 1999 for LucasNova Sensors In Fremont, CA. (Supervisor: T.R. Hsu)

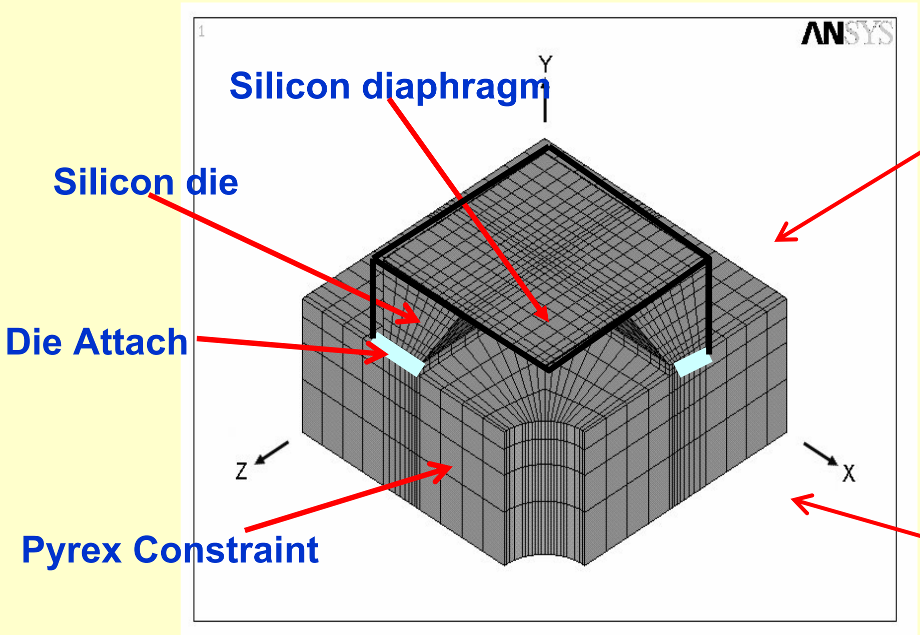

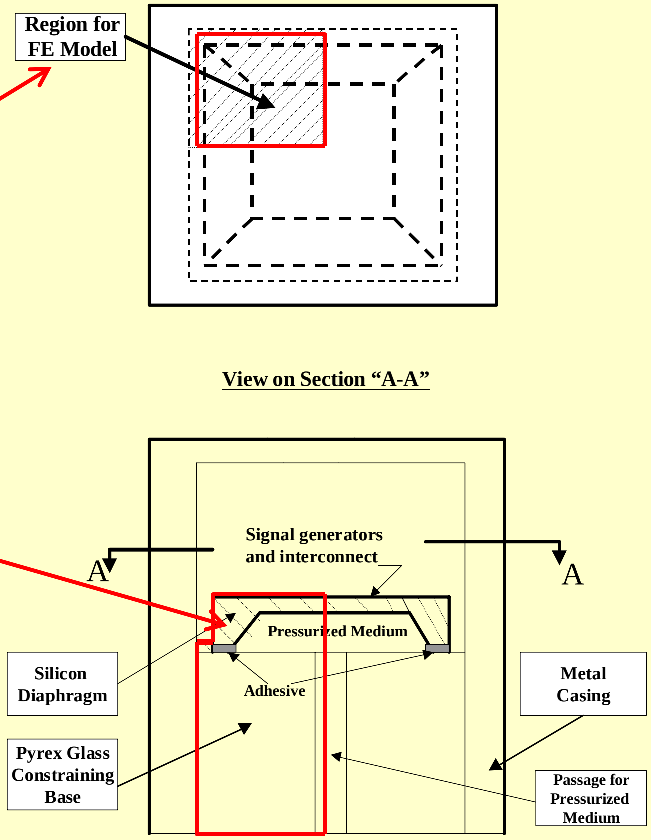

Note: **Only quarter of the die structure was in the FE model due to symmetry in geometry, loading and boundary conditions.**

SATHYABAMA
INSTITUTE OF SCIENCE AND TECHNOLOGY
(DEEMED TO BE UNIVERSITY)
Accredited "A" Grade by NAAC | 12B Status by UGC | Approved by AICTE
www.sathyabama.ac.in

SCHOOL OF MECHANICAL ENGINEERING
DEPARTMENT OF MECHATRONICS ENGINEERING

Unit – IV : MEMS Devices

Micro Electro Mechanical Systems: (MEMS) :SMR1301

MICROSENSORS AND MICROACTUATORS WORKING PRINCIPLE:

MICROSENSORS:

- A sensor element is a device that converts one form of energy into another (e.g., ZnO, a piezoelectric material, which converts mechanical energy into electricity) and provides the user with a usable energy output in response to a specific measurable input.
- Measurands may belong to the radiation, thermal, electrical, chemical, mechanical, or magnetic field domains. The sensor element may be built from plastics, semiconductors, metals, ceramics, etc.
- A microsensor must be in micro scale in dimension.
- A sensor includes a sensor element or an array of sensor elements with physical packaging and external electrical or optical connections. Synonyms for –sensorǁ are *transducer* and *detector*.
- A sensor system includes the sensor and its assorted signal processing hardware (analog or digital).
- *Transducer* sometimes refers to a sensor system, especially in the process control industry.
- In the case of silicon-based sensors, some additional jargon has developed. A Si sensor element is called a *sensor die*, which refers to a micromachined Si chip.
- It typically sells for $0.10 to $2 as a commodity product, although the price tag can rise to $50 or more for a high-performance structure sold in smaller quantities.

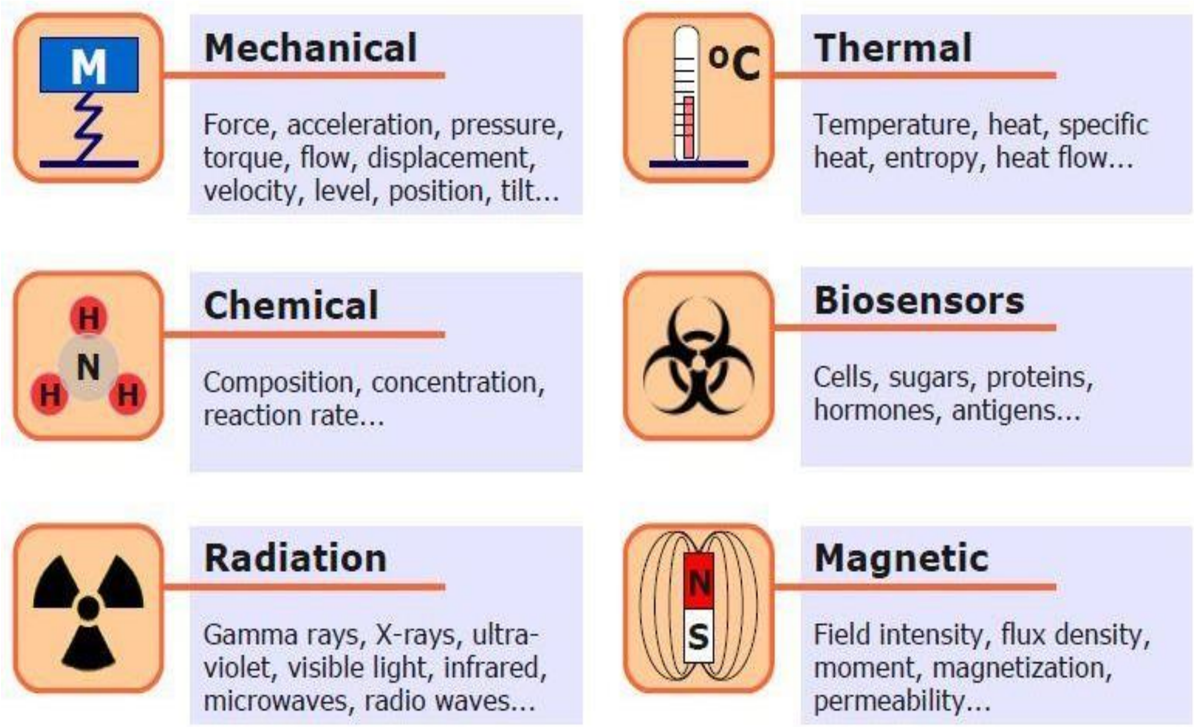

Fig-1: Application of microsensors in different fields of interest

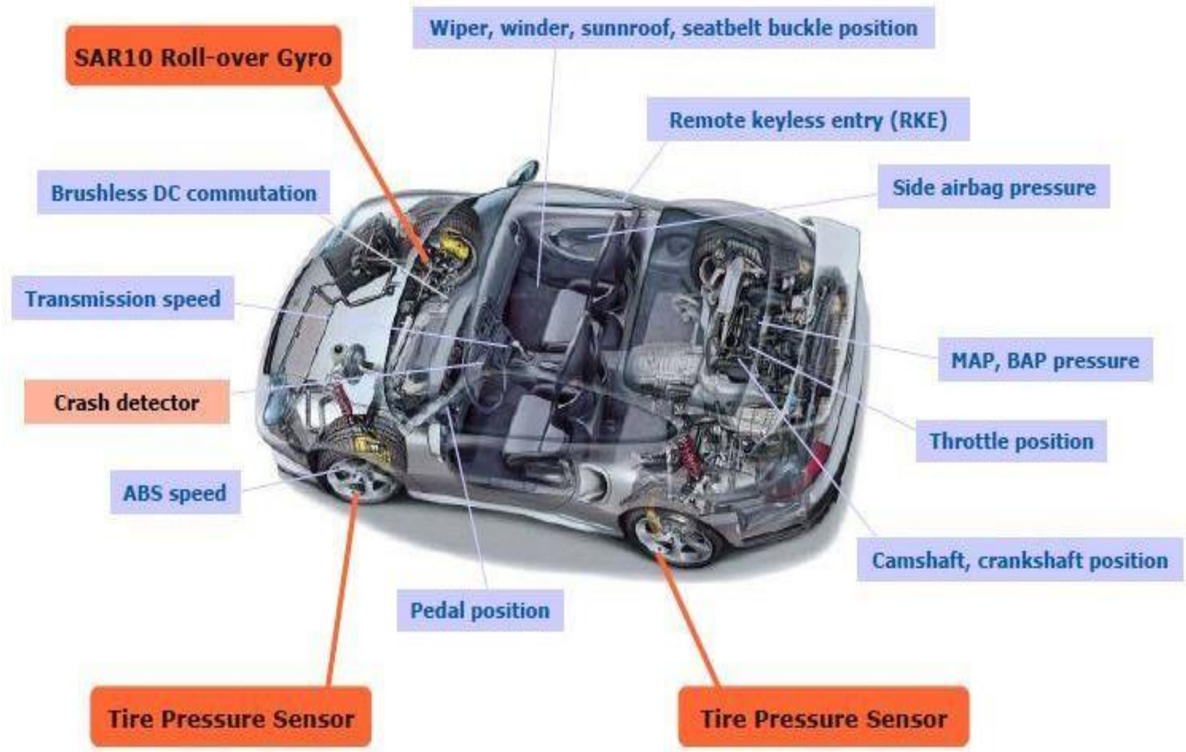

Fig-2: Typical example of microsensors used in cars

Biomedical Applications of Microsensors:

1) Disposable blood pressure sensors (17 million units per year)

2) Intrauterine pressure sensor (1 million units per year)

3) Infusion pump pressure sensor (2,00,000 units per year)

4) Catheter type pressure sensors

5) Lung Capacity meters

6) Kidney dialysis equipment

7) Human care support systems

The silicon sensor die is shown in figure below. It has sensor element that takes input from various process variables like pressure, temperature, viscosity, flow, level, etc. The outputs obtained from the sensor are fed directly to the calibration device and are converted into a suitable form. There is a modulating device which helps in the manipulation of the process variables. The Data conversion element performs the conversion of the obtained process variable from one form to another form while data transmission element transfers the energy from one location to another through bus. It is possible to interface the smart silicon sensor with the module.

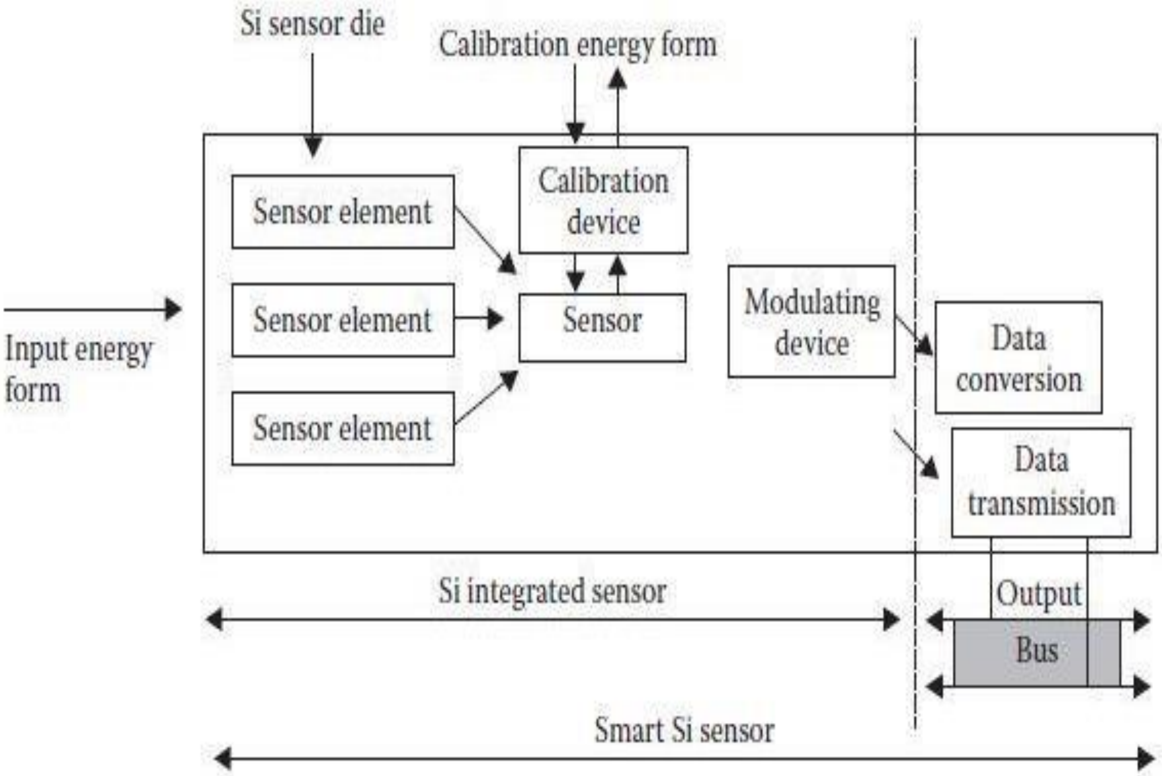

Fig-3: Silicon sensor die

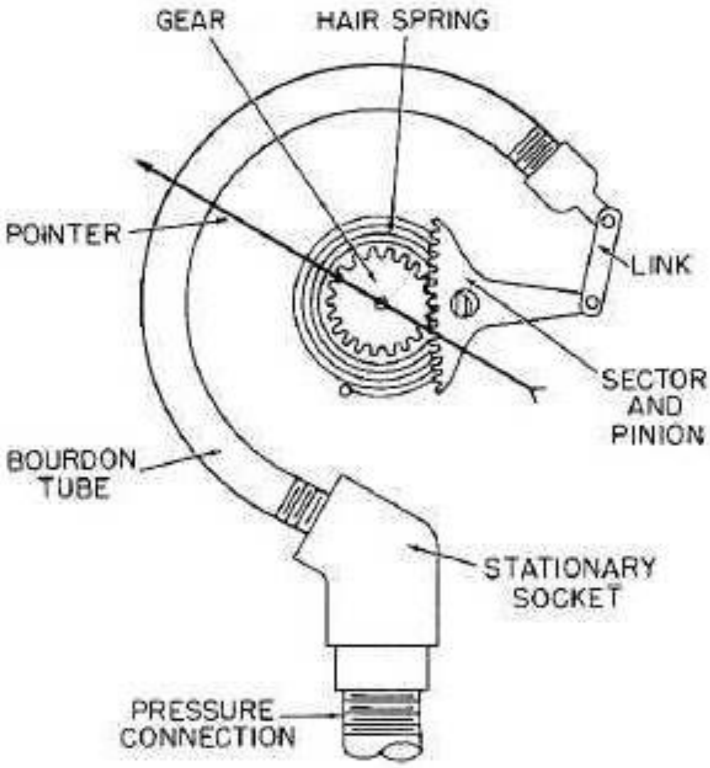

Fig-4: Example measurement system

- At yet a higher level is a *smart silicon sensor*, which is a packaged integrated sensor containing some part of the signal-processing unit to provide performance enhancement for the user.
- Signal processing might include autocalibration, interference reduction, compensation for parasitic effects, offset correction, and self-test.

Example of microsensor:

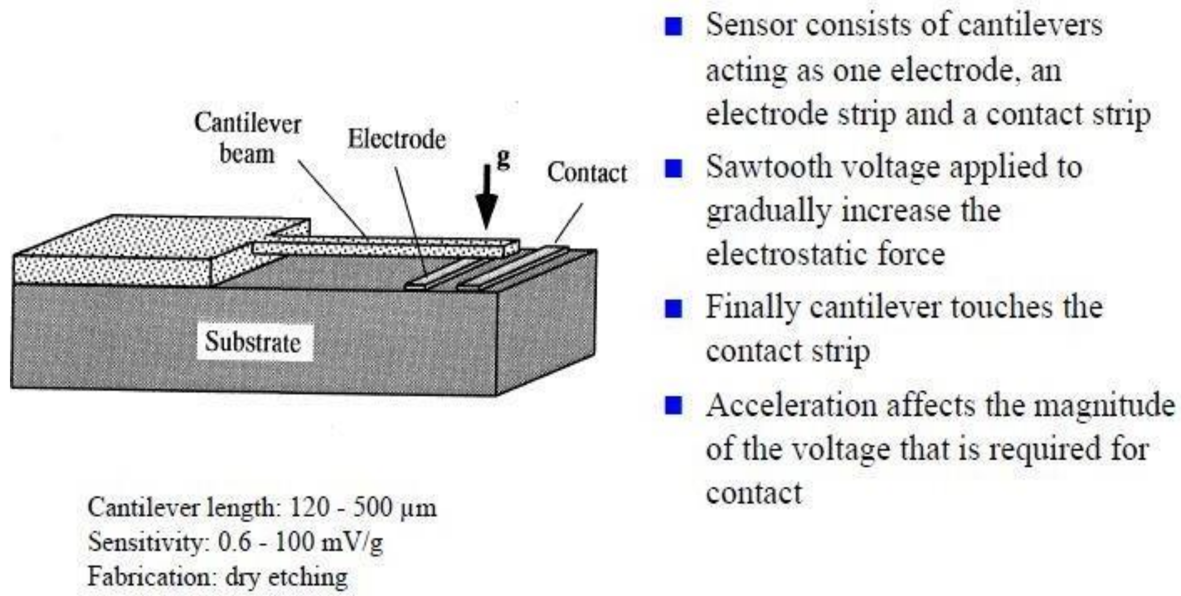

Fig-5: Capacitive cantilever micro sensor

MICROACTUATORS:

An actuator is a component of a machine that is responsible for moving and controlling a mechanism or system, for example by opening a valve. In simple terms, it is a "mover–. Its main energy source may be an electric current, hydraulic fluid pressure, or pneumatic pressure. When it receives a control signal, an actuator responds by converting the source's energy into mechanical motion. They facilitate a function such as opening a valve, positioning a mirror, moving a plug of liquid, etc.

Since an actuator –acts,‖ some power is usually needed. The selling price for Si-based actuators in large quantities may range from $5 to $200

Working Principle:

- Microactuators are based on three-dimensional mechanical structures with very small dimensions which are produced with the help of lithographic procedures and non-isotropic etching techniques.
- For an actuator-like displacement the most different principles of force generation are used, such as the bimetal effect, piezo effect, shape memory effect and electrostatic forces.
- Characteristic for microactuators in a more narrow sense is the fact that the mechanism of force generation is integrated monolithically

- Movable structural parts are made up of surface micromachining based on single crystal silicon, techniques like electrical discharge machining (EDM), micro injection molding.

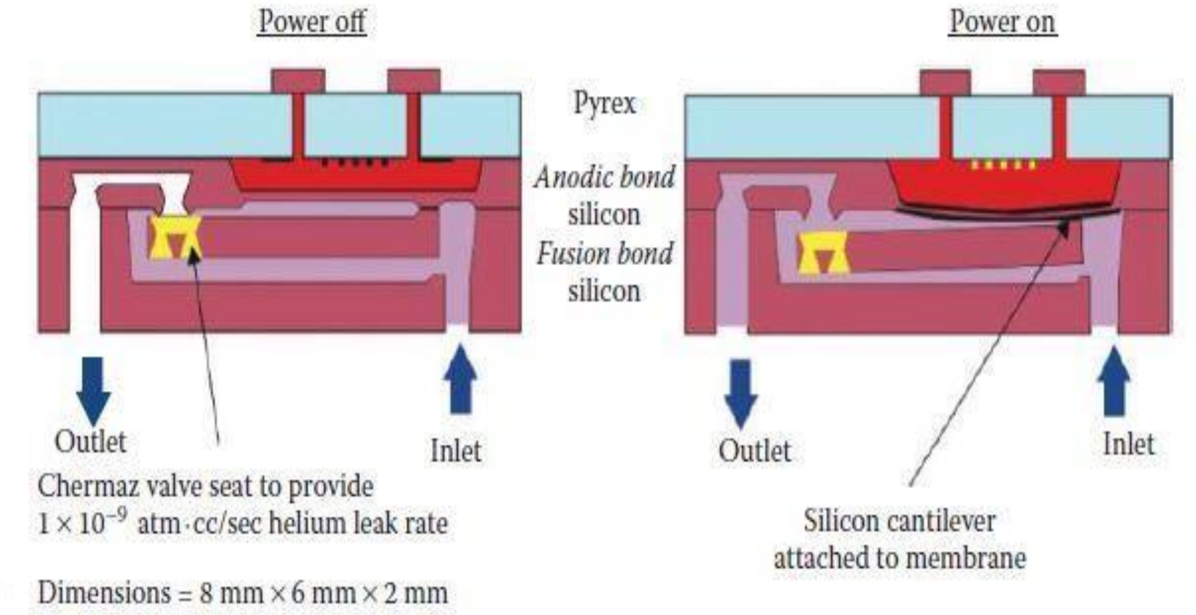

Fig-6: Examples of commercially available actuators. Thermopneumatic valves by Redwood Microsystem s (Fluistor). Normally closed shut-off microvalve featuring a liquid-filled cavity, which flexes a silicon diaphragm when heated, forcing the valve cover to lift off the valve seat.

EXAMPLE OF MICROACTUATOR- ELECTROMAGNETIC MICRO MOTORS:

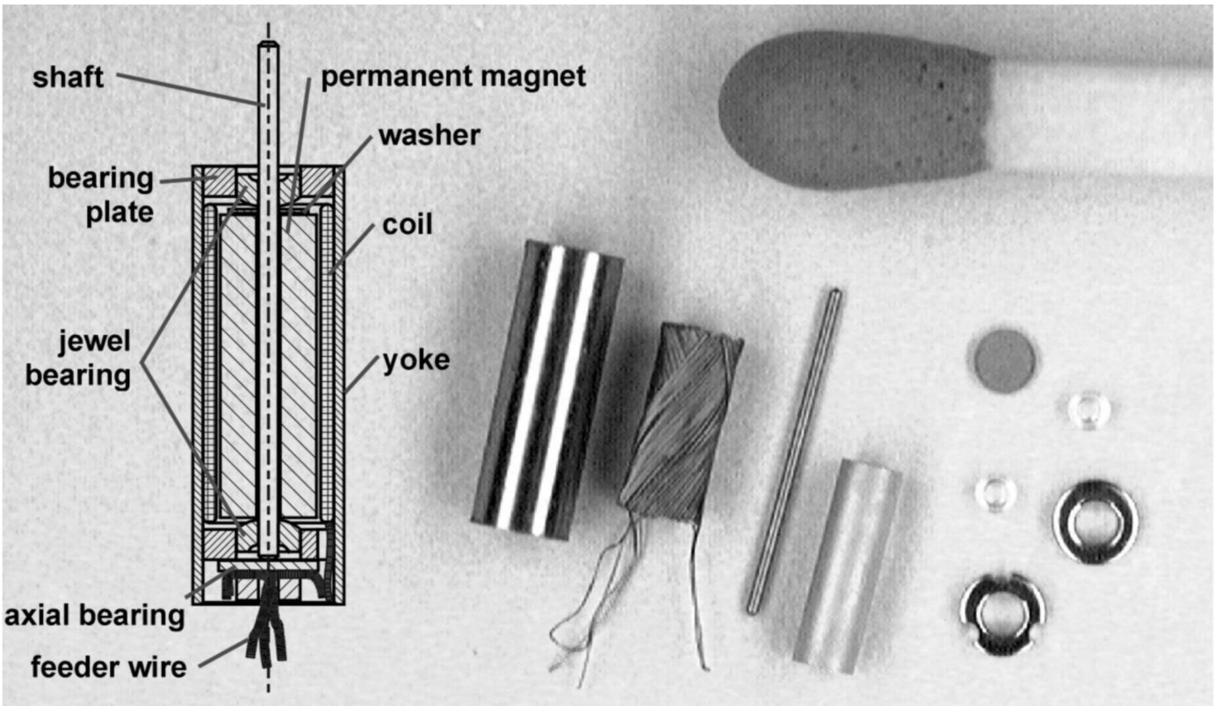

Fig-7: Construction and components of a electromagnetic micromotor

The electromagnetic micromotor has a permanent magnet placed at two sides of the system. It has a bearing plate, shaft, yoke, bearing jewel and axial bearing which are the mechanical components of the electromagnetic micromotor. When current flows in the conductor in the presence of magnetic field, then there is a rotational movement produced in the shaft which is the output obtained across the micromotor.

MICROGRIPPERS:

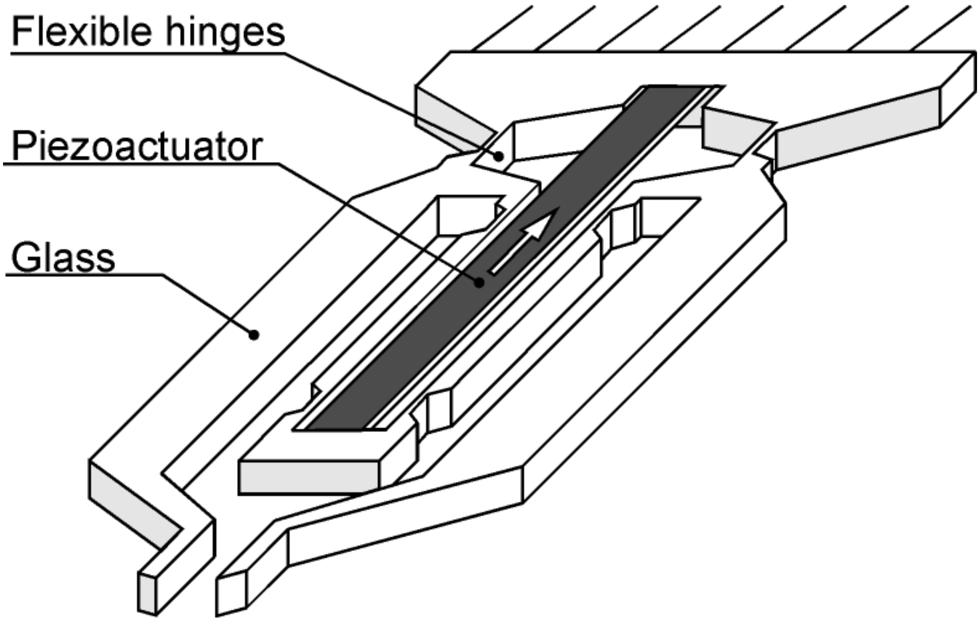

Fig-8: MEMS microgripper

PIEZOELECTRIC CRYSTAL:

- The meaning of the word –piezoelectric‖ implies –*pressure electricity*‖- the generation of electric field by applying pressure.
- Piezoelectricity is observed if a stress is applied to a solid, like by bending , twisting or squeezing it.
- The material exhibiting the direct piezoelectric also exhibit the reverse piezoelectric effect (the internal generation of a mechanical strain resulting from an applied electric field).

Fig-9: Piezoelectric crystal electricity generation

Table-1:Natural & Synthetic material

NATURAL	SYNTHETIC
1. Quartz	Lead Zirconate Titanate(PZT)
2. Rochelle Salt	Zinc oxide (ZnO)
3. Topaz	Barium Titanate($BaTiO_3$)
4. Silk	Lead Titanate($PbTiO_3$)
5. Dentin	Langasite ($La_3Ga_5SiO_{14}$)
6. DNA	Sodium tungstate (Na_2WO_3)
7. Tendon	Potassium Niobate($KNbO_3$)

Working of Piezoelectric:

- Normally, the charges in a piezoelectric crystal are exactly balanced, even if they're not symmetrically arranged .
- The effects of the charges exactly cancel out, leaving no net charge on the crystal faces.(More specifically, the electric dipole moment is zero).
- Now the effect of the charges (their dipole moments) no longer cancel one another out and net positive and negative charges appears on the crystal faces.
- By squeezing the crystal, we have produced a voltage across it's opposite faces– and that's PIEZOELECTRICITY.
- If we squeeze the crystal ,you force the charges out of balance.

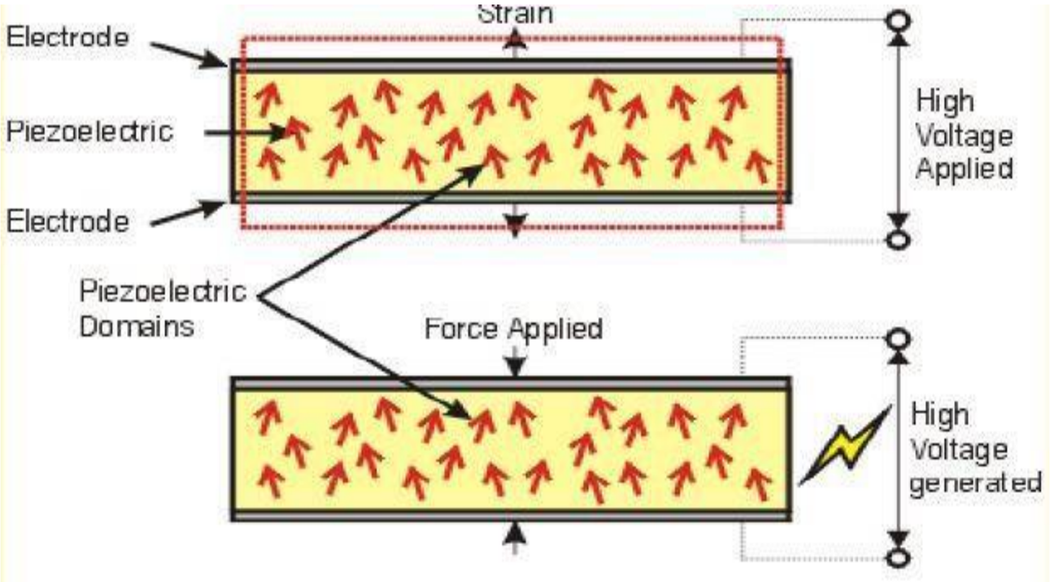

Fig-10: Movement of charges under applied stress

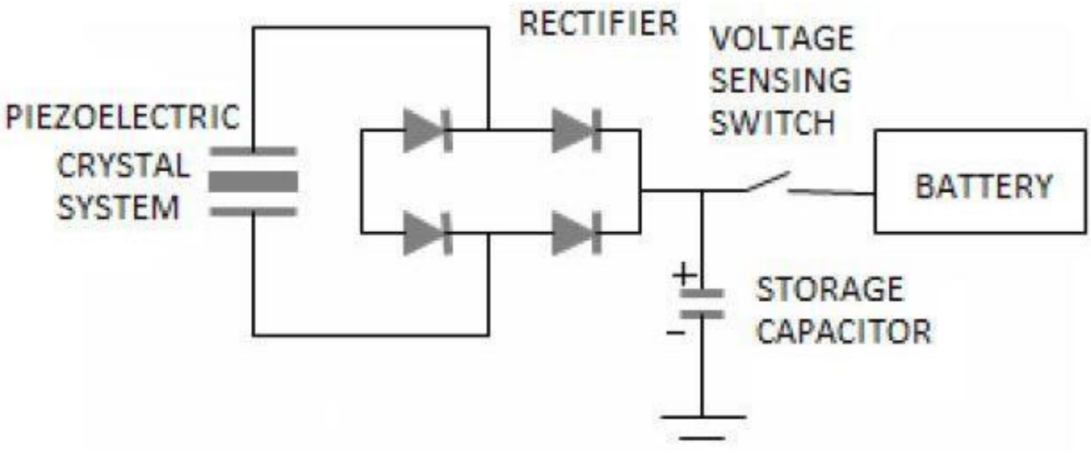

Fig-11: Piezoelectric crystal coupled with rectifier and battery for storing

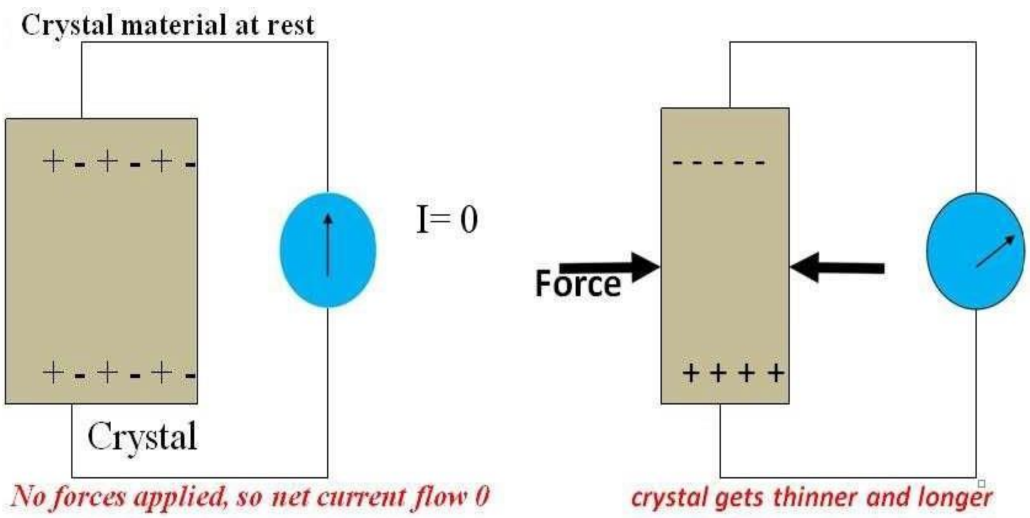

Fig-12: Piezoelectric effect

Applications of Piezoelectric materials:

Sensor:

- -Microphones, Pick-ups
- -Pressure sensor
- -Force sensor
- -Strain gauge

Actuators

- -Loudspeaker
- -Piezoelectric motors
- -Nanopositioning in AFM or STM
- -Acoustic-optical modulators

- -Valves

High voltage and power source

- -Cigarette lighter
- -Energy harvesting
- -AC voltage multiplier

Implementation of Piezoelectricity in practical life:

• **Energy Harvesting**: Vibrations from industrial machinery can also be harvested by piezoelectric materials to charge batteries for backup supplies or to power low-power microprocessors and wireless radios. Piezoelectric elements are also used in the detection and generation of sonar waves.

• **Inkjet printers**: On many inkjet printers, piezoelectric crystals are used to drive the ejection of ink from the inkjet print head towards the paper.

• **Diesel engines**: High-performance common rail diesel engines use piezoelectric fuel injectors, first developed by Robert Bosch , instead of the more common solenoid valve devices.

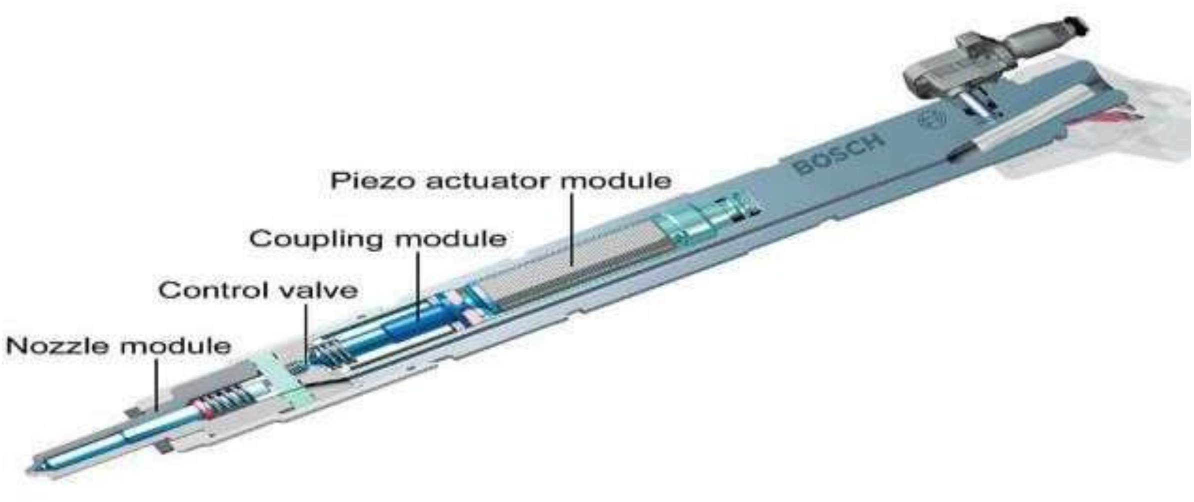

Fig-13: TYPICAL PIEZOELECTRIC INJECTION SYSTEM

Table-2: Advantages and disadvantages of Piezoelectric property materials

ADVANTAGES	DISADVANTAGES
Unaffected by external electromagnetic fields.	They cannot be used for truly static measurements
Pollution Free	Can pick up stray voltages in connecting wires.
Low Maintenance	Crystal is prone to crack if overstressed.
Easy replacement of equipment.	May get affected by long use at high temperatures.

- Piezoelectricity is a revolutionary source for –GREEN ENERGY‖
- Flexible piezoelectric materials are attractive for power harvesting applications because of their ability to withstand large amounts of strain.
- Convert the ambient vibration energy surrounding them into electrical energy.
- Electrical energy can then be used to power other devices or stored for later use.

PRESSURE SENSORS:

- Several types of pressure sensor can be built using MEMS techniques.
- Most common: piezoresistive and capacitive.
- In both of these, a flexible layer is created which acts as a diaphragm that deflects under pressure but different methods are used to measure the displacement.

MEMS capacitive pressure sensors

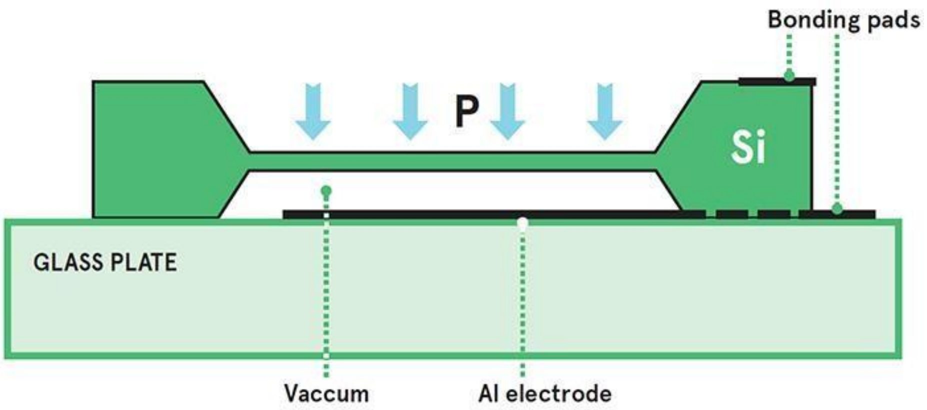

Fig-14: MEMS Capacitive pressure sensor

To create a capacitive sensor, conducting layers are deposited on the diaphragm and the bottom of a cavity to create a capacitor. The capacitance is typically a few picofarads. Capacitive pressure sensors measure pressure by detecting changes in electrical capacitance caused by the movement of a diaphragm. Deformation of the diaphragm changes the spacing between the conductors and hence changes the capacitance.

The change can be measured by including the sensor in a tuned circuit, which changes its frequency with changing pressure.

A capacitor consists of two parallel conducting plates separated by a small gap. The capacitance is defined by:

$$C = \varepsilon_r \varepsilon_0 \frac{A}{d}$$

where:

- ε_r is the dielectric constant of the material between the plates (this is 1 for a vacuum)
- ε_0 is the electric constant (equal to 8.854×10^{-12} F/m),
- A is the area of the plates
- d is the distance between the plates

❑ The capacitance of the sensor is typically around 50 to 100 pF, with the change being a few picofarads.

❑ The diaphragm can be constructed from a variety of materials, such as plastic, glass, silicon or ceramic, to suit different applications.

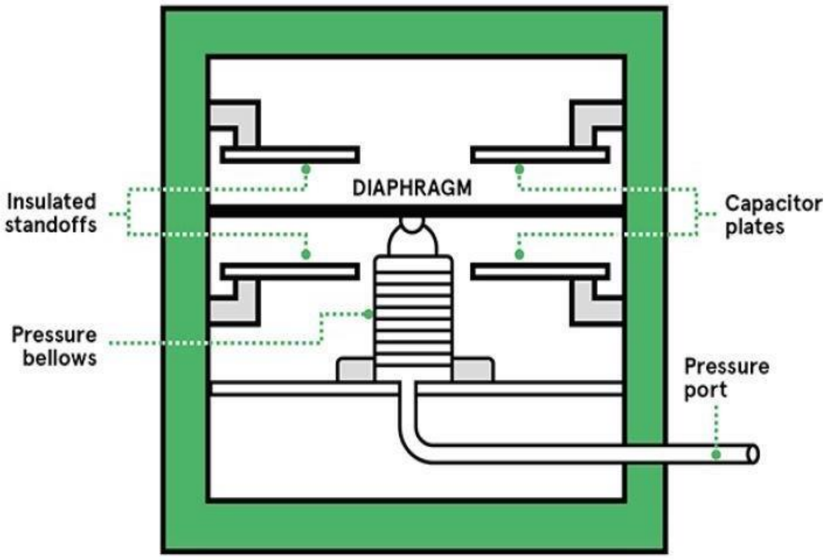

Fig-15: Diaphragm Pressure sensor system

The stiffness and strength of the material can be chosen to provide a range of sensitivities and operating pressures. To get a large signal, the sensor may need to be fairly large, which can limit the frequency range of operation. However, smaller diaphragms are more sensitive and have a faster response time.

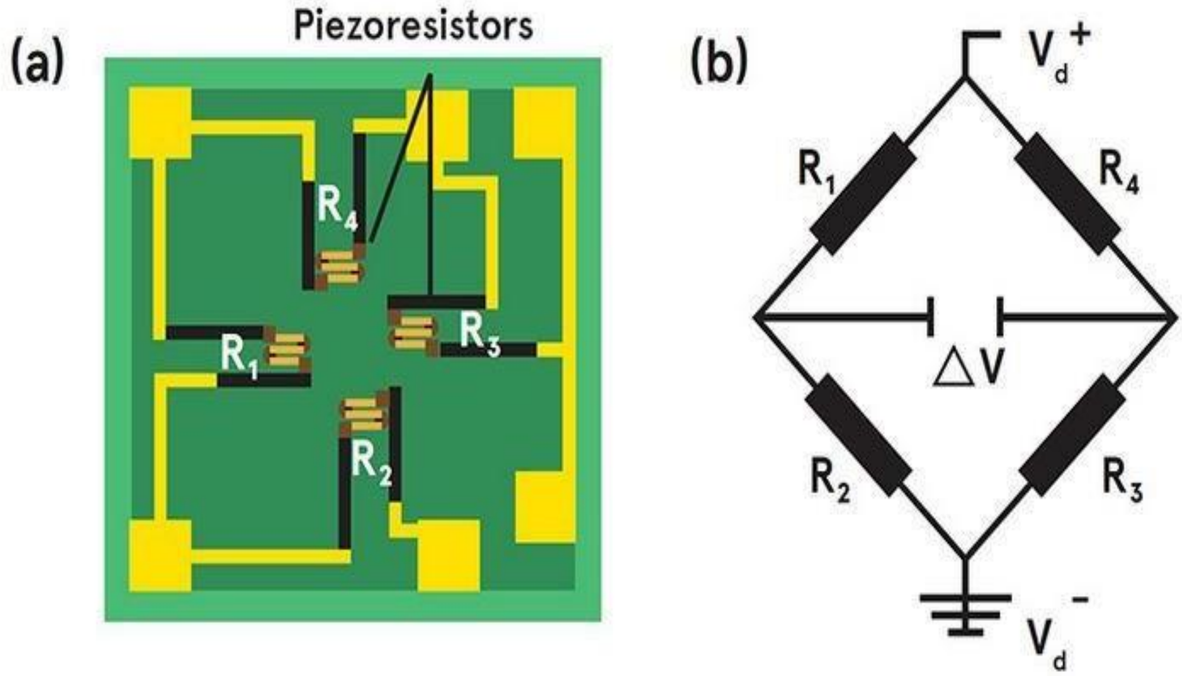

Fig-16: (a) Arrangement of Piezoresistors (b) Wheatstone bridge connection

THERMAL SENSORS AND ACTUATORS:

- One of the primary methods for electrical measurement of temperature involves changes in the electrical resistance of certain materials.
- In this, as well as other cases, the principal measurement technique is to place the temperature-sensing device in contact with the environment whose temperature is to be measured.
- The two basic devices used are the *resistance-temperature detector* (RTD), based on the variation of metal resistance with temperature, and the *thermistor*, based on the variation of semiconductor resistance with temperature

Metal Resistance versus Temperature Devices

- A metal is an assemblage of atoms in the solid state in which the individual atoms are in an equilibrium position with superimposed vibration induced by the thermal energy.
- As electrons move throughout the material, they collide with the stationary atoms or molecules of the material.

- When a thermal energy is present in the material and the atoms vibrate, the conduction electrons tend to collide even more with the vibrating atoms.
- This impedes (delays) the movement of electrons and absorbs some of their energy; that is, the material exhibits a *resistance* to electrical current flow.
- The graph in Figure 19 shows the effect of increasing resistance with temperature for several metals.
- To compare the different materials, the graph shows the relative resistance versus temperature.

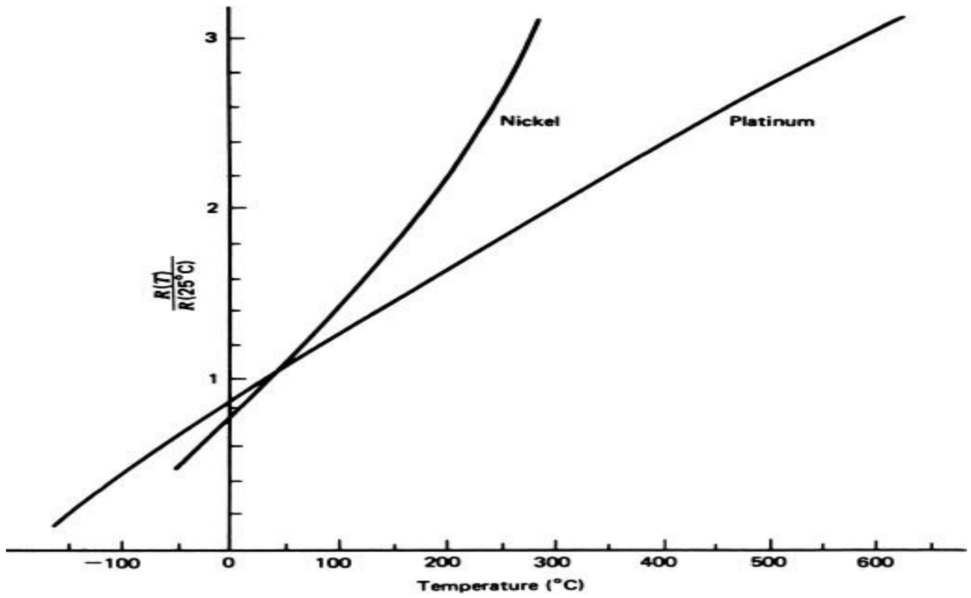

Fig-17: Temperature Vs resistance for different metals

The equation of this straight line is the linear approximation to the curve over the spanT_1 to T_2 . The equation for this line is typically written as

$$R(T) = R(T_0)[1 + \alpha_0 \Delta T] \qquad T_1 < T < T_2$$

where $R(T)$ = approximation of resistance at temperature T
$R(T_0)$ = resistance at temperature T_0
$\Delta T = T - T_0$
α_0 = fractional change in resistance per degree of temperature at T_0

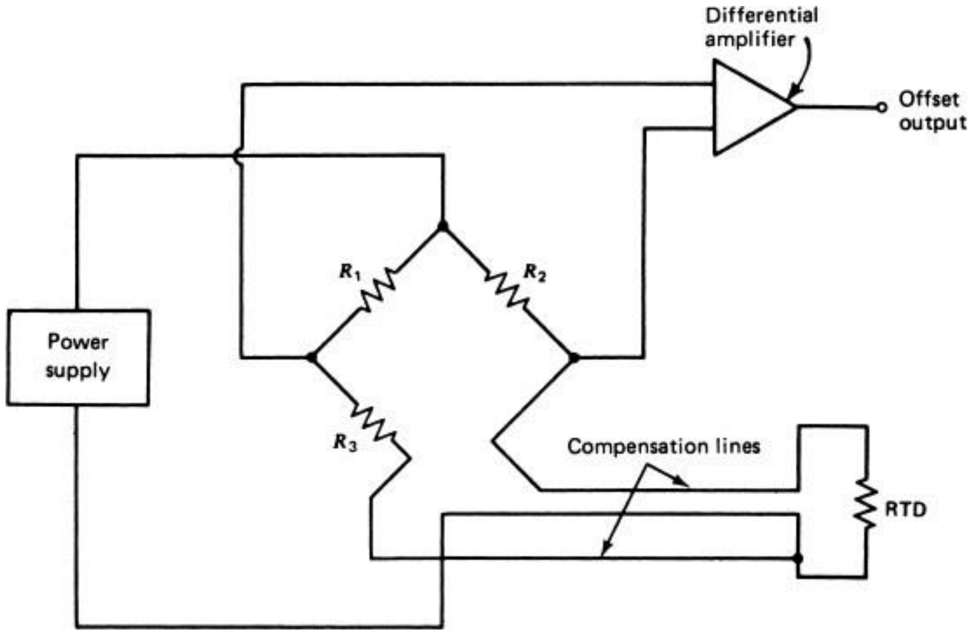

Fig-18: Typical RTD Circuit

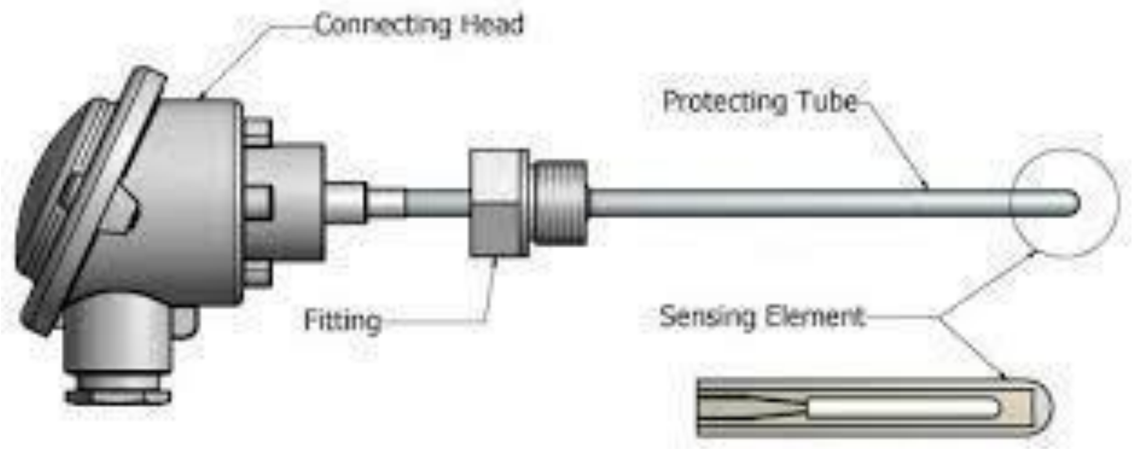

Fig-19: Picture of RTD

THERMISTORS:

The thermistor represents another class of temperature sensor that measures temperature through changes of material resistance. The characteristics of these devices are very different from those of RTDs and depend on the peculiar behavior of semiconductor resistance versus temperature.

Semiconductor Resistance versus Temperature

In contrast to metals, electrons in semiconductor materials are bound to each molecule with sufficient strength that no conduction electrons are contributed from the valence band to the conduction band.

- When the temperature of the material is increased, the molecules begin to vibrate. In the case of a semiconductor, such vibration provides additional energy to the valence electrons. When such energy equals or exceeds the gap energy.
- As the temperature is further increased, more and more electrons gain sufficient energy to enter the conduction band.
- It is then clear that the semiconductor becomes a better conductor of current as its temperature is increased—that is, as its resistance decreases.

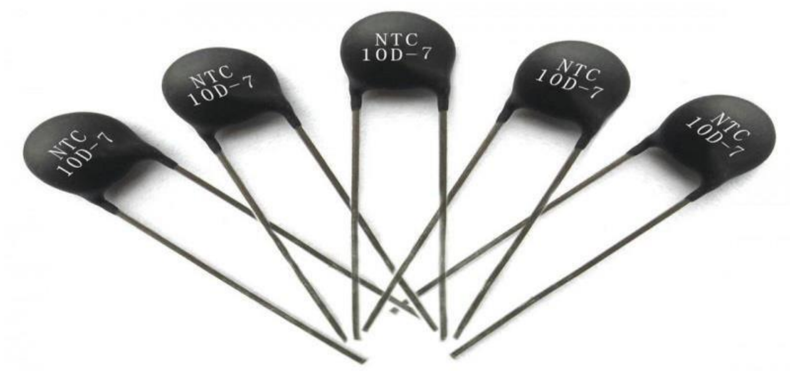

Fig-20: Thermistor Bead

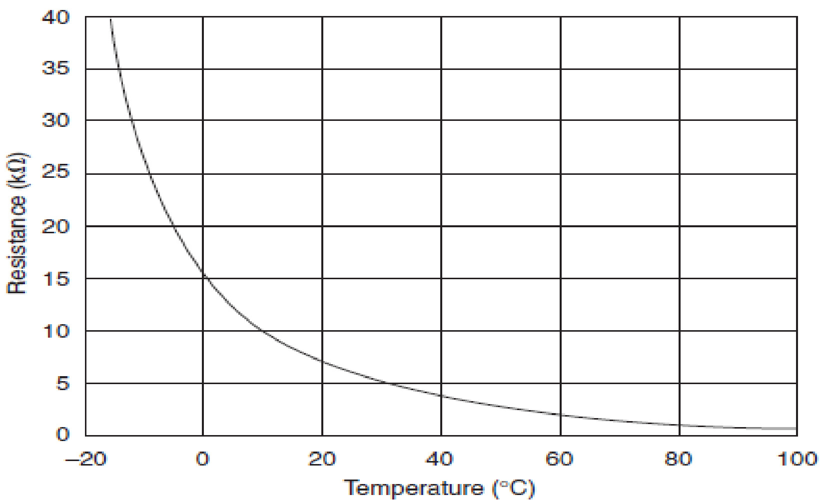

Fig-21: Temperature versus resistance response of Thermistor

THERMAL ACTUATORS:

- Actuation of microscale devices and structures can be achieved by injecting or removing heat.
- Temperature of microstructure raised by absorption of electromagnetic waves (including light), ohmic heating (joule heating), conduction and convection heating.
- Cooling achieved via conduction dissipation, convection dissipation, radiation dissipation, and active thermoelectric cooling.
- Many ink-jet printers eject ink droplets using thermal expansion of liquid links.

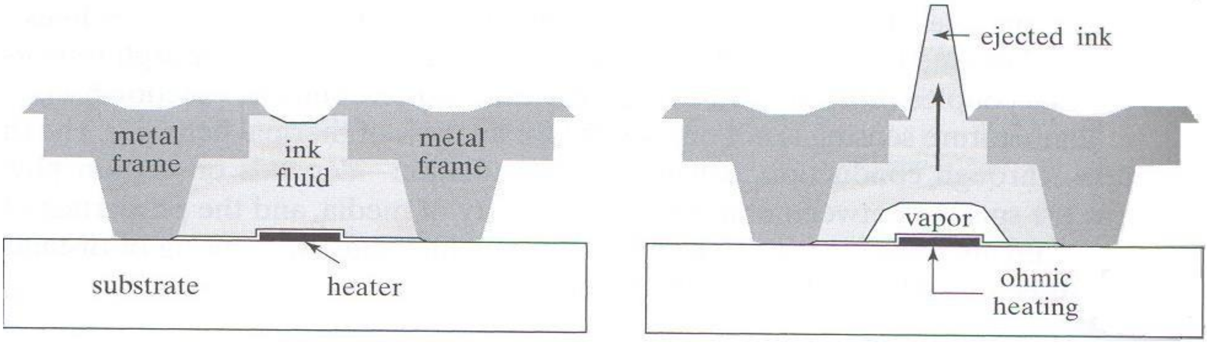

Fig-22: Example thermal actuator

Example: Thermal Inkjet Print Head

- Using resistive heating to produce tiny ink droplets. Also known as bubble jet. A typical MEMS inkjet print head has up to 600 nozzles (~10µm)

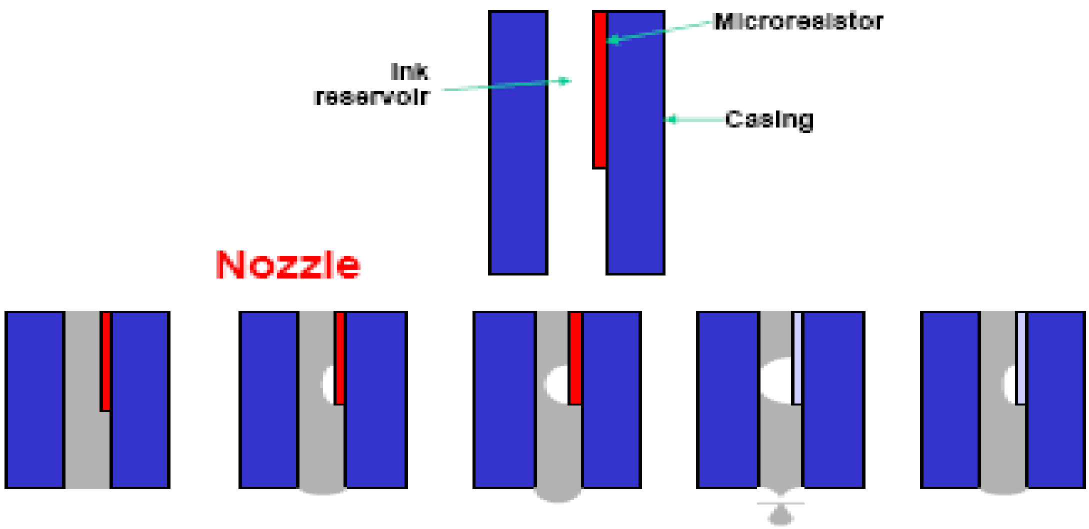

Fig-23: Inkjet Printer working phenomenon

The working procedure of the inkjet printer is as follows:

A micro-resistor creates heat → Heat vaporises ink to create a bubble → Bubble expands → A drop of ink is pushed out of a nozzle onto the paper → Heat turned off → Bubble collapses and vacuum is created → More ink into the print head from the cartridge.

Sensors and actuators based on thermal expansion:

Thermal expansion is the tendency of matter to change in volume in response to a change in temperature.

- The volumetric thermal expansion coefficient (TCE)

$$\alpha = \frac{\frac{\Delta V}{V}}{\Delta T}$$

- The linear expansion coefficient

$$\beta = \frac{\frac{\Delta l}{l}}{\Delta T}$$

- Relationship:

$$\alpha = 3\beta$$

•The thermal gases due to temperature change can be derived from the ideal gas law. For an ideal gas:

$$PV = nRT = NkT$$

•*P* is absolute pressure, *V* the volume, *T* the absolute temperature, *n* the number of moles, *N* the number of molecules, *R* universal gas constant (R= 8.3145 J/molK), k the boltzman constant (1.30866 x 10^{-23} J/K), N_A *is Avogadro no.*(N_A = 6.0221 x 10^{23})

$$k = R/N_A$$

Thermal bimorph principle:

This mechanism allows the temperature variation in microstructures to be shown as the transverse displacement of mechanical beams.

Consist of two materials joined along their longitudal axis acting as a single mechanical element.

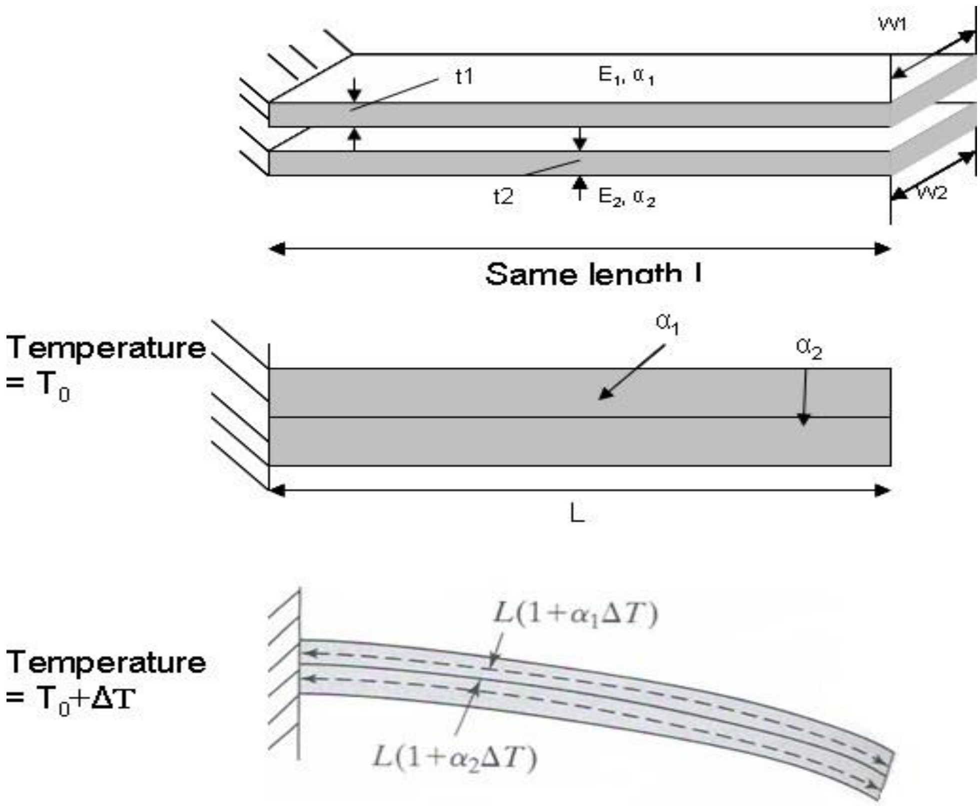

Fig-26: Thermal Bimorph principle.

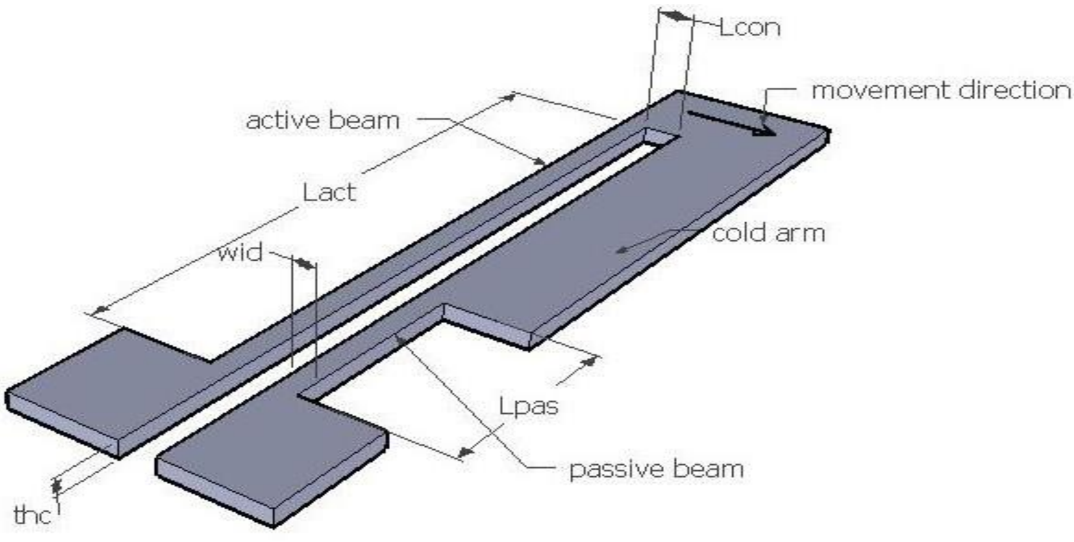

Fig-24: Full image of thermal bimorph transducer

A thermal bimorph actuator consists of a hot and cold region which are connected together. The bimorph actuator is made of one material. For a bimorph actuator only a portion of it is heated. If a current is passed through the entire system between the two fixed pads, the higher Joule heating in the thinner active beam would cause its expansion while the temperature of the cold arm will remain relatively unchanged.

The cold arm is connected to the fixed pad via a passive beam of the same cross-sectional area as the active beam. The passive beam allows flexibility of the cold arm and at the same time can be used to control the deflection based on its length.

The hot and cold arms are connected together by a connecting link which has an influence on the deflection. This design interface can be used to determine the deflection and actuation force for a thermal bimorph actuator as shown above. The deflection and force are estimated at the free tip of the actuator. The influence of the different geometric features of the actuator on its deflection can be examined.

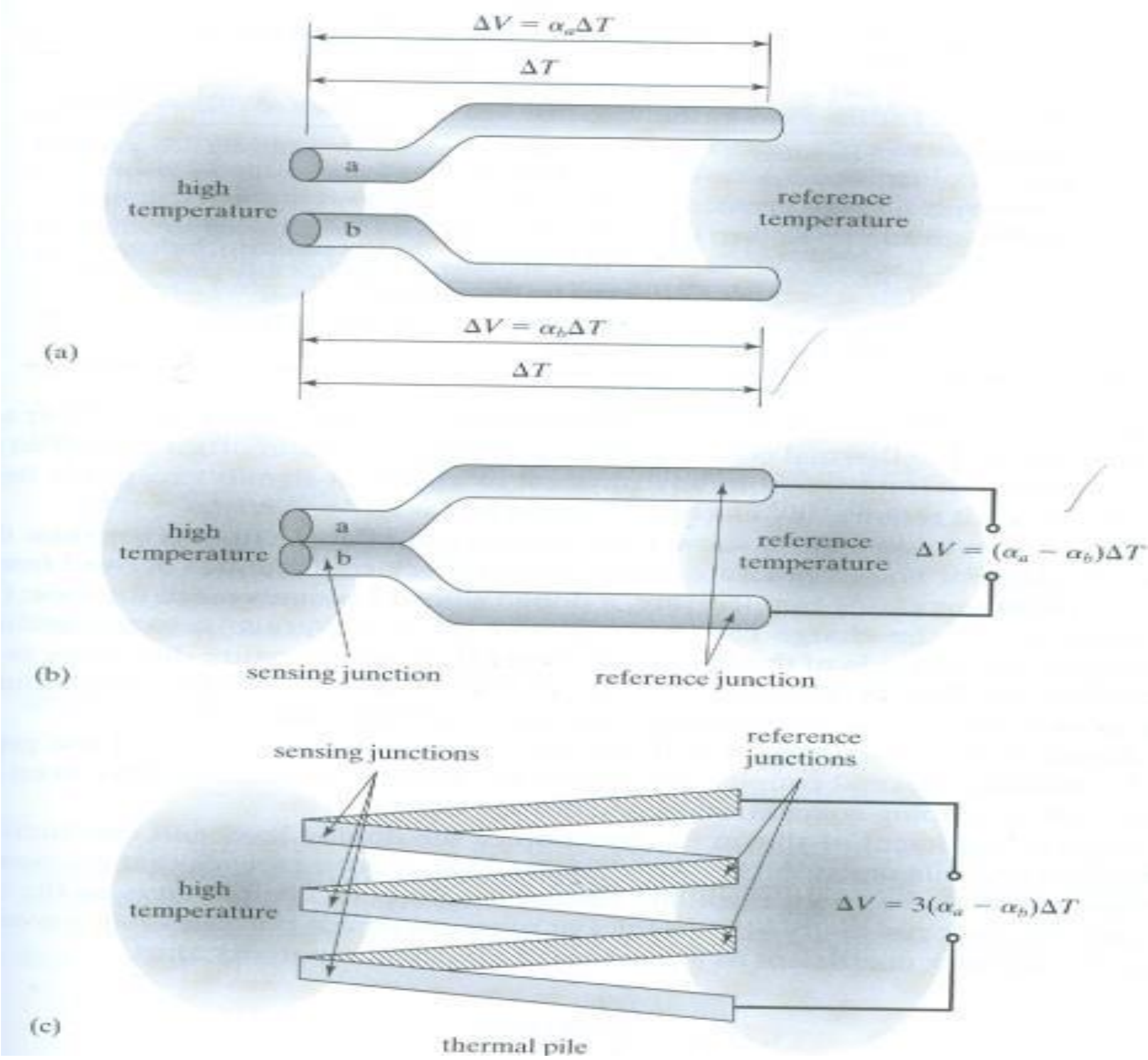

Fig-25: Thermocouple effect

Seebeck coefficient of thermal, $\alpha_{ab} = \alpha_a - \alpha_b$

Advantages of Thermal Couple:

1. Provides an output without offset and offset drift.

2. Not suffer from interference from any physical or chemical signals except for light.
3. Not require any electrical biasing and is self powered.

For non-degenerate silicon, Seebeck coefficient is derived from 3 main effects:

1. With increasing temperature, a doped silicon becomes more intrinsic
2. With increasing temperature, the charge carrier acquire a greater average velocity (buildup charge on the cold side of the semiconductor)
3. The temperature difference in a piece of silicon causes a net flow of phonons from hot to cold end.

Applications:

- Inertia Sensors
- Flow sensors
- Infrared sensors

THERMAL BIOSENSORS:

- THERMAL biosensors measure thermal energy released or absorbed in biochemical reactions.
- Thermal activities exist ubiquitously in Biological Processes, and hence widely applicable.
- Requiring no labeling of reactants, thermal bio sensing is a universally useful method, allowing direct interrogations of elementary processes in biochemistry without sophisticated cascades of reaction steps.

MEMS thermal sensors are often based on temperature detection.

I. Thermistors

- Rely on changes in their electric resistance with temperature.
- Allow measurement of absolute temperatures.
- Limited in sensitivity

II. Thermopile

- Set of Thermocouple Junctions connected in series.
- Allows measurement of differences in temperature between two Junctions.

- Offers excellent common-mode noise cancellation and zero offset, and therefore can be highly
- Sensitive.

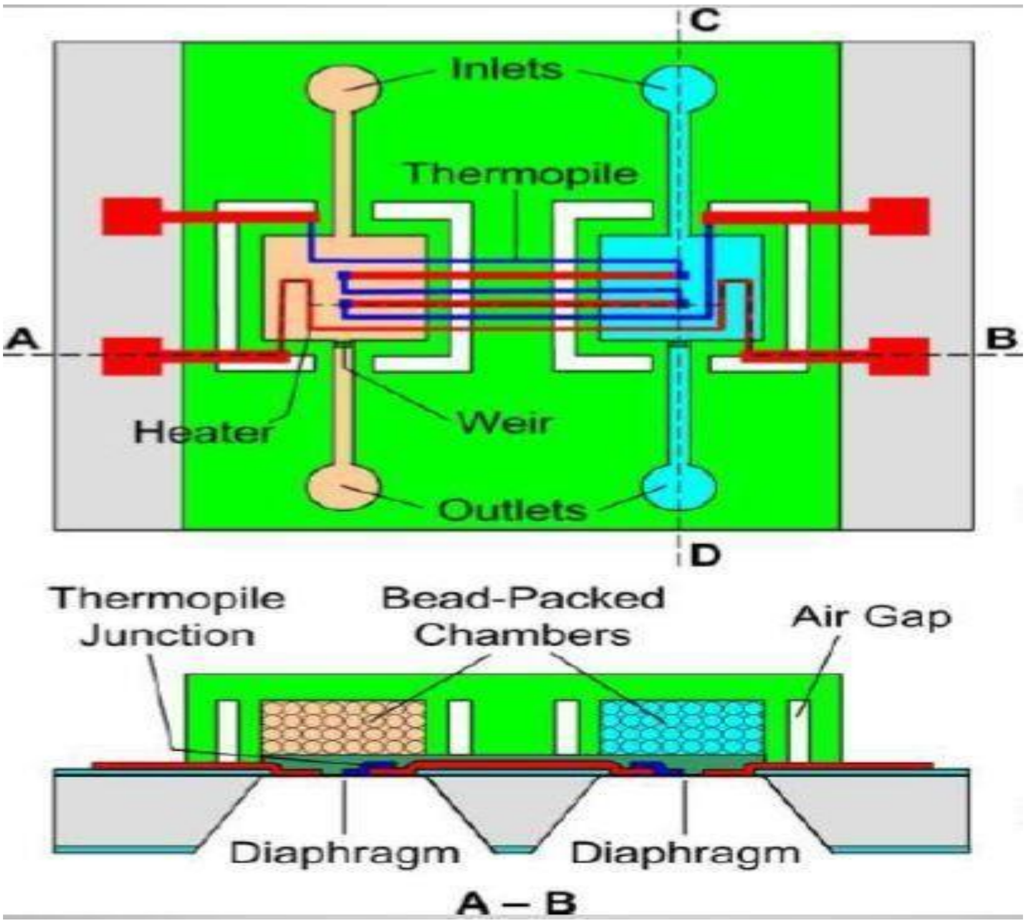

Fig-26: Thermal sensors in MEMS

- Device consists of a thermal sensor chip integrated with a microfluidic system featuring two identical chambers.
- An analyte sample solution and a reference buffer solution are respectively loaded into the chambers.
- The device can be used in Two modes: Flow-Injection mode and Flow-Through mode.
- An important feature of the microfluidic system is that the chambers are each based on a freestanding polymer diaphragm.
- The temperature difference induces a voltage in the thermopile, which is the device's direct output

INTELLIGENT MATERIALS AND STRUCTURES:

Table: 3 List of few intelligent materials and structures

Stimulus	Hydrogel	Mechanism
pH	Acidic or basic hydrogel	Change in pH—swelling—release of drug
Ionic strength	Ionic hydrogel	Change in ionic strength—change in concentration of ions inside gel—change in swelling—release of drug
Chemical species	Hydrogel containing electron-accepting groups	Electron-donating compounds—formation of charge/transfer complex—change in swelling—release of drug
Enzyme substrate	Hydrogel containing immobilized enzymes	Substrate present—enzymatic conversion—product changes swelling of gel—release of drug
Magnetic	Magnetic particles dispersed in aliginate microspheres	Applied magnetic field—change in pores in gel—change in swelling—release of drug
Thermal	Thermoresponsive hydrogel poly(N-isopropylacrylamide)	Change in temperature—change in polymer-polymer and water-polymer interactions—change in swelling—release of drug
Electrical	Polyelectrolyte hydrogel	Applied electric field—membrane charging—electrophoresis of charged drug—change in swelling—release of drug
Ultrasound irradiation	Ethylene-vinyl alcohol hydrogel	Ultrasound irradiation—temperature increase—release of drug

MAGNETIC SENSORS AND ACTUATORS:

- A magnetic sensor is a sensor that detects the magnitude of magnetism and geomagnetism generated by a magnet or current. There are many different types of magnetic sensors

Coiled:

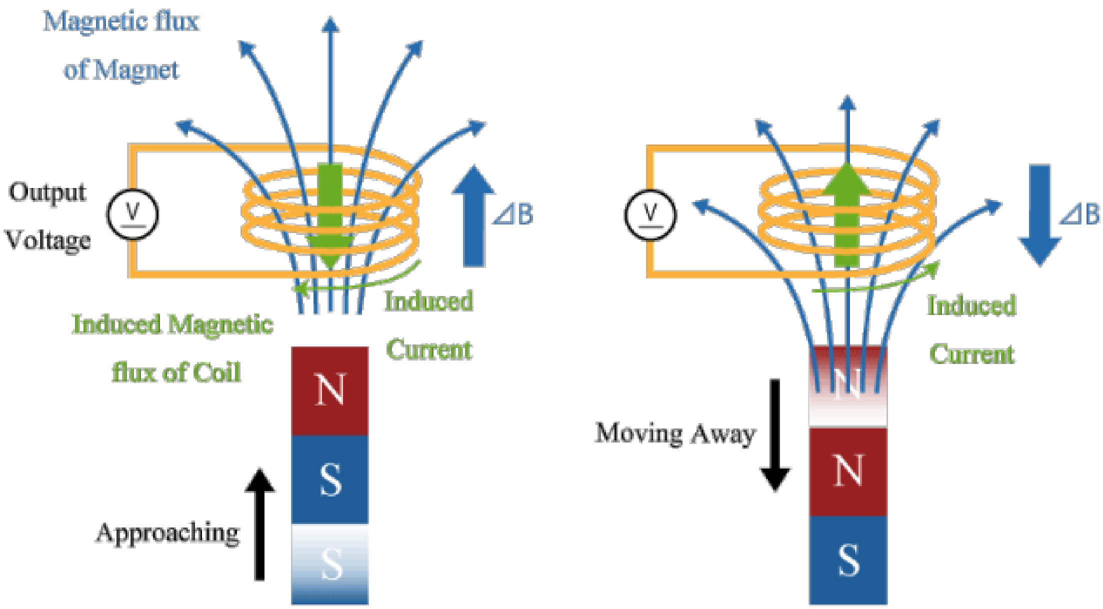

Fig-27: Principle of magnetic sensors

Coils are the simplest magnetic sensors that can detect changes of the magnetic flux density. As shown in Figure, when a magnet is brought close to the coil, the magnetic flux density in the coil increases by ΔB. Then, an induced electromotive force/induced current that generates a magnetic flux in a direction that hinders an increase in magnetic flux density is generated in the coil.

Conversely, moving the magnet away from the coil reduces the magnetic flux density in the coil, so induced electromotive force and induced current will be generated in the coil to increase the magnetic flux density.

Also, since there is no change in the magnetic flux density when the magnet is not moved, no induced electromotive force or induced current will be generated. By measuring the direction and magnitude of this induced electromotive force, it is possible to detect the change in magnetic flux density.

Because of its simple structure, a coil is not easily damaged. However, the output voltage depends on the rate of change of the magnetic flux. It may not be possible to use a coil to detect a fixed magnet or magnetic flux that changes very slowly.

REED SWITCH:

- A reed switch is a sensor in which metal pieces (reed) extending from both the left and right sides are enclosed in a glass tube with a gap at the overlapping position of the reeds. When a magnetic field is applied externally, these reeds are magnetized. When the reeds are magnetized, the overlapping parts attract each other and come into contact, then the switch turns on.

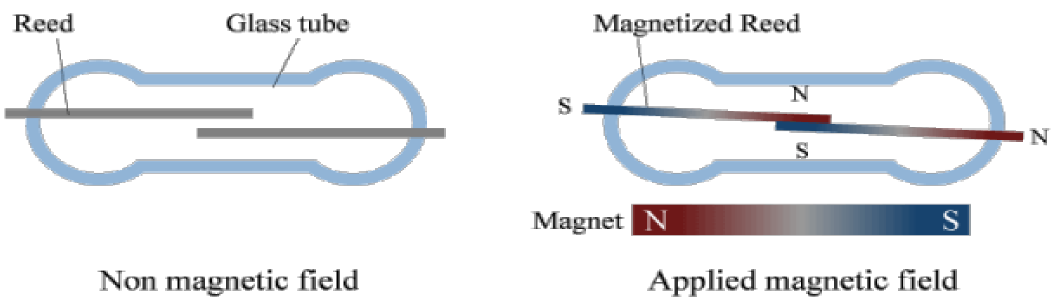

Fig-28: Reed Switch

HALL ELEMENTS:

It is based on the phenomenon that the electromotive force appears in the direction orthogonal to both the current and the magnetic field when applying a magnetic field perpendicular to the current to the object through which current is flowing.

When a current is applied to a thin film semiconductor, a voltage corresponding to the magnetic flux density and its direction is output by the Hall effect. The Hall effect is used to detect a magnetic field.

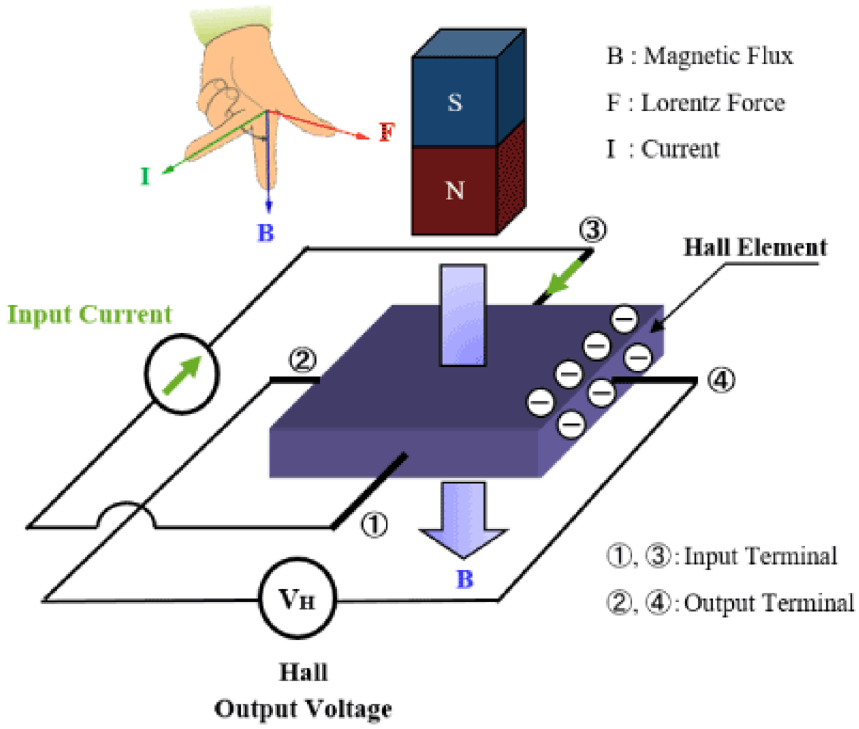

Fig-29: Hall Element principle

MAGNETORESISTIVE ELEMENT:

- An element that detects a magnetic field using a material, that resistance changes when magnetic force is applied, is called a magnetoresistive, (MR), element.
- Other than semiconductor magnetoresistive element, (SMR), there are three kinds of sensors as representative examples of the magnetoresistive element using a ferromagnetic thin film material such as anisotropic magnetoresistive element, (AMR), giant magnetoresistive element, (GMR), and tunnel magnetoresistive element, (TMR).

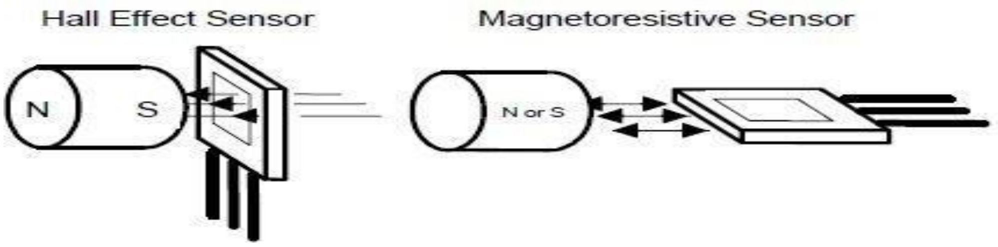

Fig-30: Magnetostrictive Element

SEMICONDUCTOR MAGNETORESISTIVE ELEMENT(SMR):

- Whereas the Hall element is a sensor that measures the Hall voltage generated by the Lorentz force, the magnetoresistive element is a sensor that utilizes the change in the resistance value caused by the Lorentz force.
- Figure shows how the resistance value of an N-type semiconductor magnetoresistive element (SMR: Semiconductor Magnetoresistive), changes. Metal electrodes are placed on a semiconductor thin film in the structure of SMR. When a clockwise current as shown in the figure flows through the semiconductor thin film, electrons which are carriers of N-type semiconductors flow counterclockwise, and the velocity of the vector is assumed as "v". When applying a magnetic field B oriented as shown in the figure, electrons undergo Lorentz force and the path becomes longer as being bent, so that the resistance value increases.

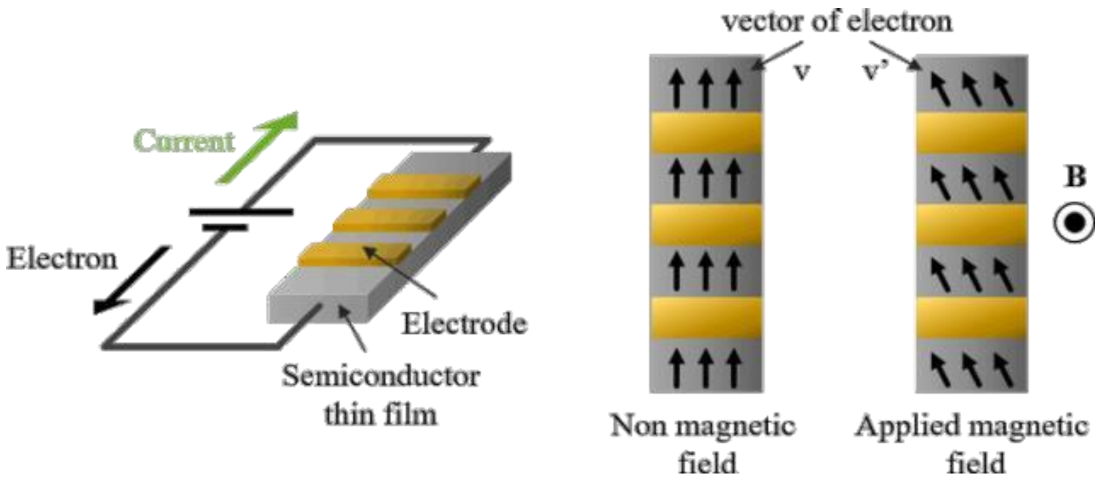

Fig-31 Magnetostrictive property using semiconductors

MAGNETIC ACTUATORS:

- Magnetic actuators and sensors use magnetic fields to produce and sense motion.

- Magnetic actuators allow an electrical signal to move small or large objects.
- To obtain an electrical signal that senses the motion, magnetic sensors are often used.
- Since computers have inputs and outputs that are electrical signals, magnetic actuators and sensors are ideal for computer control of motion.
- Hence magnetic actuators and sensors are increasing in popularity.

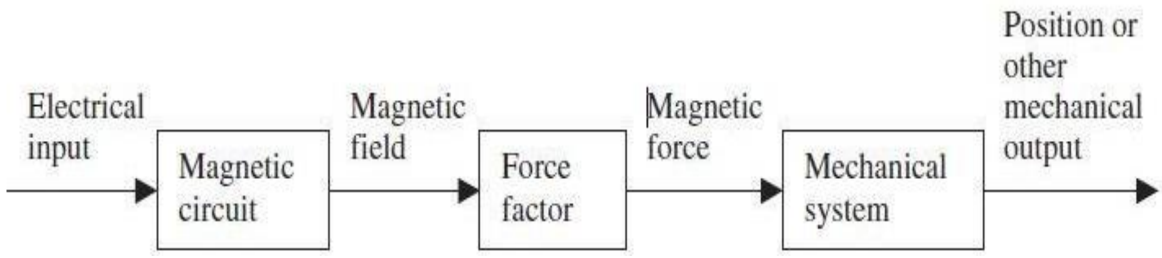

Fig-32: Block diagram of magnetic actuator

Input electrical energy in the form of voltage and current is converted to magnetic energy. The magnetic energy creates a magnetic force, which produces mechanical motion over a limited range. Thus magnetic actuators convert input electrical energy into output mechanical energy.

Typical magnetic actuators include

- Electrohydraulic valves in airplanes, tractors, robots, automobiles, and other mobile or stationary equipment
- Fuel injectors in engines of automobiles, trucks, and locomotives
- Biomedical prosthesis (artificial body) devices for artificial hearts, limbs, ears, and other organs
- Head positioners for computer disk drives
- Loudspeakers
- Contactors (electrically controlled switch), circuit breakers, and relays to control electric motors and other equipment
- Switchgear and relays for electric power transmission and distribution

ACTUATORS AND SENSORS IN MOTION CONTROL SYSTEMS:

Motion control systems can use nonmagnetic actuators and/or nonmagnetic sensors. The head assembly is a magnetic sensor that senses (―reads‖) not only the computer data magnetically recorded on the hard disk but also the position (track) on the disk. To position the heads at various radii on the disk, a magnetic actuator called a voice coil actuator is used.

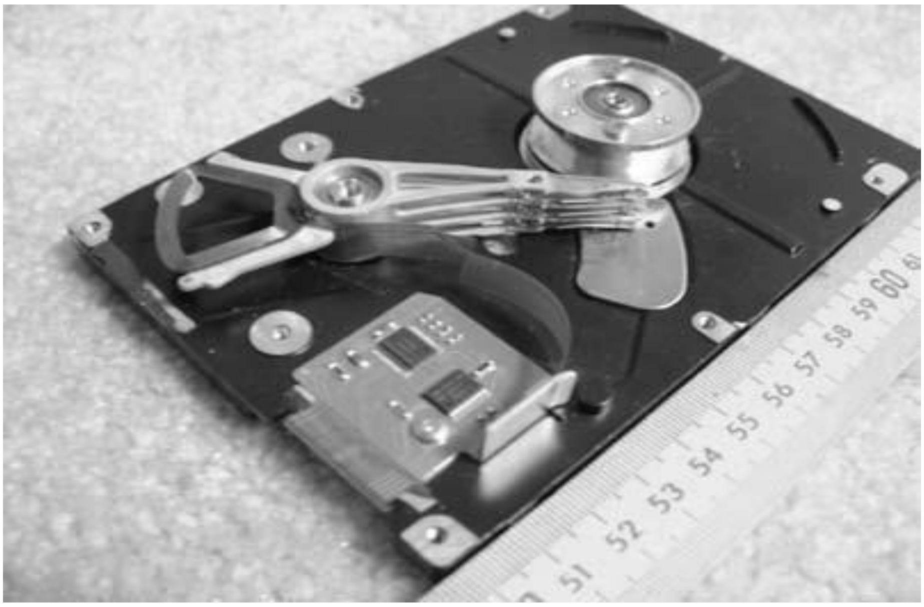

Fig-33: Typical Computer disk assembly

The actuator coil is the rounded triangle in the upper left. The four heads are all moved inward and outward toward the spindle hub by the force and torque on the actuator coil. Portions of the actuator and all magnetic disks are removed to allow the coil and heads to be seen.

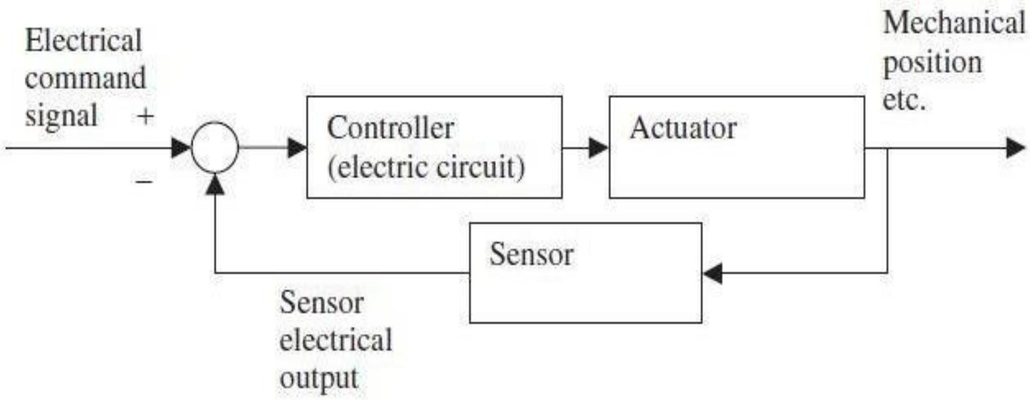

Fig-34: Basic feedback control system that may use both a magnetic actuator and a magnetic sensor.

An example of a motion control system that uses both a magnetic actuator and magnetic sensor is the computer disk drive head assembly shown in above figure.

- It contains both an actuator and a sensor. The sensor may be a magnetic sensor measuring position or velocity.
- The actuator may be a magnetic device producing a magnetic force.
- It is found that accurate control requires an accurate sensor.

Voice Coil Actuator:

- Instead of forces on steel, Lorentz force on current-carrying coils is used in many actuators. They are called –voice coil actuators‖ because of their common use in loudspeakers.
- From the Lorentz force equation, the force on an *N*-turn coil of average turn length *l* is

$F = NBIl$.

where *B* is the magnetic flux density perpendicular to the coil direction and *F* is perpendicular to both B and the coil direction. The directions follow the right-hand rule.

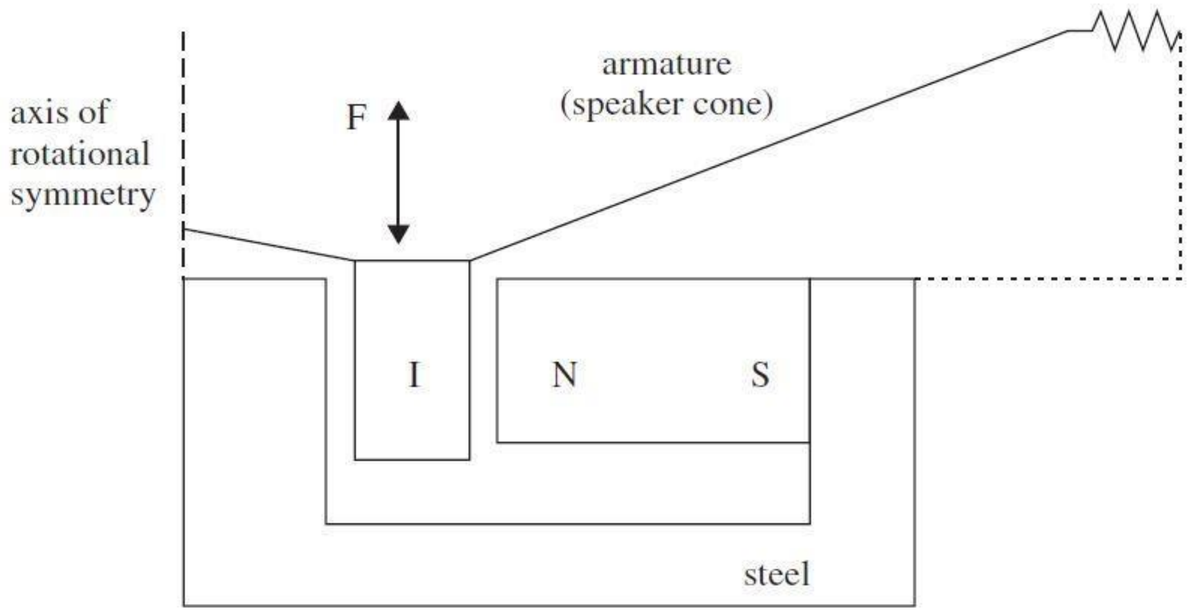

Fig-35: Typical voice coil actuator, shown driving a loudspeaker. The movable voice coil carries the current *I* and is subjected to the magnetic field from a permanent magnet with north (N) and south (S) poles.

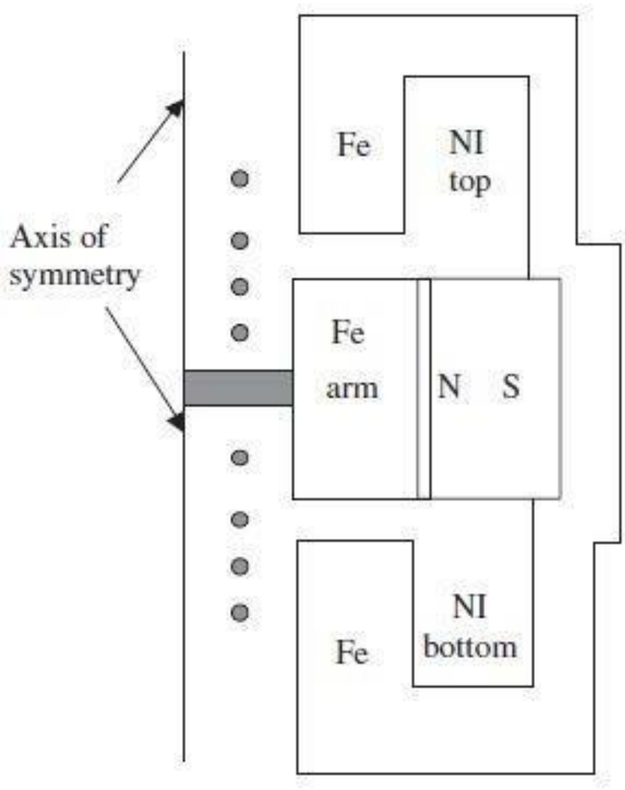

Fig-36: Actuator with both permanent magnet and coils in stator. The armature labeled "arm" moves either up or down.

- Other actuators are available that use both permanent magnets and coils. The advantage of using permanent magnets is that the **B** they produce does not require current or power loss as do coils.
- The **B** of the permanent magnets interacts with the **B** of coils to produce the force.
- It is a long-stroke actuator with one radially magnetized permanent magnet, a steel or iron armature, and two coils. The coils are wound and connected so that they both carry current in the same direction.
- For example, if they both carry current out of the page, then the lower pole of the moving iron armature has higher flux than the upper pole, and the armature experiences a downward force.
- Reversal of the current gives an upward force, and no current gives zero (balanced) force on the armature. Thus the armature experiences bidirectional force.
- The force varies with position because of the variation in both airgaps.

MAGNETIC MATERIALS USED FOR MEMS:

- Based on their B-H (Total magnetic flux density-Externally applied magnetic field) behavior, engineering materials are also typically classified into soft and hard magnetic materials.
- Soft magnetic materials are easy to magnetize and demagnetized, hence require relatively low magnetic field intensities.
- Soft magnetic materials are typically suitable for application where repeated cycles of magnetization and demagnetization are involved, as in electric motors, transformers, and inductors, where magnetic field varies cyclically
- Hard magnets, also referred to as permanent magnets, are magnetic materials that retain their magnetism after being magnetised.
- Permanent magnet (usually is hard magnetic material) is a passive device used for generating a magnetic field, and is useful in a variety of situations where it is difficult to provide electrical power or there are severe space restrictions where electromagnets are not allowed.
- The energy needed to maintain the magnetic field has been stored previously when the permanent magnet was magnetized and then left in a high state of remanent magnetization.
- The important properties of permanent magnetic materials are coercivity Hc and remanence Br. Samarium-cobalt is a permanent magnetic material used widely in 1960s

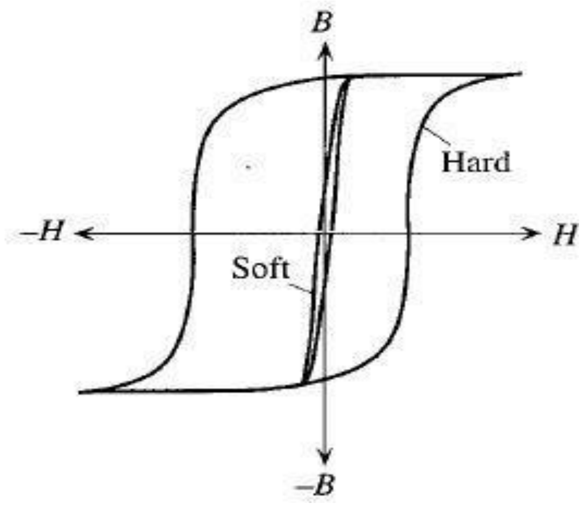

Fig-37: SOFT AND HARD MAGNETIC MATERIALS B-H Curve

- In the early 1980s, neodymium-iron-boron was developed as a low-cost high performance permanent magnet
- The presence of $Nd_2Fe_{14}B$(Neodymium Magnet), a very hard magnetic phase with greater coercivity and energy product (H*B), is what leads to the superior magnetic properties.
- Disadvantage of the above material is the need for powder sintering process which is complex.
- $Nd_2Fe_{14}B$ film has found wide application in compact recording devices, magnetic sensors and other integrated electromagnetic components

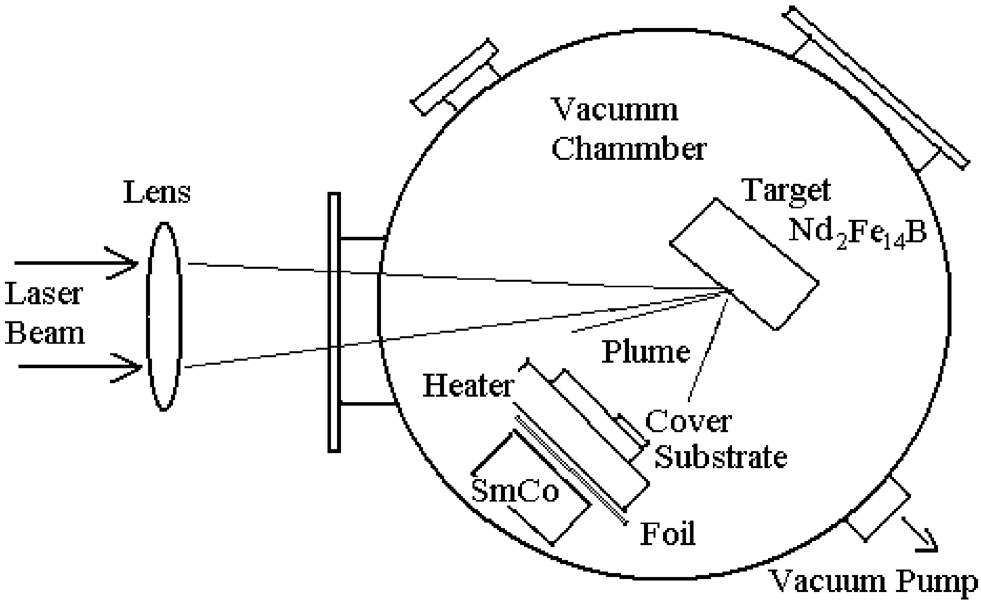

Fig-38: Illustration of the Experiment Setup

MICROFLUIDIC SYSTEMS:

The study of transportation of fluids and their mixtures at a microscale level is known as microfluidics.

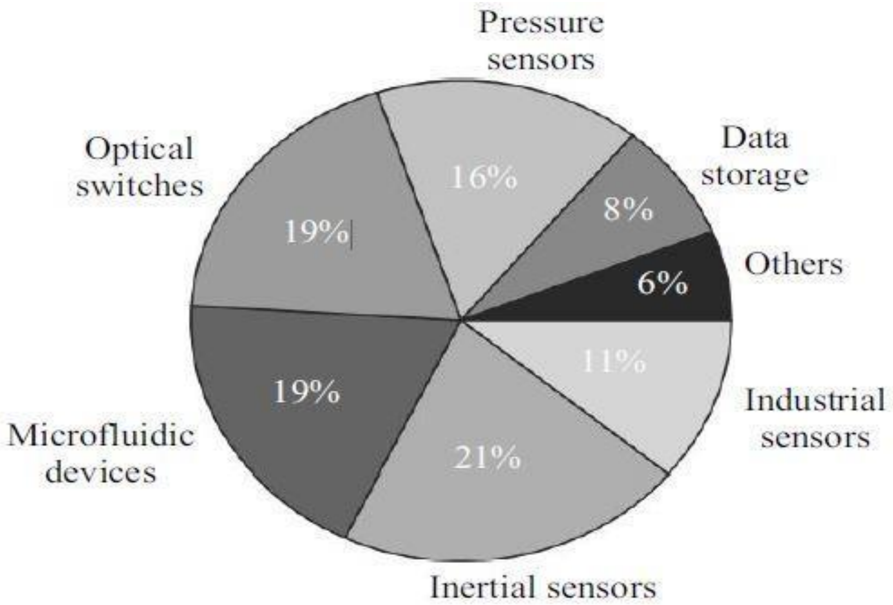

Fig-39: An approximate illustration of MEMS products in various sectors

Microdevices, which are used to transport and store fluid are called microfluidic systems (MFS). Typically the MFS handle fluid volumes in the order of nanoliter.

Some of the important building blocks of microfluidic systems are:

1)Microchannel

2) Microvalves

3) Micronozzles

4) Microreservoirs

5) Micropumps

Some important applications of microfluidics are

- Ejection of inkjet droplets in printers
- Microfluidic oscillator and micro heat exchangers
- Tuning of optical-fiber properties
- Micropumping of gases and liquids
- Drug screening and delivery
- In-vitro diagnostics
- Biological and genetic analysis (e.g. DNA detection)
- Chemical analysis and synthesis
- Environmental pollutant detection and analysis.

Advantages of MEMS microfluidics compared to conventional fluidic systems are:

- The miniaturized system requires less reagent (species or samples) resulting in faster, accurate and reliable measurements
- The capillary action changes significantly when the fluids pass through microscale diameter channels.
- As the scale becomes smaller, the dimensions of a device reach a certain size and the fluid particles or the solvent become comparable in size with the channel or the device itself.

LAB ON CHIP (LoC):

The chemical, clinical and bio-clinical laboratories the instrumentation and analytical equipment and devices are becoming smaller, simpler, and smarter suggesting miniaturization Microfluidics prefers to the design & development of tools, devices related to microscale levels for medical, chemical and biotechnological research. These devices are rather called tools, which have been emerged as biochip or lab-on-a-chip (macroscale test-tube based instrumentation and analytical equipment within the laboratory)

The advantages of LoC (Lab on Chip) are,

• Smaller liquid consumption

• Good response time

• Faster analysis and diagnosis

• Better statistical results and certainty

• Improved possibilities for automation

• Decrease in health and environmental risks

• Reduced costs

IMPORTANT CONSIDERATIONS ON MICROSCALE FLUID:

The behavior of fluid is significantly changed as geometric scale decreases. In this respect following considerations are to be noted. The physical, technological, and biological significance in flows of gases and liquids at the microscale level necessitate the study of properties of fluids. The dominant physical quantities change in the micro-world. Because of scaling effect the large surface forces, high shear and extensional rates, high heat and mass transfer rates make microfluidics a challenging technology.

The control of fluid flow in miniaturized devices and porous media is critical. The physical phenomenon such as intermolecular forces, slip, diffusion and bubbles are the main active agents at the microscale level. In the microworld the surface forces and surface tension start to dominate. When the channel of the order of one micrometer the surface tension is extremely large.

The design of MFS(microfluidic systems) concerns selection of appropriate method for inletting or pumping the liquids into microchannels against two major forces such as surface tension and the externally applied pressure. The diffusion-based characteristics of the laminar flow are sometimes exploited for sample preparation and analysis. The laminar flow behavior of fluids is also considered in the design and development process of microfluidic devices.

The Newtonian fluid mechanics and flow in confined geometries are significant. The flow of thin films spreading under gravity or surface tension gradients is considered important. The handling of fluids with liquid-gas interface in micro channels, valves, pumps, mixers, separators and reactors, excels engineering and scientific challenges. Fluid transportation in a typical microchannel is accomplished based on many phenomenological methods. The control of fluid transportation apparently depends upon the wall surface physicochemistry due to the fact that the fluids exert hydrophobic or hydrophilic force from the channels. The flow behavior of fluids is influenced by the presence of ions, polymers, biomolecules, etc.

FLUID ACTUATION METHODS:

The microfluidic systems are of two types based on the way the microvolume fluid is transported (or its position is manipulated). Accordingly, the systems are called

1) Continuous flow systems

2) Liquid droplet-based system

The position manipulation of microvolume liquid is sometimes called fluid actuation. Conventional pumps, valves, and channels actuate the fluids in continuous-flow systems. In a droplet-based system, however, they are actuated by exploiting the surface tension. In essence, the systems use surface tension gradient to move, combine, and mix liquid droplets. The droplet based system is also called digital fluidic microsystem.

Fig-40: Figure illustrating the surface tension.

When we sandwich 2 electrodes with water and potential is applied, it results in the change of hydrophilic or hydrophopic character of the region. This causes the transportation of the liquid along the region, where it can then be separated into a smaller segment. Henceforth application of potential causes liquid to segment out further. This procedure results in a digitized fluidic circuit.

This procedure has attracted much attention because it eliminates the need for traditional pumps and valves. It also involves less volume of water involved. All these mechanism can control the surface tension.

Some of the important mechanisms are:

1) Dielectrophoresis

2) Thermocapillary

3) Electrowetting

4) Electro-osmosis

5) Electrothermal

6) Light-actuated microfluidic device called optoelectrowetting

DIELECTROPHORESIS (DEP):

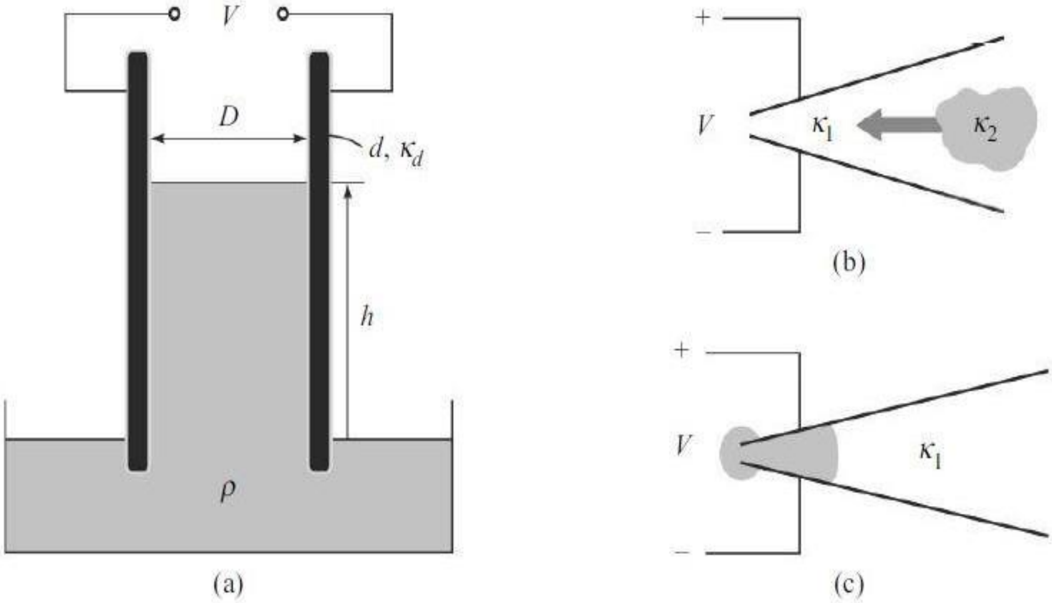

Fig-41: (a) Pellat's dielectrophoretic force experiment; (b) The dielectric liquid is attracted to regions with stronger electric field; (c) The liquid surface follows the electric field lines

Experiment was conducted by Pellat He did this by utilizing two planar, parallel and opposed electrodes, placed vertically with one end submerged into an insulating, dielectric liquid as shown in Fig (a). From the experiment it was found that if a potential difference between the two electrodes is applied, a force is exerted on the liquid, trying to impel it upward.

Because of applied potential difference, the hydrophobic and hydrophilic character of the region changes. This causes the development of a force.The magnitude of this force, and therefore the height of rise of the liquid, is proportional to the magnitude of the applied voltage.

The mathematical equation that governs the DEP phenomenon can be written as,

$$h \approx \frac{k_d \varepsilon_0 V^2}{4 g \rho d D}$$

where

V is the applied potential difference,

r is the density,

k_d is the dielectric constant of the liquid, h is height of rise of liquid,

d is the thickness of the dielectric coating, D is the distance between the planar-parallel electrode,

$\varepsilon_o = 8.854 \times 10^{-12}$ Farad/meter is the permittivity of the free space,

$g = 9.81\ m/s^2$ is the gravitational force.

The effect will be similar if the electrodes are not placed parallel as shown in Fig. (b). The force that starts to act on the liquid is called dielectrophoretic force. The dielectrophoretic force appears when a medium (liquid) is exposed to a non-uniform electric field. The liquids are pulled toward the regions of stronger electric field (Fig. (c)). In essence, the dielectrophoretic phenomenon can be utilized in microfluidics to transport and manipulate microvolume of liquid on a surface (channel).

Typical microfluidic Channel:

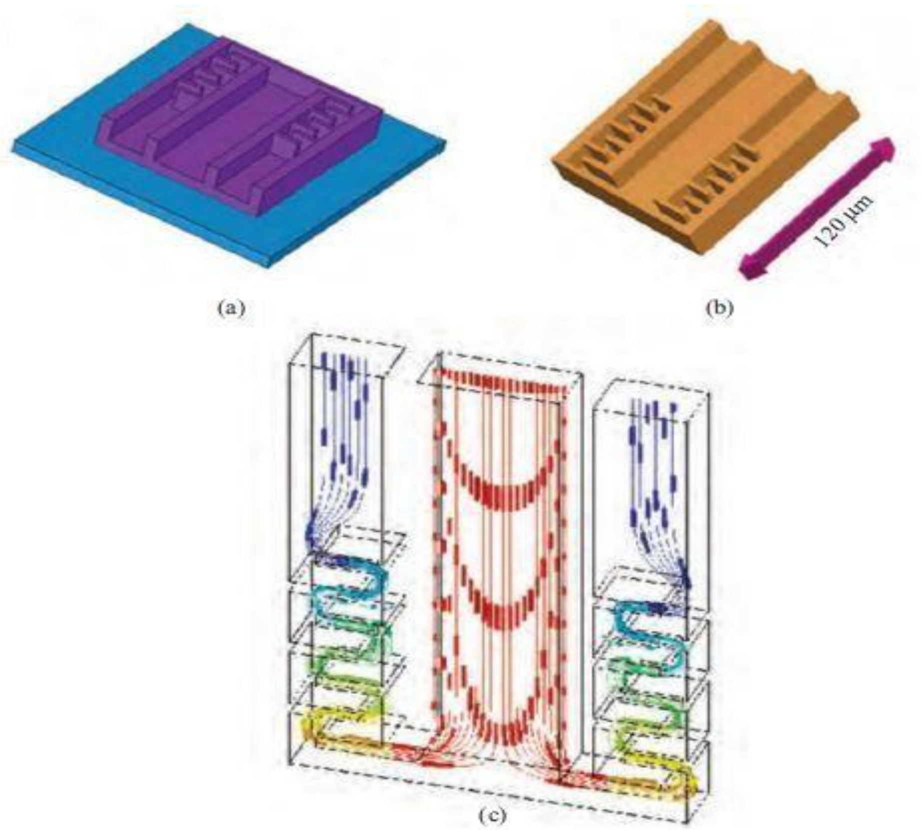

Fig-42: a)Two dimensional view of typical microfluidic channel, b) segmental view, c) Flow profile of the microfluidic channel

Above figure illustrates a typical microfluidic channel, which consists of a surface micro-machined labyrinth, having one central inlet and two outlets. This device imported from Ansys CAD software, is a model, which is approximately 100x120 mm dimension, with a channel depth of 10 mm. The top of this device is not shown because of clarity, but is made by sealing another layer onto the top surface. Fusion bonding technique can be employed to join the channel and the top layer.

The labyrinth can function as a pressure drop or pulse attenuator for blood flow and can be used in clinical diagnosis. Blood can flow into the central inlet and out through the two flanking outlets at a reduced pressure. Figure (c) shows the streamline coded in pressure (Central input channel = high pressure; Two output channel = low pressure), plus particles that follow the streamlines. In essence, the device can be utilized for the purpose of liquid analysis such as:

• Determination of pressure drop across the device

• Determination of velocity profile

• Computation of pressure applied to walls

• Transfer of heat from fluid to structure and vice-versa.

• Obviously, the above liquid (blood) parameters within the channel can be analysed.

MICROFLUID DISPENSER:

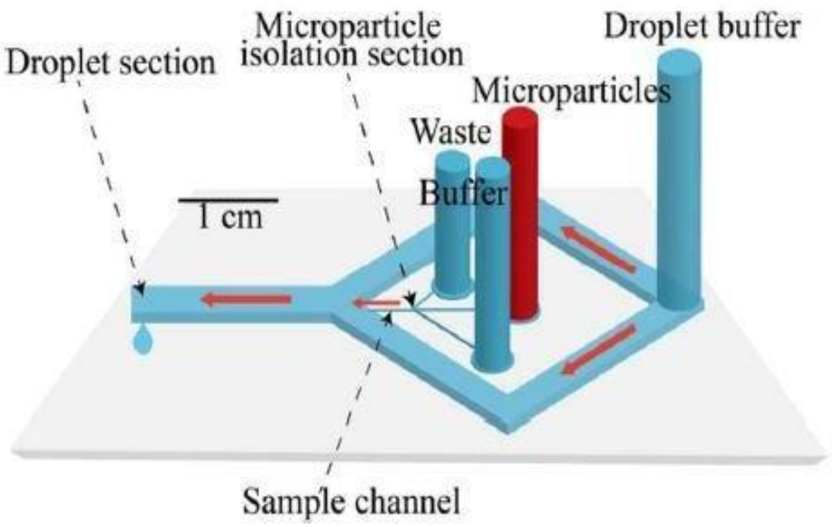

Fig-43: Typical microfluidic dispenser structure

Above figure shows the schematic of the microfluidic chip identifying individual reservoirs and flow directions. Reservoir in red supplies microparticles that flow into the waste reservoir until the optical trap isolates them into the sample channel leading to the droplet delivery section. Channels in the isolation section are 10 μm tall, the droplet buffer channels are 160 μm high and 3 mm wide, while channel lengths are according to scale. (Red arrows indicate flow direction).

The microfluidic device incorporates a separate isolation region to deliver single cells to the droplet generation section for distribution as droplets, an approach that shields the particle isolation section from the mN range surface tension forces In this, an on-chip droplet buffer reservoir generates μl s^{-1} flow rates in wide channels that bifurcate at the droplet buffer inlet and wrap around the isolation section.

Cells flowing into the intersection of these bulk channels via the sample channel at the end of the isolation section are carried by these relatively large flows along the 20 mm length of this channel to the microfluidic device exit, rapidly amplifying the μm translation achieved by the optical trap to mm range. This process moves particles away from the crowded isolation section to the exit where a hydrophobic orifice aids freefalling droplet generation making them easily accessible.

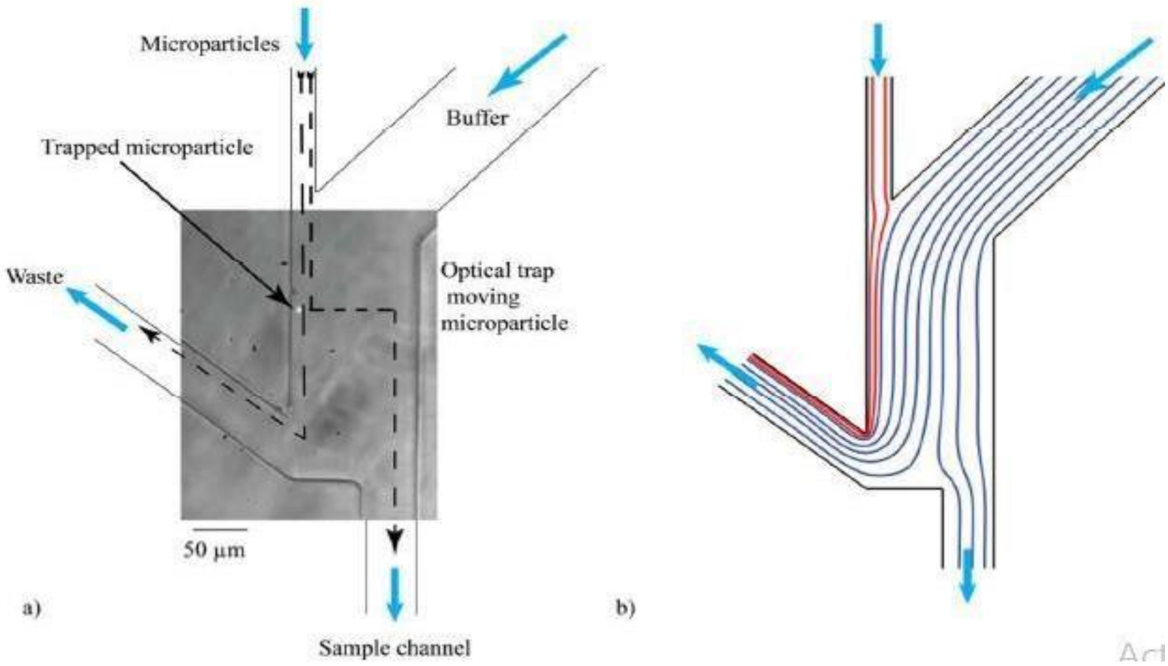

Fig-44: (a) Schematic of the microparticle isolation section, (b) Flow profile.

MICRONEEDLE:

Microfluidic systems promise to revolutionize health care by providing equipments for precise delivery and control of biological fluids. To achieve this in many situations, microneedles are used. Microneedles are attractive from a design perspective as they are also compatible with MEMS fabrication process.

Because of their small size they can be fabricated to provide a range of geometries and flow characteristics.

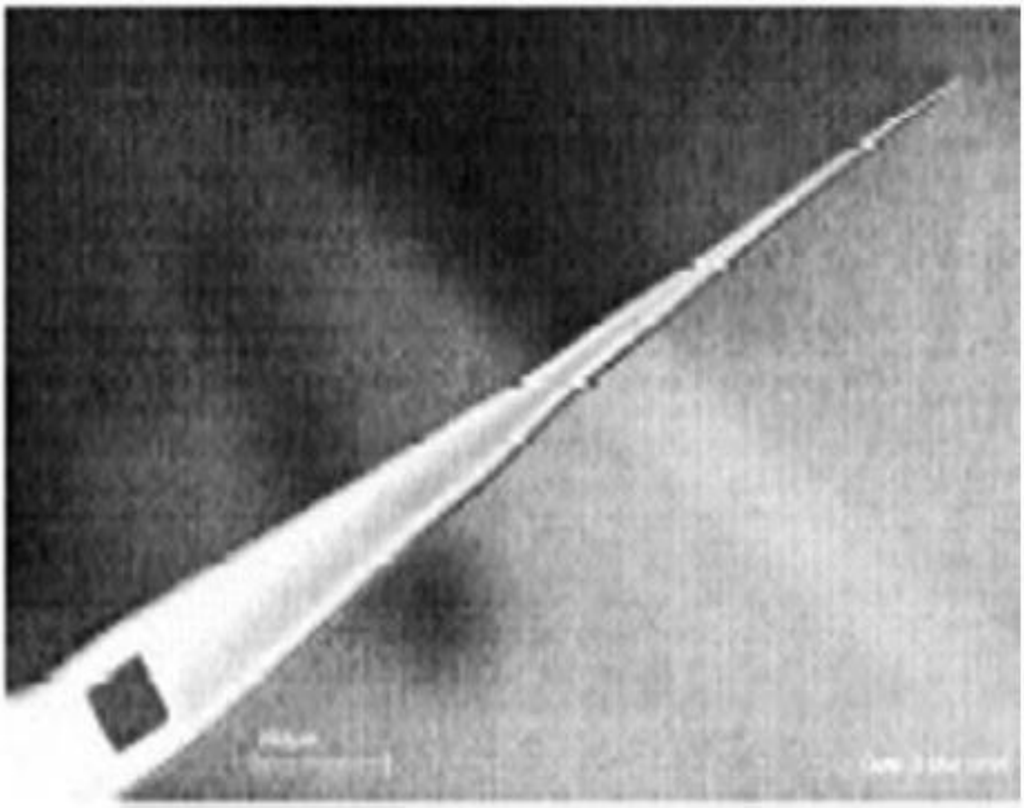

Fig-45: Microsensor of Berkeley Sensor and Actuator Center at University of California

Microneedle are considered as an important BioMEMS devices and especially very useful for the following applications. Collection of samples for biological analysis Delivery of cell or cellular extract based vaccines Providing interconnection between the microscopic and macroscopic devices Extra and Intracellular neuronal recording.

- For a laminar flow, the average flow rate Q can be expressed as,

$$Q = \frac{4ba^3}{3\mu}\left(-\frac{dP}{dx}\right)\left[1 - \frac{192a}{\pi^5 b}\sum_{i=1,3,5\ldots}^{\infty}\frac{\tan h(i\pi b/2a)}{i^5}\right]$$

which is obtained by integrating x-directed velocity profile of a rectangular duct with y and z as cross section. Here 2a is the length of the walls, 2b the length of other wall, dP/dx is the pressure gradient which can be estimated to be,

$$\frac{dP}{dx} = -\frac{4\tau_s}{D}, \text{ where } \tau_s = \frac{0.332\mu U}{x}\sqrt{\Re_x}$$

τ_s is shear stress of the plate, x is the distance along the plate, $\Re_x$ is the Reynolds number based on the distance x. The above expression is based on the assumption that the rectangular fluid duct behaves as a collection of four places. The average velocity can be expressed as

$$U = \frac{Q}{4\,ab}$$

MICROPUMPS:

It‟s a continuous flow system. A mechanical machine that moves fluid or gas continuously by suction pressure is known as a pump. Micropumps are MEMS devices, which are primarily used for microfluidic applications. The cost-effective transport of small quantities of biochemical fluidic samples, in the range of microliters per minute, has been an important challenge for micropumps

These devices operate with flow rates in the range of nanoliter to microliter per minute. Diaphragm based micropumps shown in fig. below are common

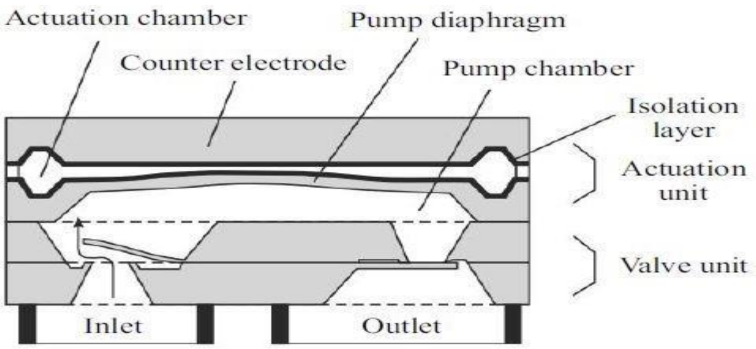

Fig-46: Cross-sectional view of a diaphragm-based micropump assembly

The important part of the micropumps is the diaphragm. The back and forth operation of the diaphragm is achieved by applying AC signal. The material should have high electromechanical properties such as high electrostrictive strain, high energy density, and (iii) high displacement voltage ratio. Polymer is chosen as the suitable material. Mostly, vinylidene fluoride-trifluoroethylene polymers are used, as they possess these properties.

These are called high-energy electron irradiated poly. Besides diaphragm, the other parts and sections of the micropumps are listed below.

- Counter electrode
- Isolation layer
- Actuation chamber
- Pump chamber
- Inlet valve
- Outlet valve
- Inlet microtube
- Outlet microtube

As mentioned, the pump is electrically driven. The AC supply with appropriate frequency is applied across the two electrodes. The diaphragm itself constitutes one electrode.

The other terminal of the AC supply is applied to the counter electrode. Isolation layer is a design criterion and it has high impedance. The operation of the micropump is shown in Fig. 21. The figure shows cross-sectional view of a pump assembly. By applying AC voltage the diaphragm can be deflected up and down (back-andforth). During positive cycle of the applied signal, the diaphragm makes upward movement. Because of this a suction pressure is developed within the pump chamber. The pressure makes it possible to open the cap of the inlet valve and to allow fluids to enter into the pump chamber. During this half-cycle the cap of the outlet valve is closed, as the cap exists at the other end of the orifice.

During negative excursion of the applied AC signal the diaphragm makes downward

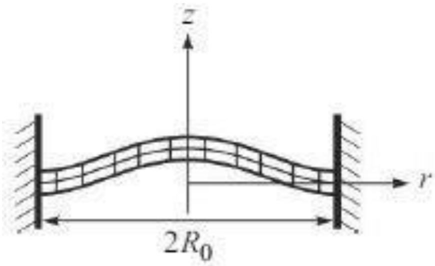

movement causing the cap of the outlet valve to open. The downward movement makes it possible to allow the fluid to pump away from the chamber.

Fig-47: Deflection of diaphragm under an electric field

The pump can be modeled by considering the diaphragm as a circular plate. It is assumed that the circular plate with clamped edges is subjected to uniform mechanical pressure in the lateral direction. Let the radius of the plate be R_0 and the horizontal and vertical axes are denoted as r and z, respectively as shown in Fig.22.

where f_d is the frequency of diaphragm. Typical values of pumping rate are 50–70 microliter per minute at the applied voltage of 2–3 Vpp. The pump pressure can be about 600 Pa at this voltage. The operational frequency ranges from 10–30 Hz. The overall dimensions of MEMS micropump can be approximately 5000x5000x1000 μm with respect to the length, width and height, respectively. Other driving methods such as electromagnetic, electrothermal etc. can be employed to vibrate the diaphragm.

SATHYABAMA

INSTITUTE OF SCIENCE AND TECHNOLOGY

(DEEMED TO BE UNIVERSITY)

Accredited "A" Grade by NAAC | 12B Status by UGC | Approved by AICTE

www.sathyabama.ac.in

SCHOOL OF MECHANICAL ENGINEERING

DEPARTMENT OF MECHATRONICS ENGINEERING

Unit – V: Micro System Packaging and Design

Micro Electro Mechanical System (MEMS) :SMR1301

1. INTRODUCTION

MEMS is a relatively new field which developed so closely with silicon processing that most of the early packaging technologies were borrowed from the microelectronics field. Packaging of a micromachine is the science of establishing interconnections between the systems and providing an appropriate operating environment for the electromechanical circuits to process the gathered information. Most MEMS devices need physical access to the outside world to react mechanically with an external parameter or to sense a physical variable. MEMS not only condition the signals but also move, which requires care in handling. The state-of-the-art of current sensing technologies is that the device normally accesses the outside world via electrical connections alone and the rest of the systems are totally sealed and isolated. Inertial and optical devices are sometimes special cases, but, in general, the packaging approach of MEMS is fundamentally different from microelectronic packaging. Unlike electronic packaging, where most of the standard packages can be used for a wide variety of applications, the MEMS packaging therefore tends to be customized to the specific applications, which can be summed up in three words: cost, performance and reliability.

Packaging can span from consumer to midrange systems to high-performance weapon-grade applications. No sharp boundaries exist between these classes. However, the gradual shift of optimization parameters, controls the performance, reliability and cost. The size of the package, the choice of its shape and material, the alignment of the device, the mounting for the isolation of shock and vibration, and the seal are some of the many concerns in MEMS packaging. Many important lessons that have seen learned throughout years of experience in the microelectronics industry can be adapted to the packaging of MEMS devices. A MEMS package contains many electrical and mechanical components, which need to be interconnected. Electrical inputs need to be interfaced with the circuits. MEMS can be extremely fragile. They must be protected from mechanical damage and hostile environments. MEMS packaging involves the components of mechanical and electrical structures and the combination of there to form a system.

Webster's Collegiate Dictionary (10^{th} edition) defines *package* as a 'commodity or a unit of a product uniformly wrapped or sealed'. This chapter presents the fundamentals of microelectronic packaging adapted by MEMS technology for its packaging along with the state-of-the-art in customized MEMS packages. The theme continues to be *smaller–faster–cheaper–optimal* systems.

The key issue facing the packaging of the MEMS device is die separation. The current standard die separation method adopted for silicon is to cut the wafer using a diamond-impregnated blade. The blade and the wafer are flooded with high-purity water while the blade spins at 45 000 rpm. This creates no problem for standard integrated circuits (ICs) because the surface is essentially sealed against the effects of water and silicon dust. However, if the MEMS device is exposed to water and debris, the system may break or become clogged and the moisture may have adverse effects, for example in case of radio frequency (RF) switches. Efforts to protect these surfaces with photoresist and other coatings have had only limited success.

1.1 ROLE OF MEMS PACKAGES

The aim of a package is to facilitate the integration of all components such that it minimizes the cost, mass and complexity. The main functions of a MEMS package can be summarized as providing: mechanical support, an electrical interface to the other system components and protection from the environment. The packaging provides an interface between the chip and the physical world. The package should protect the device, at the same time letting it perform its intended functions with less attenuation of signal in a given environment at low cost (Blackwell, 2000; Elwenspoek and Wiegerink, 2001). The packaging becomes more expensive when protection is required for relatively fragile structures integrated into the device. For a standard integrated circuit, the packaging process can take up to 95% of the total manufacturing cost. Issues in MEMS packaging are much more difficult to solve because of stringent requirements in processing, handling and the nature of fragile microstructures; the diversity also complicates the packaging problem.

Many MEMS sensors often require a sensing media interface with a sensing area. For example, a pressure sensor packaging requires incorporation of a pressure port to transmit fluid pressure to the sensor. This makes a major difference between standard semiconductor device packages and MEMS packages.

9.1.1 Mechanical support

Owing to the fundamental nature of MEMS as a mechanical device, the protection and isolation of the device from thermal and mechanical shock, vibration, acceleration and other physical damage during operation become critical. The mechanical stress affecting a system depends on the application. For example, for the same space-borne application, the device package for a military aircraft is different from those used in communication satellites because the operating environments are different. The coefficient of thermal expansion of the package should be equal to that of silicon for reliability because the thermal cycle may cause cracking or delamination if the materials are unmatched. If the packaging solution is creating excessive stress in the sensing structure, it can cause a change of device performance. Once the MEMS devices are wire bonded and other electrical connections are made, the assembly must be protected by covering the base or by encapsulating the assembly in plastic or ceramic materials since the electrical connections are usually made through the walls. Managing package-induced stress in the device becomes important for MEMS package design.

1.1.2 Electrical interface

Wire bonds and other electrical connections to the device should be made by protecting the device from scratches and other physical damages. Direct current (dc) and RF signals to the MEMS systems are given through these connections to interface the MEMS device with the systems. Also, these packages should be able to distribute RF signals to other components inside the package. High-frequency RF signals can be introduced into the package by metal transmission lines or coaxial lines or the function can be electromagnetically coupled into the device. The final connection between the MEMS and the RF lines is usually made with wire bonds or flip-chip die attachments and multilayer interconnections.

1.1.3 Protection from the environment

Many of the MEMS devices and sensors are designed to measure outside variables from the surrounding environment. The hermetic packaging generally applicable to microelectronic devices is not suitable in many cases of MEMS devices. These devices might be integrated with the circuits or mounted to a circuit board and protected from mechanical damage. Only special attention to packaging will protect a micromachined device from aggressive surroundings. Protection starts at the dice level (Sparks, 2001). Elements that cause corrosion or physical damage to the metal lines as well as other components such as moisture remains a concern for many MEMS devices. The moisture that may be introduced into the package during fabrication and before sealing can damage the materials. For example, aluminum lines can corrode quickly in presence of moisture, and gold lines degrade slowly in moisture. Junctions of dissimilar metals can also corrode in the presence of moisture. MEMS packages need to be hermetic, with good barriers against liquids and gases.

In most space-borne applications, the parts are hermetically sealed to give a perceived increase in reliability and to minimize outgassing. When epoxies or cyanate esters are used for die attach, they outgas when they cure. Outgassing is a concern for many devices since the particles could deposit onto components and reduce device performance. For example, outgassing leads to stiction and corrosion of the device. Die attach materials with a low Young's modulus allow the chip to move during the ultrasonic wire bonding, resulting in low bond strength.

1.1.4 Thermal considerations

The MEMS devices used for current applications do not have a high power dissipation requirement. The thermal dissipation from MEMS devices is not a serious problem since the temperature of the MEMS devices usually does not increase substantially during the operation. However, as the integration of MEMS with other high-power devices such as amplifiers in a single package increases, the need for heat dissipation will have to be addressed to protect the MEMS device from high temperatures. This thermal management can place a high design consideration on package design.

1.2 TYPES OF MEMS PACKAGES

Methods of packaging of very small mechanical devices are not a new topic. The aerospace industry has performed well in this respect over half a century, and the watch industry for more than that. Each MEMS application usually requires new package design, depending on the application and optimization procedures. In general, the possible group of packages can be categorized into four types: (1) all-metal, (2) ceramic, (3) plastic and (4) multilayer.

1.2.2 Metal packages

IC packaging using metal packages is well advanced because of the wide applications of ICs, excellent thermal dissipation and electromagnetic shielding. Metal packages are also often used in monolithic microwave integrated circuits (MMICs) and hybrid circuits. Materials such as CuW (10/90), Silver (Ni-Fe), CuMo (15/85) and CuW (15/85) are good thermal conductors and have a higher coefficient of thermal expansion (CTE) than silicon. All these metals, with copper, gold or silver plating are good choices for MEMS packages.

1.2.3 Ceramic packages

One of the most common packages used in the microelectronics industry is the ceramic package because of features such as low mass, low cost and ease of mass production. The ceramic packages can be made hermetic, adapted to multilayer designs and can be easily integrated for the signal feedthrough lines. Multilayer packages reduce the size and cost of integration of multiple MEMS into a single package. The electrical performances of the packages can be tailored by incorporating multilayer ceramics and interconnect lines.

These types of packages are generally referred as *co-fired multilayer ceramic packages*.

Co-fired ceramic packages are constructed from individual pieces of thin films in the ‘green’ or unfired state. Metal lines are deposited in each film by thick-film processing, such as screen printing, and via holes for interconnections are drilled. After these lines and interconnecting holes are done, the unfired layers are stacked and aligned and laminated together and fired at high temperature. MEMS and the necessary component are then attached using epoxy, or solder, and wire bonds are made the same as the metal packages.

There are several problems associated with ceramic packaging. The green state shrinks during the firing process and the amount of shrinkage depends on the number of via holes and wells cut into each layer. The ceramic-to-metal adhesion is not strong as ceramic- to-ceramic adhesion. The processing temperature of ceramics limits the choice of metal lines, and the metal should not react with the ceramic during the firing process. In *low-temperature co-fired ceramic* (LTCC), the most frequently used metal lines are tungsten and molybdenum, and the conductors are silver, gold and AuPt.

1.2.4 Plastic packages

Plastic packages are common in the electronic industry because of their low manufacturing cost. However, hermetic seals are not possible with plastic packages, which is generally required for highly reliable applications. Plastic packages are also susceptible to cracking during temperature cycling.

1.2.5 Multilayer packages

Figure 9.1 shows a cross-sectional view of a three-dimensional multilayered packaging for MEMS structures on silicon substrate. Passive elements such as filters and matching circuits are formed in each layer and active devices are assembled on the top layer using flip-chip technology. The structure is a three-dimensional hybrid IC using silicon, which is more cost-effective than GaAs. Figure 9.2 shows a 25.0-GHz receiver front-end incorporating a built-in micromachined filter along with the measured responses (Takahashi *et al*., 2000). The whole down converter and filter were built into a size of 11 × 11 mm with overall conversion gain of 22 dB and a noise figure less that 4 dB.

1.2.6 Embedded overlay

An embedded overlay (Butler and Bright, 2000) concept for packaging of micro-opto-electromechanical systems (MOEMS) and RF MEMS devices is derived from chip-on-flex (COF) process currently used for microelectronics packaging. COF is a high-performance multichip packaging technology in which dies are encased in a moulded plastic substrate and interconnections are made via a thin-film structure formed over the components. The electrical interconnections are made through a patterned overlay while the die is embedded in a plastic substrate, as shown in Figure 9.3. Chips are attached face down on the COF overlay using polyimide or thermoplastic adhesives. The substrate is formed after bonding the chips around the components using a plastic mould-forming process such as transfer, compression or injection moulding at 210 °C. The electrical connections are made by drilling via holes using a continuous argon ion laser at 35 m nm. Ti/Cu metallization is sputtered and patterned to form the electrical interconnections. The use

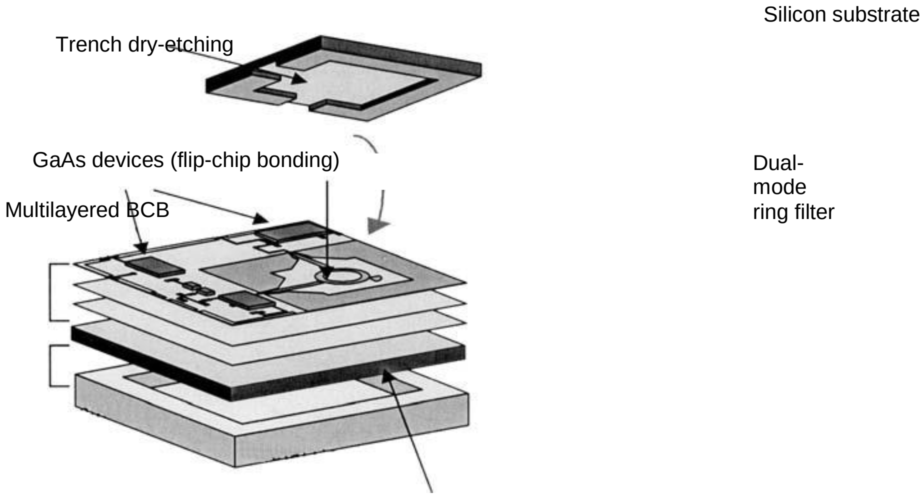

Figure 1 Three-dimensional millimeter-wave MEMS integrated circuit. Reproduced from K. Takahashi, U. Sangawa, S. Fujita, M. Matsuo, T. Urabe, H. Ogura and H. Yubuki, 2001, ‘Packaging using microelectromechanical technologies and planar components’, *IEEE Transactions or Microwave Theory and Techniques* **49**(11): 2099 – 2104, by permission of IEEE, © 2001 IEEE

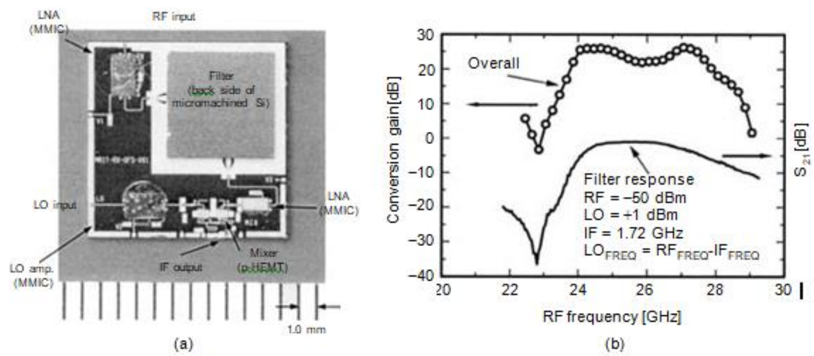

s i s t i v i t y

Figure .2 (a) Fabricated 25-GHz receiver front-end integrated circuit with micromachined fil- ter and (b) measured response. Note: LNA, low noise amplifier; MMIC, monolithic microwave integrated circuit; RF, radio frequency; LO, local oscillator; IF, intermediate frequency; HEMT, high electron mobility transistor. Reproduced from K. Takahashi, U. Sangawa, S. Fujita, K. Goho, T. Uare, H. Ogura and H. Yabuki, 2000, ‘Packaging using MEMS technologies and planar components’, in *2000 Asia Pacific Microwave Conference*, IEEE, Washington, DC: 904 – 907, by permission of IEEE, © 2000 IEEE

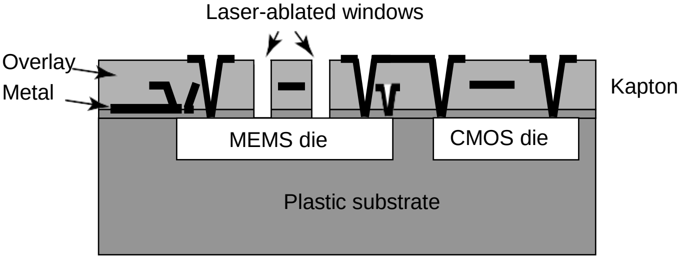

Figure.3 Chip-on-flex MEMS packaging concept. Reproduced from J.T. Butler and V.M. Bright, 2000, 'An embedded overlay concept for microsystems packaging', *IEEE Transactions on Advanced Packaging* **23**(4): 617 – 622, by permission of IEEE, © 2000 IEEE

of varying laser ablation power levels with plasma cleaning and high-pressure water scrubs provide an effective means of removing the COF overlay without damaging the embedded MEMS devices. Figure 9.4 shows the 5×5 array of micromirrors packaged in COF/MEMS modules with integrated micromirror control circuitry.

1.2.7 Wafer-level packaging

MEMS packaging should be considered from the beginning of device development. Cost-efficient MEMS packaging focuses on wafer-level packaging (Gilleo, 2001a, Reichal and Grosser, 2001). Designing the packaging schemes and incorporating then into the device manufacturing process itself can reduce the cost. Versatile packaging may be needed for many devices in which MEMS and microelectronics are on a single chip. Each MEMS device may have its own packaging methods, which may be absolutely suitable for its functioning. Since MEMS devices have movable structures on the surface of the wafer, addition of a cap wafer on the silicon substrate makes them suitable for many applications.

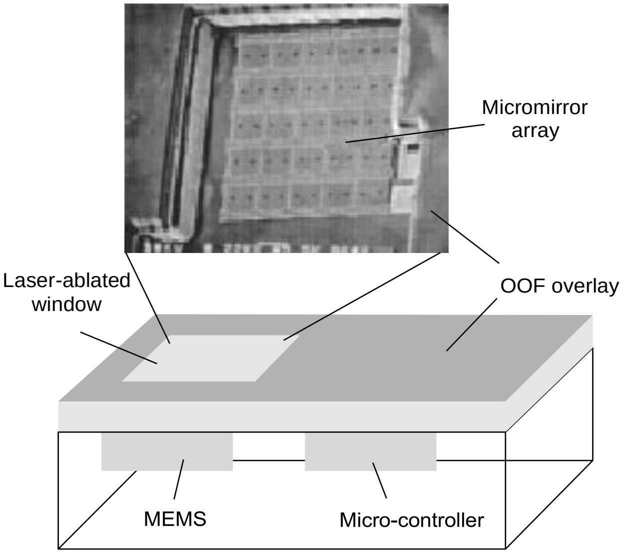

Figure .4 COF/MEMS package of 5 5 array of micromirrors. Note: COF, chip-on-flex. Repro- duced from J.T. Butler and V.M. Bright, 2000, ‘An embedded overlay concept for microsystems packaging’, *IEEE Transactions on Advanced Packaging* **23**(4): 617 – 622, by permission of IEEE, © 2000 IEEE

The cap provides protection against handling damage as well as avoiding atmospheric damping. This is done by bonding the substrate with an active device to a second wafer, either of the same material or of different material. The bonding is done by using glass frit or by anodic bond created by electrical potential. Precision-aligned wafer bonding is the key technology for high-volume, low-cost packaging of MEMS devices (Helsel *et al*., 2001; Mirza, 2000). State-of-the-art silicon wafer bonding can provide assembly level packaging solutions for many MEMS devices.

The wafer-level package, which protects the device at the wafer stage itself, is a clear choice to make at the product design stage itself. This involves an extra fabrication process, where a micromachined wafer has to be bonded to a second wafer with appropriate cavities etched on it. Figure 9.5 shows a schematic diagram of wafer-level packaging. This enables the MEMS device to move freely in vacuum or inert atmosphere with hermetic bonding, which prevents any contamination of the structure. Etching the cavities in blank silicon wafer and placing it over the MEMS device and bonding them together can make a hermetic seal.

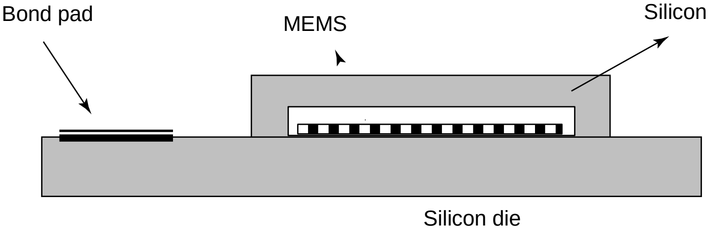

Figure .5 Silicon wafer-level packaging of RF MEMS

Anisotrophic wet etching of bulk silicon along certain crystal planes using strong alkaline solutions such as KOH can create thin diaphragms, through-wafer via holes and V-grooves. The fastest etch rates for the silicon are the (1 0 0) and (1 1 0) crystal planes and the slowest is for the (1 1 1) plane with typical masking layers such as silicon dioxide or low-pressure chemical vapor deposition (LPCVD) silicon nitride. Examples of successful development and packaging using silicon micromachining are the ink-jet heads and silicon piezoresistive pressure sensors for automotive and industrial control applications. Many of these devices require silicon wafer bonding to another substrate as a first-level packaging solution. Anodic (electrostatic) bonding of silicon to glass, low-temperature glass-frit bonding of silicon to silicon, silicon direct wafer bonding, eutectic bonding and epoxy bonding are examples of a few methods available to bond silicon wafer to other silicon, as explained in Section 9.6.1.

1.2.8 Microshielding and self-packaging

The micromachining technology has proved a flexible approach for the development of low-loss transmission lines (Dryton, 1995) as well as micropackages that provide

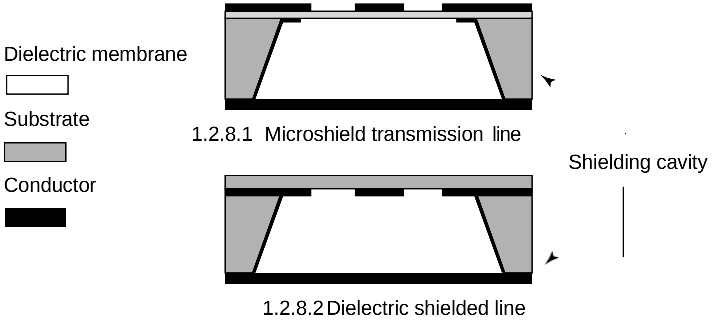

Figure .6 Topology of self-packaging transmission lines: (a) dielectric membrane supported line; (b) dielectric shielded line. Reproduced from R.F. Dryton, 1995, *The Development and Characterization of Self-packages using Micromachining Techniques for High Frequency Circuit Applications*, PhD dissertation, University of Michigan, Ann Arbor, MI, by permission of the University of Michigan

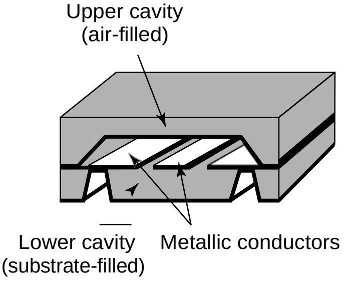

Figure .7 Self-packaged circuit constructed out of two silicon wafers. Reproduced from R.F. Dryton, 1995, *The Development and Characterization of Self-packages using Micromachining Tech- niques for High Frequency Circuit Applications*, PhD dissertation, University of Michigan, Ann Arbor, MI, by permission of the University of Michigan

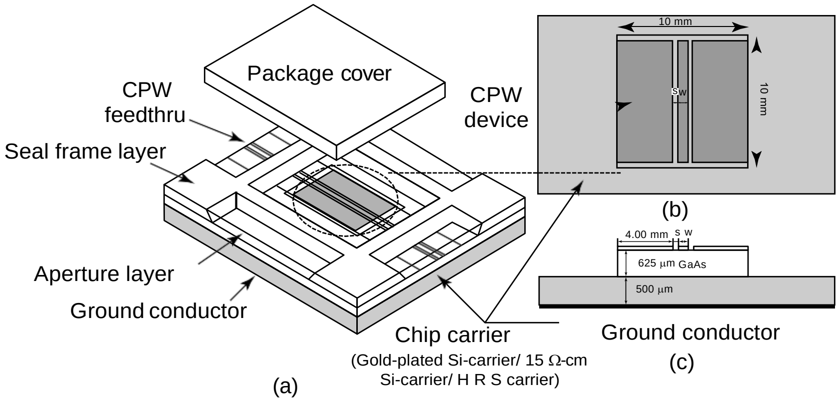

Figure .8 (a) Typical MEMS packaging with co-planar waveguide (CPW) line; (b) top view and (c) side view Note: HRS, high-resistivity silicon. Reproduced from S.J. Kim, Y.S. Kwon and H.Y. Lee, 2000, 'Silicon MEMS Packages for coplanar MMICs', in *Proceedings of 2000 Asia-Pacific Microwave Conference, Australia, December 2000*, IEEE, Washington, DC, by per- mission of IEEE, © 2000 IEEE

self-packaging (Hindreson *et al*., 2000) to individual planar circuit components. As shown in Figure 9.6, the metal conductors are supported by membrane and a lower cavity is below the conducting line. In Figures 9.7 and 9.8, the upper wafer has an air-filled cavity that is mounted over the metallic conductors. Integration of both upper and lower shielded circuits results in a self-packaged RF circuit.

1.3 FLIP-CHIP ASSEMBLY

Flip-chip is the most favored assembly technology for high-frequency applications because the short bump interconnect can reduce parasitic impedances. In flip chips, an IC die is placed on a circuit board with bond pads facing down and directly joining the bare die with the substrate. The bumps form electrical contact as well as a mechanical joint to the die. This reduces the electrical path length and the associated capacitance and inductance, which is particularly suited for high-density RF applications. The minimization of parasitic capacitance and inductance can reduce the signal delay in high-speed circuits.

Flip-chip bonding involves the bonding of die, top-face down on a package substrate. Electrical connections are made by means of plated solder bumps between bond pads on the die and metal pads on the substrate (Oppermann *et al*., 2000). The attachment is intimate with relatively small spacing (100 μm) between the die and the substrate. In flip-chip assemblies the bumps form the electrical contacts to the substrate as well as serving as a mechanical joint.

Figure 9.9 shows the flip-chip design of a MEMS package. Since the active surface of the MEMS is placed towards the substrate, the cavity will protect the movable MEMS. The stand-off distance can be accurately controlled by the bump height. Flip-chip technology is a very flexible assembly method for different applications. Another concept in wafer-level packaging is to apply a microcap to the device and then package with standard procedures. Figure 9.10 shows the concept of cap-on-chip packaging

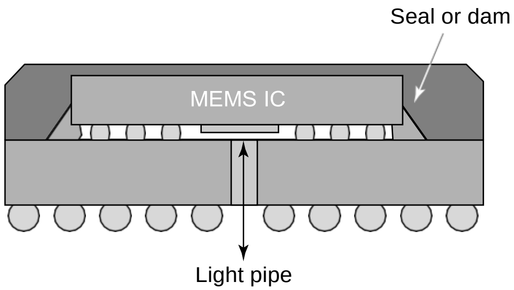

Figure .9 Flip-chip MEMS package. Reproduced from S.J. Kim, Y.S. Kwon and H.Y. Lee, 2000, 'Silicon MEMS Packages for coplanar MMICs', in *Proceedings of 2000 Asia-Pacific Micro- wave Conference, Australia, December 2000*, IEEE, Washington, DC, by permission of IEEE, © 2000 IEEE

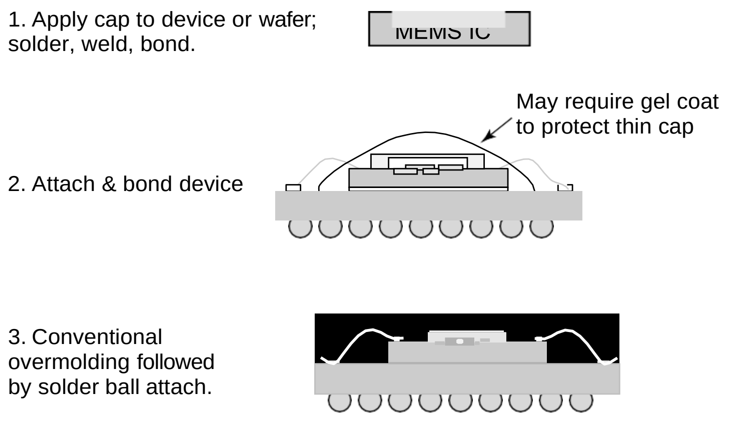

Figure .10 Cap-on-chip packaging. Reproduced from K. Gilleo, 2001b, 'MEMS packaging issues and materials', in *Proceedings of IEEE International Symposium on Advanced Packaging: Process, Properties and Interfaces*, IEEE, Washington, DC: 1 – 5, by permission of IEEE, © 2001 IEEE

for MEMS. Figure 9.11(a) presents the flip-chip bonding process on a ceramic-based (alumna) substrate and (Figure 9.11(b)) shows the gold bumps formed on pads of the substrate. The bump with an acute tail makes it easy to deform and to make the bonding area more stable under thermal conditions.

Flip-chip bonding is attractive to the MEMS industry because of its ability to package closely a number of dice on a single package substrate with multiple levels of electrical traces. Similar systems can built with wire bonding, but the area usage will be greater and the number of gold wires within the package may present a reliability issue. However, flip-chip may not be compatible with the packaging of MEMS that include microstructures exposed to the open environment.

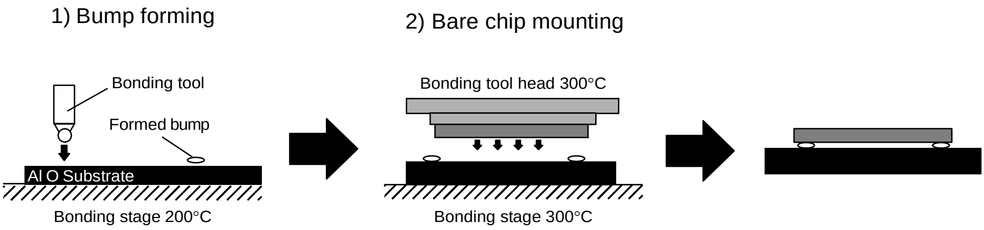

(a)

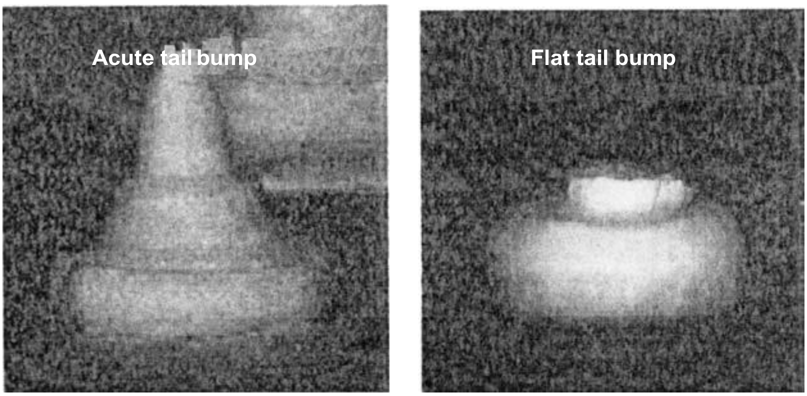

(b)

Figure .11 (a) Flip-chip bonding procedure; (b) photograph of acute and flat-tail bump used for flip-chip bonding. Reproduced from H. Kusamitsu, Y. Morishita, K. Murushashi, M. Ito and K. Ohata, 1999, 'The flip-chip bump interconnection for millimeter wave GaAs MMIC', *IEEE Transactions on Electronics Packaging and Manufacturing* **22**(1): 23 – 28, by permission of IEEE, © 1999 IEEE

1.4 MULTICHIP MODULE PACKAGING

The incompatibilities in fabrication of MEMS and ICs make them difficult for monolithic integration. Multichip module (MCM) packaging provides an efficient solution to integrate MEMS with microelectronic circuits because it supports a variety of die types in a common substrate without the need for many changes in either the MEMS or microelectronics fabrication processes. It adopts the high-density interconnect (HDI) process, consisting of embedding bare die into premilled substrate.

The micro module system (MMS) multichip module-deposited (MCM-D) process is the more traditional approach. The interconnect layers are first deposited on the substrate, and the die are mounted above the interconnect layers. The interconnect is mainly done by wire bonding (Butler, Bright and Comtios, 1997; Butler *et al.*, 1998; Cohn *et al.*, 1998; Coogan, 1990; Sardborn, Swaminathan and Subramanian, 2000).

Modifying the HDI process allows physical access to MEMS devices. Figure 9.12(a) shows the HDI process flow and Figure 9.12(b) shows an augmented HDI process for MEMS packaging by an additional laser ablation step to allow physical access to the MEMS die. The windows in the dielectric overlay above the MEMS device were selectively etched using laser ablation. Figure 9.13 shows a photograph of an MCM-D/MEMS a package.

Among various types of MCMs, the MCM-C (ceramic-based multichip module) is a multiplayer substrate based on aluminum oxide, and MCM-V (Gotz *et al*., 2001) is the vertical multichip module. The lines and vias are printed on different layers. All the layers are then co-fired (high-temperature co-fired ceramic) at the same time at high temperature. The metal parts, such as lead frames and heat sinks if necessary, can be soldered with eutectic.

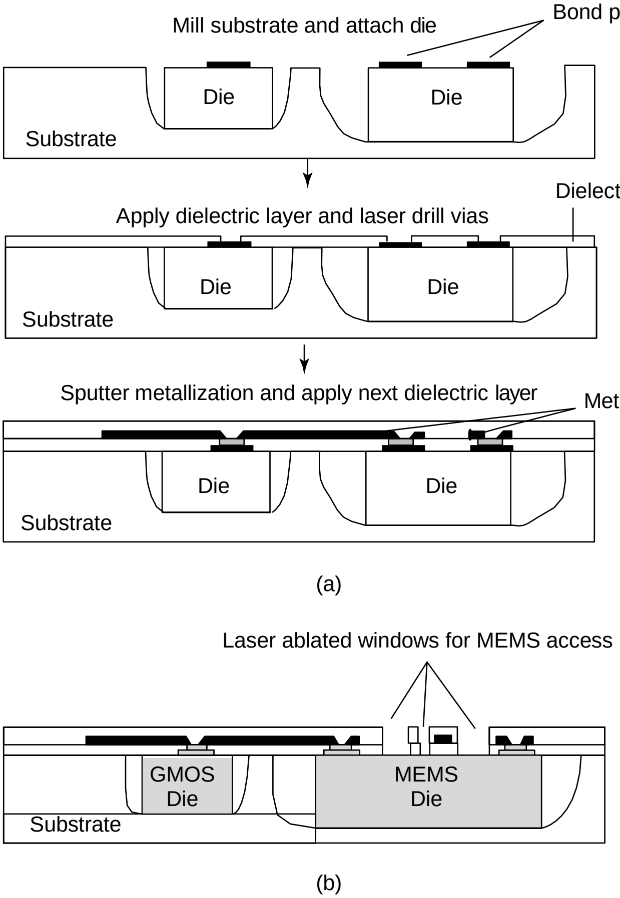

Figure .12 (a) High-density interconnected (HDI) process; (b) MEMS access in HDI process. Reproduced from J.T. Butler, V.M. Bright, P.B. Chu and R.J. Saia, 1998, 'Adapting multichip module foundries for MEMS packaging', in *Proceedings of IEEE International Conference on Multichip Modules and High-Density Packaging*, IEEE, Washington, DC: 106 – 111, by permission of IEEE, © 1998 IEEE

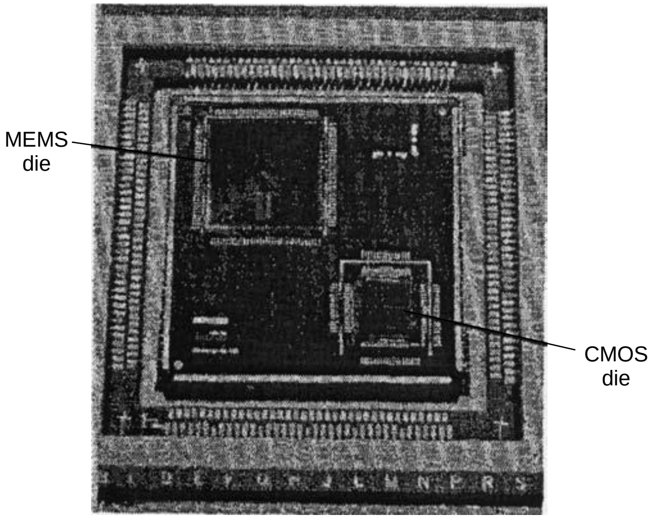

Figure .13 MCM-D/MEMS package. Note: CMOS, complementary metal oxide semiconductor; MEMS, microelectromechanical system; MCM-D, multichip module-deposited. Reproduced from J.T. Butler, V.M. Bright and J.H. Comtios, 1997, ‘Advanced multichip module packaging of micro-electromechanical systems’, in *Transducers ’97*, IEEE, Washington DC: 261 – 264, by permission of IEEE, © 1997 IEEE

1.4.2 Wafer bonding

MEMS packaging can also be done by bonding a recessed cap onto a micromachined wafer. However, conventional wafer bondings such as line fusion or anodic bonding cannot be employed because the micromechanical circuits can be damaged by to high temperatures or high electric fields. The low-temperature bonding techniques may increase the cost of packaging. If MEMS devices can be packaged at the device level first then the remaining packaging can be done with the IC packaging using common procedures. Microscale riveting (Lin, 1993; Shivkumar and Kim, 1997) or eutectic bonding (Cheng, Lin and Najafi, 2000) can be performed by directional etching of silicon for the rivet moulds and directional electroplating in an electric field for rivet formation. The wafer joining can be done at room temperature and low voltages. The protected devices after microriveting can be treated the same as the IC wafer during the dicing process. Once the joining is complete, the resulting chips can be handled in the same way as IC chips during the remaining packaging steps, such as wire bonding and moulding for plastic packages. Figure 9.14 shows the concept of a protected chip with MEMS device. Rivets are formed all around the cap wafer to hold the cap– base pair together. Figure 9.15 shows the prepared cap and base wafers and the electroplating setup. Nickel can easily be electroplated as a rivet material.

A seed layer of 125 Å of Chromium and 750 Å of Nickel is deposited on the surface of the base wafer by thermal evaporation. The cap and the base wafers are held together during the plating process so that the plating can start at the exposed area of the seed layer, grow through the rivet hole in the cap wafer and form the rivet. Simple mechanical clamping of the wafer together in the electrolyte is sufficient to rivet them together since electroplating does not occur in the microscopic wafer gap.

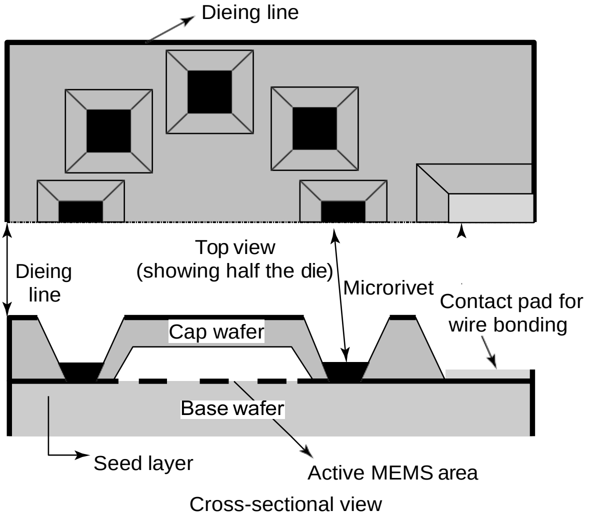

Figure .14 View of a packaged chip using microrivets. Reproduced from B. Shivkumar and C.J. Kim, 1997, 'Microrivets for MEMS packaging: concept, fabrication and strength testing', *Journal of Microelectromechanical Systems* **6**(3): 217–225, by permission of IEEE, © 1997 IEEE

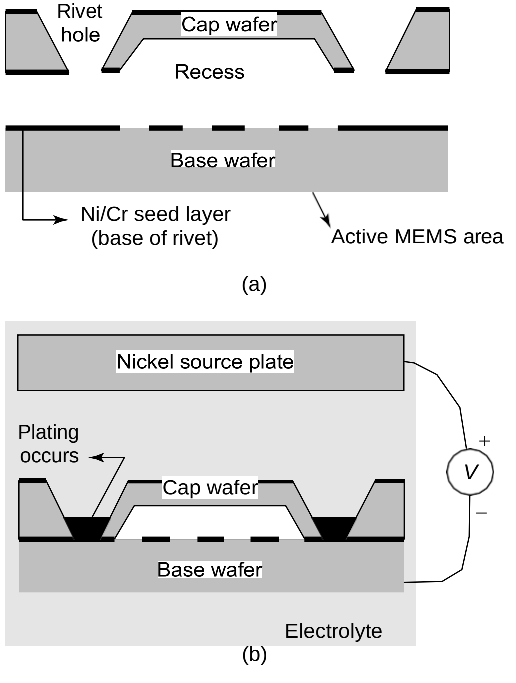

Figure .15 Schematic diagram of (a) the prepared cap and (b) the electroplating setup. Repro- duced from B. Shivkumar and C.J. Kim, 1997, 'Microrivets for MEMS packaging: concept, fabrica- tion and strength testing', *Journal of Microelectromechanical Systems* **6**(3): 217 – 225, by permission of IEEE, © 1997 IEEE

In fusion bonding, polysilicon is deposited and patterned as the heating and bonding material. Fusion bonding is used mostly in silicon-on-insulator (SOI) technology such as Si-SiO_2 (Laskey, 1986; Li *et al*., 2002; Mirza, 2000) and silicon bonding (shimbo *et al*., 1986). Aluminum-to-glass (Cheng, Lin and Najafi, 2001) bonding using localized heating can be applied for hermetic packaging. In eutectic bonding, gold resistive heaters are sputtered and used as heating and bonding material. The temperature of the microheater rises upon the flow of current, which activates the bonding process. The principle of localized bonding is shown in Figure 9.16. The effectiveness of the microheater depends on the selection of materials and the design of the geometrical shape of the structure. For example, a high temperature of 1000 °C can be created using microheaters, while the temperature at less than 2 μm away can drop to 100 °C (Mirza, 2000). Figure 9.17 shows the experimental setup for localized eutectic bonding. The conventional bonding takes one hour to reach the temperature, while localized eutectic heating will take only less than 5 minutes.

Phosphorous-doped polysilicon and gold resistive heaters are used in the silicon-to-glass fusion and the silicon-to-gold eutectic bonding process, respectively. Both processes can be accomplished in less than 5 minutes.

The aligned wafer-bonding process typically consists of two separate steps (Table 9.1). The wafers are aligned initially to each other in a bond aligner. This system can align a mask to a wafer for conventional photolithography as well as being able to align two wafers to each other. The aligned wafers are clamped with an appropriate separation gap

Table .1 Typical wafer bonding process conditions for anodic, glass frit and silicon direct wafer (DW) bonding

Condition	Bonding process		
	anodic	glass frit	DW
Temperature (°C)	300 – 500	400 – 500	1000
Pressure (bar)	N/A	1	N/A
Voltage (kV)	0.1 – 1	N/A	N/A
Surface roughness (nm)	20	N/A	0.5
Precise gap?	Yes	No	Yes
Hermetic seal?	Yes	Yes	Yes
Vacuum level during bond (Torr)	10^{-5}	10	10^{-3}

N/A Not applicable.
Source: Mirza and Ayon, 1998.

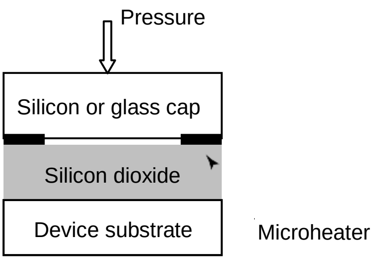

Figure .16 Schematic diagram of the localized microheater setup

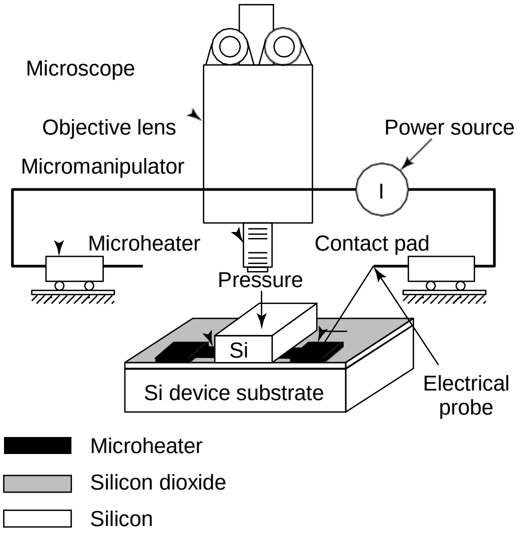

Figure .17 Experimental setup for the localized heating and bonding test. Reproduced from L. Lin, 2000, 'MEMS post-packaging by localized heating and bonding', *IEEE Transactions on advanced Packaging* **23**(4): 608 – 616, by permission of IEEE, © 2000 IEEE

between them in a bond fixture. The next step is to load the bond fixture into a vacuum bond chamber where the wafers are contacted together.

1.5 RF MEMS PACKAGING: RELIABILITY ISSUES

1.5.2 Packaging materials

Since MEMS devices have also to be fabricated other than silicon substrate, the compatibility with materials other than silicon and manufacturing in a silicon IC foundry is a major issue. One of the major capital investments needed is the equipment for automated packaging. For example, for automotive sensors, the environment in which the devices are going to operate must be considered at the beginning of package design. Table 9.2 shows the conditions in which most automotive components operate.

1.5.3 Integration of MEMS devices with microelectronics

The integration of a MEMS sensor with electronics has advantages, in particular when dealing with small signals. However, in such cases it is important that the process used for MEMS fabrication does not adversely affect the added electronics, required for the device to function correctly. MEMS devices can be fabricated as pre- or post-processing modules, which are integrated within the standard processing. The choice of whether or not to integrate depends on the application of the sensors and different aspects of the implementation technology. The state-of-the-art in MEMS is combining MEMS with ICs and utilizing advanced packaging techniques to create system-on-a-package (SOP) or system-on-a-chip (SIP) (Malshe *et al.*, 2001).

Table .2 Operating parameters of automobile sensors

Environment	Parameter value
Temperature (°C)	
driver interior	40–85
under the bonnet	125
on the engine	150
in the exhaust and combustion area	200–600
Mechanical shock (g)	
assembly (drop test)	3000
on vehicle	50–500
Mechanical vibration at 15g (Hz)	100–2000
Electromagnetic impulses (V m^{-1})	100–200

Note: depending on the application, there may also be exposure to humidity, salt spray, fuel, oil, break fluid, transmission fluid, ethylene glycol, freon and exhaust gas.
Source: Sparks, Chang and Eddy, 1998.

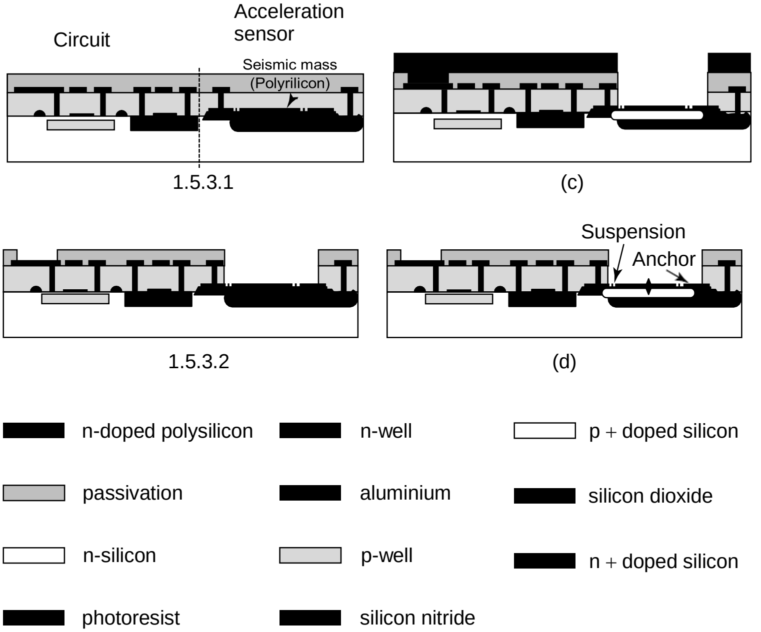

Figure .18 Integration of surface micromachining with CMOS. Reproduced from P.J. French, 1999, 'Integration of MEMS devices', in *Proceedings of SPIE Device and Process Technologies for MEMS and Microelectroncis, Queensland Australia*, SPIE volume 3892: 39 – 48, by permission of SPIE

The simplest form of integrated MEMS device is where existing layers are used for mechanical and sacrificial layers (French, 1999; Hsu, 2000; Ramesham and Ghaffarian, 2000). Standard processes have a number of layers on top of the wafer such as oxide, polysilicon, metal and nitride. This requires only the additional steps of masking and etching, as explained in Figure 9.18. Surface micromachining using post-processing additional layers is but maintaining standard processing by adding depositions at the end of processing. This may cause limitations on the thermal budget if aluminum is used as the metallization. Plasma-enhanced chemical vapor deposition (PECVD) can lower the temperature compatible with aluminum metallization.

In general, there are three main methods that have been used for monolithic integration of CMOS and MEMS; (a) electronics first (University of California, Berkeley, CA), (b) MEMS in the middle (Analog Devices, Cambridge, MA), and (c) MEMS first (Sandia National Laboratories, Livermore, CA) (O'Neal *et al*., 1999). Each of these methods has its own advantages as well as disadvantages. Sandia fabricated MEMS first and etched a trench and covered it with sacrificial oxide, which protects the MEMS devices from the CMOS processing steps. After the trench is completely filled with SiO_2, the surface is planarized, which serves as the starting material for CMOS foundry. The sacrificial oxide covering the MEMS device is removed after the fabrication of the CMOS device.

The alternative approach for monolithic integration with MEMS is the multi-chip-module (MCM) in which IC and MEMS dice can be placed in the same package. Several sensors, actuators or a combination can be combined in a single chip using the MCM technique (Butler *et al*., 1998). The main disadvantage is the probable signal loss due to parasitic effects between the components and the apparent added packaging expenses.

Co-planar MMICs packaged using a silicon (1 to 300 ▲ cm) substrate is found to reduce the parasitic effects, coupling and resonance compared with the unpackaged devices (Kim, Kwon and Lee, 2000). Common resistive silicon without gold plating can be an ideal packaging solution for low-cost and high-performance co-planar lines.

1.5.4 Wiring and interconnections

MEMS packages must protect the micromachined parts from environments and at the same time provide interconnections to electrical signals as well as access to and interaction with external environments. In hermetic packages, the electrical interconnections through a package must confirm hermetic sealing. Wire bonding is the popular technique to connect the die to the package electrically. Bonding of gold wires is easier than bonding of aluminum wires. The use of wire bonding has serious limitations in MEMS packaging because of the application of ultrasonic energy at a frequency between 50 and 100 kHz. Unfortunately, these frequencies may simulate oscillation of microstructures. Since most microstructures have resonant frequencies in the same range, the chance of structural failure during the wire bonding is high (Maluf, 2000).

1.5.5 Reliability and key failure mechanisms

Reliability requirements for various MEMS will be significantly different for different applications, especially with systems with unique MEMS devices. Hence standard reliability testing is not possible until a common set of reliability requirements is developed. The understanding of reliability of the systems comes from the knowledge of failure behavior and the failure mechanisms. The main failure mechanisms of MEMS devices are summarized as follows.

- Stiction: stiction and wear are the real concern and cause for most of the failure of MEMS. Stiction occurs as a result of microscopic adhesion when two surfaces come into contact. Wear due to corrosive environment is another aspect of failure.

- Delamination: MEMS may fail because of the delamination of bonded thin-film materials. Bond failure of dissimilar and similar materials such as wafer-to-wafer bonding can also cause delamination (Sandborn, Swaminathan and Subramanian, 2000).
- Dampening: dampening is critical for MEMS because of the mechanical nature of the parts and the resonant frequency. Dampening can be caused by many variables, including atmospheric gases. Good sealing is critical for MEMS devices. Since MEMS devices have mechanical moving parts, they are more susceptible to environmental failure than are packaging systems.
- Mechanical failure: the changes in elastic properties affect the resonant and damping characteristics of the beam and that will change the sensor performance.

1.6 THERMAL ISSUES

Heat-transfer analysis and thermal management become more complex by packing different functional components into a tight space. The miniaturization also raises issues such as coupling between system configurations and the overall heat dissipation to environment. The configuration of the system shell becomes important for the heat dissipation from system to the environment (Lin, 2000; Nakayama, 2000). Heat spreading in a thin space is one of the most important modes of heat transfer in compact electronic equipment and microsystems. As the system shrinks, the space available for installation of a fan or pump inside the system shell disappears and the generated heat has to be dissipated through the shell to the surrounding environment. In general, strategies of heat transfer in a microsystem can be presented as: first, to diffuse heat as rapidly as possible from the heat source; second, to maximize the heat dissipation from system shell to the environment.

1.7 CONCLUSIONS

The three levels of packaging strategy may be adaptable for MEMS packaging. There are: (1) die level, (2) device level and (3) system level. Die-level packaging involves the passivation and isolation of the delicate and fragile devices. These devices have to be diced and wire bonded. The device-level packaging involves connection of the power supply, signal and interconnection lines. System-level packaging integrates MEMS devices with signal conditioning circuitry or ASICs (application-specific integrated circuits) for custom applications.

The major barriers in the MEMS packaging technology can be attributed to lack of information and standards of materials and a shortage of cross-disciplinary knowledge and experience in the electrical, mechanical, RF, optics, materials, processing, analysis and software fields. Microsystem packaging is more a combination of engineering and science, which must share and exchange experiences and information in a dedicated fashion. Table 9.3 presents different challenges and solutions faced during microsystem packaging.

Packaging design standards should be unified. Apart from certain types of pressure and inertial sensors used by the automotive industry, most MEMS devices are custom built. A standardized design and packaging methodology is virtually impossible at this time because of the lack of data available in these areas. However, the joint efforts of industry and academic and research institutions can develop sets of standards for the design of

Table .3 Current packaging parameters, challenges and suggested solutions

Packaging parameters	Challenges	Possible solutions
Release etch and dry	Stiction of devices	Use freeze drying; use supercritical CO_2 drying; roughen contact surfaces such as dimples and nonstick coatings
Dicing and Cleaving	Contamination risks, elimination of particles generated	Release dice after dicing; cleave wafers; use laser swing; use waferlevel encapsulation
Die handling	Device failure, top die face is very sensitive to contact	Use fixtures that hold the MEMS dice by the sides rather than by the top face
Stress	Performance degradation and resonant frequency shifts	Use low-modulus die attach; use annealing; use compatible CTE match-ups
Outgassing	Stiction, corrosion	Use low-outgassing epoxies, cyanate esters, low-modulus solders, new die-attach materials, remove outgassing vapors
Testing	Applying nonelectric stimuli to devices	Test all that is possible using wafer-scale probing, and finish with cost-effective specially modified test systems

Note: CTE, coefficient of thermal expansion.
Source: Malshe *et al.*, 2001.

microsystems. Also, the thin-film mechanics that includes constitutive relations of thin-film materials used in the FEM (finite element method) and other numerical analysis systems need to be thoroughly investigated.

REFERENCES

Blackwell, G.R. (Ed.), 2000, *The Electronic Packaging Handbook* , CRC Press, Boca Raton, FL.

Butler, J.T., Bright, V.M., Comtios, J.H., 1997, 'Advanced multichip module packaging of micro-electromechanical systems', in *Transducers '97* , IEEE, Washington, DC: 261 – 264.

Butler, J.T., Bright, V.M., Chu, P.B., Saia, R.J., 1998, 'Adapting multichip module foundries for MEMS packaging', in *Proceedings of IEEE International Conference on Multichip Modules and High Density Packaging* , IEEE, Washington, DC: 106 – 111.

Butler, J.T., Bright, V.M., 2000, 'An embedded overlay concept for microsystems packaging', *IEEE Transactions on Advanced Packaging* **23**(4): 617 – 622.

Cheng, Y.T., Lin, L., Najafi, K., 2000, 'Localized silicon fusion and eutectic bonding for MEMS fabrication and packaging', *Journal of Microelectromechanical Systems* **9**(1): 3 – 8.

Cheng, Y.-Y., Lin, L., Najafi, K., 2001, 'A hermetic glass-silicon package formed using localized aluminum/silicon-glass bonding', *Journal of Microelectromechanical Systems* **10**(3): 392 – 399.

Cohn, M.B., Bohringer, K.F., Noworolski, J.M., Singh, A., Keller, C.G., Goldberg, K.Y., Howe, R.T., 1998, 'Microassembly technologies for MEMS', *Proceedings of SPIE Conference on Microfluidic Devices and Systems* **3515**(September): 2 – 16.

Coogan, S.A., 1990, 'System engineering: a summary of electronics packaging techniques available for present and future systems', in *Proceedings of Third Annual IEEE ASIC Seminar and Exhibit* , IEEE, Washington, DC: P4-3.1 – 3.4.

Dryton, R.F., 1995, The Development and Characterization of Self-packages using Micromachining Techniques for High Frequency Circuit Applications, Ph.D. dissertation, University of Michigan, Ann Arbor, MI.

Elwenspoek, M., Wiegerink, R., 2001, *Mechanical Microsensors* , Springer, Berlin.

French, P.J., 1999, 'Integration of MEMS devices', *Proceedings of SPIE Device and Process Technologies for MEMS and Microelectronics; Queensland Australia, SPIE* **3892**: 39 – 48.

Gilleo, K., 2001a, 'Overview of new packages, materials and Processes', *IEEE International Symposium on Advanced Packaging Materials* , IEEE, Washington, DC: 1 – 5.

Gilleo, K., 2001b, 'MEMS packaging issues and materials', in *Proceedings of IEEE International Symposium on Advanced Packaging: Process, Properties and Interfaces* , IEEE, Washington, DC: 1–5.

Gotz, A., Garcia, I., Cane, C., Morrissey, A., Aldreman, J., 2001, 'Manufacturing and packaging of sensors for their integration in a vertical MCM microsystem for biomedical applications', *Journal of Microelectromechanical Systems* **10**(4): 569 – 579.

Helsel, M.P., Berger, J.D., Wine, D.W., Osborn, T.D., 2001, 'Wafer scale packaging for a MEMS video scanner', in *Proceedings of SPIE Symposium on MEMS Design, Fabrication, Characterization and Packaging* **4407**: 214 – 220.

Hindreson, R.M., Herrick, K.J., Weller, T.M., Robertson, S.V., Kihm, R.T., Katehi, L.P.B., 2000, Three-dimensional high frequency distribution network, part II: packaging and integration, *IEEE Transactions on Microwave Theory and Techniques* **48**(10): 1643 – 1651.

Hsu, T.-R., 2000, 'Packaging design of microsystems and meso-scale devices', *IEEE Transactions on Advanced Packaging* **23**(4): 596 – 601.

Kim, S.J., Kwon, Y.S., Lee, H.Y., 2000, 'Silicon MEMS packages for coplanar MMICs', in *Proceedings of 2000 Asia-Pacific Microwave Conference, Australia, December 2000* , IEEE, Washington, DC: 17 – 20.

Kusamitsu, H., Morishita, Y., Marushashi, K., Ito, M., Ohata, K., 1999, 'The flip-chip bump interconnection for millimeter wave GaAs MMIC', *IEEE Transactions on Electronics Packaging and Manufacturing* **22**(1): 23 – 28.

Laskey, J., 1986, 'Wafer bonding for silicon-on-insulator technologies', *Applied Physics Letters* **48**(1): 78 – 80.

Li, Z., Hao, Y., Zhang, D., Li, T., Wu, G., 2002, 'An SOI– MEMS technology using substrate layer and bonded glass as wafer level package', *Sensors and Actuators A* **96**: 34 – 42.

Lin, L., 1993, *Selective Encapsulations of MEMS: Micro Channels, Needles, Resonators and Electromechanical Filters, Ph.D. dissertation, University of California at Berkeley, Berkeley, CA*.

Lin, L., 2000, 'MEMS post-packaging by localized heating and bonding', *IEEE Transactions on Advanced Packaging* **23**(4): 608 – 616.

Malshe, A.P., O'Neal, C., Singh, S., Brown, W.D., 2001, 'Packaging and integration of MEMS and related microsystems for system-on-a-package (SOP)', *Proceedings of SPIE Symposium on Smart Structures and Devices* **4235**: 198 – 208.

Maluf, N., 2000, *An Introduction to Micromechanical System Engineering* , Artech House, Boston, MA.

Mirza, A.R., Ayon, A.A., 1998, 'Silicon wafer bonding', *Sensors* December: 24 – 33.

Mirza, A.R., 2000, 'One micron precision wafer-level aligned bonding for interconnect, MEMS and packaging applications', in *Proceedings of IEEE 2000 Electronic Components and Technology Conference*: 676 – 680.

Mirza, A.R., 2000, 'Wafer level packaging technology for MEMS', in *Proceedings of IEEE 2000 Inter Society Conference on Thermal Phenomena*, IEEE, Washington, DC: 113 – 119.

Nakayama, W., 2000, 'Thermal issues in microsystems packaging', *IEEE Transactions on Advanced Packaging* **23**(4): 602 – 607.

O'Neal, C.B., Malshe, A.P., Singh, S.B., Brown, W.D., 1999, 'Challenges in packaging of MEMS', *IEEE International Symposium on Advanced Packaging Materials* , IEEE, Washington, DC: 41 – 47.

Oppermann, H.H., Kallmayer, C., Klein, C., Aschenbrenner, R., Reichl, H., 2000, 'Advanced flip chip technologies in RF, microwave and MEMS applications', *Proceedings of SPIE Design, Test, Integration and Packaging of MEMS/MOEMS* **4019**: 308 – 314.

Ramesham, R., Ghaffarian, R., 2000, 'Challenges in interconnection and packaging of microelec- tromechanical systems (MEMS)', in *Proceedings of 2000 Electronic components and Technology Conference*, IEEE, Washington, DC: 666 – 675.

Reichal, H., Grosser, V., 2001, 'Overview and development trends in the field of MEMS packag- ing', in *Proceedings of the 14th IEEE International Conference on MEMS* , 2001, IEEE, Wash- ington, DC: 1 – 5.

Sandborn, P., Swaminathan, R., Subramanian, G., 2000, 'Test and evaluation of chip-to-chip attach- ment of MEMS devices', in *Proceedings of IEEE 2000 Inter Society Conference on Thermal Phenomena*, IEEE, Washington, DC: 133 – 140.

Shimbo, M., Furukawa, K., Fukuda, F., Tanzawa, K., 1986, 'Silicon-to-silicon direct bonding method', *Journal of Applied Physics Letters* **60**: 2987 – 2989.

Shivkumar, B., Kim, C.J., 1997, 'Microrivets for MEMS packaging: concept, fabrication and strength testing', *Journal of Microelectromechanical Systems* **6**(3): 217 – 225.

Sparks, D.R., Chang, S.C., Eddy, D.S., 1998, 'Application of MEMS technology in automotive sensors and actuators', in *Proceedings of IEEE International Symposium on Micromechatronics and Human Science*, IEEE, Washington, DC: 9 – 15.

Sparks, D.R., 2001, 'Packaging of microsystems for harsh environments', *IEEE Instrumentation and Measurement Magazine*: 30 – 33.

Takahashi, K., Sangawa, U., Fujita, S., Goho, K., Urabe, T., Ogura, H., Yabuki, H., 2000, 'Pack- aging using MEMS technologies and planar components', in *Proceedings of 2000 Asia Pacific Microwave Conference, Australia, December 2000* , IEEE, Washington, DC: 904 – 907.

Takahashi, K., Sangawa, U., Fujita, S., Matsuo, M., Urabe, T., Ogura, H., Yabuki, H., 2001, 'Pack- aging using Microelectromechanical technologies and planar components', *IEEE Transactions on Microwave Theory and Techniques* **49**(11): 2099 – 2104.